UNIVERSITY OF
LINCOLN

The Roles of JAB1 and NOTCH1 in the Development of Cardiovascular Disease

A S Karountzos

Doctor of Philosophy

2019

The Roles of JAB1 and NOTCH1 in the Development of Cardiovascular Disease

Anastasios Stylianos Karountzos, BSc, MSc, MSc, MRSB

A thesis submitted in partial fulfilment of the requirements of the University of Lincoln for the degree of Doctor of Philosophy

This research programme was carried out in collaboration with the King's College London, UK

June 2019

The Roles of JAB1 and NOTCH1 in the Development of Cardiovascular Disease

Anastasios Stylianos Karountzos

ABSTRACT

Background

Pulmonary arterial hypertension (PAH) and Adams-Oliver syndrome (AOS) are rare vascular disorders, characterised by severe late-onset and developmental cardiac abnormalities respectively. Both of them are clinically associated in a proportion of cases. PAH is a progressive condition that is clinically characterized by sustained elevation in mean pulmonary artery pressure, through vascular remodelling with luminal obliteration of small vessels and increased vascular resistance, while AOS is characterized by congenital limb defects and scalp cutis aplasia. In a proportion of AOS-cases, notable cardiac development is also apparent. PAH may be hereditary (HPAH), idiopathic (IPAH) or associated with other conditions, for example AOS. Most of HPAH and 25% of IPAH cases are associated with heterozygous mutations of a TGF-β superfamily member transmembrane receptor type-II, known as *BMPR2*. The majority of mutations suggest haploinsufficiency as the molecular mechanism of disease. In addition, monoclonal proliferation and uncontrolled growth in pulmonary artery endothelial (PAEC) and smooth muscle (PASMC) cells result in perturbation and muscularization of the arterial tone. This study aims to identify the cause of a further loss of BMPR-II expression in previous immunohistochemical studies of patient's lung sections, that cannot be explained by haploinsufficiency. The defective BMP/TGF-β signalling in PAH will be addressed as well. This study also aims to identify novel genetic determinants of AOS, along with the hitherto unresolved underlying molecular defects, for the majority of affected subjects.

Methods and Results

Protein-protein interaction experimentation revealed a BMPR-II novel interacting partner, namely JAB1 protein, which through association with the kinase domain of the receptor, functions as the first identified proteasomal-associated inhibitor of BMPR-II. In addition, the linked experimental data of this study are indicative of BMPR-II degradation via the proteasomal pathway in the normal circulation. In addition, transient transfection studies demonstrated that JAB1 down-regulates BMPR-II in a dose-dependent manner. It is also confirmed that JAB1 is over-expressed during PAH progression, and proliferation studies revealed that JAB1 promotes uncontrolled cell proliferation and survival. Furthermore, functional studies supported the hypothesis that JAB1 appears to be a key regulator of BMP and TFG-β signalling pathways in PASMC cells, regulating differentially all stages of the pathways' cascades in SMAD-dependant and SMAD-independent manners. Apart its up-stream action of promoting the proteolytic degradation of BMPR-II, RT-qPCR experimentation and further functional studies proved that it

also acts down-stream, by suppressing *ID1* transcription factor or by promoting *ID* expression via up-regulation of SMAD-dependant and SMAD-independent signalling pathways, via activation of TAK1 and p38 MAPK mitogenic cascades, thus enhancing the pro-proliferative state of healthy and/or *BMPR2* mutated PASMC cells. Knock-down of JAB1 in healthy and *BMPR2* mutant PASMC cells resulted in control of their proliferation, an outcome which is indicative of the essential role of JAB1 in positively regulating the cell proliferation. The anti-proliferative effect of BMP4-ligand stimulation on hyper-proliferating *BMPR2* mutant PASMC cells was also established, highlighting the suppressive regulatory role of BMP signalling on cell proliferation and differentiation. Regarding AOS disease, *NOTCH1* mutations were found as the primary cause of AOS, in a proportion of cases of a cohort study (17%) with further cardiovascular complications. Novel identification of 10 mutations [3 frameshifts, 6 missense (EGF-like domain) and 1 nonsense] of the *NOTCH1* gene in AOS-patients, along with a significant reduction of *NOTCH1* expression in leukocyte-derived RNA from subjects, suggested that *NOTCH1* plays a key role in the AOS pathogenesis. Transient transfections of mutagenized *NOTCH1* missense constructs also revealed significant reduction in gene expression. Likewise, assessment of NOTCH1 target genes *HEY1* and *HES1* expression via RT-qPCR studies, verified the dysregulation of the NOTCH1 canonical signalling pathway in AOS-patients. Lastly, functional studies demonstrated the cross talk of BMP and NOTCH1 signalling as a synergistic effect in AOS pathology, underlined by forms of non-canonical signalling, potentiating the suppressive BMP cell signalling effect in AOS-cases of dysfunctional NOTCH1 signalling and further cardiovascular defects.

Conclusions

These findings manage to provide further insight into JAB1 mediated BMPR-II down-regulation and degradation via the proteasomal pathway, and determination of JAB1 dysregulation and role in the aggressive mitogenic proliferation potential, through reduction of SMAD signalling and consequently p38 MAPK and TAK1 activation, observed in PAH cells. This study highlights the significance of this molecule in the vasculature and sets it as a potential novel target in PAH therapy, and for drugs against PASMC cells in pro-proliferating state harbouring or not *BMPR2* PAH-associated mutations. Finally, it is established that haploinsufficiency of the NOTCH1 receptor is a primary cause of AOS, while solidifies *NOTCH1* as an important genetic factor in AOS with associated cardiovascular complications. Further X-ray crystallography studies of the identified *NOTCH1* missense mutations of the EGF-like domain will also elucidate the extend of the structural perturbation of the receptor and subsequent impairment of the signalling cascade.

ACKNOWLEDGEMENTS

Firstly, I would like to thank to my former supervisors, Dr Rajiv D. Machado and Dr Laura Southgate, for their guidance and support throughout this research project. It was great to have the opportunity to work with you and gain my very first publication. Furthermore, I would like to express my immense gratitude to my supervisor Dr Stephen Bevan, for I have received the best advice possible to conclude and edit my experimental work.

Special thanks goes to the Life Sciences department, past and present, especially Dr Timothy Bates, Dr Alan Goddard, Dr Ron Dixon and Dr Timea Palmai-Pallag for the friendly and help-insisted environment that created during the project. Also, thank you Maria, Tammy and James, and all the MSc students for it was great to share the lab with all of you.

I am also extremely grateful for being one of the winners of 2014 Primerdesign Ltd. Gold sponsorship, funds that were well utilized for the accomplishment of significant novel results towards Adams-Oliver Syndrome disease.

Also, I would like to thank my parents (Vasileios and Margarita), who have always encouraged me to achieve my dreams and been keen listeners to my progress. Nobody has been more important to me in the pursuit of this project than the members of my family, whose love and guidance are with me in whatever I pursue.

Equally importantly, I wish to thank Demy, for giving me all the love and wisdom needed to overcome any obstacles during my PhD progress and think of the future's unlimited perspectives.

DECLARATION

I herewith declare that I autonomously carried out the PhD thesis entitled “The Roles of JAB1 and NOTCH1 in the Development of Cardiovascular Disease”. The following third-party assistance has been enlisted: -

- Where stated, work was conducted in King’s College London, as part of collaborative work within the Cardiovascular department of Life Sciences & Medicine at KCL and the School of Life Sciences at the University of Lincoln.

I did not receive any assistance in return for payment by consulting agencies or any other person. No-one has received any kind of payment for direct or indirect assistance in correlation to the content of the submitted thesis.

I conducted the project in the School of Life Sciences at the University of Lincoln. The thesis has not been submitted elsewhere for an exam, as thesis or for evaluation in a similar context.

I hereby affirm the above statements to be complete and true to the best of my knowledge.

Signature.....Anastasios S. Karountzos, MSc, MRSB

TABLE OF CONTENTS

TABLE OF TABLES

TABLE OF FIGURES

LIST OF ABBREVIATIONS

ACC	Aplasia cutis congenital
ALK	Activin receptor-like kinase
ANK	Ankyrin repeat domain
AOS	Adams-Oliver syndrome
APAH	Associated pulmonary arterial hypertension
ARHGAP31	Rho GTPase activating protein 31
AVM	Visceral arteriovenous malformation
bHLH	Basic helix-loop-helix
BMP	Bone morphogenetic protein
BMPR2	Bone morphogenetic protein receptor, type 2
cDNA	complementary deoxyribonucleic acid
CFP	Cyan fluorescent protein
CHD	Congenital heart disease
COP9	Conference of the Parties 9
co-SMAD	common SMAD
CRL	Cullin-RING ligases
CSN	COP9 signalosome
CVD	Cardiovascular disease
DAPI	4',6-diamidino-2-phenylindole
DMEM	Dulbecco’s modified Eagle’s medium
DMSO	Dimethyl sulfoxide
DOCK6	Dedicator of cytokinesis 6
ECL	Enhanced chemiluminescence
EDTA	Ethylenediaminetetraacetic acid
EGF	Epidermal growth factor
eGFP	enhanced green fluorescent protein
ENG	Endoglin
EOGT	EGF domain-specific o-linked n-acetylglucosamine transferase
FBS	Foetal bovine serum
FRET	Förster resonance energy transfer

GI	Gastrointestinal tract
GST	Glutathione S-transferase
HEK293T	Human embryonic kidney cells
HeLa	Human endometrioid cancer cells
HES1	Hairy and enhancer of split-1
HEY1	Hairy/enhancer-of-split related with YRPW motif protein 1
HHT	Hereditary hemorrhagic telangiectasia
HPAH	Hereditary PAH
HPV	Hypoxic pulmonary vasoconstriction
hTERT	Human telomerase reverse transcriptase
ID-1	DNA-binding protein inhibitor
IPAH	Idiopathic PAH
JAB1	c-Jun activation domain-binding protein-1
JAMM	JAB1/MPN/Mov34 metalloenzyme motif
JBD	JNK binding domain
KD	Kinase domain
LNR	Lin-12 NOTCH repeat domain
MAML	mastermind-like transcriptional co-activator
MAPK	Mitogen-activated protein kinase
MPN	Mpr1-Pad1-N domain
mRNA	messenger ribonucleic acid
MTT	3-(4,5-dimethylthiazol-2-yl)-2,5-diphenyltetrazolium bromide
NEDD8	neuronalprecursor-cell-expressed developmentally down-regulated protein 8
NES	nuclear export signal
NICD	Notch intracellular domain
NMD	Nonsense mediated decay
NOTCH1	Neurogenic Locus Notch Homolog Protein 1
PAEC	Pulmonary arterial endothelial cells
PAH	Pulmonary arterial hypertension
PASMC	Pulmonary arterial smooth muscle cells

PBS	Phosphate buffered saline
PDB	p27-binding domain
PEST	Sequence rich in proline (P), glutamic acid (E), serine (S), and threonine (T)
PVD	Pulmonary vascular disease
PVD	Pulmonary vascular diseases
PVH	Pulmonary venous hypertension
qPCR	quantitative polymerase chain reaction
RAM	Rbp-associated molecule
RBPJ	Recombination signal binding protein for immuno-globulin kappa J region
RING	Really interesting new gene
R-SMAD	Receptor-regulated SMAD
SCF	Skp1-Cullin-F-box protein complex
SDS-PAGE	Sodium dodecyl sulphate-Polyacrylamide gel electrophoresis
siRNA	small interfering RNA
SMAD	Orthologues of the Drosophila protein, mothers against decapentaplegic and the Caenorhabditis elegans protein SMA
SmGM-2	Smooth muscle growth medium-2
TAD	Transcriptional activation domain
TAK1	Transforming growth factor beta-activated kinase 1
TGF-β	Transforming growth factor beta
TM	Transmembrane domain
TTLD	Terminal transverse limb defects
WHO	World health organization
XIAP	X-linked inhibitor of apoptosis protein
YFP	Yellow fluorescent protein

CHAPTER 1: INTRODUCTION

1.1 PULMONARY VASCULAR DEVELOPMENT

The formation of the vascular network in embryonic stages is mainly defined of the two distinct developmental mechanisms of vasculogenesis and angiogenesis. Vasculogenesis gives rise to new blood vessels along with the heart, which form the first primitive vascular plexus of the embryo. This process occurs by *in situ* differentiation of the angioblasts of the mesoderm and further *de novo* production of endothelial cells. The mesodermal hemangioblast cells are multipotent precursor cells, which also contribute to the differentiation of hematopoietic stem cells and the vascular endothelium. On the other hand, angiogenesis is the main mechanism responsible for the formation, remodelling and expansion of new blood vessels from the pre-existing network (sprouting). This process elaborates with the primitive vascular structures for the endothelial cell migration, proliferation and tube formation. Specifically, a layer of vascular smooth muscle cells encircles the endothelium and the vascular wall is formed by the recruitment of additional cellular and extra-cellular material. The vascular smooth muscle of the great vessels is derived from mesenchymal precursors, and in part from the neural crest, whereas the smooth muscle cells of smaller vessels are developed from the differentiation of the surrounding mesoderm (Patan 2004). The establishment of the lung formation and the pulmonary vascular system initiates at embryonic developmental stages and continues postnatally. It involves the vasculogenic differentiation of endothelial cells from the ventral foregut endoderm for the embryonic lung development, and the subsequent lung endoderm protrusion into the surrounding mesoderm, as the heart tube elongates and folds into structurally distinct chambers (Peng, Morrisey 2013). During that process, the six already developed pharyngeal arches outgrow in an angiogenic way in order to form sections of the pulmonary arteries. Up to date, many genes that initiate lung organogenesis and morphogenesis along with vasculogenesis and angiogenesis, have been identified, such as fibroblast growth factor, vascular endothelial growth factor, transforming growth factor beta and angiopoietin-1/2, in conjunction with several growth factor receptors and regulatory non-coding microRNAs (Jones, Capen et al. 2014). However, genes regulating the above processes are increasingly being identified, as it is becoming clear that early lung and vascular development directs epithelial and endothelial morphogenesis for

normal branching, alveolarization and maintenance of the distal air spaces (Jones, Capen et al. 2014).

1.1.1 GENERAL MORPHOLOGY OF NORMAL PULMONARY VASCULATURE

Blood vessels except for capillaries, share the same basic structure (Figure 1-1). Essentially, the wall of arteries and veins is composed of three discrete layers or tunics. The outermost layer is the tunica externa, the central section is the tunica media and the innermost layer is the tunica intima. The tunica externa or else tunica adventitia is composed of connective tissue and merges with the extracellular matrix. The tunica media is composed primarily of circumferential smooth muscle and varying amounts of connective tissue. The tunica intima consists of three parts: a) the endothelium, which is an innermost simple squamous epithelium and lines the lumina of all blood vessels, b) a basement membrane comprised of a layer of glycoproteins, and c) the internal elastic lamina, which is mainly a layer of elastic fibers.

Although blood vessels have the same basic structure, there are significant differences between arteries and veins, and also amongst arteries themselves. Arteries are more muscular for their diameters when compared to similarly sized veins, allowing them to withstand high blood pressure, as opposed to the thinner muscle layer of veins, which allows them to distend when increased blood volume enters them. In addition, capillaries are the smallest blood vessels and they are composed of a wall of endothelial cell thick, which facilitates the rapid exchange of many substances, such as water, oxygen, glucose, CO_2, uric and lactic acid along with urea and creatinine, between the blood and the interstitial fluid surrounding them (Maton 1993).

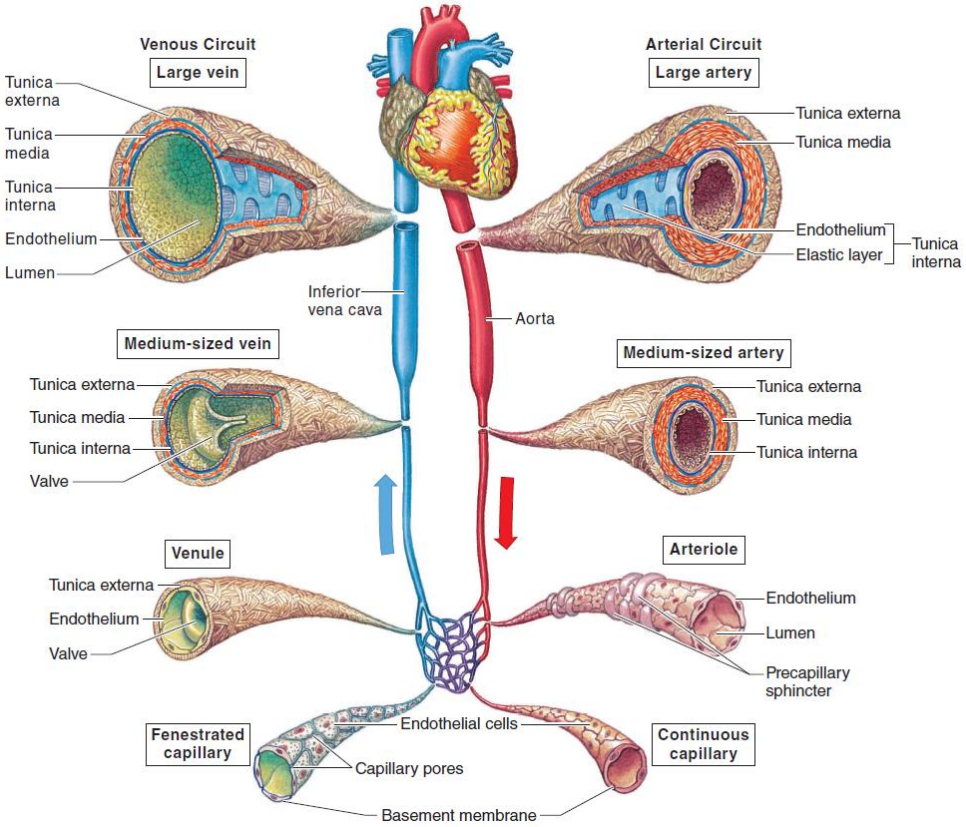

Figure 1-1 The structure of blood vessels
The three structural layers (tunics) of arteries and veins. (Fox, 2016).

1.1.1.1 MORPHOLOGY OF SPECIALISED PULMONARY BLOOD VESSELS

1.1.1.2 ARTERIES

The artery is a type of blood vessel that transports oxygenated blood from the heart to the rest of the body. The two exceptions of this rule are the umbilical and pulmonary arteries, which carry deoxygenated blood from the periphery of the body and through the right ventricle of the heart, to the organs that oxygenate it. More specifically, the blood supply of the human organism originates from the aorta, a large artery that protrudes from the left ventricle. The development and specialization of the rest of the arterial system relies upon two major factors: a) blood pressure produced by heart contractions, and b) regulation of the blood volume to target tissues of the artery. This specialization mainly concentrates in the tunica media layer of the arterial wall.

1.1.1.3 ELASTIC ARTERIES

They receive blood directly from aorta and pulmonary artery. Elastic arteries also exhibit greater thickness than muscular arteries.

Tunica intima: It is composed primarily of endothelial cells and an internal elastic membrane of loose connective tissue.

Tunica media: It is composed of smooth muscle cells and numerous layers of elastin and collagen fibers to support distensibility. The walls need to stretch in order to accommodate the ejected blood from the heart contractions.

Tunica adventitia: It is composed of collagen deposits along with a) vasa vasorum; network of small blood vessels that supply the walls of large blood vessels, and b) nervi vasorum; nerve fibers that innervate arteries and veins.

Size: >10 mm diameter.

1.1.1.4 MUSCULAR ARTERIES

They distribute blood from the elastic arteries to the rest of the body.

Tunica intima: It is composed of endothelium of flattened endothelial cells

Tunica media: It is composed of smooth muscle cells and an internal elastic layer (IEL) of elastin and collagen, in-between tunica intima and tunica media.

Tunica adventitia: It is very broad structure containing collagen and elastin fibers, which vary in thickness.

Size: 0.1-10 mm diameter

1.1.1.5 ARTERIOLES

The arterioles are small diameter blood vessels of that extend and branch out from an artery, leading to the capillaries.

Tunica intima: It is composed of a single endothelial layer and an internal elastic membrane.

Tunica media: It has a clearly defined internal elastic lamina (thick layer) of one to two layers of smooth muscle cells.

Tunica adventitia: As it is extremely thin, it is difficult to be distinguished from the external elastic lamina and the extracellular matrix.

Size: 5-100 μm diameter

1.1.1.6 CAPILLARIES

The capillaries are the smallest type of micro-vessels with size ranging from 5 to 10 μm in diameter. They only consist of tunica intima structured by a single thick endothelial cell wall, a basal lamina and a discontinuous external layer of pericyte cells.

1.1.1.7 VEINS AND VENULES

Unlike arteries, which are designed to provide resistance to the blood flow from the heart, veins are able to expand as they accumulate additional blood volume from the rest of the body. Specifically, veins accumulate 70% of total blood volume, 25% of which it is contained in venules. In terms of pressure, the average blood pressure in veins is 2 mmHg, opposed to a much higher average arterial pressure of approximately 100 mmHg.

Tunica intima: They are composed primarily of endothelial cells.

Tunica media: They are composed of smooth muscle cells and varying amounts of collagen. Also, they are much less muscular than the arteries or arterioles of the same size in diameter. Of note, the muscular layer may be absent in smaller venules.

Tunica adventitia: It is a thick outer layer of 2 types of connective tissue: a) dense collagen clusters, and b) interspersed elastic fibers. Vasa vasorum is also present.

Size: Veins: 1 mm to 1-1.5 cm diameter; Venules: 7 μm to 1 mm diameter.

1.1.2 THE NORMAL PULMONARY CIRCULATION

The heart is divided into four chambers, two atria which receive venous blood, and two ventricles which pump blood through the blood vessels of the circulatory system. The deoxygenated blood from the systemic circulation returns to the right atrium from the superior and inferior venae cavae, and passes to the right ventricle, which in turn pumps it into the pulmonary circulation, though the pulmonary arteries. The lungs receive the deoxygenated and rich in CO_2 blood, where gas exchange occurs between the lung capillaries and the air sacks (alveoli) of the lungs. Specifically, oxygen diffuses from air to the capillary blood, while CO_2 diffuses in the opposite direction (Fox 2016). Then, the oxygenated blood returns to the left atrium by the pulmonary veins and passes through the left ventricle to the aorta, in order to be pumped out to the systemic circulation. The aorta is a very large elastic artery, which ascends for a short distance, makes a U-turn, and then descents through the thoracic and abdominal cavities into several arterial branches, which supply the oxygenated blood to all organ systems of the body; thus, aorta and its branches are part of the systemic circulation (Fox 2016). The blood circuit from the right ventricle of the heart, through the lungs, and back to the left atrium is termed as the pulmonary circulation (Figure 1-2). Any part of the pulmonary circulation can become injured or blocked, leading to pulmonary vascular disease (PVD).

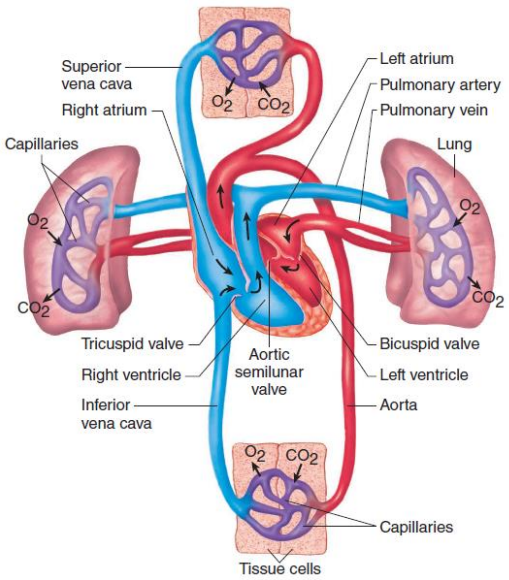

Figure 1-2 The circulatory system
The systemic circulation includes the aorta and venae cavae; the pulmonary circulation includes the pulmonary arteries and pulmonary veins. (Fox, 2016)

1.1.2.1 TRANSITIONAL HEMODYNAMICS AND STRUCTURAL ADAPTATION IN FOETAL AND NEONATAL PULMONARY CIRCULATION

The placenta is the main site of gas and metabolic exchange for the early developmental stages of the foetus. During foetal development, the patent foramen ovale and the patent ductus arteriosus are open. Thus, the foetus blood from placenta skips the lung route in order to get oxygenated and redirects through the ductus arteriosus, as a result of the high resistance of the newly developed pulmonary vasculature. This resistance is consequent of the morphology of elastic and transitional muscular arteries and arterioles, in which the smooth muscle layer is thicker narrowing down the lumen. At term, a decrease in pulmonary vascular resistance is accomplished as a result of lung expansion and utilization, increase of systemic vascular resistance because of placenta removal and closure of patent foramen ovale and patent ductus arteriosus, and dilatation of the pulmonary artery and arterioles. In the preterm infant, this difference in resistance is not linked with morphological modifications in the vasculature (Jones, Capen et al. 2014, Wu, Azhibekov et al. 2016).

1.1.2.2 HEMODYNAMICS AND STRUCTURAL FEATURES IN POSTNATAL AND ADULT PULMONARY CIRCULATION

The hydrostatic pressure of the blood in the pulmonary vasculature raises significantly after the increase of the blood flow through the lungs via the closure of the ductus arteriosus and the foramen ovale. As a consequence, the elastic and muscular arteries along with muscular arterioles undergo significant structural changes, during the first 3 weeks of postnatal life. The tunica media of the muscular arteries exhibits medial thinning, simultaneously with luminal widening of the vessel. The pulmonary vasculature reaches a steady-state after one and a half years of life; during that period, the media width is gradually decreases over time. Structurally, the adult pulmonary circulation mechanistically stabilizes into a low-pressure system of between 7 and 15 mmHg, with an average of approximately 9 mmHg (Jones, Capen et al. 2014, Wu, Azhibekov et al. 2016).

1.2 CARDIOVASCULAR DISEASE

Cardiovascular diseases (CVD) comprise a large spectrum of pathophysiological alterations that affect the heart and the vessels. The main manifestations of CVDs in the heart include a broad range of diseases such as cardiomyopathy, hypertensive heart disease, heart failure, pulmonary heart disease, cardiac dysrhythmias, inflammatory, valvular, rheumatic and congenital heart disease (Mendis, Puska et al. 2011). CVD manifestations also can be found in the arterial and venous system and include but not limited the blood vessels. They are known as vascular diseases. Typical examples are coronary artery disease, peripheral arterial disease, pulmonary vascular disease (PVD), cerebrovascular disease, renal artery stenosis and aortic aneurysm (Mendis, Puska et al. 2011).

CVD is the leading cause of death globally, except the African region. The wide spectra of CVD resulted in 17.9 million verified deaths (32.1%) in 2015, an up-rising result from 12.3 million (25.8%) in 1990. (Mendis, Puska et al. 2011, GBD 2015 Mortality and Causes of Death Collaborators 2016). Although the advancement of new diagnostic and imaging modalities are promising, CVD morbidity and mortality is increasing steadily in the developed world (Moran, Forouzanfar et al. 2014). Of note, coronary artery disease and stroke account for 80% of CVD deaths in males, following a 75% of the same causes in females (Mendis, Puska et al. 2011). Typically, the broad range of CVDs affects older individuals. More specifically, 11% of people between 20 and 40 suffer from CVD in the United States, while the percentage raises to 37% between 40 and 60, escalates to 71% between 60 and 80, and reaches to 85% for people over the age of 80 (Go, Mozaffarian et al. 2013). The average age of death from coronary artery disease in the developed world is around 80 while it is approximately 68 in the developing world. Interestingly, the disease onset is usually 7 to 10 years earlier in men when compared to women (Moran, Forouzanfar et al. 2014).

The underlying pathophysiological mechanisms of CVD vary, as they are dependent on each individual disease. However, a major component that triggers the pathophysiological alterations are risk factors that span throughout the lifespan of an individual. Risk factors such as gender, age, tobacco use, physical inactivity, excessive alcohol consumption, obesity, genetic predisposition and

family history of cardiovascular disease, high blood pressure (hypertension), high blood sugar (diabetes mellitus), high blood cholesterol (hyperlipidaemia), psychosocial factors, poverty and low educational status, and air pollution (GBD 2015 Mortality and Causes of Death Collaborators 2016). Epidemiological studies reveal the magnitude of high blood pressure resulting in 13% of CVD deaths, while tobacco resulting in 9%, diabetes 6%, lack of exercise 6% and obesity 5% (Mendis, Puska et al. 2011).

It is evaluated that 90% of CVD is preventable in the event that the above risk factors could be avoided. The up-to-date practiced measures to prevent CVD include tobacco cessation, a low-fat, low-sugar high-fiber diet, systematic physical exercise per week, limit alcohol consumption, lower blood pressure if elevated, decrease body fat if overweight or obese and decrease of psychological stress (McGill, McMahan et al. 2008).

1.3 PULMONARY VASCULAR DISEASE

1.3.1 DEFINITION OF PULMONARY VASCULAR DISEASE

Vascular disease is a subgroup of CVD and is the other end of the manifestation of CVD involving a wide array of diseases of the blood vessels; the arteries and veins of the circulatory system of the body. Many disorders in this vast network of vessels can cause a range of medical issues which can be serious or demonstrate lethality. A distinctive subtype of vascular disease is pulmonary vascular disease (PVD). PVD is the medical term for disorders affecting the blood vessels and causing abnormal blood flow between the heart and the lungs. Any kind of insulting stimulus that can cause blockage of the vessel or direct damage to the endothelial surface lead to pathophysiological alterations and at end PVD.

Characteristically, there are two main types of PVD: pulmonary embolism and pulmonary hypertension. In Europe region, the confirmed cases of pulmonary embolism broadly range from 6 to 20 per 10,000 people per year, of which 7-11% of people do not survive, and as of pulmonary arterial hypertension, there are 1.5-5.2 cases per 100,000 people at the same district, who have a median survival

rate of 2.8 years [(WHO Hospital Morbidity Database (Oct 2011) and Eurostat (Mar 2012)].

1.3.2 CAUSES, SYMPTOMS AND TREATMENTS OF PULMONARY VASCULAR DISEASE

Up to date, there are several clinical tests for the diagnosis of PVD, based on an individual's symptoms, signs and clinical history. Computed tomography (CT scan), ventilation/perfusion scan (V/Q scan), echocardiography, right heart catheterization, chest x-ray film and pulmonary angiography are the main test for PVD identification. Also, the causes and treatments of PVD vary according to which of the pulmonary system blood vessels are affected. PVD is divided into four main categories:

Pulmonary Arterial Hypertension (PAH): There are several causes for PAH which can be summarized as autoimmune disease, lung disease or heart failure. It is characterized by increased blood pressure in the pulmonary arteries, when blood is carried away from the heart to the lungs. When the causality is not apparent, it is classified as idiopathic PAH. This disease frequently causes slow progressive shortness of breath and as the condition declines, chest pain or syncope (fainting) with exertion can occur. Several up-to-date medicinal approaches can lower blood pressure in the pulmonary arteries. Supplemental oxygen along with specific vasodilators: a) endothelin receptor antagonists like ambrisentan (Letairis), bosentan (Tracleer) and macitentan (Opsumit), b) prostacycline or prostacycline analogs like epoprostenol (Flolan), iloprost (Ventavis) and treprostenil (Orenitram, Remodulin, Tyvaso), c) prostacyclin receptor agonist selexipag (Uptravi), d) stimulator of soluble guanylate cyclase riociguat (Adempas), and e) phosphodiesterase type 5 inhibitors like sildenafil (Revatio), tadalafil (Adcirca) are some of the main drugs that are currently used (Sommer, Hecker et al. 2016)

Pulmonary Venous Hypertension (PVH): It is principally characterized by increased blood pressure in the pulmonary veins when blood is carried away from the lungs to the heart. PVH is frequently caused by congestive heart failure.

Another contributing factor could be mitral stenosis or mitral regurgitation of the heart. Similarly to PAH, PVH also causes shortness of breath, if congestive heart failure is present. This symptom is more apparent while lying flat or when blood pressure is uncontrolled; in certain cases when extra fluid (edema) is present, shortness of breath may be worse. Since congestive heart failure is the common aetiology of this disease, drugs for heart failure are typically suitable: a) diuretics, such as furosemide (Lasix) and spironolactone (Aldactone), b) angiotensin-converting enzyme (ACE) inhibitors, such as Lisinopril, c) beta-blockers, such as carvedilol (Coreg) and metoprolol (Lopressor) and d) vasodilators that reduce blood pressure, such as amlodipine (Norvasc), hydralazine (Apresoline) and isosorbide mononitrate (Imdur) (Kulik 2014).

Pulmonary Embolism: It is typically defined as a blockage of an artery in the pulmonary system, by a blood clot which breaks off from a deep vein in the body (usually in the leg). The clot moves through the bloodstream, travels into the right-side of the heart and is pumped into the lungs; typically, this occurs in sudden. In rare cases, the embolism can be occurred by a large bubble of air, fat or amniotic fluid. The most common symptoms of this disease are shortness of breath, dyspnea or tachypnea, chest pain (worsened by breathing), cough with haemoptysis, cyanosis and sudden death. The size of the blood clots is accountable for the severity of the symptoms and the treatment comprises of a) anticoagulants such as heparin, betrixaban (BEVYXXA), enoxaparin (Lovenox), warfarin (Coumadin), b) thrombolysis, c) inferior vena cava filtration and d) surgery (Konstantinides, Barco et al. 2016).

Chronic Thromboembolic Disease: As a rare consequence of pulmonary embolism, the blood clot to the lungs may never be dissolved or reabsorbed by the body. Thus, multiple small blood vessels of the pulmonary system may be diseased by a reaction which occurs gradually, and ultimately could affect a large part of the lungs. In most of these cases, pulmonary hypertension may occur with symptoms such as progressive dyspnea, exercise intolerance, and nonspecific abnormalities on physical examination. The treatment involves blood thinners and in serious cases surgery to clear out the pulmonary arteries; a process which is called thromboendoarterectomy. Riociguat (Adempas) is the only approved therapy for use after surgery or in inoperable situations, and it could also be used

from people with chronic thromboembolic pulmonary hypertension in order to improve the ability to exercise (Mahmud, Madani et al. 2018).

If PVD is the underlying condition of another syndrome or clinical condition, treating of the main condition might improve the former disease. For example, autoimmune diseases as lupus, scleroderma or Sjogren's syndrome are typically treated with immunosuppressant drugs like Prednisone, azathioprine (Imuran), and cyclophosphamide (Cytoxan) or steroids to reduce inflammation. Also, inhaled oxygen administration or FDA-approved medication such as nintedanib (Ofev) and pirfenidone (Esbriet), can slow the progression of PVD in cases of lung diseases with low blood oxygen levels such as chronic obstructive pulmonary disease, idiopathic pulmonary fibrosis and interstitial lung disease.

1.4 CLINICAL FEATURES OF PULMONARY ARTERIAL HYPERTENSION

Pulmonary arterial hypertension (PAH) is a rare form of PVD, which involves pulmonary vascular remodelling with luminal obliteration of small vessels, resultant raised pulmonary vascular resistance and ultimately right ventricular failure and death (Figure 1-3) (Simonneau, Gatzoulis et al. 2013). The annual incidence rate of this particular disorder is 1-2 cases per 1 million in the general population (Shintani, Yagi et al. 2009) and it is often fatal. PAH is characterized by sustained mean pulmonary arterial pressure (mPAP) of >25 mmHg at rest and >30 mmHg during exercise. The pathobiology behind the vascular remodeling in PAH cases (Figure 1-4) primarily corresponds to clonal proliferation of pulmonary artery endothelial cells (PAECs) and uncontrolled growth of smooth muscle cells (PASMCs) in the pulmonary arterioles, resulting in intima lesions (PASMC intima thickening, extracellular matrix fibrotic lesions, PAEC plexiform, concentric, and dilation/angiomatoid lesions) and reduction of the small pulmonary arteries luminal area (Tuder, Stacher et al. 2013). The monoclonal growth of PAECs in combination with abnormal glycolysis and mitochondrial dysfunction (Warburg phenomenon), indicates a link to pre-proliferating states and cancer progression (Ryan, Dasgupta et al. 2015).

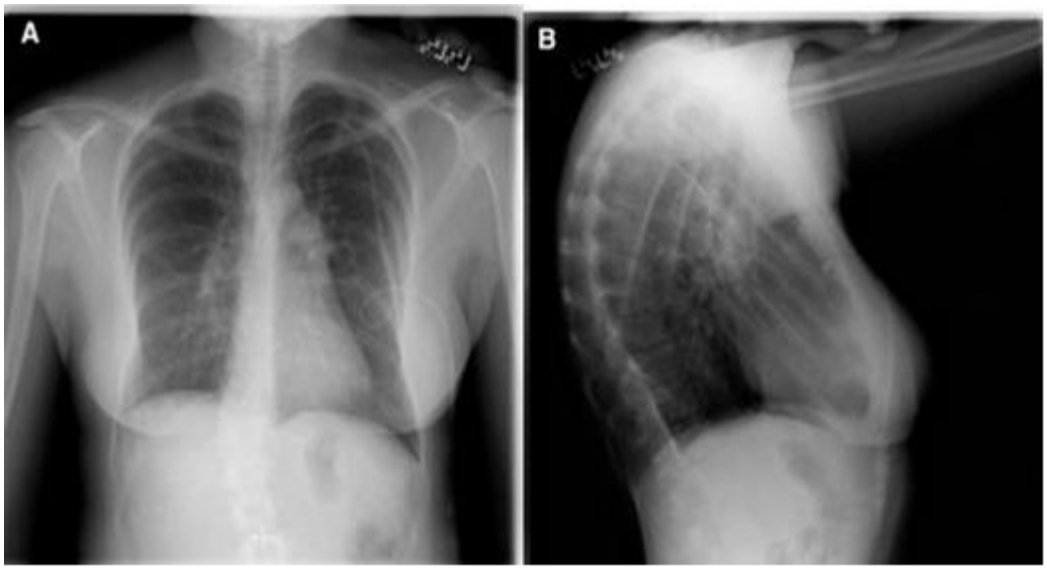

Figure 1-3 Chest x-ray of patient with PAH
A – posteroanterior, B – lateral view. Hypertrophy of right ventricle and pulmonary artery can be observed, caused by PAH (McLaughlin, McGoon 2006).

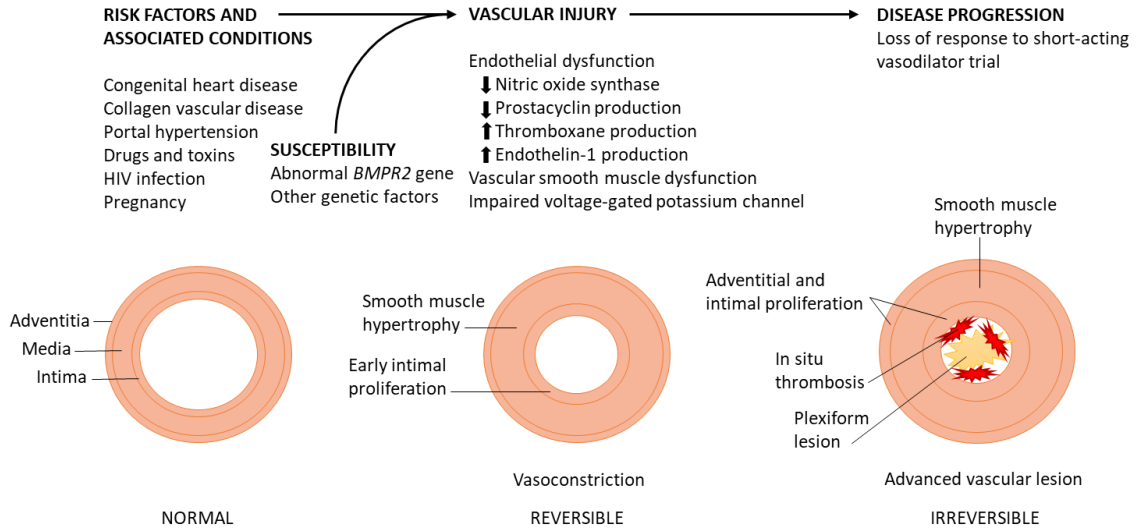

Figure 1-4 Pathogenesis of Pulmonary Arterial Hypertension
PAH occurs in susceptible patients as a consequence of an insult to the pulmonary vascular structure, resulting in an injury that initially progresses reversibly, and if not properly treated in an irreversible way, in order to produce characteristic pathological features such as smooth muscle cells hypertrophy, adventitial and intimal proliferation, *in situ* thrombosis, and plexiform lesions. [As also summarized in (Gaine 2000)].

Key: HIV, human immunodeficiency virus; *BMPR2*, bone morphogenetic protein receptor II gene

Despite the fact that in theory PAH can be present at any age, it is typically diagnosed in the fourth decade of life with an interesting gender bias towards female patients. Women are more prone to develop PAH than men with an estimated 1.7:1 ratio. Several reports of human and rodent data have proposed that altered metabolism of estrogen and abnormal estrogen levels along with differential signalling in PAH, may explain the gender predisposition of this disease (Pugh, Hemnes 2010). For adults, the mean representation age of the disease ranges from 36 to 50 years; however, individuals of any age may be affected (Soubrier, Chung et al. 2013).

If the disease is not clinically diagnosed at the time of appearance and treated accordingly, the outcome is usually fatal within 3 years (Shintani, Yagi et al. 2009). The most common vital screening tool is echocardiography, but unfortunately is not suitable for clinical diagnosis. An echocardiogram can reveal elevated right-ventricular systolic pressure (i.e. 31-46mmHg or <31mmHg with additional signs of right heart strain) but this is only indicative of PAH high probability. Thus, a clinical diagnosis of this disease depends on the right heart catheterization (RHC) method, which is the only way of accurately measuring the pulmonary artery pressures and officially diagnosing PAH. Also, pre- and post-capillary forms can be distinguished with the use of RHC. The severity is specified by means of the determinations of the feasibility, for example a cardiac arrest volume (Sommer, Hecker et al. 2016).

1.4.1 CLASSIFICATION OF PULMONARY ARTERIAL HYPERTENSION

The World Health Organization (WHO) has endorsed many international conferences and world symposiums in order to review and classify different forms of pulmonary hypertension (PH) under a clinical and pathobiological context. The 5th World Symposium on PH, which was held in Nice 2013 (Simonneau, Gatzoulis et al. 2013), revised previously established classification criteria to take into consideration the recent clinical and non-clinical published data of the various research groups globally (Table 1-1). The most common underlying causes include PAH from congenital heart disease (CHD), persistent PH of the newborn,

connective tissue disease, chronic lung diseases and hypoxemia, PH due to left-sided heart disease, and chronic thromboembolic pulmonary disease (George, Schieb et al. 2014). Demographic data from UK and France report a PH incident rate of 6.6 to 15.0 cases per million population per year, with PAH cases to reach a prevalence range of 1.1 to 2.4 cases per million population per year and a 5-year mortality of approximately 40%. PAH may be heritable (HPAH), Idiopathic (IPAH), associated with drugs, toxins, or other medical conditions such as previously mentioned connective tissue disease, human immunodeficiency virus infection (HIV), congenital heart disease and portal hypertension (Gaine 2000).

Table 1-1 Updated clinical classification of pulmonary hypertension, Nice 2013 (Simonneau, Gatzoulis et al. 2013).

* This thesis is concentrated on previous and current research summarized in the first group of the Nice 2013 PH clinical classification, and more specifically with 1.1 Idiopathic PAH, 1.2 Heritable PAH and 1.4.4 Congenital heart diseases.

1. Pulmonary arterial hypertension
1.1 Idiopathic PAH
1.2 Heritable PAH
1.2.1 BMPR2
1.2.2 ALK-1, ENG, SMAD9, CAV1, KCNK3
1.2.3 Unknown
1.3 Drug and toxin induced
1.4 Associated with:
1.4.1 Connective tissue disease
1.4.2 HIV infection
1.4.3 Portal hypertension
1.4.4 Congenital heart diseases
1.4.5 Schistosomiasis
1′ Pulmonary veno-occlusive disease and/or pulmonary capillary hemangiomatosis
1″. Persistent pulmonary hypertension of the newborn (PPHN)
2. Pulmonary hypertension due to left heart disease
2.1 Left ventricular systolic dysfunction
2.2 Left ventricular diastolic dysfunction
2.3 Valvular disease
2.4 Congenital/acquired left heart inflow/outflow tract obstruction and congenital cardiomyopathies
3. Pulmonary hypertension due to lung diseases and/or hypoxia
3.1 Chronic obstructive pulmonary disease
3.2 Interstitial lung disease
3.3 Other pulmonary diseases with mixed restrictive and obstructive pattern
3.4 Sleep-disordered breathing
3.5 Alveolar hypoventilation disorders
3.6 Chronic exposure to high altitude
3.7 Developmental lung diseases
4. Chronic thromboembolic pulmonary hypertension (CTEPH)
5. Pulmonary hypertension with unclear multifactorial mechanisms
5.1 Hematologic disorders: chronic hemolytic anemia, myeloproliferative disorders, splenectomy
5.2 Systemic disorders: sarcoidosis, pulmonary histiocytosis, lymphangioleiomyomatosis
5.3 Metabolic disorders: glycogen storage disease, Gaucher disease, thyroid disorders
5.4 Others: tumoral obstruction, fibrosing mediastinitis, chronic renal failure, segmental PH

Key: ALK-1 = activin receptor-like kinase 1 gene; APAH = associated pulmonary arterial hypertension; BMPR2 = bone morphogenetic protein receptor, type 2; CAV1 = caveolin-1; ENG = endoglin; HIV = human immunodeficiency virus; PAH = pulmonary arterial hypertension.

1.4.2 PATHOPHYSIOLOGY OF PAH

1.4.2.1 PULMONARY COMPENSATORY MECHANISM

In case of moderate hypoxia (20-60 mmHg PO2), the pulmonary circulation is affected via the mechanism of vasoconstriction, resulting in increase of pulmonary vascular resistance (PVR) in the cardio-vasculature (Aaronson, Robertson et al. 2006). This effect is termed as hypoxic pulmonary vasoconstriction (HPV) and it is observed exclusively in the pulmonary vasculature. During periods of hypoxia and resulting HPV, a vasodilation effect is also observed, primarily in systemic circulation (Ward, Aaronson 1999). Therefore, and in cases of HPV, there is a particular mechanism in which efficient ventilation-perfusion ratio is maintained by directing blood from the lungs to the systemic circulation (Mark Evans and Ward, 2009). However, this homeostatic mechanism is insufficient in sustained exposure to hypoxia and PVR increase lead to a rise in pulmonary artery pressure, causing vascular remodelling and sustained PH, even after hypoxia recedes to normoxic conditions (Ward, Aaronson 1999).

1.4.2.2 HISTOPATHOLOGY

Despite the numerous disease aetiologies, common characteristic pathophysiology and clinical manifestations are observed in each PH classification, through the use of histological examination. The proliferation of smooth muscle cells of tunica media and/or endothelial cells of tunica intima provide explanation for the occurred vascular remodelling. A certain homeostatic imbalance and dysregulation of vasodilators and vasoconstrictors lead to increased cell proliferation, intimal hyperplasia and medial thickening and adventitial proliferation (McLaughlin, McGoon 2006).

The histopathologic classification criteria that pulmonary arteries are subjected for evaluation are: a) muscularization of arterioles, b) concentric laminar intimal proliferation and fibrosis, eccentric intimal proliferation and fibrosis, plexiform and dilatation lesions, active and healed arteritis and fresh and recanalized thrombi

(Pietra, Edwards et al. 1989). It is of special interest a certain pathological PAH hallmark, which depicts a collection of disorganised and dysregulated endothelial cells as a form of plexiform lesion, and is highly associated with idiopathic PAH (IPAH) (Figure 1-5) (Jonigk, Golpon et al. 2011, Tuder, Stacher et al. 2013). There are several factors contributing in plexiform legion development, such as up-regulation of growth factors and smooth muscle cells and endothelial proliferation (Wideman, Hamal 2011, Yang, Long et al. 2011). However, the exact mechanism of this resulting up-regulation, as an initiation event of plexiform lesion formation, is not extensively researched (Machado 2012). Amongst the histological markers of PAH, plexiform lesions are indicative signs of disease progression, and could also be observed in other PH-associated diseases (Jonigk, Golpon et al. 2011). Since plexiform lesions are not specific to PAH, other biological markers could also be employed for observation in PAH-patients, such as hypertension and occlusion of the pulmonary arterial vessels. The later promotes vascular remodelling and hypertrophy, which in turn could be detected due to an elevated right-ventricle afterload, as a compensatory homeostatic mechanism to optimise the ventilation-perfusion ratio (Crosswhite, Sun 2014, Li, Qiu et al. 2014). The up to date most reliable identification of endothelial plexiform lesions is trichrome immunohistochemical assays, usually probing for factor VIII antigen present on endothelial cells.

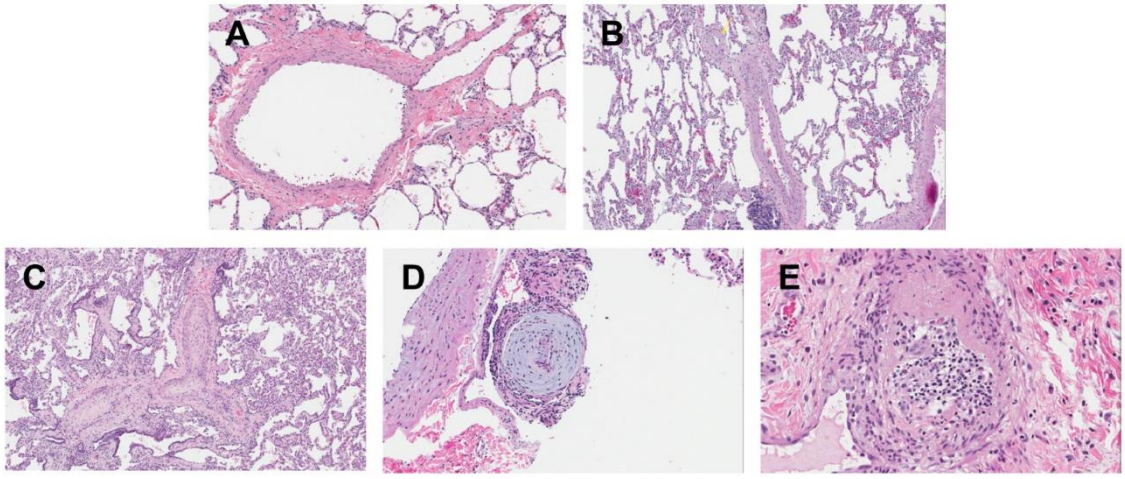

Figure 1-5 Histopathology of IPAH endothelial plexiform lesions
Control lungs with histologically normal (A) or remodeled PA with media thickening (B). IPAH lungs with both media and intima thickening (C), intima obliteration (D), and plexiform lesion with inflammation (E). Hematoxylin-eosin; A, B: 10x; C, D: 20x; E: 40x magnification. (Tuder, Stacher et al. 2013).

1.4.3 GENETICS OF PAH

Microsatellite linkage analysis in a significant number of autosomal dominant families with PAH by 2 distinct groups in 2000 (Deng, Morse et al. 2000, International PPH Consortium, Lane et al. 2000) (35 and 6 accordingly), highlighted that PAH has a genetic aetiology, which corresponds to mutations of a type II receptor of the transforming growth factor beta (TGF-β) superfamily, known as bone morphogenetic protein receptor II (BMPR-II) on chromosome 2q33. More specifically, over 70% of HPAH and approximately 25% IPAH cases harbour deleterious *BMPR2* mutations (Machado, Eickelberg et al. 2009). The majority of these mutations (70%) are frameshifts and nonsense mutations, that likely lead to elimination of *BMPR2* mRNA via nonsense-mediated mRNA decay (NMD), the remainder comprise missense mutations identified across all *BMPR2* regions (Machado, Eickelberg et al. 2009, Machado, Aldred et al. 2006) (Figure 1-6). NMD is a surveillance pathway that exists in all eukaryotes and its main functions is to reduce errors in gene expression by eliminating mRNA transcripts that contain premature stop codons (Baker, Parker 2004).

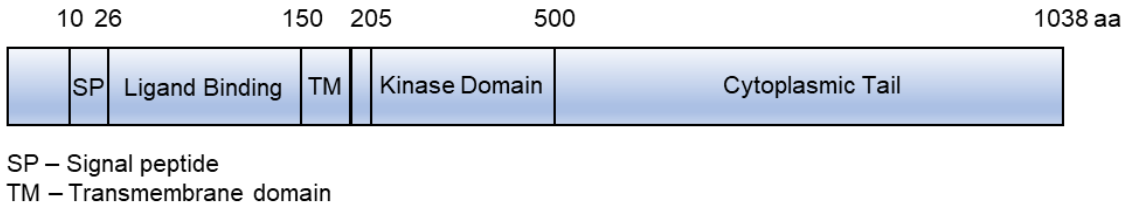

Figure 1-6 BMPR-II receptor structure illustrating the key functional domains

HPAH is inherited as an autosomal dominant trait with incomplete penetrance and an estimated life risk of 10-20%; while taking into account the recent Nice classification and the alteration of familial PAH term to hereditary, a distinctive 20% of patients that harbour identifiable *BMPR2* mutations and previously thought to be IPAH, pose hereditary risk to other family members (Machado, Southgate et al. 2015). It is rational to infer that in the majority of HPAH cases, and due to high prevalence of truncating mutations that would likely be subject to NMD, the inherited molecular mechanism of the disease is *BMPR2* haploinsufficiency (Machado, Pauciulo et al. 2001). Other mutations that much less commonly contribute to PAH phenotype are mutations in the TGF-β superfamily, Activin-like Kinase-Type I (ALK1) and Endoglin (ENG), which are associated with hereditary hemorrhagic telangiectasia (HHT) that may lead directly to the development of PAH. In addition, rare nonsense mutations of SMAD9 gene, the intracellular partner of the BMP signalling pathway, also highlight key role to the dysregulation of the canonical signalling cascade and further implication to the disease pathogenesis (Shintani, Yagi et al. 2009, Nasim, Ogo et al. 2011).

1.4.4 MOLECULAR PATHOLOGY OF PAH

Pulmonary artery smooth muscle cells (PASMC) from PAH-patients not only exhibit attenuated growth suppression by BMPs, but also irregular mitogenic response to transforming growth factor-β1 (TGF-β1) ligand (Davies, Holmes et al. 2012). Also, TGF-β ligands are regulating the endothelium (PAECs) via the BMP/TGF-β signalling pathways (Goumans, Valdimarsdottir et al. 2003).

The TGF-β superfamily of receptors is extensively characterised of associated ligands and distinctive signal transduction routes. Nevertheless, the largest group of TGF-β cytokines along with the bone morphogenetic proteins (BMPs) and their down-stream effects are not very well characterized (Machado, Eickelberg et al. 2009). The key TGF-β receptors are ALK1, endoglin-1 and BMPR-II; most importantly, all three are receptors for BMP ligands (Dyer, Pi et al. 2014). In general, the TGF-β superfamily receptors are highly conserved throughout nature, and several genetic mutations within this serine/threonine-specific protein kinase group are highly associated with the onset and pathogenesis of PAH (Machado, Eickelberg et al. 2009). The TGF-β signalling pathway is primarily involved in cell growth and differentiation along with tumour suppression, via inhibitory mechanisms that repress cellular proliferation and growth factor effects, induce apoptosis and autophagy, suppress immune response and inhibit progression of angiogenesis (Demagny, Araki et al. 2014).

1.4.4.1 BMP/TGF-β SIGNALLING PATHWAY

The BMP/TGF-β superfamily comprises over 30 members in humans and many orthologues are found in most primitive metazoan linage sequenced. BMP/TGF-β signalling plays key roles in the regulation of cell growth, differentiation and development in a wide and highly conserved range of biological systems. In general, the signalling cascade is initiated with ligand-induced oligomerization (heterotetrametric formation) of serine/threonine receptor kinases. Initially, ligand stimulation assembles two type-I and two type-II serine/threonine membrane receptors consisting of short cytoplasmic segments followed by the kinase domain and a carboxy-terminal tail, which in case of BMPR-II receptor is extended. The signal is propagated after phosphorylation of type-I components by type-II receptors. The complexity of ligand-receptor combinations and the differential stages of the BMP/TGF-β signalling pathway is demonstrated in Figure 1-7.

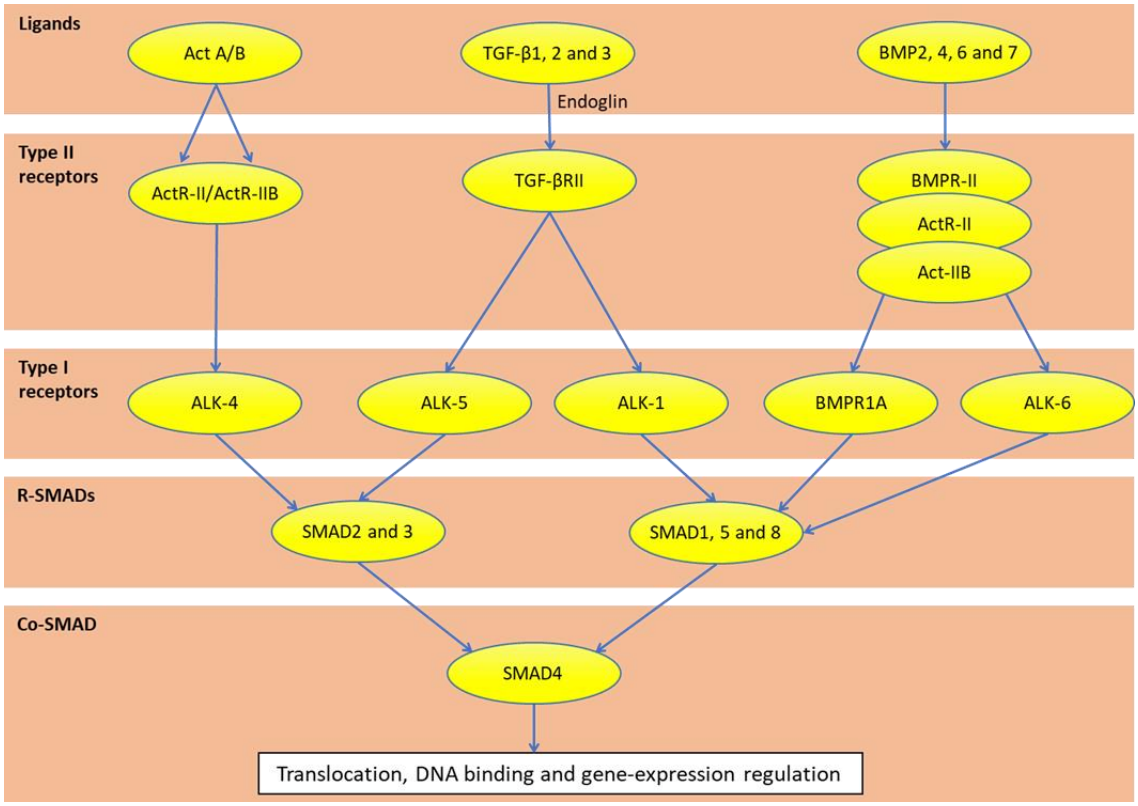

Figure 1-7 TGF-β signal transduction
TGF-β ligands bind to a range of type-II receptors to form complexes that interact with type-I receptors. Consequently, the receptors form heteroteramers, which phosphorylate and activate R-SMADs, that subsequently form complexes with the common SMAD4. Ultimately, the complexes translocate to the nucleus for direct or indirect regulation of gene transcription. Endoglin is a co-receptor for TGF-β1, 2 and 3.

Key: Act, activin; ActR, activin receptor; ALK, activin-like kinase; BMP, bone morphogenetic protein; BMPR, BMP receptor; TGF-βR, TGF-β receptor.

Subsequently, type-I receptors phosphorylate the cytoplasmic receptor regulated SMADs (R-SMAD). This sub-set of the SMAD family, orthologues of the Drosophila protein, mothers against decapentaplegic (MAD) and the Caenorhabditis elegans protein SMA (from gene sma for small body size), function as transcriptional regulators. Consequently, the carboxy-terminal phosphorylated SMAD dimers bind to the common-SMAD4 (co-SMAD4 – chaperone molecule) and this complex translocates to the nucleus, where it acts as transcription factor and regulator of gene expression. The N- and C- terminals of SMADs are highly conserved and termed as Mad homology (MH) 1 and MH2 domains, which are bridged by a linker region of variable amino acid sequences. The MH2 domain is highly conserved amongst all SMADs, in contrast to MH1,

which is conserved in R-SMADs and SMAD4, but not in other SMAD members as inhibitory SMADs (I-SMADs). The C-terminal end of R-SMADs is phosphorylated at the distinctive Ser-Ser-Val/Met-Ser sequence (SSXS motif), by the type-I receptors,. More specifically and in case of TGF-β signalling, the R-SMADs that transduce the signal are SMAD2 and SMAD3, whereas in BMP signalling are SMAD1, SMAD5 and SMAD accordingly. The regulation of the signalling cascade is orchestrated by I-SMADs 6 and 7, as part of a negative feedback loop.

Furthermore, the stability of the superfamily receptors and /or the SMADs are tightly regulated by SMURF E3 ubiquitin ligases and USP4/11/14 deubiquitinases. In addition, the BMP/TGF-β signalling pathway is modulated by MAPK signalling at a number of levels. Moreover, there are other SMAD-independent signalling cascades that affect BMP/TGF-β signalling, including ERK, SAPK/JNK and p38 MAPK pathways. Despite numerous reports of dysregulated MAPK signalling in PAH, the role of altered MAPK and Raf/ERK1/2 activation remains to be extensively investigated (Rudarakanchana, Flanagan et al. 2002, Welsh, Harnett et al. 2004, Lane, Blackwell et al. 2005, Gollob, Whilhelm et al. 2006, Wright, Ewart et al. 2015, Awad, Elinoff et al. 2016, Ge, Gram et al. 2016). Ultimately, the phosphorylated R-SMAD/SMAD4 complex enters the nucleus where it binds transcription promoters/cofactors to initiate DNA transcription. SMAD3 and 4 directly bind to SMAD-binding elements (SBEs), which include AGAC or GTCT sequences. SMAD2 indirectly binds DNA as it forms complexes with SMAD3 and 4. In contrast, SMAD1, 5 and 8 have a weak affinity for AGAC/GTCT sequences and instead they bind strongly to GCCGnCGC sequences of other target genes. The wide range of transcription factors that are activated from the BMP/TGF-β signalling consists of members of the basic helix-loop-helix (bHLH) and Fox proteins, activator-protein 1 (AP-1), and inhibitor of DNA-binding proteins (IDs), Runx family of transcription factors, targets of other signalling cascades as Wnt signalling and epithelial-mesenchymal transition mechanisms (i.e. corepressor SIP1) and several coactivators like CBP/p300 which enhance Runx-dependent transcription.

A characteristic overview of the SMAD-dependant (canonical) and SMAD-independent (non-canonical) BMP/TGF-β signalling pathways is summarized in Figure 1-8.

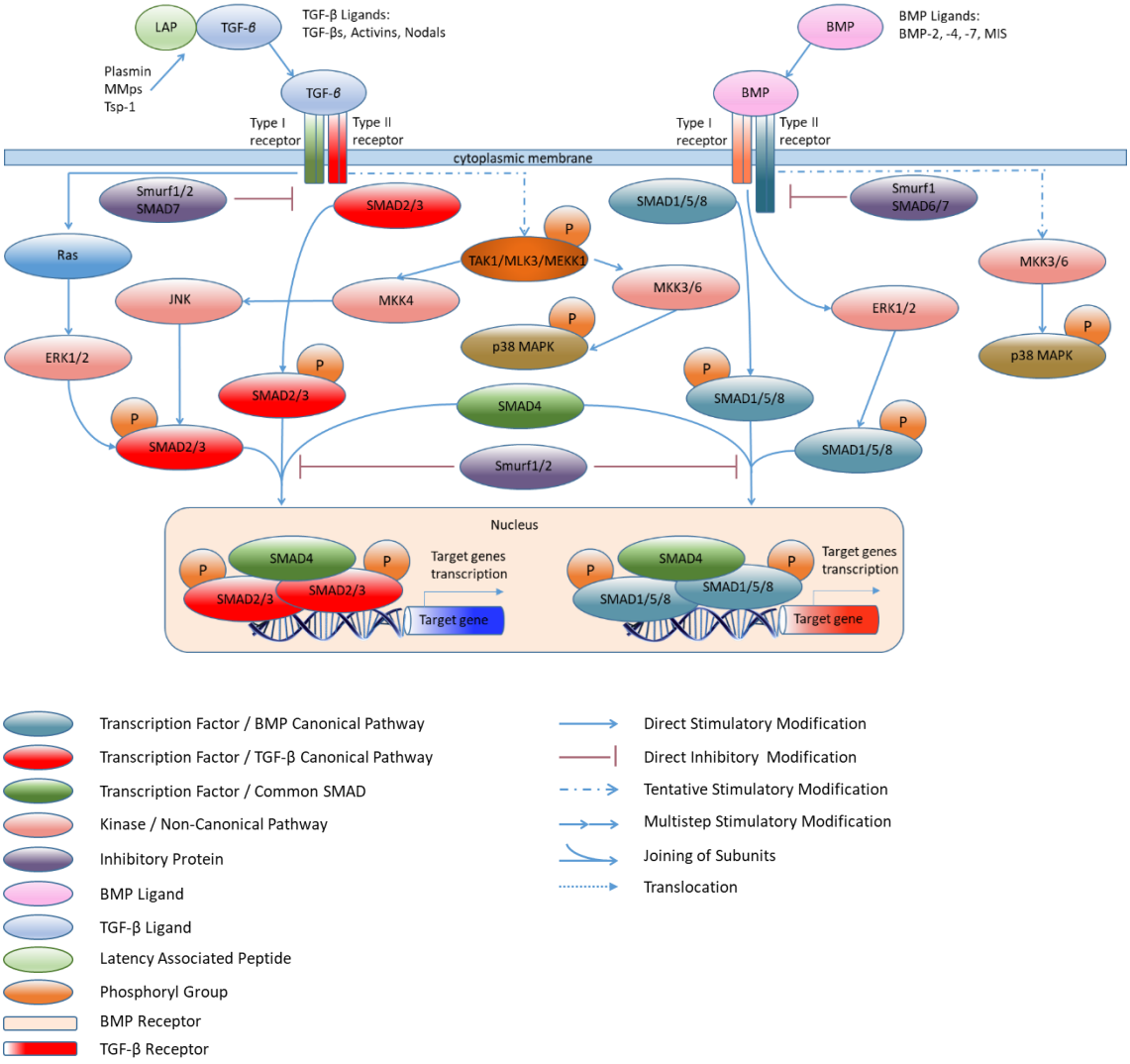

Figure 1-8 BMP/TGF-β Canonical and non-Canonical Signalling Pathways Transforming growth factor-β (TGF-β) superfamily signalling plays a critical role in the regulation of cell growth, differentiation, and development in a wide range of biological systems. In general, canonical signalling is initiated with ligand-induced oligomerization of serine/threonine receptor kinases and phosphorylation of the cytoplasmic signalling molecules SMAD2 and SMAD3 for the TGF-β/activin pathway, or SMAD1/5/9 for the bone morphogenetic protein (BMP) pathway. Carboxy-terminal phosphorylation of SMADs by activated receptors results in their partnering with the common signalling transducer Smad4, and translocation to the nucleus. Activated SMADs regulate diverse biological effects by partnering with transcription factors resulting in cell-state specific modulation of transcription. Inhibitory SMADs, i.e. SMAD6 and SMAD7 antagonize activation of R-SMADs. The expression of inhibitory SMADs (I-SMADs) 6 and 7 is induced by both activin/TGF-β and BMP signalling as part of a negative feedback loop. The stability of TGF-β family receptors and/or Smads are regulated by Smurf E3 ubiquitin ligases and USP4/11/15 deubiquitinases (not-shown). In the context of non-

canonical signalling, TGF-β/activin and BMP pathways are modulated by MAPK signalling at a number of levels. Moreover, in certain contexts, TGF-β signalling can also affect SMAD-independent pathways, including Erk, SAPK/JNK, and p38 MAPK pathways.

1.4.4.2 SIGNAL TRANSDUCTION ROUTED THROUGH BMPR-II

The *BMPR2* gene is 13 exons in length, encoding an extracellular ligand binding domain, a transmembrane domain, a highly conserved catalytic kinase domain and an extended cytoplasmic tail (Machado, Aldred et al. 2006) (Figure 1-5). The translated protein, BMPR-II, functions as a serine-threonine receptor kinase which binds bone morphogenetic proteins (BMPs), members of the TGF-β superfamily of ligands that are involved in paracrine signalling. BMPR-II has a molecular weight of 115 kiloDaltons (kDa) and forms heteroterameric complexes with the type I receptors (ALK3, ALK6, and ACVR1) (50-55 kDa) in order to transduce the BMP signal. In general, type II receptors are capable of binding various BMP ligands (BMP7, BMP4, BMP2) in the absence of type I receptors; when the binding occurs, type I receptors are recruited and phosphorylated. In turn, the type I receptors phosphorylate the receptor regulated R-SMAD1,5 or 8. Consequently, the SMAD dimers bind to the common SMAD4 and this complex translocates to the nucleus, where it acts as transcription factor and regulator of gene expression (Figure 1-9).

This canonical SMAD signalling cascade is involved in many cellular processes in both embryo development and the adult organism, including cell growth, cell differentiation, osteogenesis, apoptosis, cellular homeostasis and other cellular functions relative to anti-proliferating effects (Miyazono, Maeda et al. 2005). In contrast, there are also non-canonical BMP cascades that result in increased cell proliferation, through activation of the Mitogen-activated protein kinase (MAPK) cascades, via BMP/TGF-β receptor activated X-linked inhibitor of apoptosis protein XIAP protein, which in turn activates the intermediary signalling molecule Mitogen-activated protein kinase kinase kinase 7 (TAK1), which directly activates the MKK/ERK signalling nexus (Figure 4-10) (Rudarakanchana, Flanagan et al. 2002, Nishihara, Watabe et al. 2002, Kaur, Wang et al. 2005, Augeri, Langenfeld et al. 2016). Previous protein-protein interaction studies have revealed that there

are several other interacting partners of BMPR-II, including LIMK1 and Tctex-1 (Foletta, Lim et al. 2003, Machado, Rudarakanchana et al. 2003), that are involved in PAH pathogenesis, through activation of the mitogenic p38MAPK and subsequent activation of AP-1 transcription factor, which controls a number of cellular processes including differentiation, inflammation, enhanced cell proliferation, cell survival and apoptosis (Ameyar, Wisniewska et al. 2003).

BMPR-II target genes of particular importance are the ID proteins, which almost certainly are activated by BMP stimulation in diverse cell types (Figure 1-9) (Miyazono, Maeda et al. 2005). They have two main roles as they function as negative regulators of cell differentiation and positive regulators of cell proliferation (Yang, Li et al. 2013). The group consists of 4 members (ID1, 2, 3 and 4) that exhibit similar biological activities, and they are part of the family of HLH transcription factors. They basically interact with other tissue-specific bHLH transcription factors activating genes (like MyoD/myogenin in muscle and NuroD/Mash1/neurogenin in neurons) that contain enhancer E-box sequences (CANNTG, with a palindromic canonical sequence of CACGTG) (Lopez-Rovira, Chalaux et al. 2002). In the context of vascular remodelling, they are important regulators of vascular cell function, as they are widely involved in vasculogenesis and angiogenesis and cardiovascular diseases as PH and atherosclerosis (Yang, Li et al. 2014). For example, ID proteins stimulate the migration and proliferation of endothelial cells and promote survival and vessel regeneration after BMP/TGF-β and VEGF stimulation, while they suppress the de-differentiation and proliferation of smooth muscle cells and limit tunica-media thickness as they are involved in the cell proliferative responses to thrombin, angiotensin II and oxidized low-density lipoprotein (ox-LDL) (Yang, Li et al. 2014). Of interest, ID proteins are also down or up-regulated by BMP/TGF-β-independent signalling cascades as ERK1/2 and intracellular signalling mediators like XIAP and TAK1 respectively (Figure 1-8) (Augeri, Langenfeld et al. 2016, Nasim, Ogo et al. 2012).

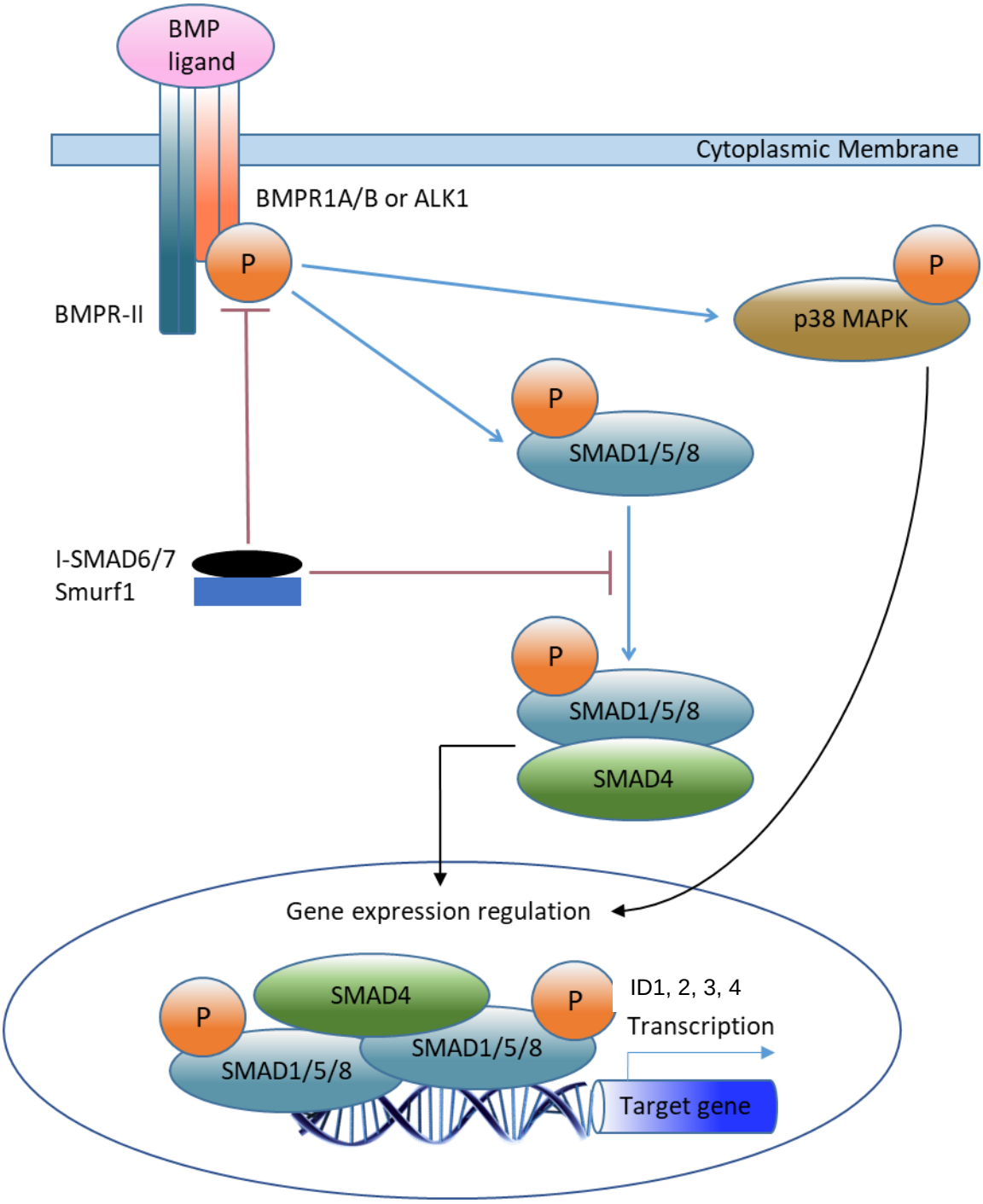

Figure 1-9 BMP signalling pathway
Upon BMP4/7/9/10 ligand binding, the BMPR-II receptor activates and phosphorylates through its kinase domain, type-I receptors such as BMPR1A/B. In turn, type-I receptors phosphorylate R-Smads 1/5/8, or independently activate the p38MAPK pathway. Smad4 acts as a chaperone molecule and makes a trimer with receptor-activated SMADs, which translocate to the nucleus and form complexes with other transcription co-factors, regulating targeted gene expression. BMPR-II main target genes are ID proteins, which function as negative regulators of cell differentiation and positive regulators of cell proliferation

1.4.4.3 FUNCTIONAL CONSEQUENCES OF BMPR-II MUTATION

Mutations predicting premature truncation is likely to result in NMD of BMPR-II transcript. The majority of amino-acid substitutions outside the cytoplasmic tail lead to a diminution of SMAD activation as indicated by in vitro luciferase assays (Rudarakanchana, Flanagan et al. 2002, Nishihara, Watabe et al. 2002). A common outcome of mutation is activation of the mitogen p38MAPK. Of interest, immunohistochemical analysis of lung sections with PAH denote further loss of BMPR-II, than is expected by haploinsufficiency by as yet unknown mechanisms (Atkinson, Stewart et al. 2002).

The BMPR-II tail has numerous poorly understood functions, including regulation of p38 MAPK and p42/44 MAPK and interaction with c-Src, LIMK, and Tctex-1 (West, Harral et al. 2008).

In order to identify the extent of key pathways in regulation of the pulmonary circulation, Machado et al. conducted in novel experimentation a yeast-two hybrid system, using the catalytic kinase domain of BMPR-II as bait in a lung cDNA library, which was assembled in order to identify potential interacting partners of the wild-type receptor (unpublished data - refer to Chapter 3.1). The preliminary results identified Jun activation domain-binding protein 1 (JAB1) as an interacting partner of BMPR-II.

1.5 CHARACTERIZATION OF THE NOVEL BMPR-II INTERACTING PROTEIN JAB1

JAB1 is a subunit of the COP9 signalosome (CSN), which is a protein complex, highly conserved across species, with crucial functions in the ubiquitin-proteasome pathway (Wei, Serino et al. 2008). The last two decades of research have revealed that the CSN consists of 8 distinct subunits, each named CSN1-CSN8, which appears to have co-evolved with the 26S proteasomal lid, it displays proteasomal activity reliant on deneddylation of the cullin- RING ligases (CRL) of ubiquitin E3 complexes. Neddylation is the process of the ubiquitin-like protein NEDD8 conjugation to its target proteins. These eight subunits harbour different

domains and as a result illicit different functions within whole living organisms, animal models or cells (*in vivo*). The two key domains within the CSN are the proteasome-COP9 signalosome-initiation factor 3 (PCI) and MPR1-PAD1-N-terminal (MPN) domain (Pan, Wang et al. 2014). Interestingly, these two domains have been identified as components of the 'lid' sub-complex of the 26S proteasome and the eukaryotic translation initiation complex (eIF3); meaning these structural and functional homologies may predict that the PCI and MPN domain have additional roles (Shackleford, Claret 2010).

CSN5/JAB1 contains the catalytic centre of the CSN isopeptidase activity; Interestingly, can also stably exist and act independently of the complex, promoting a diverse range of protein-protein interactions with its targets. Of note, overexpression or down-regulation of JAB1 protein levels have little effect in its presence in the CSN holo-complex, an observation that led to conclusion that JAB1 is an active mediator of crucial biological functions, both as part of the CSN-complex or independently (Yoshida, Yoneda-Kato et al. 2010).

It is of note that JAB1 is the CSN subunit with the vastest number of protein interactions with significant cellular regulators and the resulting down-steam effects are largely dependent on the target (Chun, Lee et al. 2013). In general, JAB1 stabilizes or de-stabilizes the target protein. For example, key regulatory proteins like C-JUN, AP-1, HIF1-α and MDM2 are stabilised by JAB1, whereas p27Kip, p53, 9-1-1 (Rad9-Rad1-Hus1) DNA repair complex, Cyclin E and oestrogen receptor alpha (ERalpha) are destabilised (Shackleford, Claret 2010). Table E-1 in Appendix E summarizes these interactions along with primary research data that contributed to JAB1 role in intracellular distribution, as a transcriptional activator, a member of the CSN holo-complex as well as other reported JAB1 interactions. In case of protein de-stabilization, JAB1 and through a CRM1-dependent pathway is nuclear exporting its target to the cytoplasm and more specifically in the peri-nuclear region for degradation (Wei, Serino et al. 2008). Therefore, a way to prevent JAB1-mediated degradation is prevention of the nuclear export. However, the specific mechanism in which JAB1 drives nuclear export of its binding partners is not yet known.

JAB1 is closely associated with both apoptotic and cellular proliferative mechanisms along with implication to efficient DNA repair, genome integrity and cell survival. JAB1 knockdown animal models displayed a disrupted development at embryonic day 6.0 (no longer viable at day 8.5), than knockdowns of other CSN subunits like CSN2, 3 and 8, because of increased expression of several JAB1 targets, including p27, p53, c-myc and cyclin E (Shackleford, Claret 2010). Furthermore, apoptosis in JAB1-deleted thymocytes is correlated with increased expression of proapoptotic protein BCL2-associated X protein (BAX) and a decrease in expression of the anti-apoptotic protein family B-cell CLL lymphoma 2 (Bcl-2), most notably Bcl-xL (Wei, Serino et al. 2008). In case of cell cycle and in particular its tight regulation by cyclin-dependent kinases (CDK) inhibitors, JAB1 notably interacts with $p27^{Kip}$, a crucially important CDK inhibitor (Shackleford, Claret 2010). Increased JAB1 expression correlates with reduced $p27^{Kip}$ levels, driving cell proliferation (Wei, Serino et al. 2008).

Recent studies through pathological investigation of JAB1 expression in several types of human cancer, suggest that JAB1 is up-regulated in breast, colon, pancreatic and lung carcinomas (Fukumoto et al. 2006, Hsu et al. 2008). Of note, JAB1 antagonises TGF-β signalling by inducing targeting the chaperone SMAD4 and SMAD5 and 7 for proteolytic degradation (Wan, Cao et al. 2002, Haag, Aigner 2006, Kim, Lee et al. 2004) and also controls multiple events in the mammalian cell cycle, mainly by inhibition of tumour suppressor genes as p53 and $p27^{Kip1}$ (Tomoda, Kubota et al. 2002). In regard to BMPR-II, there is no published research that indicates a potential interaction of JAB1 with the BMP type-II receptor, a fact that makes the initial experimental yeast-two hybrid system results unique, and further drives this particular investigation of verifying the interaction and its signalling consequences.

$P27^{Kip1}$ interactions and metalloproteinase activity of JAB1 have been associated with specific domains of the mature protein (Figure 1-10). The direct binding of JAB1 with $P27^{Kip1}$ is facilitated by the p27-binding domain (PBD) of JAB1, which is closely located to the nuclear export signal (NES) domain of the protein. NES domain is responsible for the CRM1-dependent shuttling of $P27^{Kip1}$ between the nucleus and the cytoplasm. Also, JAB1 contains a Mpr1-Pad1-N (MPN) domain with a metalloenzyme (JAMM) motif. The JAMM motif is accountable for the

deneddylation activity of the JAB1/CSN5 subunit within the context of the CSN holo-complex and further loss of any CSN subunit will result into reduced JAMM activity (Wei, Serino et al. 2008). In addition, it has been postulated that the MPN domain serves as a protein-protein interaction platform, and the adjacent to the N- terminal JNK binding domain (JBD) is being reported to have a centromeric binding activity on the CENP-T/CENP-W complex, regulating its degradation (Chun, Lee et al. 2013). Further studies are required to fully elucidate the functions of the above mentioned JAB1 domains, regarding their roles within or outside the JAB1/CSN5/COP9 complex.

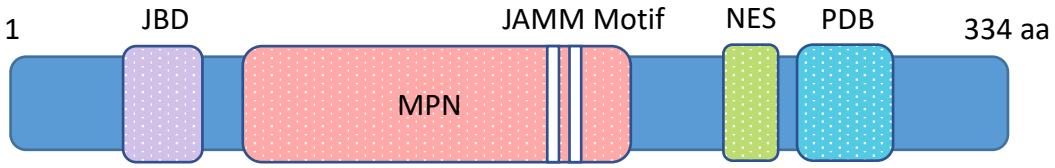

Figure 1-10 Structure of the JAB1 protein
Schematic of JAB1 protein highlighting all the critical functional domains, such as a JAMM motif-containing MPN domain and an NES domain close to the PBD domain at the C-terminal end.

Key: JBD, JNK binding domain; MPN, Mpr1-Pad1-N domain; JAMM, JAB1/MPN/Mov34 metalloenzyme motif; NES, nuclear export signal; PDB, p27-binding domain

1.5.1 JAB1 AND THE UBIQUITINATION PATHWAY

The ubiquitin pathway is a mechanism of post-translational modification, that affects proteins in varying ways, most importantly by degradation through the ubiquitin-proteasome pathway. It is mediated via ubiquitin, an 8.5 kDa regulatory protein which is found in most tissues of eukaryotic organisms, that apart degradation of the tagged target may also contribute to cellular relocation or prevent protein-protein interactions (Glickman, Ciechanover 2002, Chao 2015).

The ubiquitination process requires three types of enzymes: ubiquitin-activating enzymes (E1), ubiquitin-conjugating enzymes (E2) and ubiquitin ligases (E3). These three types of enzymes form a three-stages of a reaction cascade, a) an ATP-dependent activation of ubiquitin by E1 enzymes, b) conjugation of ubiquitin from E1 to the cysteine active site of E2 via a trans(thio)esterification reaction, and c) ligation of ubiquitin to the target protein, through an isopeptide bond

between a lysine residue of the protein and the C-terminal glycine of ubiquitin. For the last stage, numerous classes of E3 enzymes act as an enzymatic scaffold between E2 enzymes, ubiquitin and the E3-recognised substrate protein. The largest class of ubiquitin E3 ligases is represented by cullin-RING ligases (CRL) that are widely involved in the formation of multi-subunit E3sm like the anaphase-promoting complex (APC) and the Skp1-Cullin-F-box protein complex (SCF), which main role is to recognise and ubiquitinate specific target proteins for degradation via the proteasome. However, a large number of ubiquitin-like proteins (UBL) exist that clearly modify target proteins in pathways akin, but distinct from ubiquitination (Welchman, Gordon et al. 2005). The most notable UBL up to date is neuronalprecursor-cell-expressed developmentally down-regulated protein 8 (NEDD8). The conjugation of NEDD8 to the SCF scaffold or its removal are termed neddylation and deneddylation respectively, and represent a distinct mechanism of CRL-SCF regulation (den Besten, Verma et al. 2012).

The COP9-CSN proteasome mediates the dennedylation process by cleavage of the NEDD8 moiety by the metalloisopeptidase activity of the JAMM motif, apparent in the JAB1/CSN5 subunit. However, the dennedylation activity is a property of the CSN holo-complex and not the JAB1/CSN5 itself (Cope, Suh et al. 2002). Instead, JAB1 protein it is widely reported that is tagging other processes for ubiquitination through the proteasomal pathway. Up to date, verified JAB1 targets for ubiquitination are p27Kip, Lutropin/choriogonadotropin receptor (LHR), p53, estrogen receptor α (ERα), West Nile virus capsid, Cyclin E, Rad9-Rad1-Hus complex, RUNX-3, DNA topoisomerase II alpha, Endothelin type A and B receptors (ET(A) and ET(B)) and SMAD4, 5 and 7. Of interest, ET(A) and (B) overexpression is associated with chronic heart failure and in infiltrating cells of atherosclerotic lesions, whereas SMAD4, 5 and the I-SMAD7 are positive and negative regulators respectively of the previously described BMP/TGF-β signalling (Yoshida, Yoneda-Kato et al. 2010). Therefore, since novel data (extensively described in Chapter 3) reveal JAB1 and BMPR-II interaction, it is only rational to hypothesise that JAB1 binds BMPR-II as a target for degradation via the 26S proteasome pathway. As previously described, PAH has been associated with *BMPR2* mutations; however, this is a potential for wild-

type BMPR-II to be down-regulated by specific intracellular JAB1-BMPR-II interactions. Ultimately, researching this potential BMPR-II down-regulation, and other down-stream effects of such interaction, may help to elucidate the portions of HPAH and IPAH cases, where *BMPR2* mutations are absent, and/or further decrease of the receptor's expression that is observed in clinical immunohistochemical samples which cannot be explained by *BMPR2* loss of function mutations and haploinsufficiency (Machado, Pauciulo et al. 2001, Pietra, Edwards et al. 1989, Atkinson, Stewart et al. 2002, Rajkumar, Konishi et al. 2010).

1.6 ASSOCIATED FORMS OF PAH

As determined in the Evian-Venice and later in Nice PH classification (Simonneau, Gatzoulis et al. 2013, van Albada, Berger 2008) it is of critical importance to state that PAH can be clinically associated in patients suffering from vascular diseases such as hereditary hemorrhagic telangiectasia (HHT) (Harrison, Flanagan et al. 2003) and Adams-Oliver syndrome (AOS) (Patel, Taylor et al. 2004, Piazza, Blackston et al. 2004, Snape, Ruddy et al. 2009). HHT is clinically characterized by epistaxis, mucocutaneous telengiectases and visceral arteriovenous malformations (AVMs), particularly in the brain (CAVMs), lungs (PAVMs), liver (HAVMs), and gastrointestinal tract (GI) (Sabba, Pasculli et al. 2007). Of interest, the predominant causes of HHT, demonstrated at both the molecular and functional level, are diverse heterozygous mutations in endoglin (ENG) and activin receptor-like kinase 1 (ALK1), encoding type III and type I receptor members of the TGF-β superfamily, both are known to form heterotetramers with BMPR-II (Harrison, Flanagan et al. 2003). By contrast, AOS is a developmental disorder, predominantly characterised by the combination of aplasia cutis congenita (ACC) and terminal transverse limb defects (TTLD). However, a number of neurological and cardiovascular features, including pulmonary hypertension, are also seen in conjunction with the limb and scalp defects, suggesting that this condition represents an aggregation of clinical findings resulting from a vasculopathy during embryogenesis (Swartz, Sanatani et al. 1999). The recent identification of pathogenic mutations in the NOTCH1

receptor add significant weight to this hypothesis and support a genotype/phenotype correlation between Notch pathway mutations and AOS-related cardiovascular disease (Stittrich, Lehman et al. 2014).

1.6.1 ADAMS-OLIVER SYNDROME AND PAH

Adams-Oliver syndrome (AOS) is a rare congenital disorder with highly variable prevalence (Martinez-Frias, Arroyo Carrera et al. 1996), and an estimated incidence of 1 in 225,000 live births. Its primary features are a specific abnormality in skin development (aplasia cutis congenita, ACC) and several malformations of the limbs and digits (terminal transverse limb defects, TTLD). ACC, a condition characterized by localized areas of missing skin ordinarily happening on the highest point of the head, is the second most common condition, affecting 75% of people that are suffering from AOS; abnormalities involving abnormal development of the hands and feet (syndactyly, brachydactyly or oligodactyly) are the major feature in AOS, manifesting in 86% of cases (Figure 1-11). In approximately 20% of AOS cases, AOS patients can develop cardiovascular conditions like cutis marmorata telangiectatica congenita, hepatoportal sclerosis, arterio-venous malformations and PAH (Patel, Taylor et al. 2004, Snape, Ruddy et al. 2009). Moreover, congenital heart defects (CHDs) affect approximately 13-20% of cases with ACC and TTLD (Digilio, Marino et al. 2008). These include Tetralogy of Fallot, aortic coarctation and valvular defects. AOS is also associated with neurological problems, such as developmental delay, structural abnormalities of the brain and learning disabilities of cognitive deficit nature.

Early clinical investigations (Zapata, Sletten et al. 1995), report that 13.4% cases of AOS have been associated with congenital heart defects and Swartz et al., 1999 identified a case of a young girl diagnosed with AOS and PH associated with double outlet right ventricle and portal hypertension. They suggested that the development of PAH in patients suffering from AOS may have a shared genetic aetiology, especially in cases where no thromboembolic episodes in large vessels are recorded, and generalized abnormalities in small vessels are likely to

be causing a disruption of blood flow. A more recent clinical review (Snape, Ruddy et al. 2009) reports several identified cases of AOS associated with pulmonary vascular anomalies including PAH, implicating a common aetiology to pulmonary vascular disease and AOS.

A) Aplasia cutis congenita (ACC):

B) Terminal transverse limb defects (TTLD):

Figure 1-11 The primary features of AOS
A) aplasia cutis congenita (ACC) and B) terminal transverse limb defects (TTLD). (Images reproduced courtesy of Dr L. Southgate, St George, UoL)

1.7 GENETICS OF ADAMS-OLIVER SYNDROME

AOS may be inherited as an autosomal dominant or autosomal recessive trait, as well as occurring in isolated cases. Mutations in four genes so far have been recognised as a principal genetic aetiology in the appearance of AOS phenotypes in all forms of inheritance. *ARHGAP31*, *DOCK6*, *EOGT* and/or *RBPJ* genes play

significant roles during embryonic development and functional changes in their transcripts and expression underlie different types of AOS (Table 1-2) (Shaheen, Faqeih et al. 2011, Southgate, Machado et al. 2011, Hassed, Wiley et al. 2012, Shaheen, Aglan et al. 2013, Cohen, Silberstein et al. 2014).

Table 1-2: AOS candidate genes

Locus	AOS1	AOS3	AOS2	AOS4
Inheritance	Autosomal dominant	Autosomal dominant	Autosomal recessive	Autosomal recessive
Gene	*ARHGAP31*	*RBPJ*	*DOCK6*	*EOGT*
Description	Rho GTPase-activating protein 31	Recombination signal binding protein for immuno-globulin kappa J region	Dedicator of cytokinesis 6	EGF domain-specific O-linked N-acetylglucosamine transferase
Chromosome	3q13.33	4p15.2	19p13.2	3p14.1
Gene span	126.34 Kb	111.95 Kb	63.16 Kb	38.41 Kb
# of exons	12	12	48	15
CDS length	4,335 bp	1,503 bp	6,144 bp	1,332 bp
Protein length	1,444 aa	500 aa	2,047 aa	443 aa
Mutations identified	p.Gln683X p.Lys1087SerfsX4	p.Glu63Gly p.Lys169Glu	p.Thr455SerfsX24 p.Asp416X p.Arg841SerfsX6 p.Thr1370MetfsX19	p.Trp207Ser *p.Gly359AspfsX28 p.Arg377Gln [*recurrent mutation: n=9]

References	Southgate *et al.*, 2011	Hassed *et al.*, 2012	Shaheen *et al.*, 2011 Shaheen *et al.*, 2013	Shaheen *et al.*, 2013 Cohen *et al.*, 2014

Heterozygous mutations in the *ARHGAP31* (*AOS1*) or *RBPJ* (*AOS3*) genes cause an autosomal dominant pattern of inheritance. Conversely, mutations in both copies of *DOCK6* (*AOS2*) or *EOGT* (*AOS4*) lead to AOS development in an autosomal recessive manner. The ARHGAP31 and DOCK6 proteins are equally involved in the regulation of hydrolyse enzymes called GTPases (i.e. Cdc42 and RAC1), which cycle between an inactive form bound to GDP and an active form bound to GTP; this regulatory circle is critical for several aspects of embryonic development. On the other hand, both RBPJ and EOGT proteins are associated with the NOTCH signalling pathway. More specifically, RBPJ is an internal part of the signalling pathway, acting downstream as the major transcription factor of NOTCH target genes (e.g. *HEY1, HES1*). The role of EOGT is less clear but it is believed to act by transferring a molecule called N-acetylglucosamine to the NOTCH extracellular domain. In 2014, a novel report by Stittrich et al., identified mutations of the *NOTCH1* gene in a proportion of a AOS cohort, only to be rapidly followed by Southgate et al. 2015, in order to provide solid evidence of haploinsufficiency of NOTCH1 receptor as a cause of AOS with variable cardiac abnormalities (Southgate, Sukalo et al. 2015).

1.7.1 OVERVIEW OF THE NOTCH1 SIGNALLING PATHWAY

1.7.1.1 DOMAIN ARCHITECTURE OF NOTCH1 RECEPTOR

The NOTCH1 receptor is a single-pass transmembrane protein of 2555 amino acids length in human pre-protein isotype (Figure 1-12A), which may be subjected to further cleavage and modification in the trans-Golgi to form non-covalent heterodimers on the cell surface. The extracellular domain (ECD) of the receptor varies in length from species to species; for example, mammalian ECDs spanning a much larger length than of Caenorhabditis elegans counterparts. Both

Drosophila and human NOTCH1 contain a distinct 36 EGF-like domains at the N- terminal part, a subset of which contain calcium binding sites (cbEGF). Adjacent to the EGF-like repeats, there are 3 Lin-12-Notch (LNR) repeats, and hydrophobic region which mediates heterodimerization of the receptor (HD). Together, LNR and HD regions form the negative regulatory region (NRR), next to the cell membrane. There are 3 main cleavage sites for NOTCH1 proteins termed S1, S2 and S3. S1 is target for proteolysis of the receptor and along with the S2, they are lying in the NRR area, which is responsible for protecting the cleavage sites from post-translational modifications. The final S3 cleavage site lies within the transmembrane segment to liberate Notch intracellular domain (NICD). NICD consists of a RAM domain (RBPjk associated molecule), followed by seven ankyrin repeats (ANK), a transcription activation domain (TAD) and a C- terminal OPA/proline/glutamic acid/serine/threonine-rich (PEST) domain which is involved in NICD degradation by proteolysis.

1.7.1.2 NOTCH1 CANONICAL AND NON-CANONICAL SIGNALLING PATHWAYS

Canonical NOTCH1 signalling is initiated on the binding of the receptor to Delta/Serrate/LAG-2 (DSL) ligands, which are predominantly expressed on opposing cell-surfaces. Upon DSL-NOTCH1 interaction, a series of proteolytic cleavages take place in the extracellular NOCH1 compartment at S2 site by ADAM metalloproteases, and within the transmembrane counterpart at S3 site by γ-secretase respectively. Finally, the cleaved NICD domain translocates to the nucleus and interact with the RBPJκ/CSL transcription repressor, which in turn is being converted to a transcriptional activator. A simplified schematic of the canonical pathway is illustrated in Figure 1-12B. This active transcription complex induces the expression of bHLH family of genes such as Hairy and enhancer of split (Hes) family genes (*HES*1, 3, 5 and 7), and Hes-related with YRPF motif (Hey) family genes (*HEY*1, 2 and *HEYL*) (Zanotti, Canalis 2016).

Hey and *Hes* genes are the main transducers of NOTCH1 signalling in mammals, during vast diverse developmental stages, like somitogenesis and neurogenesis, coordinated spatiotemporal patterning of the mesoderm, and embryonic heart

and vascular development (Fischer, Schumacher et al. 2004). Of note, *HEY1* is well known to have a discrete role in cardiovascular development with HEY1/HEY2 double-knockout mice exhibiting defects of vasculogenesis and remodelling particularly in the head region, along with *HES1* at a lesser extend (Fisher, Schumacher et al. 2004, Southgate, Sukalo et al. 2015).

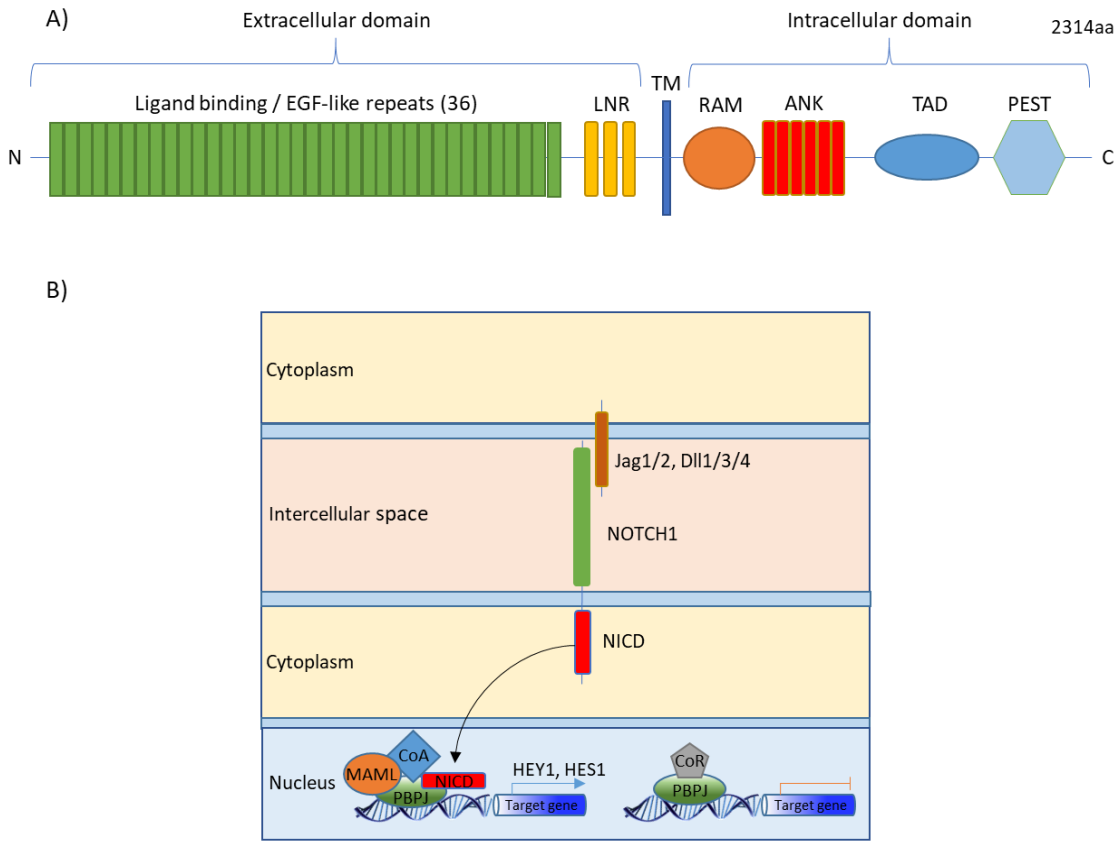

Figure 1-12 The NOTCH1 protein and the canonical NOTCH1 signalling pathway
A) The human NOTCH1 protein structure illustrating all the critical functional domains. B) Simplified schematic of the canonical NOTCH1 signalling cascade. EGF-repeat domain is glycosylated by EOGT in mammalian cells. The signal transduction is initiated by 1 of 5 ligands (Jag1/2, Dll1/3/4) via direct contact of adjacent cells. Following ligand activation, the intracellular domain NICD is initially cleaved and subsequently translocates to the nucleus to form an active transcriptional complex with MAML, RBPJ, and CoA. When Notch signalling is inactive, RBPJ complexes with CoR to repress the transcription of down-stream genes.

Key: EGF, epidermal growth factor-like repeat domain; LNR, Lin-12 NOTCH repeat domain; TM, transmembrane domain; RAM, RBPJ-associated molecule; ANK, ankyrin repeat domain; TAD, transcription activation domain; PEST, OPA/proline/glutamic acid/serine/threonine-rich domain; EOGT, EGF Domain-Specific O-Linked N-Acetylglucosamine Transferase; NICD, Notch intracellular domain; MAML, mastermind-like transcriptional co-activator (CoA); CoR, transcriptional co-repressor; RBPJ, Recombining Binding Protein Suppressor Of Hairless transcriptional regulator

Finally, there are also highly conserved non-canonical Notch signalling pathways that are exert their biological functions by targeting the Wnt/β-catenin signalling pathway, inducing arterial fate in vascular progenitors and play key suppressor roles in human cancers (Figure 1-13) (Andersen, Uosaki et al. 2012). Up to date, there are well characterized interactions of Notch signalling with also other signalling pathways, such as hypoxia and BMP/TGF-β signalling cascades (Andersson, Sandberg et al. 2011, Fu, Chang et al. 2009). These signalling cross-talks are generating the notion that signalling mechanisms do not operate in isolation, rather than being implemented in to far greater signalling networks (Figure 1-13).

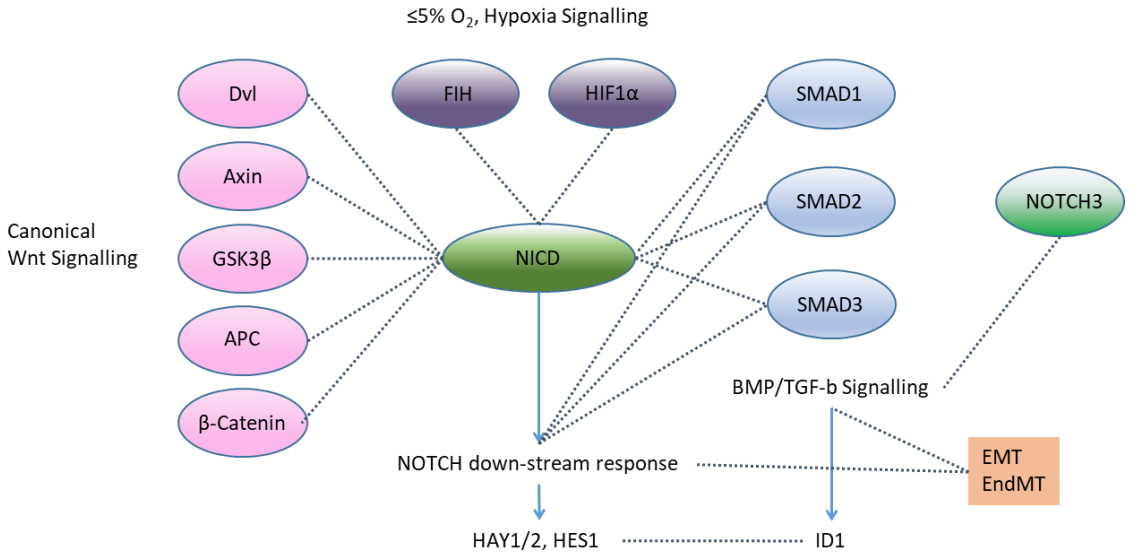

Figure 1-13 Cross-talk between the Notch pathway and other signalling pathways
Key intracellular mediators of the Wnt, hypoxia and BMP/TGF-β pathways are depicted. Interactions between Notch ICD and key intracellular mediators in the other signalling mechanisms are indicated by dashed lines. Active Notch/BMP/TGF-β signalling is implicated in Epithelial-to-Mesenchymal (EMT) and endothelial-to-mesenchymal transition (EndMT) programming in he developing heart. TGF-β down-regulates the expression of Notch3, but up-regulates HES1 expression, during smooth muscle differentiation.

Key: Dvl, Dishevelled; GSK3β, Glycogen synthase kinase 3 beta; APC, adenomatous polyposis coli; FIH, asparagine hydroxylase factor-inhibiting HIF1α; HIF1α, Hypoxia-inducible factor 1-alpha, NICD, Notch ICD; HEY1/2, Hairy/enhancer-of-split related with YRPW motif proteins 1/2; HES1, Hairy and enhancer of split 1; SMAD1/2/3, Mothers against decapentaplegic homolog 1/2/3; EMT, epithelial-to-mesenchymal transition; EndMT, endothelial-to-mesenchymal transition

Taken all into account, Notch signalling acts in certain cases synergistically with BMP/TGF-β signalling, whereas in other cases antagonises the down-stream

effects of the later in the context of vascular development and remodelling in disease states (Itoh, Itoh et al. 2004).

1.7.2 THE *NOTCH1* GENE IN AOS

Despite the identification of four causal genes, each of these genes only accounts for a small proportion of AOS cases, collectively explaining around 10% of affected individuals. To further define the molecular genetic factors involved in AOS pathogenesis, Southgate *et al., 2015* performed whole-exome sequencing of 12 probands with a clinical diagnosis of AOS and identified 2 novel truncating mutations (c.1649dupA; p.Y550* and c.6049_6050delTC; p.S2017Tfs*9) in the *NOTCH1* gene. Further mutation screening of a patient cohort comprising of 50 unrelated AOS subjects (Appendix D – Table D-1) detected *NOTCH1* mutations in an additional 7 individuals, including two *de novo* variants (Table 1-3). All mutations were predicted to be pathogenic by bioinformatic software (Appendix D – Table D-2). Of note, 47% of mutation carriers also had a congenital heart or vascular abnormality, highlighting a genotype/phenotype correlation between *NOTCH1* mutation and cardiovascular defects. These findings are highly correlated with existing vast literature reviews that linking *NOTCH1* mutations with cardiovascular and lung conditions (Zong, Ouyang et al. 2016, Rusanescu, Weissleder et al. 2008, Kerstjens-Frederikse, van de Laar et al. 2016, Zhou, Liu 2014); (Southgate, Sukalo et al. 2015)

Table 1-3: List of identified and AOS-associated NOTCH1 variants (Southgate, Sukalo et al. 2015)

Exon	Coding variant	Protein variant	Variant type	Protein domain
7	c.1220C>G	p.P407R	Missense	EGF 10
8	c.1343G>A	p.R448Q	Missense	EGF 11
8	c.1345T>C	p.C449R	Missense	EGF 11
8	c.1367G>A	p.C456Y	Missense	EGF 11
10	c.1649dupA	p.Y550*	Frameshift	EGF 14
25	c.4120T>C	p.C1374R	Missense	EGF 35
26	c.4663G>T	p.E1555*	Nonsense	LNR 3
26	c.4739dupT	p.M1580lfs*30	Frameshift	-
28	c.5218G>T	p.A1740S	Missense	TM
32	c.6049_6050delTC	p.S2017Tfs*9	Frameshift	ANK 4

It is of particular interest to establish how the novel AOS-related *NOTCH1* missense mutations affect the regulation of NOTCH1 signalling. Specifically, c.1220C>G, c.1343G>A and c.1345T>C affect amino acids that are located in or adjacent to the NOTCH1 ligand-binding domain, specified by EGF repeats 11-13 (Figure 5A, B). Similarly, the c.4120T>C (p.C1374R) mutation affects a cysteine residue within an EGF domain which is likely to adversely affect the protein structure. By comparison, the c.5218G>T mutation is located in the transmembrane domain and its significance on the structural integrity of the molecule has to be assessed. Thus, quantitative studies will be undertaken to assess the NOTCH1 potential down-regulation in AOS-affected individuals, along with its implication in the signalling cascade.

1.8 AIMS AND OBJECTIVES

Hypothesis: The primary hypothesis to be tested in this thesis is that JAB1 and NOTCH1 are involved in the development of CVD, in the regulation of BMPR-II expression and key intracellular pathways including BMP/TGF-β and NOTCH1 canonical signalling. In order to test this hypothesis, the following areas will be investigated:

1. Hypothesis: JAB1 functions as the first identified proteasomal-associated inhibitor of BMPR-II.

   Aims and Objectives: The interaction of JAB1 and BMPR-II will be analysed *in vitro* and *in vivo* in a panel of cancer cell lines* followed by the confirmation of down-regulation of BMPR-II by JAB1 through proteasomal ubiquitination.

2. Hypothesis: Dysregulation of JAB1 leads to abnormal BMPR-II receptor loss and PAH progression by disruption of the homeostatic BMP/TGF-β signalling balance.

   Aims and Objectives: Through the use of transient transfections of JAB1 into cancer cell lines and primary pulmonary artery smooth muscle cells**, the potential BMP/TGF-β stochiometric imbalance will be investigated along with alterations in the phenotypic proliferation rates of the cells. Additionally, transient RNA interference will be employed to reverse abnormal proliferation of cells in PAH.

3. Hypothesis: *NOTCH1* mutations are significantly associated with AOS and cardiac abnormalities via a loss of structural integrity of the receptor.

   Aims and Objectives: *NOTCH1* expression and signalling will be assessed for novel missense and nonsense mutations identified in AOS patients, through the use of quantitative RT-PCR and ectopic protein expression.

Finally, a potential cross-talk between NOTCH1 and BMP signalling will be investigated.

*The use of human cancer cell lines (HeLa and HEK293T) as experimental model systems for the *in vitro* investigation, was decided based on their highly proliferative phenotype, stable growth, availability and easiness to be cultured and transfected into two-dimensional culture environments. They were purchased free of contamination from ATCC company.

** The use of human primary pulmonary artery smooth muscle cells as an experimental model system for the *in vivo* investigation, was decided based on their isolation directly from the tissue of interest, normal cell morphology and maintenance of the important markers and functions seen *in vivo*. They were provided by Dr R.D. Machado (holder of Patient Consent Forms and associated Patient Information Sheets). Finally, PCR-based testing for bacterial and mycoplasma contaminants revealed no detection of contamination.

CHAPTER 2: MATERIALS AND METHODS

2.1 CHEMICALS AND REAGENTS

Unless stated otherwise, the reagents were purchased from Sigma-Aldrich, Gibco, life-technologies, Lonza and BIO-RAD.

Table 2-1 Reagents

Reagent/ Kit	Company	Catalogue Number
XL1-Blue Competent Cells	Agilent Technologies (Santa Clara, California, USA)	200249
High Capacity cDNA reverse transcription kit	Applied Biosystems (Foster City, California, USA)	4368814
DC Protein Assay Kit II	Bio-Rad (Hertfordshire, UK)	5000112
Cell Counting Slides for TC20 Cell Counter		1450015
30% Acrylamide/Bis Solution		1610154
Precision plus protein prestained standards, dual colour		161-0374
Fluoromount G	Cambridge Bioscience (Cambridge, UK)	0100-01
Glycerol (Laboratory reagent grade)	Fisher Scientific (Hampton, New Hampshire, USA)	G/0600/08
Methanol (HPLC grade)		67-56-1
Ethanol (HPLC grade)		64-17-5
2-Propanol (HPLC grade)		67-63-0
HighRanger 1kb DNA Ladder	Geneflow (Staffordshire, UK)	L3-0020-S
Heat inactivated foetal bovine serum (FBS)	Gibco (Thermo Fisher Scientific)	10082147
DBPS, no calcium, no magnesium		14190169
Penicillin-Streptomycin (PS) (100X)		15140122
Trypsin-EDTA (0.25%), phenol red		25200056
Trypan Blue Solution, 0.4%		15250061
Lipofectamine™ 2000	Invitrogen (Paisley, UK)	11668-027
Miller's LB Broth Base® (Luria Broth Base)		12795-027
Ultra-pure water		10977-049
Neon Transfection System 10 & 100ul Kit		MPK1096 & MPK10096
LB Agar, powder (Lennox L Agar)		22700-025
SmGM-2 Smooth Muscle Growth Medium-2	Lonza (Slough, UK)	CC-3182
HEPES >99.5%, Free Acid	Melford (Ipswich, UK)	B2001
Purified BSA 100X	New England Biolabs (Ipswich, Massachusetts, USA)	B90015
COPS5-Human, 4 unique 29mer shRNA constructs in pRS	OriGene Technologies (Rockville, Maryland, USA)	TR313776
Protein G Sepharose beads		TP790005
Marvel Dried Skimmed Milk Powder	Premier brans	N/A
Custom designed real-time PCR assay kit with Double-Dye probe (Taqman-style, 2x PrecisionPLUS Mastermix)	Primerdesign Ltd (Southampton, UK)	DD-hu-300
FuGENE HD Transfection Reagent	Promega	E2311

CellTiter 96® Non-Radioactive Cell Proliferation Assay (MTT)	(Madison, Wisconsin, USA)	G4000
HiSpeed Plasmid Maxi Kit	QIAGEN (West Sussex, UK)	12662
RNeasy Plus Mini Kit		74134
Recombinant Human BMP-4 Protein	R&D Systems (Minneapolis, Minnesota, United States)	314-BP-050
cOmplete, mini EDTA-free protease inhibitor cocktail tablets	Roche Applied Science (West Sussex, UK)	11 836 153 001
Dulbecco's modified eagle media (DMEM) high glucose with L-Glutamine, Sodium Pyruvate and Sodium Bicarbonate	SIGMA-ALDRICH (GmbH, Hannover, Germany)	D6429
2-Mercaptoethanol >99%		M6250
Ammonium persulphate		A3678
Lactacystin >90% (HPLC)		L6785
Sodium Dodecyl Sulphate (SDS) (Molecular Biology Grade)		71725
N,N,N′,N′-Tetramethylethylenediamine		T9281
Tris base		000000010708976001
Bromophenol Blue		B0126
Ampicillin sodium salt		A9518
Kanamycin sulphate		60615
Sodium Chloride (Molecular Biology Grade)		S3014
Sodium hydroxide solution (Molecular Biology Grade)		72068
Hydrochloric acid (Molecular Biology Grade)		H1758
Potassium Chloride (Molecular Biology Grade)		P9541
Ponceau S solution		P7170
Dimethyl sulfoxide (Molecular Biology Grade)		D8418
Ethidium bromide solution (Molecular Biology Grade)		E1510
Triton X-100 (Molecular Biology Grade)		T8787
Tween-20 (Molecular Biology Grade)		P9416
Glycine >99%		G8898
Sodium orthovanadate 99.98%		450243
Sodium fluoride (Molecular Biology Grade)		S7920
Magnesium chloride anhydrous >98%		M8266
Phenylmethanesulphonyl fluoride (Molecular Biology Grade)		78830
Phosphate buffered saline tablets		P4417
Hoechst Stain solution		H6024
Pierce ECL Western Blotting Substrate	Thermo Scientific (Waltham, Massachusetts, USA)	32106

Table 2-2 Buffers

Reagent Name	Components
DNA loading dye (6X)	0.25% (w/v) xylene cyanol and/or bromophenol blue; 30% glycerol (v/v); ddH_2O
Glycerol dye	0.5 mg/ml bromophenol blue; 50% (v/v) glycerol
Laemmli sample buffer (2X)	10% (w/v) SDS; 1 M Tris-Cl (pH 6.8); 0.02% (w/v) bromophenol blue; 5% (v/v) 2-mercaptoethanol; dH_2O
Lysis buffer for Western blots	1M Tris base (pH 7.4); 5M NaCl; 1M $MgCl_2$; 10% SDS; 1% Triton X-100; 20 mM sodium fluoride (NaF); 1 mM sodium orthovanadate (Na3VO4); 1 mM phenylmethylsulphonyl fluoride (PMSF); 10x Protein Inhibitors Cocktail; dH_2O
Phosphate buffered saline (PBS)	Dissolve 10 PBS tablets/1 litre ; (g/L:- 8.0 sodium chloride; 0.2 potassium chloride; 1.15 di-odium hydrogen phosphate; 0.2 potassium dihydrogen phosphate; pH 7.3± 0.2 at 25 ^oC)
Ponceau S staining solution	0.1% (w/v) Ponceau S; 5% (v/v) acetic acid
Protein loading buffer	0.2% (w/v) bromophenol blue; 1% (v/v) 2-mercaptoethanol
Protein running buffer	25 mM Tris-HCl; 192 mM glycine; 0.1% (w/v) SDS
Protein transfer buffer	25 mM Tris, 192 mM glycine, 20% (v/v) methanol; pH 8.3
Stripping Buffer	100 mM 2-mercaptoethanol, 2% SDS, 62.5mM tris-HCL pH 6.7
Tris-borate EDTA buffer (TBE)	(1X) 89 mM Tris; 89 mM boric acid; 2 mM EDTA
Tris-buffered saline with Tween (TBS-T)	50mM Tris-HCl (pH 8.0); 150 mM NaCl; 0.1% (v/v) Tween-20
TBS-T with bovine serum albumin (BSA)	TBS-T; 5% BSA
TBS-T with milk	TBS-T; 5% (w/v) Marvel dried milk powder
Tris-EDTA (TE) buffer	10 mM Tris-HCl (pH 7.5); 1 mM EDTA (pH 8.0)
Tris-SDS buffer	0.05 M Tris (pH 8); 0.1% SDS

Table 2-3 Primary antibodies

Antibody	Product number	Company	Isotype	Migration in SDS/PAGE (kDa)	Immunogen	Dilution
α-tubulin	Ab7291	Abcam	Mouse monoclonal IgG1 [DM1A]	50	Raised against amino acids 426-450 of chicken α-tubulin	1:8000 WB
Jab1	GTX70203	GeneTex	Mouse monoclonal IgG2b	38	Raised against the full-length mouse JAB-1 gene (expressed in E.coli)	1:3000 WB 2 µg for 10^7 cells IP
BMPR-II	AF811	R&D SYSTEMS	Goat polyclonal IgG	115	Raised against the mouse myeloma cell line NS0-derived recombinant human BMPR-II	0.05 µg/ml WB
Smad 5	12534S	Cell Signalling	Rabbit monoclonal IgG [D4G2]	60	Raised against a synthetic peptide corresponding to residues surrounding Pro249 of human Smad5	1:1000 WB
phospho-Smad1/5 (Ser463/465)	9516S	Cell Signalling	Rabbit monoclonal IgG [41D10]	60	Raised against a synthetic phosphopeptide corresponding to residues surrounding Ser463/465 of human Smad5	1:1000 WB
p38 MAPK	9212S	Cell Signalling	Rabbit polyclonal IgG	43	Raised against a synthetic peptide corresponding to the sequence of human p38 MAPK	1:1000 WB
phospho-p38 MAPK (Thr180/Tyr182)	9215S	Cell Signalling	Rabbit monoclonal IgG [3D7]	43	Raised against a synthetic phosphopeptide corresponding to residues surrounding Thr180/Tyr182 of human p38 MAPK	1:1000 WB
Smad2/3	3102S	Cell Signalling	Rabbit polyclonal IgG	52, 60	Raised against a synthetic peptide corresponding to residues in the amino-terminal region of Smad2/3	1:1000 WB

phospho-Smad2 (Ser465/467)/ Smad3(Ser423/425)	8828S	Cell Signalling	Rabbit monoclonal IgG [D27F4]	52, 60	Raised against a synthetic peptide corresponding to residues surrounding Ser465/467 of human Smad2	1:1000 WB
TAK1	5206S	Cell Signalling	Rabbit monoclonal IgG [D94D7]	78 to 82	Raised against a synthetic peptide corresponding to residues surrounding Gln600 of human TAK1	1:1000 WB
phospho-TAK1 (Thr184/187)	4508S	Cell Signalling	Rabbit monoclonal IgG [90C7]	82	Raised against a phosphopeptide (KLH-coupled) corresponding to residues surrounding Thr184 and Thr187 of human TAK1	1:1000 WB
RAC1	Ab33186	Abcam	Mouse monoclonal IgG2b [0.T.127]	21	Raised against recombinant full-length protein corresponding to Human Rac1	1 µg/ml WB 2 µg for 10^7 cells IP
c-Myc	M4439	SIGMA-ALDRICH	Mouse monoclonal IgG1 [9E10]	-	Raised against a synthetic peptide corresponding to residues 408-439 of the human p62c-Myc	1:5000 WB 2.5 µg for 10^7 cells IP
FLAG M2	F3165-.2MG	SIGMA-ALDRICH	Mouse monoclonal IgG1	-	Raised against FLAG sequence at the N-terminus, Met-N-terminus, C-terminus, or at an internal site of FLAG fusion proteins	1:5000 WB 1 µg for 10^7 cells IP
HA	H6908	SIGMA-ALDRICH	Rabbit polyclonal IgG	-	Raised against a synthetic peptide corresponding to amino acid residues 98-106 (Tyr-Pro-Tyr-Asp-Val-Pro-Asp-Tyr-Ala) of the human Influenza hemagglutinin (HA), conjugated to KLH.	1:1000 WB 5 µg for 10^7 cells IP

Table 2-4 Secondary antibodies

Antibody	Product number	Company	Type	Dilution
Anti-Mouse Immunoglobulins/HRP	Ab97023	Abcam	Polyclonal Goat	1:3000 WB
Anti-Rabbit Immunoglobulins/HRP	Ab16284	Abcam	Polyclonal Donkey	1:1000 WB
Anti-Goat Immunoglobulins/HRP	Ab97100	Abcam	Polyclonal Rabbit	1:5000 WB

Table 2-5 4 unique 29mer shRNA constructs sequences in pRS (retroviral untagged vector) for silencing Human COPS5

Oligo Name	Sense sequence 5'-3'	Anti-sense sequence 5'-3'	References
Scrambled Negative Control (TR30012)	GCACTACCAGAGCTAACTCAGATAGTACT	AGTACTATCTGAGTTAGCTCTGGTAGTGC	-
TR313776A (TI355097)	GCCAACAACATGCAGGAAGCTCAGAGTAT	ATACTCTGAGCTTCCTGCATGTTGTTGGC	(Okoh *et al*., 2015)
TR313776B (TI355098)	TACTCAGATGCTCAATCAGCAGTTCCAGG	CCTGGAACTGCTGATTGAGCATCTGAGTA	
TR313776C (TI355099)	TCTGCTGAAGATGGTGATGCATGCCAGAT	ATCTGGCATGCATCACCATCTTCAGCAGA	
TR313776D (TI355100)	AGAAGCTATCCATGGATTGATGTCTCAGG	CCTGAGACATCAATCCATGGATAGCTTCT	

2.2 CELL CULTURE

2.2.1 ROUTINE CELL MAINTAINANCE

All tissue culture procedures were performed in a class II laminar flow cabinet (Aura 2000 B.S., Bioair Instruments) and the cell lines were incubated at 37 ^{o}C, 5% CO2 and 100% humidity (Hera Cell, Heraeus). The range of primary cells and cell lines that were used can be found in Table 2.6, referring also on the type of tissue culture media used. The media storage temperature was 4 ^{o}C following warming up to 37 ^{o}C prior to the use. Tissue culture flasks T-25, T-75 and T-175 (SARSTEDT) were used each time for the different experimental purposes (i.e. qPCR or Western Blotting). All cell cultures consisted of adherent cell types that were grown up to 80% of flask confluence, and then split by trypsinization method. All types of cells were not passaged more than 10 times. The cells were sub-cultured after two-times washing with phosphate-buffered saline (PBS) and trypsinization by using the appropriate volume of 1X sterile Trypsin/EDTA. Trypsin-EDTA was activated within 2 to 4 minutes at 37 ^{o}C, and the flasks were gently tapped for cell detachment to occur. The neutralization of trypsin-EDTA was made possible with addition of complete (10% FBS) cell culture media. The cell suspensions were transferred to 50 ml centrifuge tubes (SIGMA) and pelleted via 5 minutes centrifugation at 200 ×g, following pellet re-suspension in 1 ml of appropriate media. Each cell line was seeded at the correct cellular density, utilizing the appropriate flask size and media volume, following immediate return to proper culture conditions.

2.2.2 CELL COUNTING

The cells were counted using a TC20 Automated Cell Counter (1450102 BIO-RAD). Each time, the cells were washed, detached, pelleted and re-suspended in 1 ml of PBS. 10 µl of the cellular suspension were added to the counting slides (1450011 BIO-RAD), and the cell viability was defined by the trypan-blue method, when mixed in 1:2 dilution with the chemical. The cell counter was set to detect cells within the range of 6 to 20 µm with a dilution factor of 1000. The correct cell

number required for passaging or further experimentation was defined using the following formula:

$V = (REQ/DET) \times DIL$

(V: volume of cells required in µl, REQ: required number of cells, DET: detected cell count, DIL: dilution factor)

For proliferation assay studies, the cells were counted manually using Neubaouer haemocytometers (1127884 camlab).

2.2.3 FREEZING AND THAWING CELL LINES

Following routine cell maintenance and counting procedures, the cells were re-pelleted and re-suspended to a density of 1×10^6 cells per 1 mL of freezing media (75% cell culture media with glutamine; 20 % FBS; 5 % DMSO) and aliquoted into Nalgene™ general long-term storage cryogenic tubes (Thermo Scientific). These tubes were placed in isopropanol filled Mr. Frosty Freezing Containers (Thermo Scientific) and stored at -80 ^oC overnight, prior transfer to liquid nitrogen containers for long-term storage.

The thawing procedure of cells stored in liquid nitrogen occurred by immediate placement in a 37 ^oC water bath for approximately 1 minute, to ensure optimal cell recovery. Following that, 10 ml of tissue culture media were added under sterile conditions, and the cells were pelleted by centrifugation. The pellets were re-suspended in 5 to 10 mL of complete tissue culture media in order to be transferred to the appropriate cell culture flask and finally placed in the incubator.

Table 2-6 Cell lines

Cell line	Culture media	Cellular origin	*BMPR2* status	References
HeLa	DMEM; 10% FBS; 1% P/S	Human cervix epithelial; adherent cells	WT	Supplied by ATCC
HEK293T	DMEM; 10% FBS; 1% P/S	Human embryonic kidney epithelial; adherent cells	WT	Supplied by ATCC
hTERT PASMC	SmGM-2 Smooth Muscle Growth Medium-2	Human immortalized smooth muscle cells	WT / *BMPR2*$^{+/R899X}$	In lab
pPASMC	SmGM-2 Smooth Muscle Growth Medium-2	Human primary smooth muscle cells	WT / *BMPR2*$^{+/W9X}$	Supplied by Lonza

2.2.4 TRANSIENT TRANSFECTIONS

Appropriate high-quality Plasmid DNA (Table 2-7) and shRNA (Table 2-5) amounts at the required concentration were transiently transfected into cells using the Neon® Resuspension Buffer R in combination with the Neon® Transfection System-electroporator from ThermoFisher Scientific (MPK5000), which was set at optimised settings for every used cell line (Table).

Cells were washed in PBS (without Ca^{2+} and Mg^{2+}), trypsinized, pelleted and counted, and 2.5×10^5 cells per each 10 µl Neon® Tip or 1.5×10^6 cells per each 100 µl Neon® Tip were electroporated for most optimised protocols. Afterwards, the cells were aliquoted in desired densities and plated in 24 or 12 well plates with pre-warmed media for proliferation studies, or 10cm dishes for protein-based analysis, and returned to the incubator. For each set of transfections, a negative control for transfection was included, which consisted of transfection with the pCMV-Tag3-empty plasmid (Table 2-7). Cell viability was determined the following day and cell culture media replaced.

In preliminary studies, HeLa and HEK293T cell lines were transiently transfected at 80% confluence with plasmid DNA using liposomal reagent Lipofectamine 2000 (Life Technologies) or with the non-liposomal reagent Fugene HD (Promega) at 3:1 ratio of transfection reagent (µl) to plasmid DNA (µg), and cells were incubated for 48h, prior to fluorescent imaging or Western blotting. The

above reagents were selected after comparison of transfection efficiency against the other commercial liposomal reagents Metafectane PRO, K2 (Biontex), and Lipofectamine 3000 (life technologies) (Appendix C). After the 48h incubation the cells were fixed with 4% para-formaldehyde and nuclei stained with Hoechst (1:20000 dilution).

Table 2-7 Plasmids constructs and vectors

Plasmid name	Plasmid	Insert	Use	Company
pCMV-Tag 3 (empty)	pCMV-Tag 3	-	negative control	Stratagene
pCMV-Tag 3 Myc-JAB1	pCMV-Tag 3	mouse *JAB1* with N-terminal Myc-tag	JAB1 expression in transient transfections	Stratagene
pCMV-Tag 2 FLAG-JAB1	pCMV-Tag 2	mouse *JAB1* with N-terminal FLAG-tag	JAB1 expression in transient transfections	Stratagene
pCMV-Tag 5 Myc-BMPR2	pCMV-Tag 5	human *BMPR2* with N-terminal Myc-tag	BMPR-II expression in transient transfections	Stratagene
pcDNA 3.0 BMPR2	pcDNA 3.0	human *BMPR2*	BMPR-II expression in transient transfections	Invitrogen
pFN21A-Notch1 WT	pFN21A	human *NOTCH1* WT	NOTCH1 WT expression in transient transfections	Promega
pFN21A-Notch1 c.1345T>C	pFN21A	human *NOTCH1* c.1345T>C	NOTCH1 c.1345 expression in transient transfections	Promega
pFN21A-Notch1 c.1649dupA	pFN21A	human *NOTCH1* c.1649 dupA	NOTCH1 c.1649 expression in transient transfections	Promega
pRK5-HA-Ubiquitin-WT	pRK5-HA	human ubiquitin with N-terminal HA-tag	Full length ubiquitin expression in transient transfections	addgene

2.2.5 CHEMICAL TREATMENTS

For hBMP4 treatment, the cells were left in transfection media for 24 hours following a starvation period of 12 hours with 0.5% FBS in DMEM. Afterwards, 10ml of cell culture were treated with 10ng/ml of hBMP4 (from a stock solution of

100µg/ml in sterile 4 Mm HCl containing 0.1% bovine serum albumin) for 1 hour for Smad phosphorylation or 4 hours for ID1 transcription (cite that).

For lactacystin-based studies, 24 hours after transfection with Jab1, the cells were incubated for 6 hours with or without the proteasome inhibitor lactacystin at 20µM and were further subjected to SDS-PAGE and western blotting.

2.2.6 CELL PROLIFERATION ASSASYS AND GROWTH CURVES

HeLa cells were transfected with JAB1-pCMVTag3 or pCMV-Tag 3 empty vector (control) and seeded in triplicate in 6 well plates at a density of 25,000 cells per well (day 0). On days 1, 2, 3, 4 and 5, the cells were harvested by trypsinization and counted by haemocytometer.

A 7-day SMC proliferation assay was conducted to independently assess the proliferation of the PAH-associated human p.R899X PASMCs against WT PASMCs. The cells were seeded in technical triplicates in 12 well plates at a density of 50,000 cells/well and counted by haemocytometer.

HeLa, HEK293T and hTERT-SMC WT growth curves were constructed by maintaining the cells in 6 well plates for 7 days and counting every 24 hours by haemocytometer (Appendix B).

For each proliferation assay, the cell media was replaced every second two days and the cell viability was determined by using 0.4% filtered Trypan Blue solution.

MTT ASSAY

3-(4,5-dimethylthiazol-2-yl)-2,5-diphenyltetrazolium bromide (MTT) conversion to insoluble formazan as colorimetric assay to assess cells viability and proliferation, was employed to verify manual cell counts. The MTT method was used in 96-well plate experiments at a final concentration of 1mg/ml in DMEM with 10% FBS. MTT-treated cells were incubated for 3.5 hours, MTT media removed and DMSO added. Absorbance of the viable cells was read by SpectraMax Plus 384 Microplate Reader at 540 nm.

2.2.7 LIVE CELL AND FLUORESCENT IMAGING

Adherent cell morphology and confluence was observed using a Nikon Eclipse TE2000-S inverted microscope, equipped with Dn100 digital net camera and Nikon Dn100 web interface software. The expression of fluorescent proteins and 4',6-diamidino-2-phenylindole (DAPI) staining of cell nuclei were visualized by use of Nikon Eclipse 80i fluorescent microscope.

2.3 MANIPULATION OF NUCLEIC ACIDS

2.3.1 RNA EXTRACTION

The RNA extractions were performed with RNeasy Plus Mini kit (74134 QIAGEN). The cell cultures were washed thrice with sterile PBS buffer, trypsinized and further re-suspended in tissue culture media. The suspended cells were transferred to RNase-free tube and pelleted by centrifugation. Cell lysis was accomplished by addition of 600µl of RLT Plus buffer (with 1% β-mercaptoethanol) and vortexing. QIAshredder spin column homogenized cell lysates were transferred in gDNA eliminator spin columns and the flow-through were subjected in 70% ethanol prior RNA precipitation in RNeasy spin column. The column was washed thrice and the final total RNA was eluted in 30 µl of Elution Solution and further kept at -80 ^{o}C for short-term storage.

2.3.2 NUCLEIC ACID QUANTIFICATION

The DNA or RNA concentrations and the sample purity (total yield) were determined using the NanoDrop ND-1000 Spectrophotometer (NanoDrop Technologies, USA). Before and after each measurement, the pedestal and the lid were cleaned with 70% alcohol. The computer program was initialized and further blanked with the Elution Buffer used for nucleic acid dissolvement. The sample volume applied onto the pedestal was 1.2 µl and triplicates were measured each time. The overall sample purity was analogue to absorbance readings of 260 and 280 nm, with DNA and RNA optimal A260/280 ratios of 1.8 and 2.1 respectively.

2.3.3 VISUALISATION OF NUCLEIC ACIDS

The DNA fractionation or the quality of the RNA extracts were performed and determined respectively by 1% Agarose gel electrophoresis in TBE (45 mM Tris-borate, 1 mM EDTA) buffer containing ethidium bromide (E1510 SIGMA) to a final concentration of 2 µg/ml. Each time, the gels casts allowed to set within a fume hood utilizing Bio-Rad gel equipment. DNA or RNA was mixed with 5X Loading Buffer (100mM Tris pH 8, 10mM EDTA pH 8, 50% Glycerol and 0.5%w/v bromophenol blue) and electrophoresed at 60V for 40 minutes. DNA bands or RNA 18S and 28S rRNA subunits were visualized under ultraviolet light using a BIO-RAD transilluminator (ChemiDoc XRS+) and gel images were taken.

2.3.4 TWO STEP REVERSE TRANSCRIPTASE QUANTITATIVE PCR (RT-qPCR)

2.3.4.1 cDNA SYNTHESIS

Generation of cDNA from total RNA was performed with the High-Capacity cDNA Reverse Transcription Kit (Applied Biosystems). All components, including the RNA, were stored on ice throughout.

The 20 µl reactions were synthesized by 10 µl MasterMix (Table 2-8) complemented with 1 µg of total RNA. The optimised thermal cycler conditions for first strand cDNA synthesis, RNA denaturation, cDNA synthesis and termination of reaction are described in Table 2-9.

Monitoring of forms of contamination, such as presence of genomic DNA or reagent contamination within the cDNA samples, was made possible by performing reverse transcriptase-minus and no template reactions within each experimentation. The cDNA samples were stored at -80 ^{o}C prior further use.

Table 2-8 2x RT Master Mix Composition (Adopted and Modified from AB High Capacity cDNA Reverse Transcription Kit - Life Technologies)

Component	Volume/Reaction (µL)
10x RT Buffer	1.0
25x dNTP Mix (100mM)	0.4
10x RT Random Primers	1.0
MultiScribe Reverse Transcriptase	1.0
Nuclease-free H2O	6.6
Total per Reaction	10

Table 2-9 Thermal Cycler Conditions for cDNA synthesis

	Step 1	Step 2	Step 3	Step 4
Temperature (℃)	25	37	85	4
Time	10 min	120 min	5 min	∞

2.3.4.2 QUANTITATIVE PCR (qPCR)

Quantitative Real-Time PCR was performed on a StepOne Plus real-time PCR machine (Applied Biosystems), using double-dye Taqman-style detection chemistry with the PrimerDesign 2x PrecisionPLUS MasterMix (Table 2-10) and custom-designed probe sets for *JAB1*, *NOTCH1, HEY1 and HES1* mRNAs (PrimerDesign). The normalization in mRNA relative quantifications was made possible by the use of *GAPDH* and *ACTB* house-keeping genes as controls. The qPCR total volume reaction was 10 µl (5 µl of master mix + 2.5 µl of diluted 1:10 cDNA template) and the qPCR amplification conditions profile is provided in Table 2-11. Gene of interest expression levels for patient and mutagenized samples were calculated by the $2^{(-\Delta\Delta Ct)}$ method relative to the wild-type baseline (Methodology originally published in Southgate, Sukalo et al. 2015).

Table 2-10 PrimerDesign 2x PrecisionPLUS qPCR MasterMix composition.

Component	1 Reaction
Resuspended primer/probe mix	0.5 µl*
PrimerDesign 2x PrecisionPLUSTM Mastermix	5 µl
RNAse/DNAse free water	2µl
Final volume	7.5 µl

*Working Concentration of primers = 150nM in a 10µl reaction

Table 2-11 Amplification Conditions using PrimerDesign 2x PrecisionPLUS qPCR MasterMix.

	Step	Time	Temperature (℃)
Cycling x40	Enzyme Activation	2 min	95
	Denaturation	15 sec	95
	Extension/Data Collection*	60 sec	60

*Fluorogenic data should be collected during this step through the FAM channel.

2.4 BACTERIAL PRODUCTION OF PLASMID DNA

2.4.1 CHEMICAL TRANSFORMATION OF COMPETENT E.COLI CELLS

The plasmid DNA of interest was chemically introduced into XL-1 blue Competent cells of golden efficiency (the cells were kindly prepared and offered by Dr Enrico Ferrari, University of Lincoln). To ensure maximal survival out of -80 ^{o}C storage, the cells were thawed on ice into pre-chilled 1.5 ml microcentrifuge tubes. 2 µl of plasmid DNA was added to 50 µl of thawed aliquoted XL-1 cells and further incubated on ice for 30 minutes. Subsequently, the cells were heat shocked in waterbath at exactly 42 ^{o}C for 50 seconds. Ultimately, the transformed samples were returned on ice for 2 minutes and then 500 µl of SOC medium (0.5% Yeast Extract, 2% Tryptone, 10 mM NaCl, 2.5 mM KCl, 10 mM $MgCl_2$, 10 mM $MgSO_4$, 20 mM Glucose) was added to the chemical reaction mix following an orbital shake for up to 1 hour at 37 ^{o}C. Separately, pUC19 DNA was used as a positive control for the transformation reaction, and a negative control free of plasmid DNA, and so antibiotically sensitive, was included to the overall transformation reactions.

After 1-minute centrifugation at 6000rpm, a maximum of 50 μl of the transformation reaction was spread on previously prepared Luria Broth (LB) Agar plate (10g Bacto-tryptone, 10 g sodium chloride, 5 g yeast extract and 15 g agar per litre), containing either ampicillin or kanamycin to a final concentration of 100 μg/ml or 50 μg/ml, respectively. After overnight incubation period at 37 ^{o}C, single uniformed bacterial colonies were selected and extracted from the plate using sterile pipette tips in order to expand the bacterial population, following the protocol of small scale pDNA production.

2.4.2 PLASMID DNA PURIFICATION

A starter culture of bacteria containing the desired plasmid DNA was generated by direct selection of colonies from the agar plate and their subsequent addition to 5 ml of LB broth (10 g Bacto-tryptone, 10 g sodium chloride, 5 g yeast extract per litre), containing the previously mentioned antibiotic concentrations. The incubation time was 8 hours at 37 ^{o}C degrees with orbital shaking. For the purpose of generating high quantities of purified pDNA, a secondary large 16 hours culture at 37 ^{o}C with orbital shaking was prepared utilizing 500 ml of LB Broth with antibiotic, along with 1:1000 dilution of the starter culture. The preparation of the pDNA extraction was based on the QIAGEN Plasmid Maxi kit (12162) and the company's protocol for high-copy plasmid purification with a recovery yield of 500 μg. At the end of the incubation period, the culture was pelleted by centrifugation at 6,000 *x g* for 20 minutes at 4 ^{o}C. After re-suspension of the bacteria pellet in lysis buffer, the plasmid DNA in the clarified lysate was bound in the silica resin column by gravity flow. The column was washed and then 1 ml DNA was eluted in Buffer QC and further precipitated by iso-propanol in a QIA precipitator. The DNA pellet was washed by 70% ethanol, air-dried and subsequently eluted in nuclease-free water. Both quantity and quality of the purified pDNA was determined and verified using the Nanodrop in order to be used in subsequent down-stream experimentation, such as transient transfections via electroporation.

2.5 MANIPULATION OF PROTEINS

2.5.1 PROTEIN ISOLATION

The cell cultures were obtained from the tissue culture incubator and washed twice with sterile PBS. The cell lysates were prepared from cell monolayers growing in 10 cm dishes and harvested after trypsinization and re-suspension in assay-dependent Extraction Buffer (Appendix A). The detached cells in the lysis buffer were transferred into a 1.5 ml microcentrifuge tube and then left on ice for 30 minutes with occasional vortexing. The samples were submitted to 3 cycles of 5 seconds sonication (Soniprep 150 Ultrasonic Disintegrator MSE) time on melting ice with 3 seconds interval for cooling, for the purpose of DNA fragmentation. Subsequently, they were centrifuged at 15000g for 20 minutes at 4 ^{O}C. The supernatant was boiled on a heat block at 94^{o}C for 5 minutes and the protein concentration of the samples was then determined for future use. Samples that were not processed immediately, they were stored at -20 ^{o}C for a maximum of a month period.

2.5.2 PROTEIN QUANTIFICATION

The determination of protein concentration was performed using the DC Protein Assay Kit II (5000112 Bio-Rad), because of its compatibility with the SDS detergent present within the Extraction Buffer. The Lowry protein assay is a colorimetric detection method for quantifying the total level of protein in a solution and it is based on the reaction of protein with an alkaline copper tartrate solution along with Folin reagent.

The mechanism of action for colour development involves the reaction of copper ions with the protein peptide bonds within an alkaline environment and the subsequent reduction of a Folin-Ciocalteu reagent by the copper-treated protein.

5 µl of pre-boiled protein sample along with 25 µl of Reagent A and 200 µl of Reagent B were mixed in 96-well microplate format wells in triplicates and a series of bovine serum albumin (BSA) protein standards was also included,

ranging from 1.4 µg/µl to 25 ng/µl. Blank samples containing Laemmli Buffer were also included. After a 30 minutes incubation period at room temperature, the 96-well plate was horizontally shaken for 5 seconds and an absorbance reading at 750 nm was obtained (SpectraMax 190 Microplate Reader) taken also into account the absorbance readings of the blacks, which were subtracted from the standards and the protein samples readings. At next, a standard curve was generated from the proteins standards (SoftMax Pro Software 5.2 Rev C), for determination of the unknown concentration of the protein samples (Appendix E - Figure E-1). Ultimately, the samples were diluted with 2X Laemmli buffer to bring their concentration at 1 µg/µl.

2.5.3 SODIUM DODECYL SULPHATE-POLYACRYLAMIDE GEL ELECTROPHORESIS (SDS-PAGE)

For the casting of 1.5 mm vertical gels, the Mini-PROTEAN Tetra Electrophoresis System (165-8006, Bio-Rad) was utilised. For optimal separation of proteins in samples, varying percentages of resolving gel were produced, comprised of dH_2O, 0.375 M Tris-HCl pH 8.8, 8-12% (v/v) polyacrylamide (37.5:1 acrylamide:bisacrylamide) and 0.1% (w/v) SDS. In addition, 0.1% (w/v) ammonium persulphate and 0.1% TEMED was added, for polymerisation of the resolving gel to occur. Immediately, the gel was poured between the two vertical glass plates and 70% ethanol applied to the top for air bubbles removal. The approximate setting time of the gel was 20 minutes. Subsequently, the 70% ethanol was removed and the top of the gel flushed with water and allowed to be dried. A 5% stacking gel was then produced as before and further applied between the glass plates, consisted of 0.125 M Tris-HCl pH 6.8, 5.0% (v/v) polyacrylamide mix, 0.1% (w/v) SDS, 0.1% (w/v) ammonium persulphate and 0.1% TEMED. A 12-well comb was placed on the top and the gel was allowed to set for an additional 40 minutes.

In the interim, the protein samples at 1 µg/µl were mixed with protein loading buffer (Table 2-2) and the samples heated to 95 ^{o}C for 5 minutes and centrifuged. The sample loading volume into the cast wells was 20 µl, including a molecular marker (26620, PageRuler Plus Prestained Protein Ladder, Thermo Scientific) for determination of each protein according to their molecular weights. The

electrophoresis was performed in protein running buffer (Table 2-2) at 125 volts for approximately 1 hour. The bromophenol blue dye line was monitored for efficient electrophoresis.

2.5.4 PROTEIN TRANSFER TO NITROCELLULOSE MEMBRANE

After SDS-PAGE electrophoresis, the gel was equilibrated in transfer buffer (Table 2-2) for 5 minutes for removal of electrophoresis buffer salts and detergents. The nitrocellulose membrane that was used was Amersham Protran Premium (10600003 GE), with pore size of 0.45 μm. For the purposes of protein transfer to the membrane, the Trans-Blot SD Semi-Dry Transfer Cell (1703940 BIO-RAD) was used, employing the philosophy of semi-dry blotting; the platinum-coated titanium and stainless-steel electron pair provides efficient and background-free blotting. Before the assembly of the unit for standard transfer, the membrane and the filter papers were soaked into transfer buffer and all components along with the gel were fit together, according to the manufacturer's instructions. Mini-gels of 0.75 mm thickness were transferred for 15-30 minutes at 15 V. After the transfer procedure, the membrane was stained with Ponceau S solution to confirm successful protein transfer and then rinsed with water to remove the red staining.

2.5.5 IMMUNOLOGICAL DETECTION OF MEMBRANE BOUND PROTEIN

The nitrocellulose membranes containing the transferred proteins were blocked in TBS-T-BSA or TBS-T-milk solution for 1 hour at room temperature with shaking in a 2D rocker. Next, the membranes were incubated with the appropriate concentration of primary antibody in TBS-T-BSA (Table 2-3) and overnight at +4 oC with agitation. The following morning and after 4x5min washes with shaking in TBS-T, the membranes were incubated with the appropriate concentration of horseradish peroxidase conjugated (HRP) secondary antibody (Table 2-4) diluted in 5% TBS-T-milk, for 45 minutes in RT with agitation. A final series of 4x5min washes in TBS-T was repeated and the peroxidase activity of the secondary

antibody was detected utilizing the enhanced chemiluminescence (ECL, Pierce) system. The Detection Reagents 1 and 2 were combined in equal volumes and 1 ml per membrane was incubated on the membrane for 3 minutes at RT. The chemiluminescence activity was detected using X-Ray film (CL-XPosure Film PN34089, Fisher Scientific) and a film developer (AGFA Curix 60) in a dark room (Figure 2-1). The appropriate duration of film exposure was specific for each cell line and primary antibody used; the optimal exposure time for the project experimental conditions was selected for all presented figures. All samples were processed in triplicates.

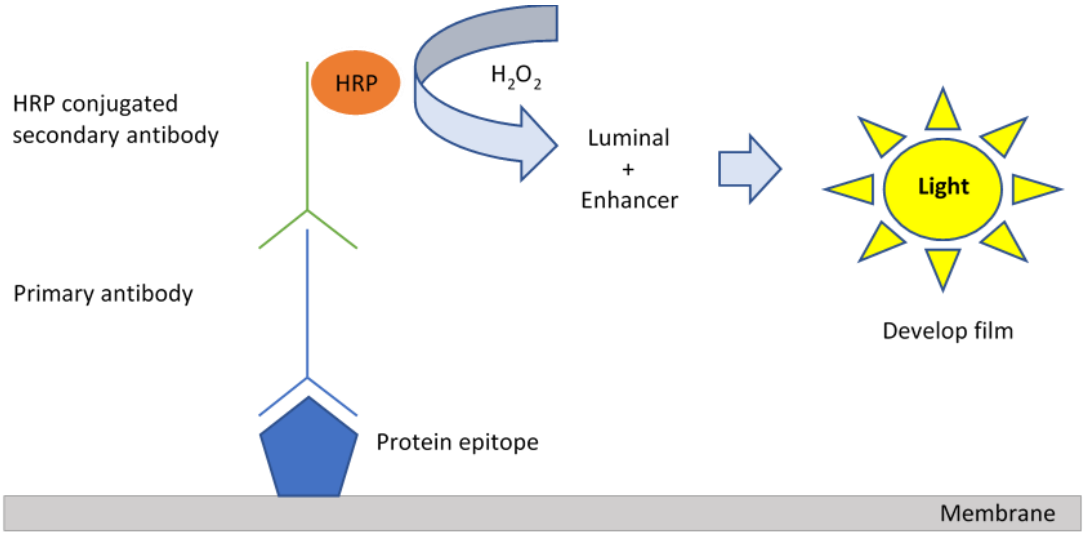

Figure 2-1 Protein detection of enhanced chemiluminescence (ECL).
The horse radish peroxidase (HRP) conjugated secondary antibody binds the primary antibody specific to the protein of interest and light is emitted, after HRP-catalysed oxidation of luminal in the presence of H_2O_2. Present to the reaction enhancers, such as modified phenols, increase and prolong the intensity of the emitted light.

The resulting visualised protein bands were scanned using a Cannon Pixma MG5550 and the density of the bands determined using the Image Studio Lite Ver. 5.2 software. The intensity and the area-covered of each protein band were then compared to control sample, followed by one-way ANOVA on the data in order to observe significant variation (P-value ≤ 0.05) in protein expression between sample types.

This method of X-ray film detection of chemiluminescence (via scanned film data) is semi-quantitative, because of the sigmoid response of the film, regarding the relationship of the signal to the amount of the analyte over a range of

concentration of analyte. A more linear approach for fluorescent quantitation is being suggested for future work, such as digital charge coupled devices (CCD) or other direct imaging devices like digital SLRs. This instrumentation will allow an increase in signal sensitivity, linearity and dynamic range, and a further decrease of laboratory costs associated with X-Ray film processing and chemical waste.

2.6 CO-IMMUNOPRECIPITATION ASSAY

The experimentation preceding the immunoprecipitation (IP) studies was involving transient transfections of selected cells with the plasmids of interest (Table 2-7). After a forty-eight hours incubation time, the media was removed from the transfected cells and the 10cm tissue culture dishes were placed on top of ice. Then, the cells were washed twice with ice-cold PBS and further removed by scrapping after the addition of 500 µl of ice-cold lysis buffer (Appendix A). The cells in the lysis buffer were kept ice-cold into 1.5 ml microcentrifuge tubes, before a three-cycles of 5 seconds sonication time with 3 seconds intervals on ice. After the sonication cycles, the cell lysates were vortexed and centrifuged at 17000 x*g* for 15 minutes at +4 ^{o}C for sedimentation of the insoluble materials. Again, the amount of protein present in the samples was quantified by the Lowry assay method.

Protein lysates were pre-cleared with Protein A or G sepharose beads alone, and 1 mg of protein extract was incubated with 2.5 µg of anti-c-myc antibody, 1µg of anti-flag antibody, 2 µg of anti-JAB1 antibody or 2 µg of anti-RAC1 antibody as negative control by rotation overnight at +4^{o}C. The antibody-lysate mixture was incubated with 50 µl of Protein A or G sepharose beads, pre-equilibrated with co-IP lysis buffer, for 5 hours at +4^{o}C. The beads were washed 4 times with 1 ml co-IP buffer without protease inhibitors, followed by centrifugation for 5 min at 500 g. The pellet was resuspended in 50ul 2X Laemmli Buffer (2%w/v SDS, 10%w/v glycerol, 50mM Tris pH 6.8, 0.025% w/v bromophenol blue, 1% v/v 2-mercaptoethanol), incubated at 96^{o}C for 10 min and centrifuged at 2500g for 3 min. The supernatant containing the immunoprecipitated proteins was then

analyzed by Western blotting (see section 2.2.1) looking for protein-protein interactions. Samples were processed in duplicate.

2.7 UBIQUITINATION ASSAY

HeLa cells were transiently transfected with Myc-tagged BMPR-II, Flag-tagged JAB1 and HA-tagged ubiquitin in the presence or absence of lactacystin. Forty-eight hours post-transfection, cell lysates were immunoprecipitated using anti-Myc tag antibody (SIGMA), boiled in SDS sample-loading buffer and re-precipitated prior to immunoblotting. The detection of ubiquitination of precipitated BMPR-II protein was observed after Western blotting with anti-HA (SIGMA) antibody, along with the exogenous expression levels of Myc-BMPR-II and Flag-JAB1 in cell lysates using antibodies against Myc or Flag (SIGMA), respectively. The degradation of BMPR-II was visualized by a distinctive ubiquitin smear on the membrane, after the Western blotting technique.

2.8 STATISTICAL ANALYSIS

One-way ANOVA or unpaired t-tests were performed on the densitometric analysis data of immunoblots, to test for significant variation between different sample types, with statistical significance identified when the P-value was ≤ 0.05.

In case of qPCR data analysis, one-way ANOVA and paired t-tests were performed on the relative quantification values of gene expression at different times or after various treatments at different times, with statistical significance identified when the P-value was ≤ 0.05.

In case of proliferation studies, two-way ANOVA and paired t-tests were performed on the data to test for significant variation between the cell counts or the various treatments at different times, with statistical significance identified when the P-value was ≤ 0.05.

The complete statistical analysis was performed using GraphPad Prism Version 6.01.

*** All the mentioned project experimentation has been conducted in triplicates and repeated thrice. The wide range of powerful and reproducible techniques described above have been established by myself under the supervision and guidance of Dr R.D. Machado and Dr L. Southgate, in the available facilities of the University of Lincoln and King's College London, UK.

CHAPTER 3: UBIQUITINATION AND DEGRADATION OF BMPR-II BY JAB1

3.1 INTRODUCTION

To interrogate the extent and nature of pathways key in regulation of the pulmonary circulation, a yeast two-hybrid screening experiment was conducted by Dr R.D. Machado (former primary supervisor of the project), using the catalytic kinase domain of BMPR-II as bait in a lung cDNA library (unpublished experimentation)*****. This approach facilitated the identification of JAB1 as a novel interacting protein partner, providing insight and potentiating the explanation of BMPR-II degradation via the proteasomal pathway in the normal circulation and, further, the currently unexplained elevated receptor loss in disease progression (Atkinson, Stewart et al. 2002). Of note, the biological relevance of JAB1 to TGF-β and BMP signalling is well established as it has been demonstrated to bind to and promote degradation via the proteasomal pathway of SMADs, 4, 5 and 7 (Wan, Cao et al. 2002, Haag, Aigner 2006, Kim, Lee et al. 2004). Through the yeast two-hybrid experiment, 5 clones of different lengths, were identified, encoding the JAB1 cDNA. Further GST pull-down assays, performed by Dr R.D. Machado and utilising the tagged BMPR-II kinase domain, have confirmed the interaction *in vitro* (Figure 3-1A)*****. Of note, immunofluorescence studies have demonstrated clear subcellular co-localization of the two proteins (Figure 3-1B – Unpublished Data)*****. Of interest, over-expression of JAB1 in HeLa cells alters the normal membrane-bound appearance of BMPR-II and, instead, appears to sequester the receptor adjacent to the nucleus analogous to co-localization between JAB1 and SMADs 5 and 7, a physical interaction culminating in degradation of both SMADs (Haag, Aigner 2006, Kim, Lee et al. 2004). Magnification of the co-localization indicates a significant and reproducible enrichment of both proteins in the peri-nuclear region (Figure 3-1B). Immunofluorescence of JAB1 with the non-interacting protein SMAD1 demonstrates a markedly different localization pattern with JAB1 predominantly dispersed in the cytoplasm and no evidence of co-aggregation (preliminary studies - data not shown). Further, JAB1 protein is overexpressed in a plethora of tumour types with implication in initiation and progression of several types of cancer by promoting cell proliferation, angiogenesis, stabilization of certain oncogenes and promoting degradation of tumour suppressor genes (Shackleford, Claret 2010, Fukumoto, Tomoda et al. 2006, Tsujimoto, Yoshida et

al. 2012, Hsu, Huang et al. 2008, Augeri, Langenfeld et al. 2016, Jumpertz, Hennes et al. 2014). Here, data is presented examining whether BMPR-II and JAB1 interact, whether JAB1 is overexpressed in *BMPR2* mutant PASMC cells, the impact of JAB1 overexpression in a cancerous cell line, and finally assessing whether JAB1 down-regulation of BMPR-II is dependent on its ability to target BMPR-II for ubiquitin conjugation.

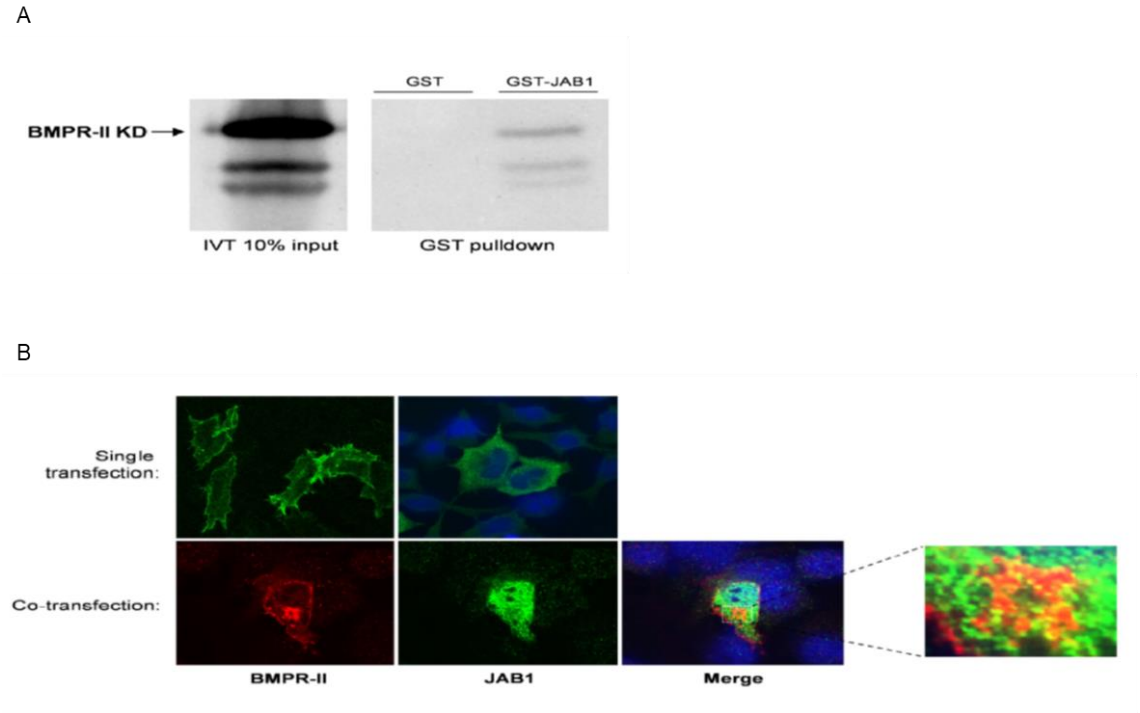

Figure 3-1 Validation of the interaction between BMPR-II and JAB1
A) Autoradiographs of the in vitro translated BMPR-II kinase domain (KD) used in GST pull-downs with GST alone and GST-JAB1. B) Subcellular localization of BMPR-II and JAB1 singly transfected (upper panels) and co-localisation of both proteins following co-transfection (lower panels). Data were provided by Dr Rajiv D. Machado with permission reprints.

***** The preliminary experimentation of this project, that is briefly mentioned in this PhD thesis sub-Chapter 3.1, was entirely conducted by Dr R.D. Machado et al., who also provided a summation of the resulted data as depicted in Figures 3-1 and 3-5. The Aims of this Chapter have been established after review on the significance of these novel data. This experimentation is currently unpublished.

3.2 AIMS

- To verify the interaction of JAB1 with BMPR-II *in vitro* and *in vivo* by co-immunoprecipitation and Western blotting analysis.
- To examine how ectopic expression of JAB1 affects BMPR-II intracellular levels, by transient transfection studies and Western blotting in cancerous generic cell line.
- To assess JAB1 expression in WT and mutant PASMC cells by Western blotting analysis.
- To validate enhanced proliferation rates of JAB1 transfected cells, by use of manual and MTT proliferation assays.
- To test the hypothesis that JAB1 down-regulation of BMPR-II is mediated via the proteasomal pathway, by Ubiquitination assay and further blockage of ubiquitination process by lactacystin, a well-studied inhibitor of the proteasomal pathway.

3.3 RESULTS

3.3.1 INTERACTION OF JAB1 WITH BMPR-II

3.3.1.1 CONFIRMATION *IN VITRO*

To verify the preliminary indication of potent JAB1 and BMPR-II interaction in mammalian cells, *in vitro* co-immunoprecipitations were conducted in a HeLa cell line. Myc-BMPR-II together with Flag-JAB1 constructs were co-electroporated in HeLa cells. Following a 48hours incubation period, the whole cell-lysates were immunoprecipitated by either anti-Flag (Figure 3-2A) or anti-Myc (Figure 3-2B) and then separated on an SDS-polyacrylamide gel and blotted to nitrocellulose. Immobilized Flag-JAB1 was incubated with either anti-Myc or anti-RAC1 (negative control) respectively. Reciprocally, immobilized Myc-BMPR-II was incubated with either anti-Flag or anti-RAC1 respectively. Thus, BMPR-II associated with JAB1 in HeLa cells when both proteins were overexpressed. The endogenous small GTPase protein RAC1 of the Rho family of GTPases was used as a negative control of the experiment, as there is no known, suspected or confirmed interaction with the BMP receptors.

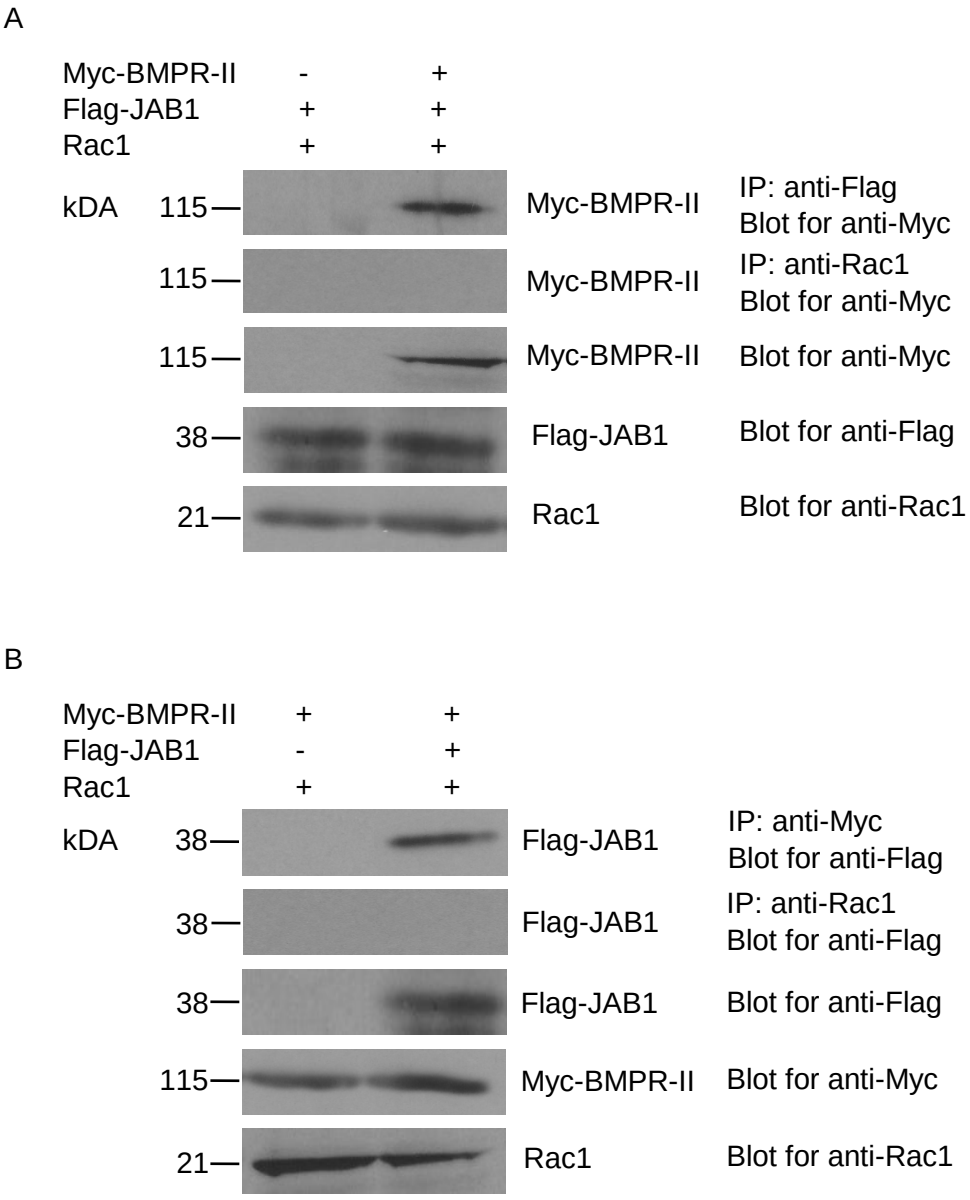

Figure 3-2 Interaction of Jab1 with BMPR-II *in vitro*
HeLa cells were transfected with 8μg Myc-BMPR-II, 6μg Flag-JAB1 and/or 6μg RAC1 (negative control) per 10-cm dish. Immunoprecipitation assays were performed using anti-Flag and anti-RAC1 (A) or anti-Myc and anti-RAC1 (B) antibody, and the immunocomplex was detected by western blotting using anti-Myc or anti-Flag antibody, respectively. The immunoblots revealed no interaction for the negative control RAC1. The expression levels of Myc, Flag fusion proteins and RAC1 in cells were also detected, as indicated in the lower panels.

3.3.1.2 CONFIRMATION *IN VIVO*

Most importantly, it has been also demonstrated that endogenous BMPR-II interacts with JAB1 in HeLa and HEK293T cancer cell lines. This has been validated by *in vivo* co-immunoprecipitation experimentation in the mentioned cell lines. Whole-cell lysates of cell monolayers in 80% confluence were immunoprecipitated with anti-JAB1 antibody and then separated on an SDS-polyacrylamide gel. The interaction of JAB1 with BMPR-II was analysed and confirmed in both cell lines, by Western blotting using an anti-BMPR-II antibody (Figure 3-3). Again, RAC1 was used as a negative control of the experiment.

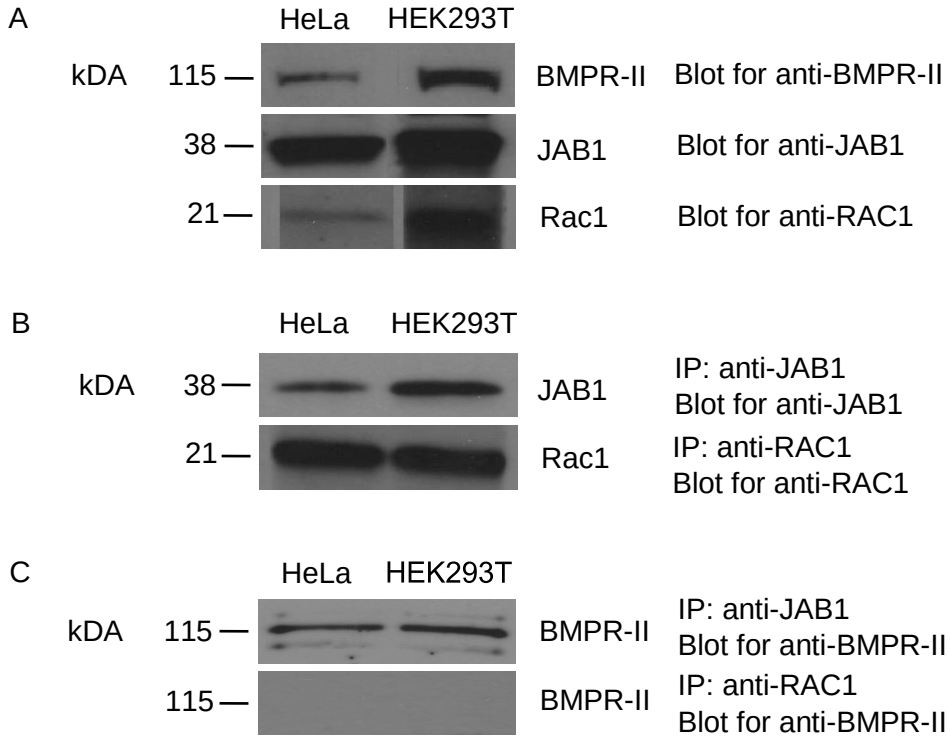

Figure 3-3 *In vivo* interaction of endogenous JAB1 with BMPR-II in HeLa and HEK293T cell lines
A) Immunoblots of endogenous BMPR-II, JAB1, and RAC1 in HeLa and HEK293T cell lines. B) Immunoprecipitation and Western Blotting of JAB1 and RAC1 in the above cell lines; anti-JAB1 and anti-RAC1 antibodies were used for both experiments to immunoprecipitate the endogenous proteins. C) Co-Immunoprecipitation of RAC1 and JAB1 probing for BMPR-II. The immunoblots revealed no interaction for the negative control RAC1 and strong interaction of JAB1 with BMPR-II in both cell lines.

3.3.2 DOWN-REGULATION OF BMPR-II BY JAB1

Since ectopic expression of JAB1 induces degradation of p53, $p27^{Kip}$, and SMADs 4, 5 and 7, it has been investigated whether JAB1 expression also affects the steady-state level of BMPR-II protein in HeLa cells. Titrated expression of increasing amounts of Myc-JAB1 resulted in a dose-depended significant decrease of BMPR-II in HeLa cells (Figure 3-4). Interestingly, JAB1 titrated over-expression decreased also the endogenous levels of SMAD5, a finding which correlates with previous evidence of JAB1 and SMAD5 protein-protein interaction and inhibition of BMP signalling (Haag, Aigner 2006). However, JAB1 expression did not decrease SMAD1 protein level, consistent with its inability to bind this SMAD, along with SMADs 2, 3 or SMAD6 (Kim, Lee et al. 2004). Densitometric and further statistical analysis was employed to show significant differences of BMPR-II and SMAD5 down-regulation (Figure 3-4B) after Myc-tagged JAB1 over-expression, compared with control groups (electroporated with empty vectors). These data suggest that JAB1 specifically targets BMPR-II protein for degradation, while having no effect on other highly homologous SMADs, apart SMAD5.

A. Immunoblot

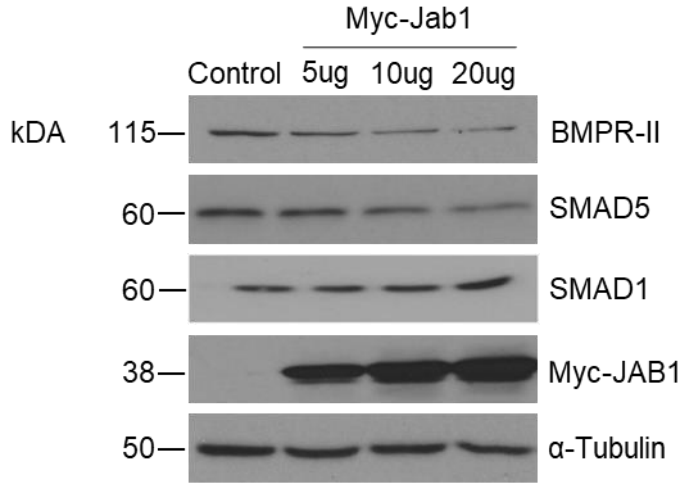

B. Densitometry

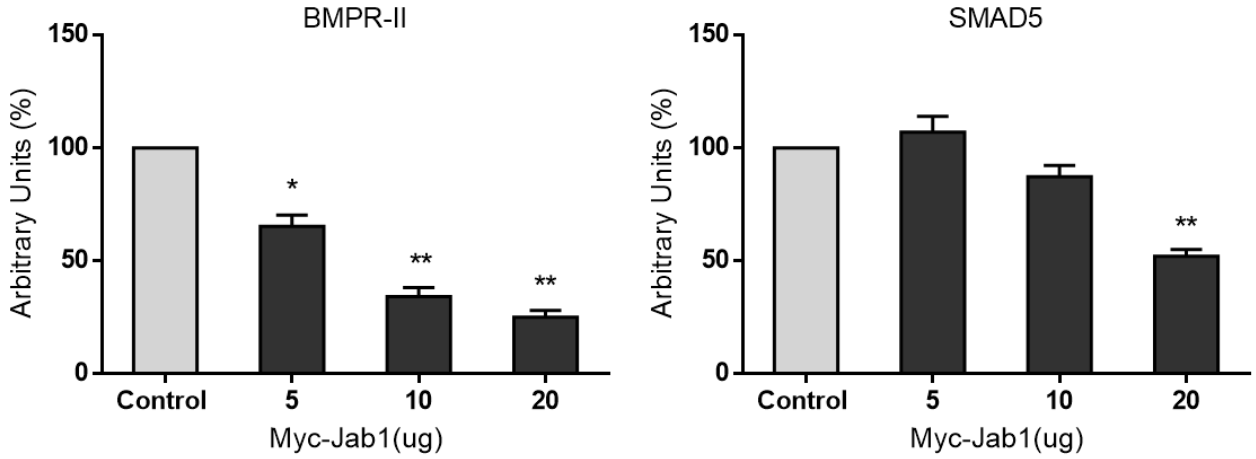

Figure 3-4 Down-regulation of BMPR-II and SMAD5 after ectopic expression of Myc-tagged JAB1

A. Immunoblots of endogenous BMPR-II, SMAD5 and SMAD1 following ectopic titrated expression of Myc-JAB1 vector or control plasmid in HeLa cell line. Ectopic expression of Myc-JAB1 decreases endogenous BMPR-II and SMAD5 steady-state levels, while SMAD1 remains unaffected. α-Tubulin was used as a loading control. B. Densitometric analysis in arbitrary units (%) from the immunoblots for BMPR-II and SMAD5. Data are means ±SD of 3 independent experiments; *P < 0.05 and **P< 0.01 vs the control group, RM one-way ANOVA.

3.3.3 JAB1 EXPRESSION IN WILD TYPE AND MUTANT PASMC

3.3.3.1 JAB1 PROTEIN EXPRESSION IS UP-REGULATED IN *BMPR2*-MUTANT CELLS *IN VIVO*

To elucidate the molecular consequence of JAB1 up-regulation and further impairment of the BMP signalling cascade, preliminary experimentation on primary PASMC cells, harbouring the HPAH-associated BMPR-II kinase domain missense mutation p.D485G, revealed enhanced JAB-1 expression when compared with healthy control cells (Figure 3-5A,B). Notably, the endogenous levels of the COP9 component CSN6 did not alter (Figure 3-5A, B), suggestive of a complex independent role of JAB1 in PAH progression. Furthermore, JAB1 expression mirrors BMPR-II expression in pulmonary arterioles (Figure 3-5C), only to enhance of its key role in BMPR-II regulation and disruption of the pulmonary vascular architecture resulting in perturbation of arterial tone and muscularization.

A. Immunoblot

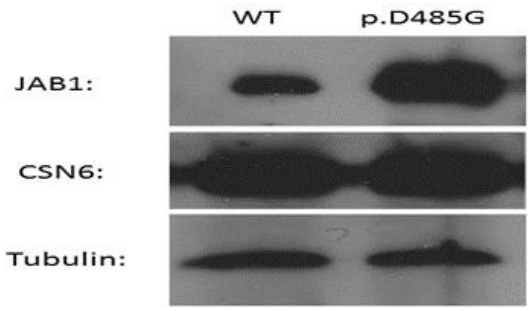

B. Densitometry

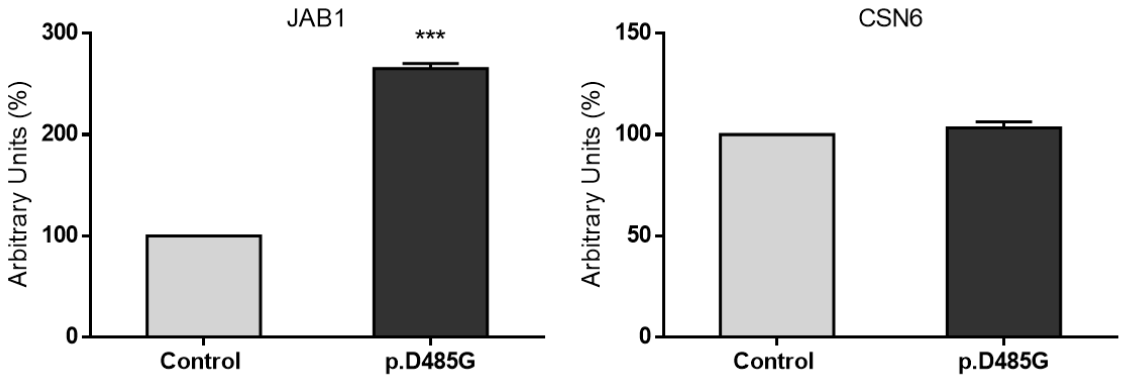

C. Immunohistochemistry

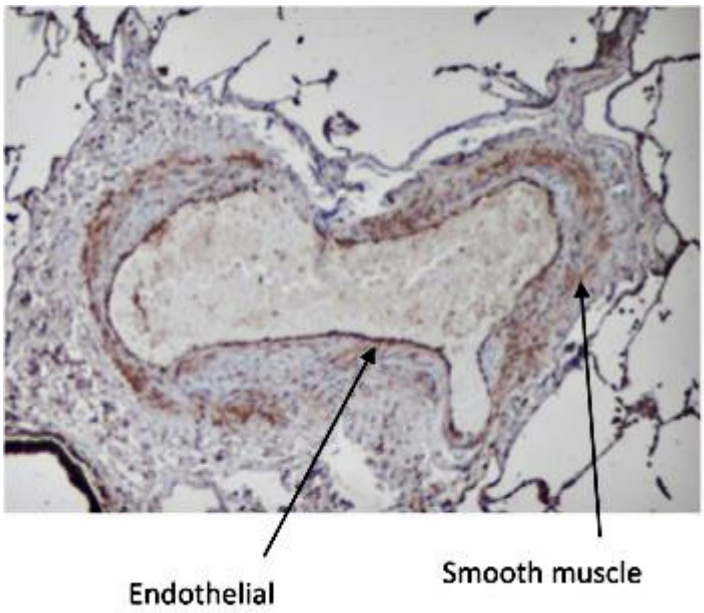

Figure 3-5 Endogenous JAB1 overexpression in Primary PASMCS harbouring p.D485G mutation

A. Preliminary experimentation revealed significant upregulation of endogenous JAB1 expression in primary PASMC-*BMPR2*$^{+/D485G}$ cells, while CSN6 levels remained

unaffected. B. Densitometric Analysis of JAB1 and CSN6. Data are means ±SD; ***P < 0.001 vs the control group, paired student-t-test. C. Immunohistochemistry of JAB1 in pulmonary arterioles demonstrating localisation to key sites of disease in PAH. Data provided by Dr Rajiv D. Machado with permission reprints.

3.3.3.2 *BMPR2*-MUTANTS STIMULATE JAB1 UP-REGULATION IN PASMC

Further *in vitro* studies were employed to investigate the potentiality of JAB1 up-regulation in the presence of PAH-associated BMPR-II mutations, as the previously described aspartate mutation p.D486G and the p.R899X, an arginine to termination tail mutation, which is a HPAH-associated recurrent dysfunction. Transfection studies with *BMPR2* constructs harbouring the missense p.D485G and the truncating p.R899X mutation accordingly, in primary WT PASMC cells, revealed significant JAB1 up-regulation in both cases (Figure 3-6). This finding comes in agreement with the preliminary *in vivo* observation, enhancing the novel regime hypothesis of dysregulated JAB1 expression in PAH cases harbouring BMPR-II specific mutations.

A. Immunoblot

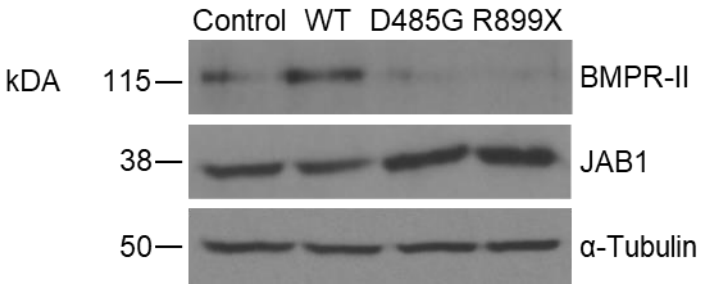

B. Densitometry

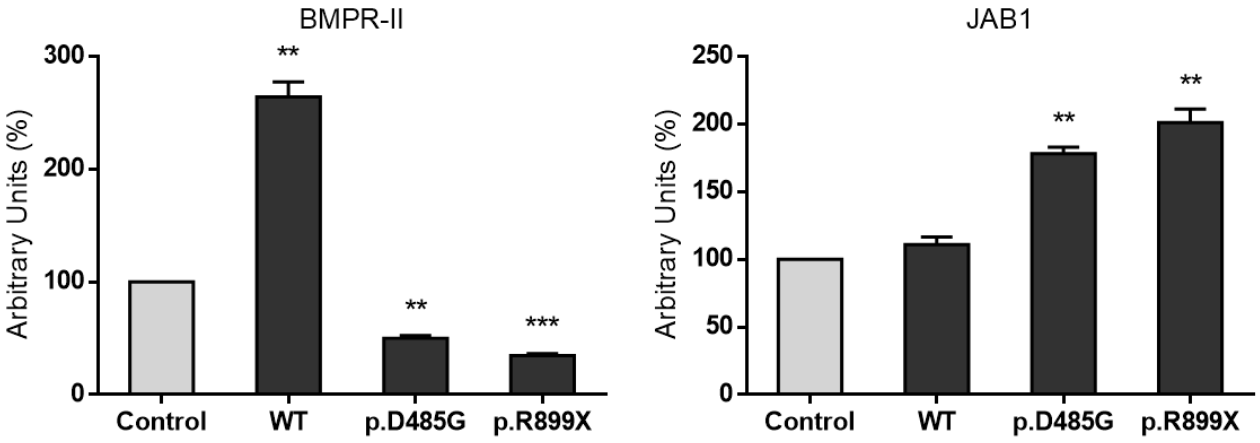

Figure 3-6 Transfection of mutant BMPR-II stimulates JAB1 up-regulation in Primary PASMCs

A. Over-expression (10ug/transfection) of p.D485G and p.R899X mutations of BMPR-II revealed significant upregulation of endogenous JAB1 protein expression in primary PASMC-*BMPR2*$^{+/+}$ cells; JAB1 levels remained unaffected when the cells were transfected with WT BMPR-II. In the cases of BMPR-II mutants, the subsequent endogenous increase of JAB1 protein resulted in a reciprocal decrease of BMPR-II receptor protein levels. Control cells were transfected with empty vector. B. Densitometric Analysis of BMPR-II and JAB1. Data are means ±SD of 3 independent experiments; **P < 0.01 and ***P<0.001 vs the control group, RM one-way ANOVA.

3.3.4 JAB1 PROMOTES PROLIFERATION IN *JAB1*-TRANSFECTED HELA CELLS

Since one of the many roles of JAB1 outside the CSN holo-complex is oncogenic through its contribution to dysregulation of the suppression mechanisms of cell proliferation, it was only rational to interconnect the down-regulation of BMPR-II due to enhanced JAB1 up-regulation in PASMC cells with their enhanced proliferation rates in PAH. For the purposes of proving the significantly increased proliferation rates of cells after over-expression of JAB1, a 5-day proliferation assay by manual counting was conducted in order to verify the suggested tumour inducer potential of JAB1, after transfection into HeLa cells. An increased pattern of cell proliferation was visible from day 3 onwards and significant differences in proliferation between control and JAB1 transfected cells were observed on day 4 and day 5 (adjusted P values < 0.0001) (Figure 3-7). The experiment was repeated in triplicate and the transfection efficiency of each experiment was evaluated through Western blotting analysis. Further MTT assay studies independently verified the same trend of increased proliferation in HeLa cells that were overexpressing JAB1. 4-day assays showed significant differences comparing control and JAB1 transfected cells (Figure 3-7B).

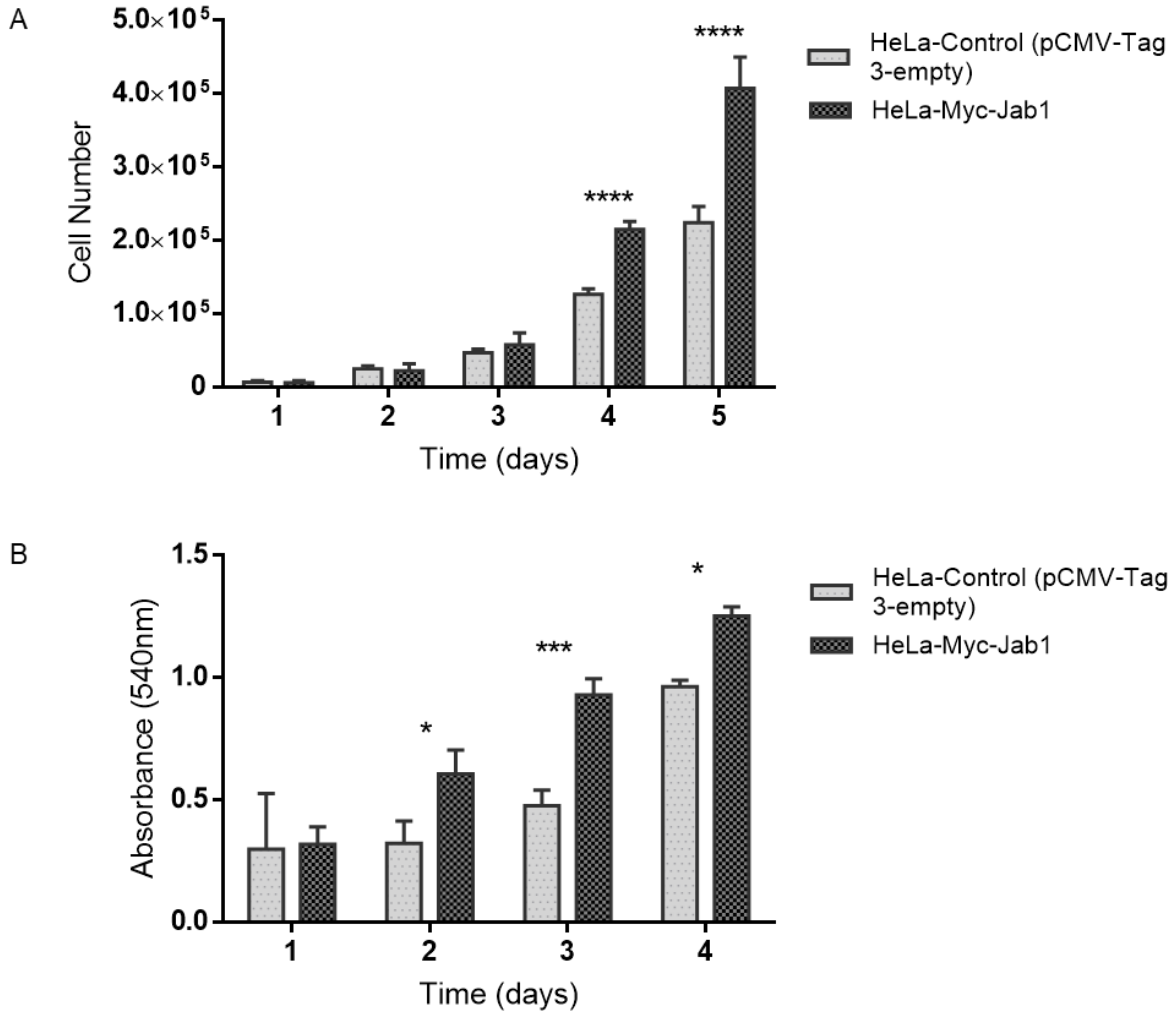

Figure 3-7 HeLa cells proliferation assays
A) A significant difference in proliferation between JAB1 transfected cells and control at days 4 and 5 was identified. B) MTT Proliferation Assays. A 4-day time-course revealed significantly increased proliferation of myc-JAB1 transfected cells at days 2, 3 and day 4 by comparison to control cells. All p values were calculated by Sidak's multiple comparison test in a 2-way Analysis of Variance (ANOVA).

Key: ****$p<0.0001$; ***$p=0.0002$; *$p\leq0.015$

3.3.5 JAB1 DRIVES BMPR-II UBIQUITINATION AND THE PROCESS IS REVERSED BY PROTEOLYTIC INHIBITION

Since ectopic expression of JAB1 induces degradation of BMPR-II, it is possible that JAB1 regulates BMP activity by also inducing degradation of BMPR-II in the BMP pathway. The interaction between JAB1 and BMPR-II suggests a mechanism of BMPR-II degradation. However, JAB1 is a component of COP9 signalosome in the nucleus, which is a multifunctional protein complex associated with regulation of protein stability, transcription, protein phosphorylation and intracellular distribution. Based on the initial preliminary findings of JAB1 and BMPR-II interaction and co-localization at the perinuclear region (Figure 3-1), all the above raised the question of whether COP9 signalosome complex is required for BMPR-II degradation. To ensure whether JAB1-dependent degradation of BMPR-II occurred through the 26S proteasome pathway, the turnover of BMPR-II in the presence and absence of lactacystin was assessed. Lactacystin inhibits protein degradation by the proteasome and JAB1-induced down-regulation of BMPR-II protein level was blocked by 20μM of lactacystin administration in HeLa cells that were over-expressing JAB1 (Figure 3-8B). Taking that into account, a ubiquitination assay was designed to assess whether the degradation of BMPR-II is mediated by the 26S proteasome. Proteins destined for degradation by the 26S proteasome are marked by covalent attachment of ubiquitin chains, which mediate recognition by the 26S proteasome. Thus, to investigate the ubiquitination of BMPR-II, an HA epitope-tagged version of ubiquitin was expressed along with Myc-BMPR-II and Flag-JAB1, and the levels of BMPR-II and ubiquitin conjugates were evaluated by immunoprecipitation with Myc antiserum followed by immunoblotting with anti-HA antibody (Figure 3-8). As shown in Figure 3-8, no BMPR-II ubiquitination was observed when HeLa cells over-expressed the HA-ubiquitin and the Myc-tagged version of BMPR-II. On the contrary, a fairly strong ladder of high-molecular-weight ubiquitin-conjugated BMPR-II products was observed when both Flag-JAB1 and HA-ubiquitin were ectopically expressed, alongside Myc-BMPR-II. This finding is the first reported indication that JAB1 could function as the first identified proteasomal-associated inhibitor of BMPR-II.

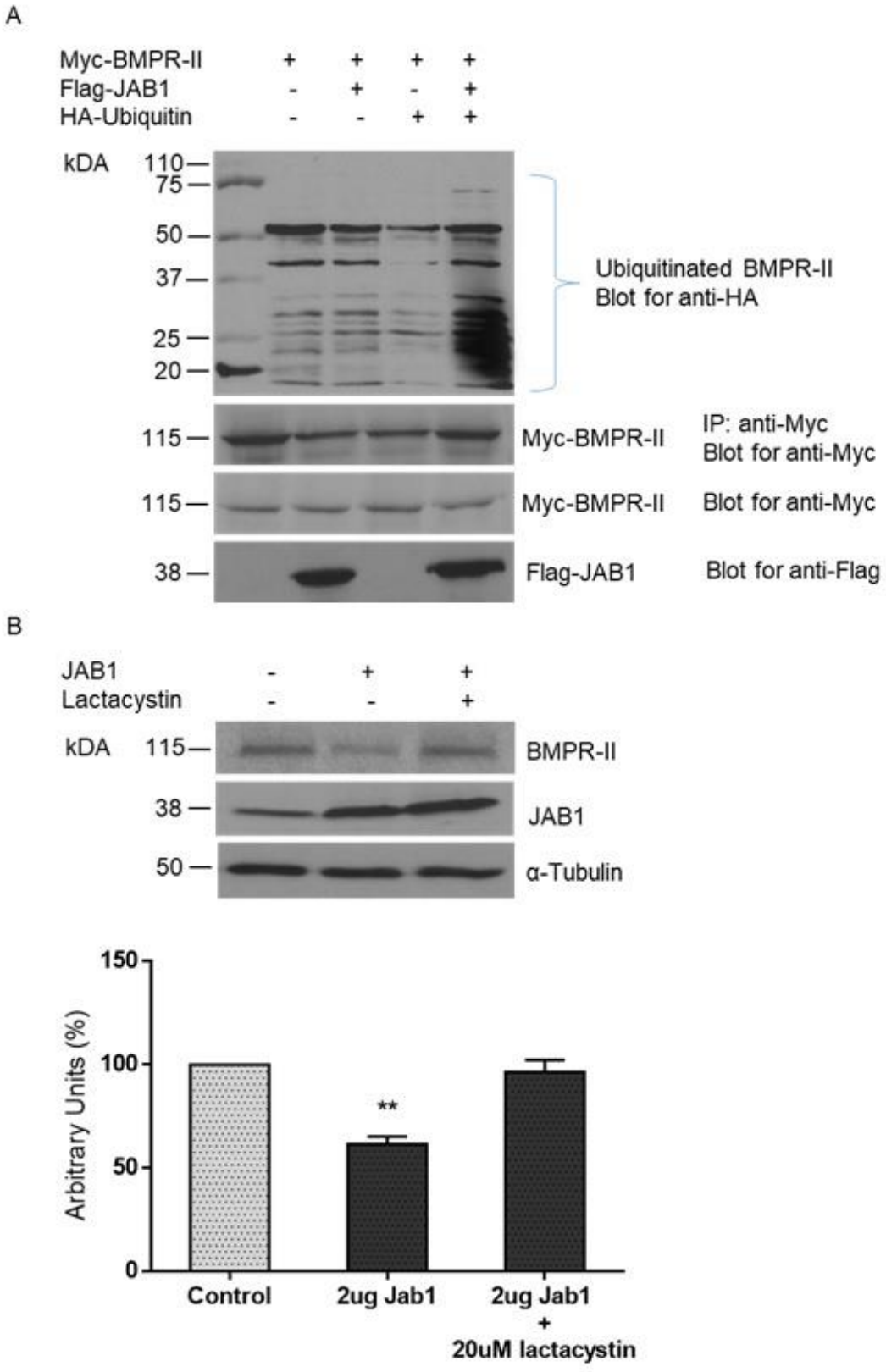

Figure 3-8 JAB1 induces degradation of BMPR-II through ubiquitination
A) Ubiquitynation of BMPR-II mediated by JAB1. HeLa cells were transfected with Myc-BMPR-II together with Flag-Jab1 or/and HA-Ubiquitin as indicated. Cell lysates were subjected to immunoprecipitation with Myc antiserum, boiled in SDS, and then re-

precipitated prior to immunoblotting. Protein expression was confirmed by immunoblotting total cell lysates. Non-specific binding of anti-HA antibody is also apparent. B) Degradation of BMPR-II is sensitive to 26S proteasome inhibitors. HeLa cells transfected with JAB1 were incubated with or without the proteasome inhibitor lactacystin (20 μM), and expression of endogenous BMPR-II was analyzed by immunoblotting and densitometry. Data are means ±SD of 3 independent experiments; **P< 0.01 vs the control group, RM one-way ANOVA.

The polyclonal anti-HA antibody (H6908, Sigma-Aldrich), that was utilized for the anti-HA blots, has an affinity for non-specific binding, ultimately increasing the background noise in the blot. This problem is evident in the company's website as well, in certain immunoprecipitation example cases. All the other co-IP blots of this study, utilizing anti-Myc and anti-Flag antibodies along with their secondary antibodies, were clean from non-specific bindings and background noise. If take into account that the same buffer recipes, IP and SDS-PAGE conditions (Table 2-2, Appendix A) along with the same nitrocellulose membrane (10600003, Amersham) and X-ray film were employed for this experiment as per all the other functional studies of this research, a greater dilution of the anti-HA and/or its secondary antibody could reduce the visual problem of non-specific banding in Figure 3-8A.

3.4 DISCUSSION

3.4.1 INTERACTION OF JAB1 WITH BMPR-II

It is widely accepted that a primary initiating factor for arterial tunica media/intima disorganization and PAH progression is loss of BMPR-II signalling (Long, Ormiston et al. 2015). *BMPR2* heterozygous mutations underlie more than 70% of HPAH and 25% of IPAH cases. Specifically, *BMPR2* nonsense mutations are likely to follow NMD pathway, and recurrent PAH-associated missense mutations of extracellular BMPR-II compartment or the kinase domain may never allow the receptor to reach the cell surface. Thus, BMPR-II haploinsufficiency is the main inherited mechanism of disease progression, contributing in the formation of pulmonary vascular lesions in PPH and vascular obliteration in severe PH

(Atkinson, Stewart et al. 2002, Machado, Pauciulo et al. 2001). BMPR-II is expressed predominantly in endothelium and in a lesser extend in vascular smooth muscle cells. However, BMPR-II expression in respiratory system is highly reduced in patients with severe PH, either harbouring heterozygous germline *BMPR2* mutations or in other mutation negative cases of primary PH (Atkinson, Stewart et al. 2002). Specifically, immunohistochemistry of PAH patient lung sections displayed a profound loss of BMPR-II beyond that which may be explained by haploinsufficiency. For that reason and to further investigate the unexplained receptor loss in PAH disease progression state, preliminary experimentation undertaken by Machado et al., identified JAB1 as a novel interacting protein partner of BMPR-II receptor, validating the interaction in vitro (Figure 3-1). Preliminary transient transfection and co-localization studies of JAB1 and BMPR-II, also undertaken by Machado et al., demonstrated the subcellular co-localization of both proteins at the perinuclear region of HeLa cells (Figure 3-1), a sequestration analogous to co-localization between JAB1 and other verified interacting proteins as p53, p27Kip and SMADs 4, 5 and 7 (Wan, Cao et al. 2002, Haag, Aigner 2006, Kim, Lee et al. 2004, Tomoda, Kubota et al. 2002, Chao 2015).

As a first aim of this study and to confirm the interaction of JAB1 with BMPR-II, co-immunoprecipitation studies were employed to validate the interaction *in vivo* and in *vitro* (Figures 3-2 and 3-3). The results indicated that JAB1 was vice versa immunoprecipitated with BMPR-II in both cases, thus this novel interaction was confirmed and opened the investigation of the potential down-regulation of the receptor by JAB1. Since ectopic expression of JAB1 is inducing the degradation of its targets in a plethora of cases (Shackleford, Claret 2010), it was also examined if JAB1 also affects the endogenous levels of BMPR-II in HeLa cell line. Figure 3-4 demonstrates that the expression of JAB1 reduced BMPR-II steady-state levels in a dose dependant manner, whereas SMAD1 levels remained unaffected as it is not a known target of JAB1. As expected, SMAD5 protein levels were also decreased verifying Haag et al., 2006 results and fulfilling the second aim of this project.

3.4.2 JAB1 EXPRESSION IN WT AND MUTANT PASMC

For the purposes of this study, it was vital to investigate if JAB1 was over-expressed in *BMPR2* mutant PASMC cells, in order to correlate the molecular consequence of the potential JAB1 up-regulation during disease progression with BMPR-II signalling impairment and further loss of the receptor. The *BMPR2* p.D485G KD mutation and p.R899X TD mutation were selected for screening of the JAB1 protein expression in primary PASMC cells, both *in vivo* and *in vitro* cases. The selection of the above mentioned mutations was made mainly because they are recurrent mutations in HPAH, allowing the receptor to reach the surface (no detected NMD in vitro), disrupting the SMAD1/5/8 signalling in the first case (p.D485G), while retaining it unaffected in the other (p.R899X) (Foletta, Lim et al. 2003, Machado, Aldred et al. 2006). Furthermore, the p.R899X tail mutation is causing disruptions to tail functions, including regulation of p38 and p42/44 MAPK (Rudarakanchana, Flanagan et al. 2002, Yang, Long et al. 2005) and interaction with LIMK (Foletta, Lim et al. 2003), c-Src (Yang, Long et al. 2005) and Tctex-1 (Machado, Rudarakanchana et al. 2003). Also, the PASMC cells was the model cells of choice because of their abnormal proliferation, de-differentiation, EC matrix production and significant contribution to the vascular lesions in PAH disease state (Morrell, Yang et al. 2001). Indeed, JAB1 protein expression in primary cells was upregulated *in vivo* and *in vitro*, comparing with healthy WT controls (Figures 3-5 and 3-6), whereas CSN6 protein levels remained unaffected, implying that the COP9 holo-complex is not participating in PAH progression, also suggesting a JAB1 independent role in disease state. This experimentation fulfilled the third aim of the project providing novel information about JAB1 dysregulation in PAH. A further final indication that JAB1 is up-regulated in primary endothelial and smooth muscle cells of pulmonary arteries in PAH is depicted in Figure 3-5C. This up-regulation mirrors BMPR-II expression and may contribute to disease progression by impairing the BMP signal and possibly by promoting the cells in a pro-proliferating or even hyper-proliferating state.

3.4.3 JAB1 CONTRIBUTION IN CELL PROLIFERATION

JAB1 as a monomer or a small complex outside the CSN holo-complex, specifically stabilizes via phosphorylation oncoprotein complexes of JNK, c-Jun or JunD with AP-1 sites contributing to cell proliferation, inhibits p53 and $p27^{Kip}$ function to induce G1 cell cycle arrest thus acting as positive regulator of cell cycle progression, acts as modulator of intracellular signalling by inducing degradation of key down-stream molecules as SMAD4, 5 and I-SMAD7 or stabilizing HIF-1α, and it is also involved in DNA damage-repair mechanisms by degrading 9-1-1 damage sensing complex or by promoting Rad51-mediated repair mechanism (Shackleford, Claret 2010, Chamovitz, Segal 2001, Tian, Peng et al. 2010). Thus, it is rational to characterize JAB1 as an onco-protein, which contributes to tumour cell proliferation and is over-expressed in many human cancers including breast, colon, pancreatic and lung carcinomas (Yoshida, Yoneda-Kato et al. 2010). Interestingly, the vascular proliferation in PPH is monoclonal, which is evocative of neoplastic proliferation, in contrast to the polyclonal cell proliferation in secondary PP (Waite, Eng 2003). It is also believed that the PAH-associated vascular proliferation is monoclonal due to the *BMPR2* haploinsufficiency model that leads to early neoplastic-like vascular proliferation (Waite, Eng 2003, Machado 2012). For the purposes of the forth aim of the project and in order to validate the tumorigenic potential of JAB1 protein, the proliferation of HeLa cells after human JAB1 ectopic expression was monitored in by manual cell counting or MTT assays (Figure 3-7). Indeed, the transfected cells exhibited enhanced proliferation as expected. Taken together, the observation that JAB1 protein is over-expressed during PAH progression and the fact that JAB1 promotes uncontrolled cell proliferation and survival, underlines the significance of this molecule in the vasculature and sets it as a potential novel target in cancer therapy, and for drugs against PASMC cells in pro-proliferating state harbouring or not *BMPR2* PAH-associated mutations.

3.4.4 UBIQUITINATION AND DEGRADATION OF BMPR-II BY JAB1

To interrogate the hypothesised proteolytic mechanism of identified BMPR-II down-regulation, by JAB1 protein-protein interaction and subsequent proteasomal degradation, it was vital to ensure that the decrease in BMPR-II steady-state levels is mediated by the 26S proteasome. Thus, the proteasomal inhibitor lactacystin was added to HeLa cells transfected with human JAB1. Interestingly, JAB1-induced down-regulation of BMPR-II protein level was blocked by lactacystin (Figure 3-8B). Proteins destined for degradation by the 26S proteasome are marked by covalent attachment of ubiquitin chains. Obviously, the degradation of BMPR-II is mediated by the 26S proteasome. Subsequently, an *in vitro* ubiquitination assay was designed in order to be evidenced whether enhanced BMPR-II turn-over by JAB1 is through its ability to promote the ubiquitination of BMPR-II. As expected, JAB1 down-regulation of BMPR-II and its subsequent degradation was mediated via the proteasomal pathway in case of JAB1 over-expression (Figure 3-8), fulfilling the last aim of the project and verifying the initial hypothesis.

This novel identified mechanism in which BMPR-II is targeted by JAB1 for proteasomal degradation is the second indication of the proteolytic degradation of BMP receptors, as it has also been identified that Smurf1 ubiquitin ligase causes down-regulation of BMPR-II and interestingly, its degradation is induced in cases of monocrotaline and hypoxia models of PAH (Murakami, Mathew et al. 2010). This finding correlates with a report that identifies Tribbles-like protein 3 (Trb3) as a BMPR-II TD-interacting protein, in which upon BMP stimulation its dissociation from the TD triggers Smurf1 degradation, thus resulting in stabilization of the BMPR-II receptor (Chan, Nguyen et al. 2007). In contrast of the above observations and against the verified BMPR-II proteasomal degradation, it has also been proposed that a lysosomal degrative pathway is regulating BMPR-II expression (Durrington, Upton et al. 2010). Further studies showed that the lysosomal inhibitor chloroquine increased cell surface BMPR-II levels and restored BMP9 signalling in EC cells harbouring *BMPR2* mutations (Dunmore, Drake et al. 2013). In comparison to this study, it has been also shown that BMPR-II could be degraded by the proteasomal pathway. This post-

translational modification of the WT receptor, driven by JAB1 protein, is a finding which also explains its further loss in PAH progression, in cases whether BMPR-II is mutated or not.

3.5 CONCLUSION AND FURTHER WORK

This report facilitated the identification of a BMPR-II novel interacting protein partner, namely JAB1, which though association with the kinase domain of the receptor, functions as the first identified proteasomal-associated inhibitor of BMPR-II. Dysregulation of JAB1 is a major factor in disruption of the pulmonary vasculature architecture, resulting in perturbation of arterial tone and muscularization. Furthermore, the linked experimental data of this report are indicative of BMPR-II degradation via the proteasomal pathway in the normal circulation and, finally, the up to date unsolved elevated receptor loss in disease progression could be explained through the identified protein-protein interaction with JAB1.

The proposed future directions, based on these findings, include the determination of the minimal JAB1 interacting regions, by domain, with the BMPR-II receptor and the definition of the real-time interaction of BMPR-II with JAB1 by fluorescence resonance energy transfer (FRET) analysis. Given the fact that PAEC cells are the primary site of disease in PAH (Long, Ormiston et al. 2015), blood outgrowth endothelial cells (BOEC) harbouring mutation specific classes (i.e. missense/truncating) could be utilised to determine JAB1 status across the *BMPR2* mutation spectrum, and further JAB1 expression and localization. BOEC cells could be also utilised to analyse proliferation, migration and adhesion in the context of JAB1 down-regulation in HPAH, and also to extend this analysis in idiopathic disease (mutation-negative) to assess ubiquity of JAB1 down-regulation (Atkinson, Stewart et al. 2002). Finally, co-immunoprecipitation studies could be undertaken in order to assess the JAB1 potential interactions with BMP type I receptors, such as BMPR1A, -1B and ALK1, and if detected, repeat the experiments described above with these additional molecules. If to continue working in the field, a recommended allowing suitable time for the

above-mentioned experimentation, would be a 2-year study, as this was the time frame for the evolution of the research described in the current chapter.

CHAPTER 4: DIFFERENTIAL REGULATION OF BMP/TGF-β SIGNALLING BALANCE BY JAB1 AND BMPR-II INTERACTION

4.1 INTRODUCTION

Following the proven down-regulation of BMPR-II by JAB1 via the proteasomal pathway, a more comprehensive analysis was undertaken to assess the dysregulation of BMP canonical signalling, after the verified loss of the receptor. To underline the fact that this effect belongs to a model post-translational modification of BMPR-II, a HeLa generic cell line was selected to impact the severity of BMP signal loss and more specifically of its signalling intermediaries.

Based on the initial findings of JAB1 up-regulation in primary PASMC cells harbouring the p.D485G KD of BMPR-II and the concomitant *in vitro* work of inserting the p.D458G mutation and the p.R899X TD mutation in primary PASMC cells following observation of the increased levels of JAB1 protein expression, the p.W9X nonsense mutation of the extra-cellular ligand-binding domain of BMPR-II was selected and investigated in terms of proliferation, defective BMP signalling (intermediaries and down-stream target), endogenous JAB1 protein expression and TGF-β signalling. The p.W9X mutation is related to HPAH and is frequently recurrent in patients with PAH (Machado, Aldred et al. 2006). In addition, a first approach to reverse the proliferation potential of p.W9X mutants was also addressed by enhancing the BMP pathway with BMP4-ligand stimulation. While the reduced antiproliferative effect of BMP-ligand stimulation of BMP pathway in PAH-associated mutant PASMC and PAEC cells has already been demonstrated alone or with reference to various drug approaches like iloprost (Yang, Li et al. 2010, Yang, Li et al. 2013, Waite, Eng 2003), herein a manual proliferation assay on patient p.W9X PASMC cells treated specifically with BMP4 alone, was employed to verify the potential BMP signalling enhancement and reversal of PAH phenotype.

Recent evidence suggests that alternate pathways, independent of BMP-related SMADs, are critical to the context-specific nature of TGF-β superfamily signalling. These alternative SMAD-independent signalling cascades include kinases such as ERK1/2, JNK, TAK1 and p38 MAPK (Awad, Elinoff et al. 2016). Therefore, it is crucial to investigate the potential dysregulation of p38 MAPK, which has been shown to be up-regulated after functional loss of the BMPR-II receptor in PAH cases following PAH-associated *BMPR2* mutations (Rudarakanchana, Flanagan

et al. 2002). For the purposes of this investigation, the model cell line which was selected for experimentation was again the same cancerous cell line, in order to potentiate the activation of p38 MAPK signalling, a SMAD-independed signalling cascade after JAB1 mediated down-regulation of BMPR-II. Subsequently, p38 MAPK potential induction was investigated in PAH p.W9X mutant PASCM cells in order to correlate the results with the cancer cell line. Furthermore, previous studies have addressed the activation of canonical TGF-β signalling cascade, in cells where JAB1 targets the inhibitory SMAD7 for degradation, or the regulation of TGF-β and the BMP signalling, because of the common-SMAD4 and SMAD5 degradation after JAB1 over-expression (Haag, Aigner 2006, Wan, Cao et al. 2002, Kim, Lee et al. 2004). Putting that into context, a full expression profile analysis of endogenous levels of BMP/TGF-β intermediaries, p38 MAPK and TAK1, along with JAB1 and BMPR-II protein expression, was carried out in p.W9X PASMC cells, to determine potential activation of SMAD-dependent or SMAD-independent BMP/TGF-β signalling outcomes. To end this, a similar investigation in the BMP/TGF-β-dependent or independent signalling, after JAB1 mediated down-regulation of BMPR-II, was undertaken in HeLa cell line.

Finally, to investigate whether JAB1 down-regulation could effectively reverse the abnormal proliferation of primary PASMC-*BMPR2*$^{+/W9X}$ mutants, the RNA interference technique was employed to specifically deplete the JAB1 protein in both p.W9X and healthy human PASMCs.

4.2 AIMS

- To assess BMP defecting signalling and p38 MAPK pathway activation in Hela cells after ectopic JAB1 overexpression, by transient transfection studies and Western blotting analysis.
- To examine and validate the antiproliferative effect of BMP4-ligand stimulation on PASMC-*BMPR2*$^{+/W9X}$ cells, by manual counting assays.
- To assess *JAB1* mRNA and protein expression levels in PASMC-*BMPR2*$^{+/W9X}$ mutants, by qPCR and Western blotting analysis respectively.
- To profile BMP/TGF-B signalling cascades in PASMC-BMPR2+/^{W9X} cells, by Western blotting analysis
- To investigate the potential differential regulation of BMP/TGF-B signalling balance in a SMAD-dependent and SMAD-independent manner, by JAB1 and BMPR-II interaction in HeLa cell line, by transfection studies and Western blotting analysis.
- To reverse the abnormal proliferation of PASMC-*BMPR2*$^{+/W9X}$ mutants via JAB1 protein knock-down, by RNA interference and further MTT proliferation assay assessment.

4.3 RESULTS

4.3.1 JAB1-MEDIATED SUPPRESSION OF THE BMP SIGNALLING PATHWAY

4.3.1.1 JAB1 OVER-EXPRESSION LEADS TO REDUCED BMP SIGNALLING

In order to assess the potential dysregulation of BMP signalling after the verified loss of expression of the BMPR-II receptor preceded by ectopic over-expression of JAB1, the protein levels of phosphorylated SMAD1/5 were assessed through Western blotting analysis in HeLa cells. The p-SMAD1/5 levels were significantly down-regulated in both titrated and non-titrated manners of JAB1 overexpression after BMP4 ligand stimulation (Figures 4-1 and 4-3). The down-regulation of SMAD5 was also observed, verifying the previous experimentation.

4.3.1.2 JAB1 OVER-EXPRESSION PROMOTES DOWN-REGULATION OF P38 MAPK

To define abnormalities in alternate pathways specific to down-regulation of BMPR-II after ectopic over-expression of JAB1, the expression of p38 MAPK, which is an important mediator of BMP non-canonical signalling, was analysed in HeLa cells. Interestingly, the levels of phosphorylated p38 MAPK protein were significantly down-regulated in the presence of excess JAB1 and the down-regulated WT receptor (Figure 4-2). This finding was also consistent after stimulation with BMP4 ligand and activation of the BMP pathway in both titrated and non-titrated manners of JAB1 overexpression (Figures 4-1 and 4-3), which in this case was also disrupted due to down-regulated BMPR-II expression.

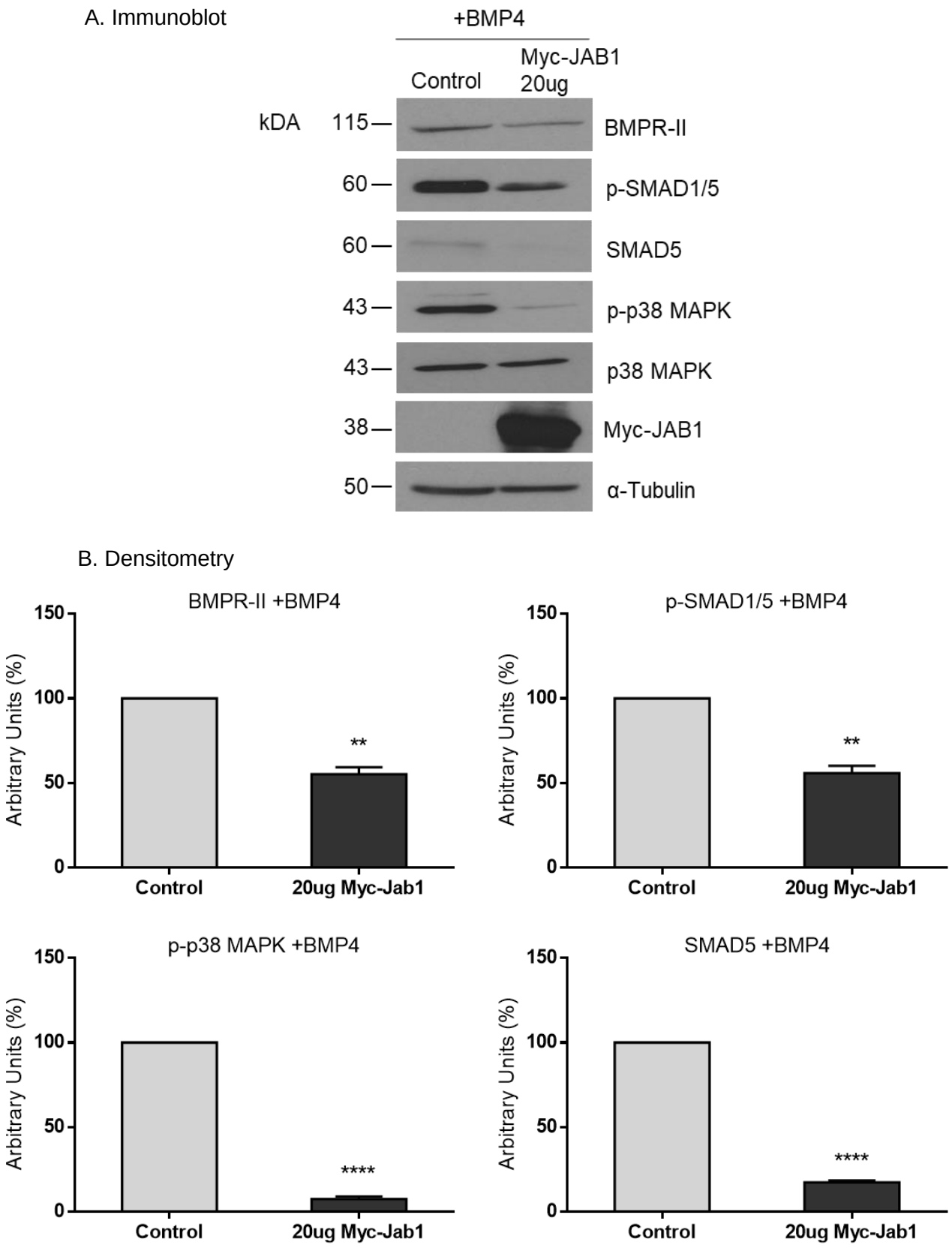

Figure 4-1 Down-regulation of BMPR-II, p-SMAD1/5, SMAD5 and p-p38 MAPK after ectopic expression of JAB1 stimulated with BMP4

A) A. Immunoblots of endogenous BMPR-II, p-SMAD1/5, SMAD5, p-p38 MAPK and p-38 MAPK following ectopic over expression of JAB1 vector or control plasmid in HeLa cell line. Ectopic expression of JAB1 decreases endogenous BMPR-II, p-SMAD1/5, SMAD5 and p-p38 MAPK steady-state levels, while p-38 MAPK remains unaffected. α-Tubulin was used as a loading control. B. Densitometric analysis in arbitrary units (%) from the immunoblots for BMPR-II, p-SMAD1/5, SMAD5 and p-p38 MAPK. Data are means ±SD of 3 independent experiments; **P < 0.01 and ****P<0.0001 vs the control group, paired student-t-test.

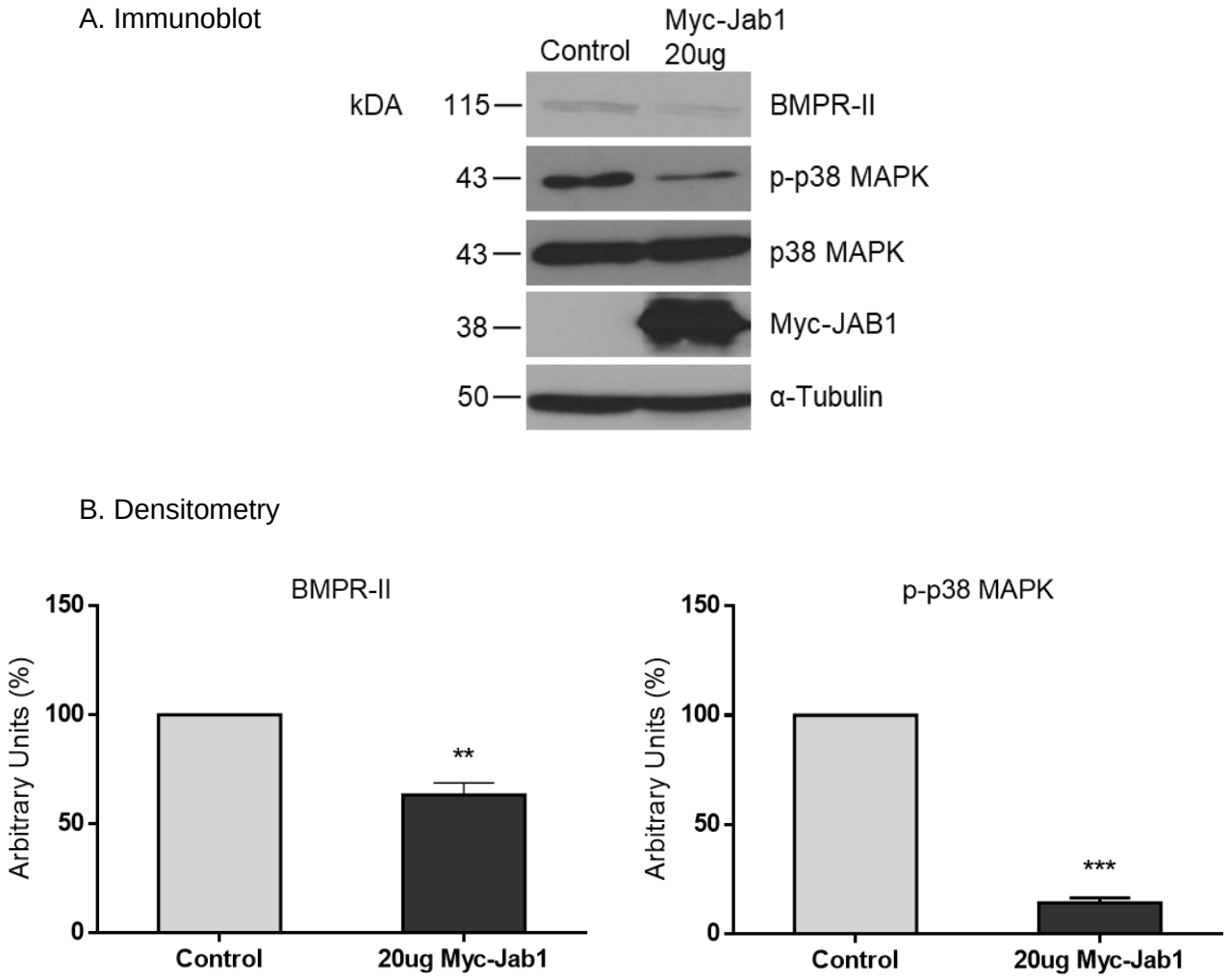

Figure 4-2 Down-regulation of BMPR-II and p-p38 MAPK after ectopic expression of JAB1

A. Immunoblots of endogenous BMPR-II, p-p38 MAPK and p-38 MAPK following ectopic overexpression of JAB1 vector or control plasmid in HeLa cell line. Ectopic expression of JAB1 decreases endogenous BMPR-II and p-p38 MAPK steady-state levels, while p-38 MAPK remains unaffected. α-Tubulin was used as a loading control. B. Densitometric analysis in arbitrary units (%) from the immunoblots for BMPR-II and p-p38 MAPK. Data are means ±SD of 3 independent experiments; **P< 0.01 and ***P < 0.001 vs the control group, paired student-t-test.

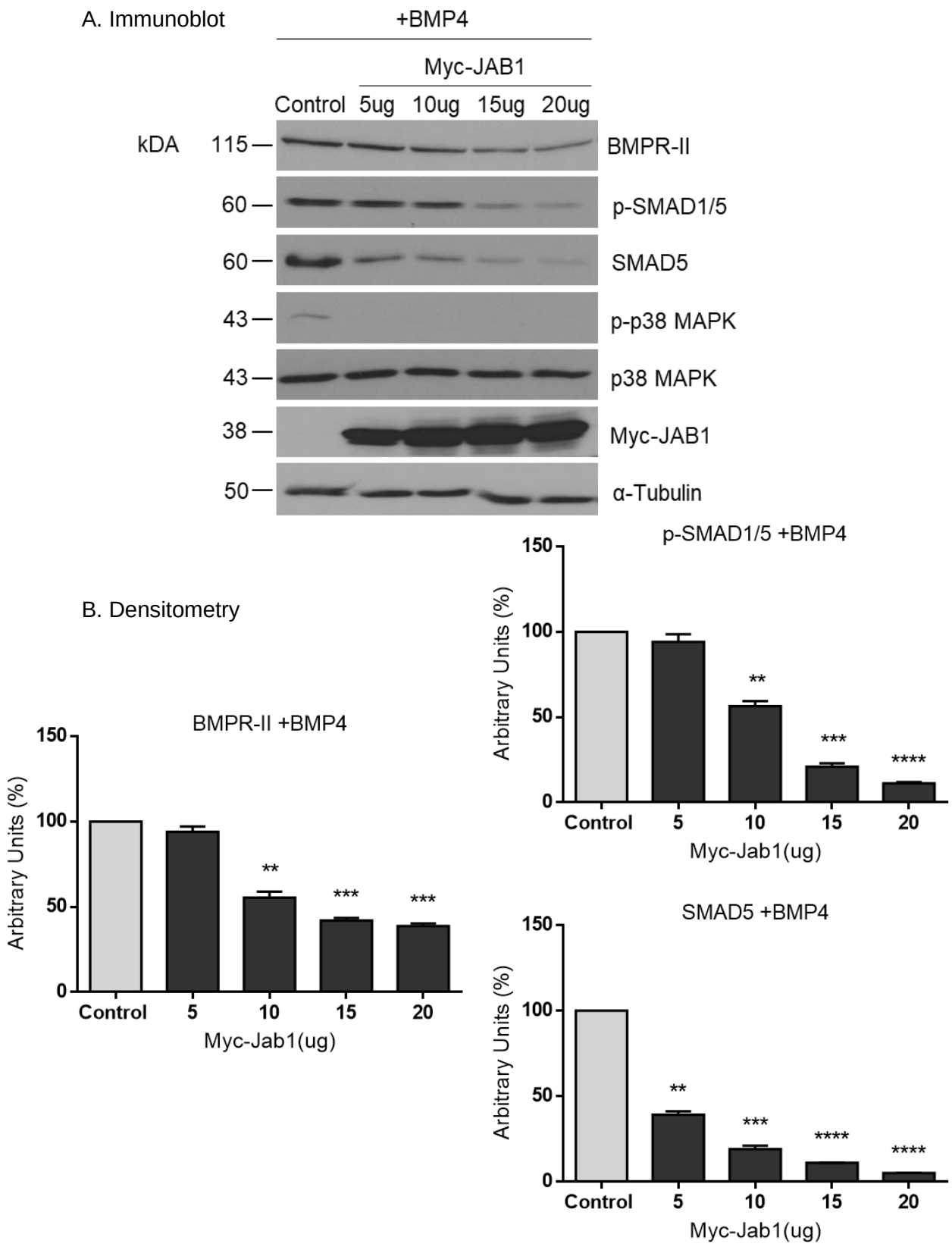

Figure 4-3 Down-regulation of BMPR-II, p-SMAD1/5, SMAD5 and p-p38 MAPK after ectopic expression of JAB1 stimulated with BMP4
A. Immunoblots of endogenous BMPR-II, p-SMAD1/5, SMAD5, p-p38 MAPK and p-38 MAPK following ectopic titrated expression of JAB1 vector or control plasmid in HeLa

cell line. Ectopic expression of JAB1 decreases endogenous BMPR-II, p-SMAD1/5, SMAD5 and p-p38 MAPK, steady-state levels, while p-38 MAPK remains unaffected. α-Tubulin was used as a loading control. B. Densitometric analysis in arbitrary units (%) from the immunoblots for BMPR-II, p-SMAD1/5 and SMAD5. Data are means ±SD of 3 independent experiments; **P < 0.01, ***P< 0.001 and ****P<0.0001 vs the control group, RM one-way ANOVA.

4.3.2 JAB1 UP-REGULATION IS BMPR-II MUTATION SPECIFIC

4.3.2.1 ABNORMAL PROLIFERATION OF PRIMARY PASMC-*BMPR2*$^{+/W9X}$ MUTANTS AND INHIBITION OF PROLIFERATION WITH SELECTIVE BMP4 TREATMENT.

The analysis of the rates of proliferation between healthy primary PASMC cells and PASMC cells harbouring the *BMPR2* p.W9X mutation, was assessed after a 4 days proliferation assay in 12-well plates (Figure 4-4). The enhanced proliferation rate of the *BMPR2*$^{+/W9X}$ cells when compared to WT cells, was visible even from the second day of the manual counting (adjusted P value <0.0001), maintaining the significant proliferation rate until the last day of the experiment. In a parallel experiment, primary PASMC-*BMPR2*$^{+/W9X}$ cells incubated with conditioned smooth muscle growth media (SmGM-2, Lonza) enhanced with 10ng/ml of BMP4, exhibited no significant proliferation when compared with healthy primaries. (Figure 4-4).

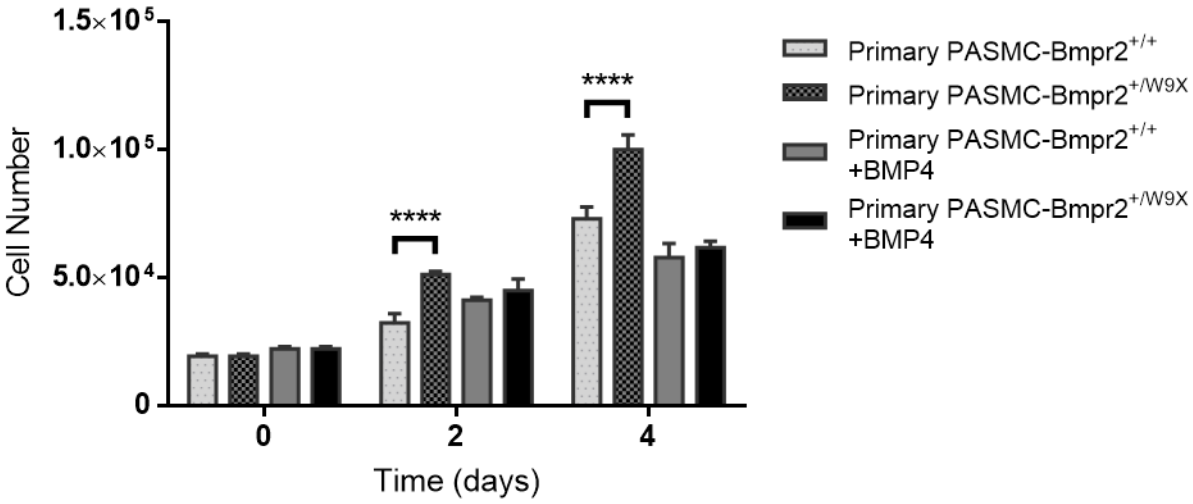

Figure 4-4 Primary PASMC proliferation assay harbouring BMPR-II p.W9X mutation
A significant difference in proliferation between PASMC *BMPR2*$^{+/+}$ and *BMPR2*$^{+/W9X}$ cells at days 2 and 4 was identified. A 4-day time-course revealed no significantly increased proliferation of WT and mutant cells when treated with 10 ng/ml BMP4. Data are means ±SD of 3 independent experiments; P values were calculated by Sidak's multiple comparison test in a 2-way Analysis of Variance (ANOVA).
Key: ****p<0.0001

4.3.2.2 DEFECTIVE BMP SIGNALLING AND JAB1 EXPRESSION PROFILE IN PRIMARY PASMC-*BMPR2*$^{+/W9X}$ MUTANTS

As expected, primary PASMC-*BMPR2*$^{+/W9X}$ mutants exhibited a heavily impaired BMP signalling, as it was verified by both quantitative RT-PCR for the BMP-responsive element ID1 (Figure 4-5), a main target gene of BMP signalling, and Western blotting analysis for phosphorylated levels of SMAD1/5 proteins (Figure 4-6), with or without BMP4 ligand stimulation. Surprisingly, the levels of *JAB1* mRNA expression were significantly reduced in the p.W9X cells, regardless of BMP4 stimulation (Figure 4-5). On the contrary, the JAB1 protein levels remained unaffected in PASMC-*BMPR2*$^{+/W9X}$ mutants compared with WT healthy primary cells.

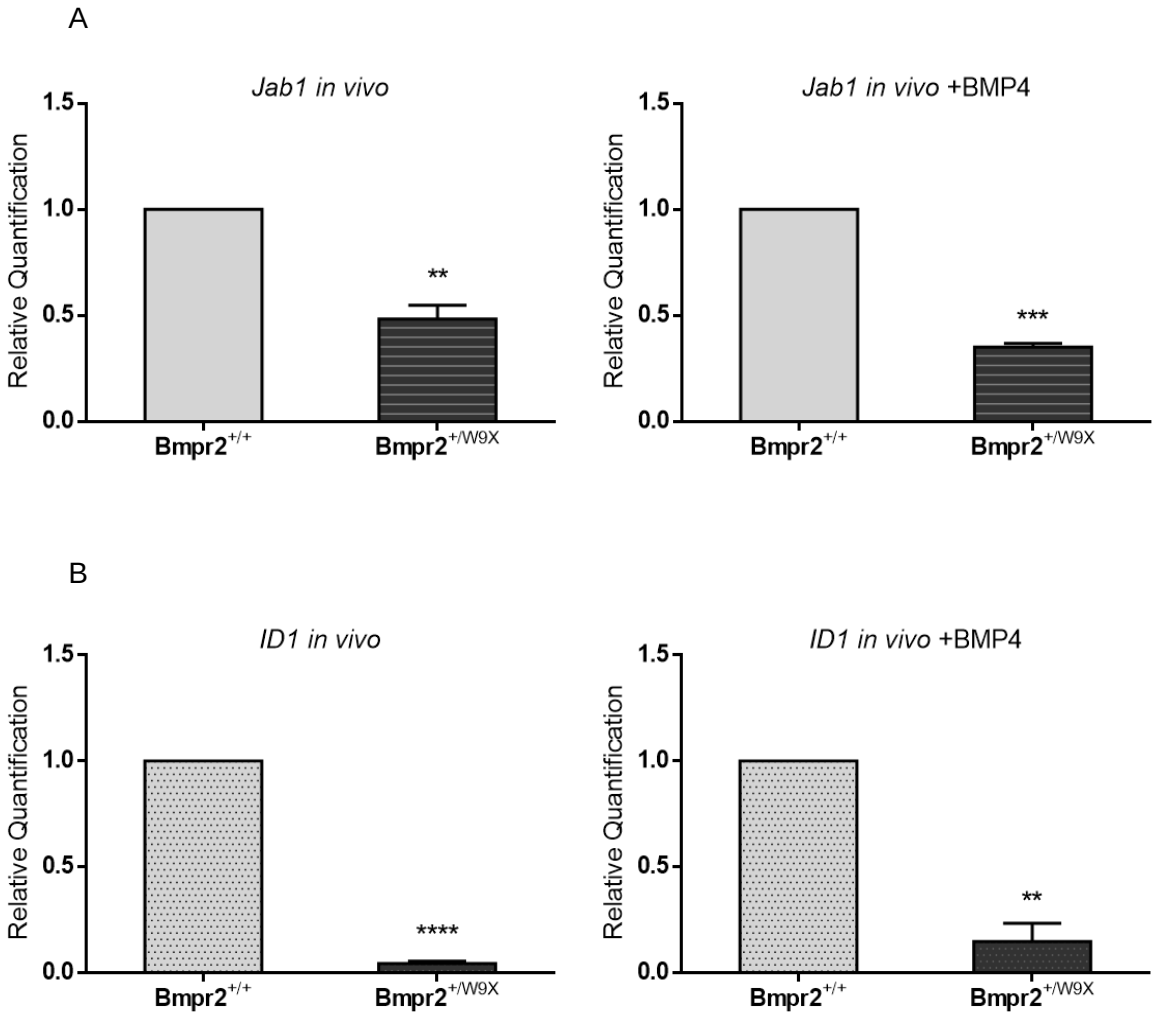

Figure 4-5 Real-time PCR of *JAB1* and *ID1* levels of expression in primary PASMC-*BMPR2*$^{+/W9X}$ cells

A) Graphs show *in vivo* levels of gene expression for *Jab1* w/o BMP4 stimulation. Surprisingly, primary PASMC cells harbouring BMPR-II p.W9X mutation, reduce Jab1 transcript levels. B) Graphs show *in vivo* levels of gene expression for *ID1* w/o BMP4 stimulation. Relative quantification (RQ) of mRNA transcripts are calculated relative to the WT baseline and normalised to ACTB levels. Data are means ±SD of 3 independent experiments; **p≤0.01; ***p<0.001; ****p<0.0001 vs the control group, paired student-t-test.

4.3.3 BMPR-II HAPLOINSUFFICIENCY POTENTIATES TGF-B SIGNALLING IN PRIMARY PASMC-*BMPR2*$^{+/W9X}$ MUTANTS

Through Western blotting analysis, the endogenous levels of phosphorylated SMAD2/3 proteins for TGF-β signalling, along with the endogenous phosphorylated levels of SMAD1/5 proteins for BMP signalling in primary PASMC-*BMPR2*$^{+/W9X}$ cells (stimulated or not with BMP4-ligand), were assessed for whole cell lysates. In case of the untreated cells, the BMP signalling was found heavily impaired, with almost no p-SMAD1/5 protein expression, whereas the signalling was partially restored after BMP4 treatment (Figure 4-6). There was no difference in p-SMAD2/3 protein expression in the *BMPR2* p.W9X PASMC cells. However, a significant sift of p-SMAD2/3 protein levels was observed after BMP4-ligand stimulation. Utilizing the same method for protein analysis, the endogenous phosphorylated levels of the SMAD-independent molecules TAK1 and p38 MAPK (with or without BMP4 stimulation) were also assessed in the diseased cells. Interestingly, p-TAK1 along with p-p38 MAPK protein levels were up-regulated in the diseased cells previously stimulated or not with BMP4-ligand (Figure 4-6). The down-regulated levels of endogenous BMPR-II protein expression and the unaltered levels of endogenous JAB1 for the mutant cells are also depicted in the Figure 4-6.

A. Immunoblot

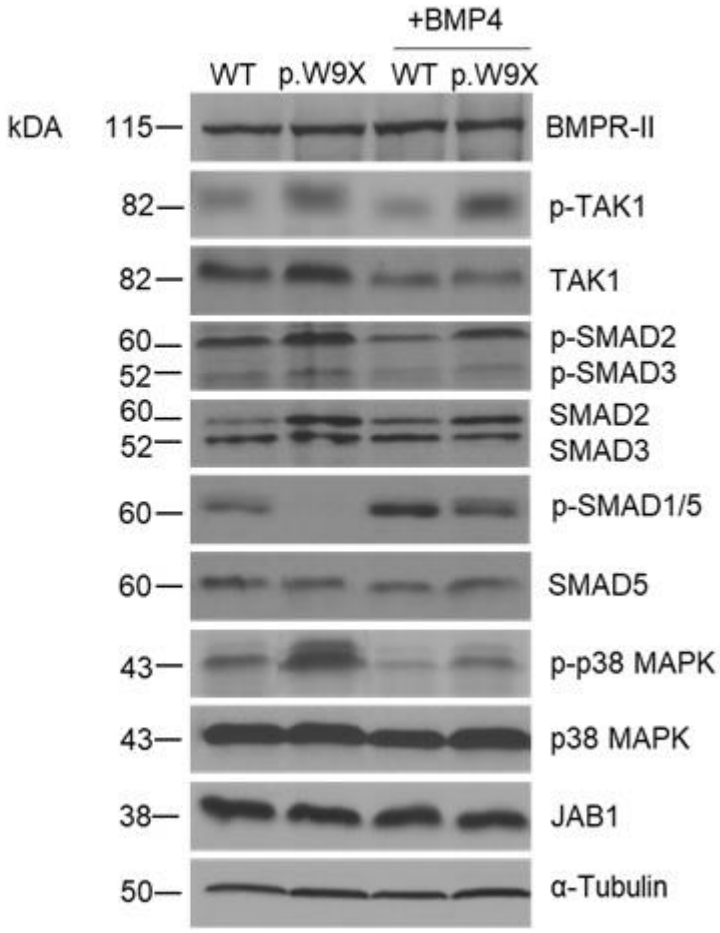

B. Densitometry

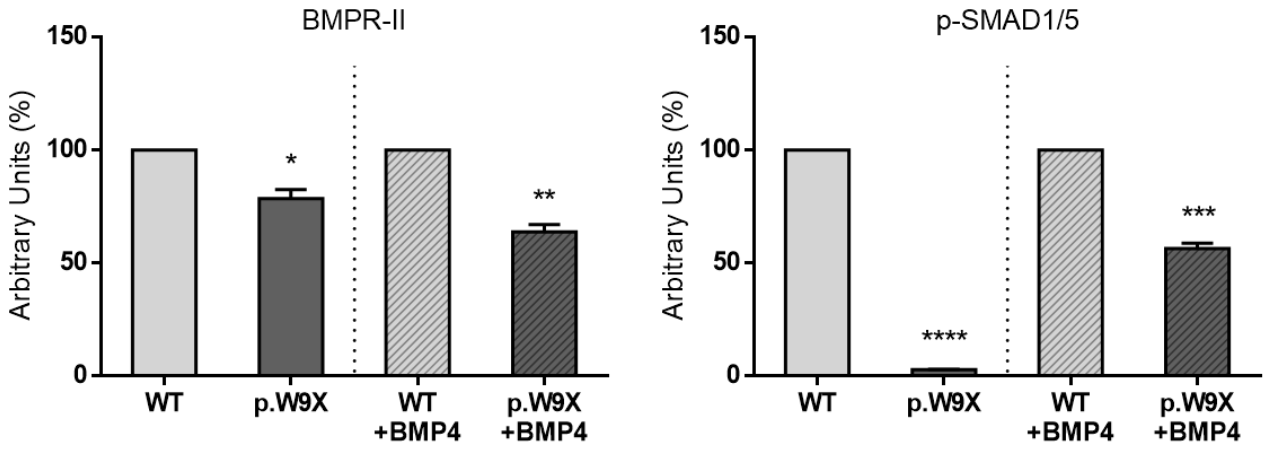

*(Continues at the next page)

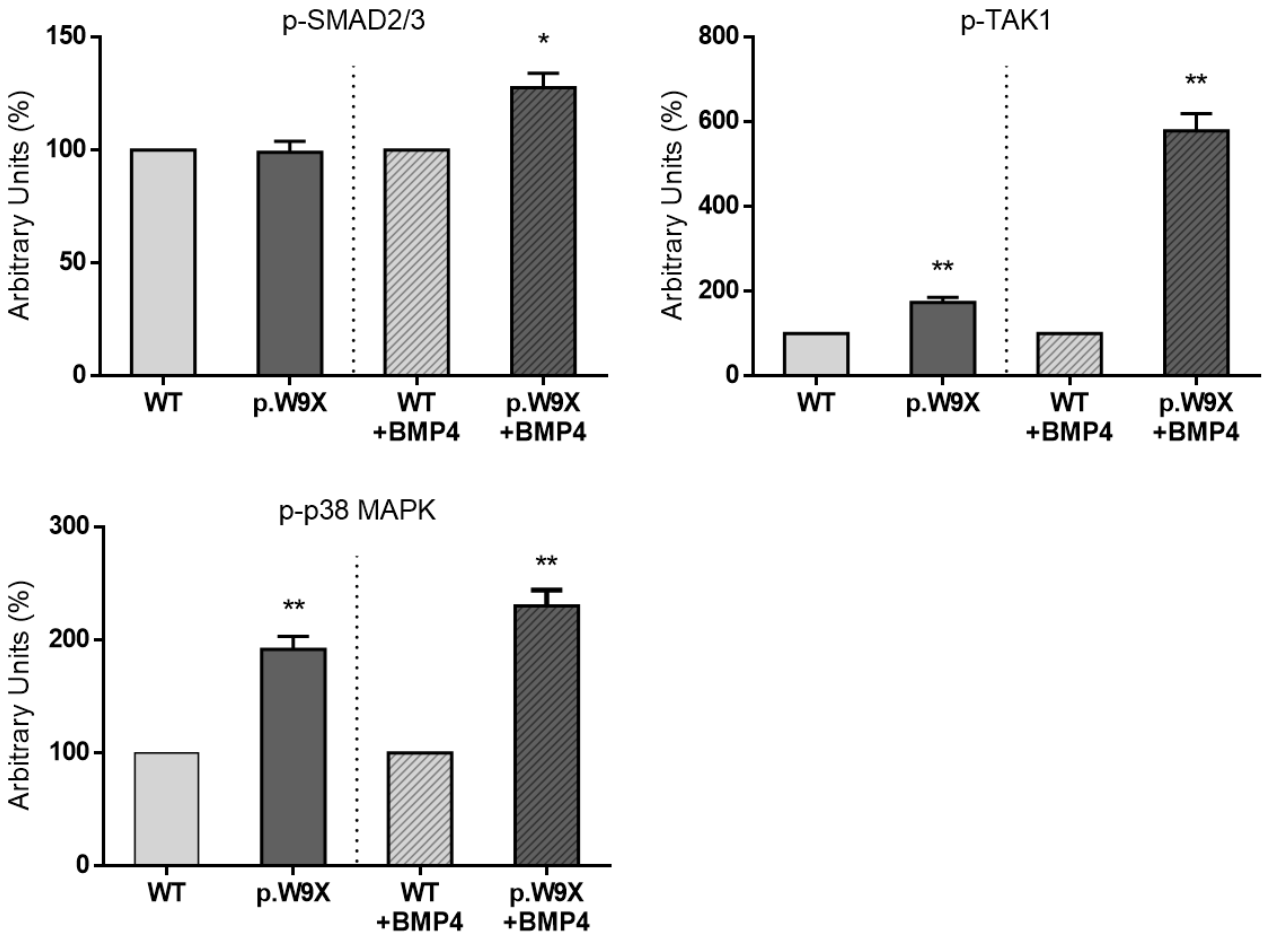

Figure 4-6 TGF-β and BMP signalling in Primary PASMC- *BMPR2*$^{+/W9X}$ cells
A. Immunoblots of endogenous BMPR-II, p-SMAD1/5, SMAD5, p-SMAD2/3, SMAD2/3, p-TAK1, TAK1, p-p38 MAPK, p-38 MAPK and JAB1, w/o BMP4 stimulation. α-Tubulin was used as a loading control. B. Densitometric analysis in arbitrary units (%) from the immunoblots for BMPR-II, p-SMAD1/5, p-SMAD2/3, p-TAK1 and p-p38 MAPK. Data are means ±SD of 3 independent experiments; *P<0.05, **P < 0.01, ***P< 0.001 and ****P<0.0001 vs the control group, RM one-way ANOVA.

4.3.4 JAB1 OVER-EXPRESSION DRIVES SMAD-DEPENDENT AND SMAD-INDEPENDENT TGF-B SIGNALLING OUTCOMES

To investigate whether SMAD-dependent and/or SMAD-independent TGF-β signalling is affected after JAB1 over-expression and impairment of BMP signalling, a JAB1 WT cDNA construct was transfected into HeLa cells and the phosphorylated levels of SMAD2/3 and TAK1 were taken into account by Western blotting analysis, with or without BMP4 stimulation. Interestingly, the excess of JAB1 protein and impairment of BMP signalling due to BMPR-II down-regulation, activated the TGF-β signalling in the cancer cell line, in a both SMAD-dependent and SMAD-independent manner (Figure 4-7). The p-SMAD2/3 protein levels were significantly up-regulated after JAB1 over-expression in the absence of BMP4 ligand stimulation, an alteration which was not observed after BMP4 stimulation. In addition, significantly increased p-TAK1 expression was also observed in JAB1 transfected cells when compared with cells transfected with empty plasmid, with or without BMP4 stimulation (Figure 4-7), suggesting activation of SMAD-independent signalling and activation of TAK1-MAPK pathways in cells where defecting BMP signalling occurs after JAB1 over-expression and down-regulation of the BMPR-II receptor. Furthermore, the levels of endogenous *ID1* mRNA transcripts were quantified by qPCR analysis, after ectopic expression of JAB1 protein in both immortalized hTERT-PASMC and Hela cell lines. Interestingly, *ID1* levels of expression were significantly up-regulated in both cell lines after *JAB1* over-expression with or without BMP4-ligand stimulation (Figure 4-8).

A. Immunoblot

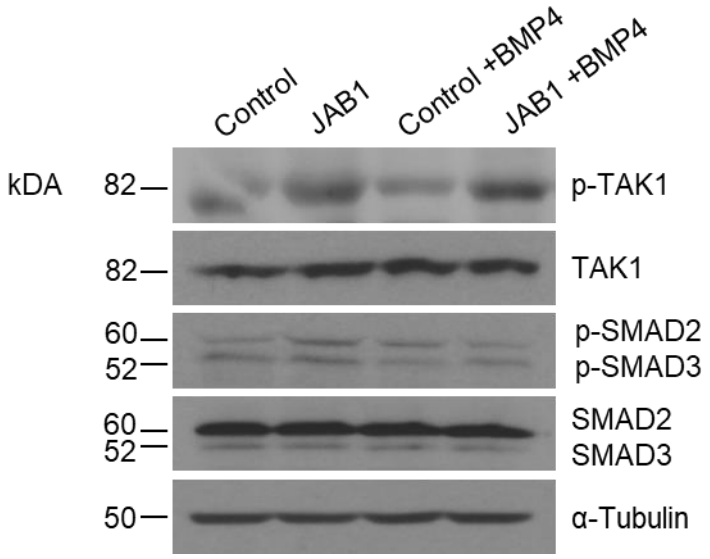

B. Densitometry

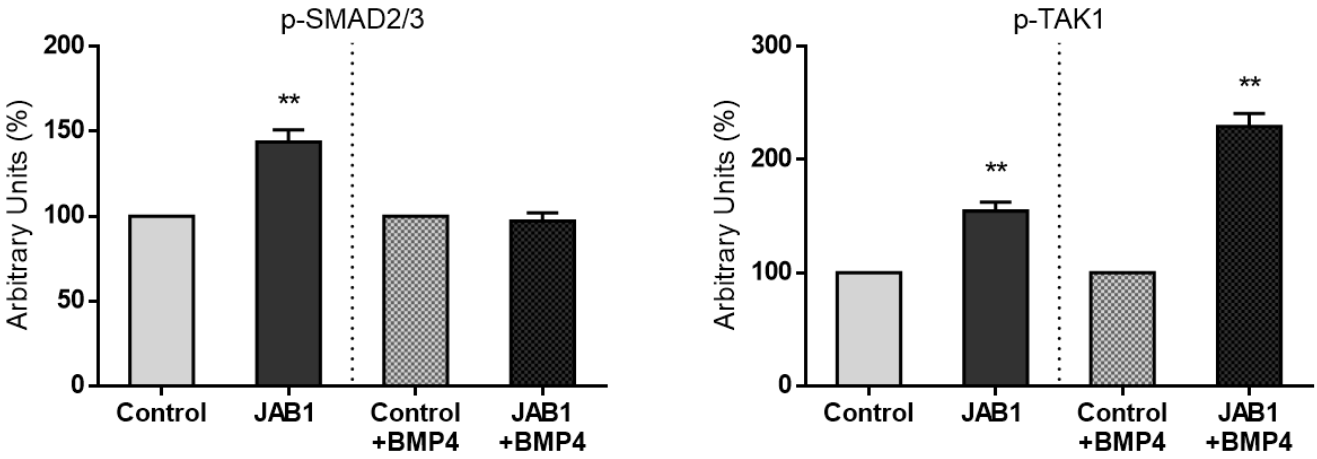

Figure 4-7 Over-expression of JAB1 activated TGF-β signalling in HeLa cells
A. Immunoblots of endogenous p-TAK1, TAK1, p-SMAD2/3 and SMAD2/3 of HeLa cells transiently transfected with JAB1 construct, w/o BMP4 stimulation. B. The levels of p-TAK1 were significantly up-regulated in the presence of JAB1 over-expression, regardless BMP4 stimulation. p-SMAD2/3 levels showed increased expression only in the case of absence of BMP4 stimulation, by comparison to cells transfected with empty plasmid (control). Data are means ±SD of 3 independent experiments; **P < 0.01, vs the control group, paired student-t-test

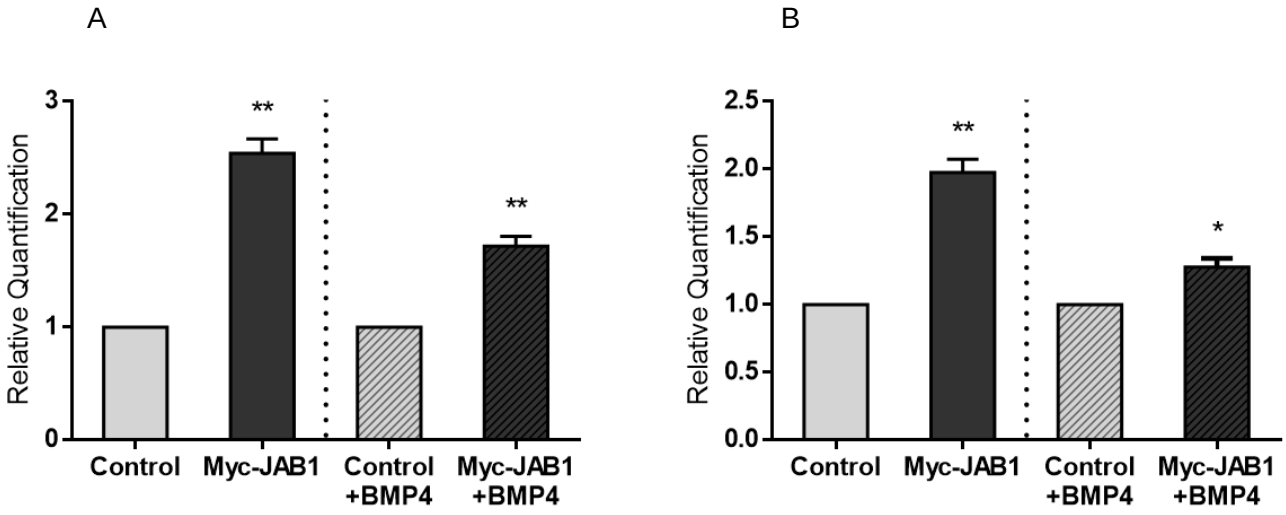

Figure 4-8 ID1 up-regulation in cell lines after ectopic over-expression of JAB1
Real-time PCR of ID1 mRNA levels of expression in hTERT-PASMC (A) and HeLa (B) cells. A) Graph show in vitro levels of gene expression for ID1 in hTERT-PASMCs after JAB1 was transiently overexpressed (20ug/transfection), w/o BMP4 stimulation. B) Graph show in vitro levels of gene expression for ID1 in HeLa cell line after JAB1 was transiently overexpressed (20ug/transfection), w/o BMP4 stimulation. Surprisingly, all cases presented significant up-regulation of ID1, regardless the presence of BMP4. Relative quantification (RQ) of mRNA transcripts are calculated relative to the control (cells transfected with empty plasmid) baseline and normalised to ACTB levels. Data are means ±SD of 3 independent experiments; *P<0.05 and **P < 0.01 vs the control group, paired student-t-test.

4.3.5 shRNA KNOCK-DOWN OF JAB1 REVERSES ABNORMAL PROLIFERATION IN PRIMARY PASMC-*BMPR2*$^{+/W9X}$ CELLS

Two specific short hairpin (sh) RNA expression vectors specific to human JAB1 (hJAB1-shRNA) were selected along with a Scramble shRNA vector for negative control, and the efficiency of transfection was tested prior the main experimentation (Appendix E). Importantly, the effect of JAB1-specific knock-down was evident at 48h after transfection. After satisfying results on JAB1 knock-down levels in HeLa cell line (Appendix E – Figure E-3), a 50-50 mix of the 2 shRNA constructs was inserted though co-transfection in both mutant and healthy WT PASMCs and after 48h of incubation time, the cells were trypsinized, diluted and seeded into 96-well plates ($4x10^3$ cells/well). MTT assay studies were employed to verify the effect on proliferation of the JAB1-knock out cells in a 2-days incubation time. At day 0 (6h after seeding of cells), there was no difference

in cell proliferation of p.W9X mutants transfected with Scramble shRNA or hJAB1-shRNA, compared to WT cells, giving an equal start on proliferation for both mutants and healthy PASMCs. As expected, the mutant cells transfected with Scramble shRNA showed significant difference in proliferation at day 2 ($P < 0.0001$). Interestingly, the pathogenic phenotype of *BMPR2* mutants and their enhanced proliferation rate was rescued at day 2, while transfected with hJAB1-shRNA and compared with the healthy individuals, also depleted of JAB1 protein (Figure 4-9).

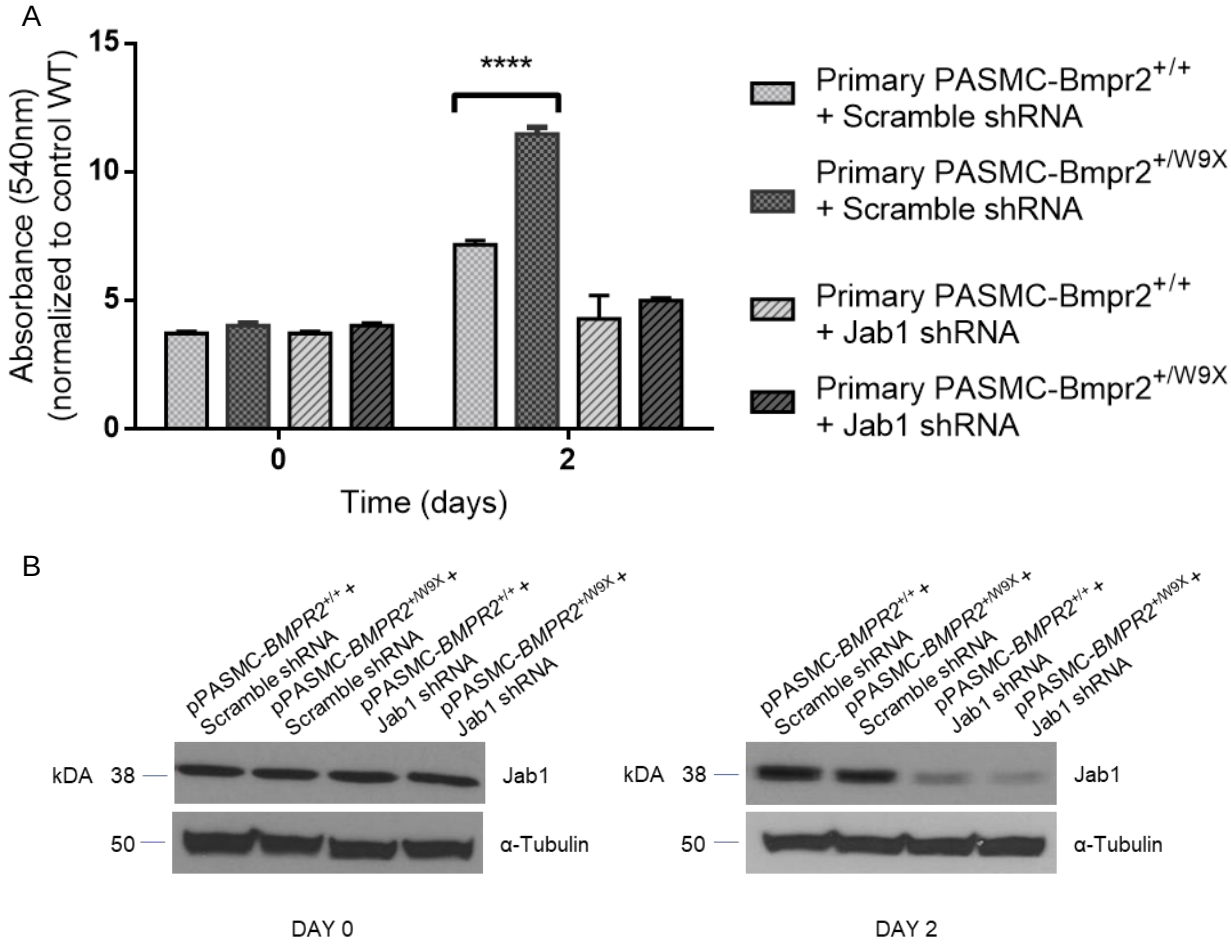

Figure 4-9 MTT Proliferation Assay of Primary PASMC-*BMPR2*$^{+/W9X}$ cells transiently transfected with specific shRNA constructs for efficient knock-down of JAB1
A. While transfected with Scramble shRNA, mutant cells showed significant difference in proliferation at day 2; Interestingly, the pathogenic phenotype rescued when JAB1 was knocked-out with combination of 2 anti-Jab1 specific shRNAs (5ug/transfection). Data are means ±SD of 3 independent experiments. The p values were calculated by Sidak's multiple comparison test in a 2-way Analysis of Variance (ANOVA). B. Immunoblottings at day 0 and day 2, revealing effective JAB1 down-regulation of protein expression. α-Tubulin was used as endogenous control. Key: ****p<0.0001;

4.4 DISCUSSION

4.4.1 JAB1-MEDIATED SUPPRESSION OF THE BMP SIGNALLING PATHWAY: RECEPTOR TO SIGNALLING INTERMEDIARIES

While BMPs have not yet explored in clinical trials, both PAECs and PASMCs are responding to BMP2, 4, 6 and 9 in terms of BMPR-II signalling enhancement and restoration of the vascular integrity, aspects that are critically dysregulated in PAH (Long, Ormiston et al. 2015). While BMP9 exhibits enhanced selectivity for endothelium, thus preventing endothelium apoptosis and increasing the stability of tunica interna, BMP4 selectivity is concentrated in tunica media, thus controlling abnormal proliferation responses and dedifferentiation of PASMC cells in disease state (Long, Ormiston et al. 2015). As a first aim of this project and to determine whether JAB1-mediated down-regulation of BMPR-II has an effect in BMP signalling, SMAD1/5 levels of protein expression have been analysed. As expected, SMAD1/5 protein expression was repressed, even after stimulation with BMP4 ligand (Figures 4-1 and 4-3). Despite the fact that this analysis was made in a generic cell line, the reduced BMP signalling is indicative of the dysregulation of the SMAD1/5 canonical signalling after ectopic JAB1-overexpression. Further to that, the endogenous levels of SMAD5 were again greatly reduced, validating the experimentation of the previous chapter.

In a SMAD-independent manner, JAB1 over-expression promoted the down-regulation of activated p38 MAPK in HeLa cells, a finding which differs with the notion of activation of p38 MAPK in the absence of exogenous ligand and defective BMP signalling, due to loss-of function of the BMPR-II receptor (Figure 4-2). Further to that, BMP4 stimulation and subsequent BMP signalling activation did not alter the down-regulation of activated p38 MAPK in the cells (Figures 4-1 and 4-3). On the contrary, Rudarakanchana et al., 2002, reported that substitution of the cysteine residues in the ligand binding or kinase domain of the receptor, prevented trafficking of BMPR-II to the cell surface and reduced BMP4 binding. Their transfection studies with BMPR-II mutant constructs led to impairment of SMAD-dependent BMP-mediated signalling and a further activation of p38MAPK. In addition, Gao, Zhu et al., 2010, indicated a positive correlation of JAB1 with p38 MAPK, as expression levels of both proteins were significantly higher in rats

with PAH compared to control subjects, and after treatment with atorvastatin also both were down-regulated. These early findings contradict with the results of the current study.

Therefore, this project novel data suggest a SMAD1/5/8 unrelated down-regulation of p-p38 MAPK in the presence of excess JAB1, which in turn triggers a) the association of p-p38 MAPK regulation with JAB1, b) the loss of BMPR-II expression with the loss of p38 MAPK activation, and c) the potentiation of activation of other SMAD-independent or SMAD-depended signalling cascades, such as the TGF-β signalling pathway, in order to investigate the proliferation potential of cells with defective BMP signalling and type II receptor, due to JAB1 over-expression. Taken all together, the BMP defective signalling and a further dysregulation of p38 MAPK signalling upon JAB1 over-expression were assessed in HeLa cell line fulfilling the first aim of this project.

4.4.2 JAB1 DYSREGULATION IS BMPR-II MUTATION SPECIFIC IN PAH CELLS

The *BMPR2* p.W9X mutation which is associated with HPAH, was selected for assessment of JAB1 potential up-regulation and profiling of BMP/TGF-β signalling in primary PASMC patient cells. While this mutation has been reported as pathogenic in several studies (Nasim, Ghouri et al. 2008, Yang, Long et al. 2011, Drake, Dunmore et al. 2013), there are no up to date data for further association with JAB1 expression nor SMAD-independent signalling activation. As expected, BMP signalling was heavily impaired in patient cells, as activated SMAD1/5 signalling was heavily down-regulated along with the expression of the down-stream target gene *ID1* (Figures 4-5 and 4-6). Of note, BMP4-ligand stimulation significantly enhanced the activation of SMAD1/5 signalling. Surprisingly, *JAB1* MRNA levels of expression were significantly down-regulated, a finding which comes in opposition with the steady-state levels of JAB1 protein expression in the mutants, when compared with the WT cells. As mRNA is eventually translated into protein, it is usually assumed that there is some sort of correlation between the levels of mRNA and protein. But, there are presumable reasons for the poor correlations generally reported between the level of mRNA

and the level of protein, and these may not be mutually exclusive. First, there are many complicated and varied post-transcriptional mechanisms involved in turning mRNA into protein that are not yet sufficiently well-defined to be able to compute protein concentrations from mRNA; second, proteins may differ substantially in their *in vivo* half-lives; and/or third, there is a significant amount of error and noise in both protein and mRNA experiments that limit our ability to get a clear picture (Greenbaum, Colangelo et al. 2003). For the purposes of the *in vitro* evaluation of JAB1 expression profile in primary PASMC-*BMPR2*$^{+/W9X}$ mutants, the protein levels will be taken into account only to deduce that dysregulation of JAB1 protein expression is *BMPR2* mutation specific and to satisfy the second aim of this project.

4.4.3 SELECTIVE ENHANCEMENT OF BMP SIGNALLING WITH BMP4 INHIBITS PROLIFERATION OF *BMPR2* MUTANT PASMC CELLS

TGF-β1 and BMPs as BMP2, 4 and 7 exerts potent effects on vascular smooth muscle cells *in vitro*, including inhibition of proliferation, extracellular matrix synthesis and cell differentiation (Morrell, Yang et al. 2001). Recently, (Long, Ormiston et al. 2015) reported the first use of BMP7 ligand to target and enhance endothelial BMPR-II signalling and reverse established PAH in animal model of disease (*BMPR2*$^{+/R899X}$ mouse). This study complements the previous mentioned research by the *in vitro* inhibition of proliferation of *BMPR2* mutant PASMC cells by selective BMP4 treatment (Figure 4-4). Expression of mutant BMPR-II in PAECs promotes apoptosis and a release of factors that stimulate proliferation of PASMCs (Yang, Long et al. 2011). These factors belong to the paracrine signalling and their excessive release act as growth factors that induce PASMC proliferation or chemokines to recruit circulating inflammatory cells. This later effect might also be a second stimulus which is involved in the initiation of the HPAH that results from defects in BMPR-II expression, as BMPR-II also regulates PAECs endothelial cell barrier function (Burton, Ciuclan et al. 2011). All the above contribute to vascular remodelling in PAH. TGF-β1 and FGF2 molecules induce the BMP/TGF-β signalling inhibitory pathway for arterial muscularization, reducing cell growth and apoptosis. In case of TGF-β1 and BMPR-II deficient

cells, an increase also in IL-6, 8 expression and NF-κB activation has also been observed (Davies, Holmes et al. 2012). The significant difference in proliferation between primary PASMC *BMPR2*$^{+/+}$ and *BMPR2*$^{+/W9X}$ cells in this experimentation validates the proliferative potential of the *BMPR2* mutant PASMCs, while the antiproliferative effect of BMP4-ligant selective stimulation of BMP pathway (Figure 4-4), contributes to significant reversal of PAH phenotype on these cells, fulfilling also the third aim of this project.

4.4.4 *BMPR2* HAPLOINSUFFICIENCY POTENTIATES TGF-B SIGNALLING IN PULMONARY ARTERIAL HYPERTENSION

As already shown, cell proliferation was increased in human PASMC-*BMPR2*$^{+/W9X}$ mutant cells compared with WT cells. To explain this increase in proliferation rate plus the effect of reduced levels of BMPR-II and BMP signalling, the potentiation of TGF-β signalling up-regulation was investigated in the mutant cells. TGF-β superfamily ligands signal through both SMAD-dependent and SMAD-independent pathways. SMAD signalling occurs via either SMAD2/3 (TGF-β) or SMAD1/5/8 (BMP), which translocate to the nucleus with the common SMAD4 to directly regulate target gene transcription (Runo, Loyd 2003). BMPs and TGF-βs have been both been reported to activate SMAD-independent mitogen-activated protein kinase (MAPK) signalling pathways, including ERK1/2, JNK and p38 MAPK. As previously mentioned, p38 MAPK has been shown to be an alternative SMAD-independent signalling pathway downstream of BMPR-II and other TGF-β superfamily receptors (Rudarakanchana, Flanagan et al. 2002). Therefore, it was questioned whether p38 MAPK intracellular signalling was altered in the presence of the mutant p.W9X BMPR-II receptor, as *in vivo BMPR2* mutations in PAEC and PASMC cells may drive PAH through multiple potentially independent downstream mechanisms, including proliferation, apoptosis, inflammation and thrombosis (Majka, Hagen et al. 2011). In relevance and similarity with the above-mentioned studies, significantly elevated activated levels of p38 MAPK were observed with or without BMP4-ligand stimulation (Figure 4-6). Next, it has been investigated whether TAK1, a known activator of the p38 MAPK pathway and intermediary of TGF-β signalling, is involved in exerting the

proliferative activity in mutant cells. Indeed, the levels of activated TAK1 protein were significantly up-regulated in mutant cells, with or without BMP4 treatment, as shown in Figure 4-6. The TGF-β signalling pathways are activated in human and experimental PAH models (i.e. *BMPR2*$^{+/R899X}$ mice) where *BMPR2* is mutated, inducing PASMC cells in a pro-proliferative and anti-apoptotic state, promoting activation of MAPK pathways via TAK1 and p38 MAPK phosphorylation *in vivo* (Nasim, Ogo et al. 2012). Specifically, BMP/TGF-β signalling cascade regulates TAK1 by increasing the expression of XIAP, through its binding to the TD of BMP type I and II receptors. Then XIAP binds TAK-1 binding-protein (TAB1) that recruits TAK1 leading to its phosphorylation (Augeri, Langenfeld et al. 2016). This SMAD-independent mechanism is also activated during embryonic developmental stages and is required for embryo ventralization (Augeri, Langenfeld et al. 2016). The TAK1 pathway has been shown to activate MKK/ERK phosphorylation, which is increased in PAH-PASMCs (Figure 4-10) (Nasim, Ogo et al. 2012).

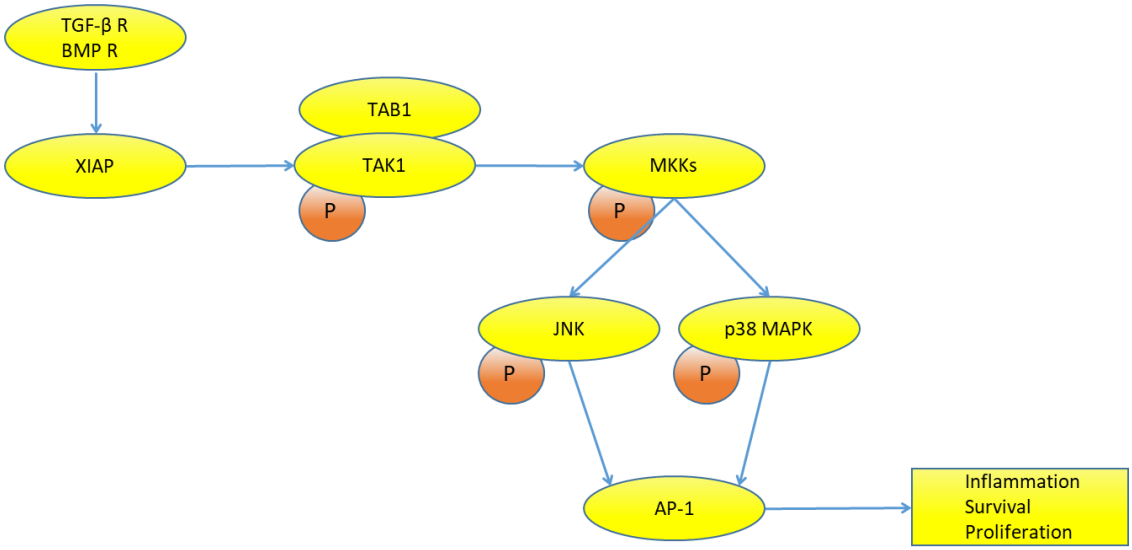

Figure 4-10 Receptor-mediated TAK1 signalling pathways
Receptor-mediated activation of TAK1 is mainly mediated by the E3 ubiquitin ligase XIAP, through the direct interaction with TAB1 downstream of TGF-β or BMP receptors activation, probably without E3 ubiquitin ligase activity. The activated TAK1 upregulates AP-1-dependent gene expression, though activating the MKK/ERK (JNK and p38 MAPK) pathways. The arrows show positive regulation and ''P'' indicated phosphorylation.

Aberrant ERK activation has been described in the pulmonary vasculature of advanced PAH patients, implicating up-steam activation of Ras/Raf/MEK/ERK in

disease pathogenesis. Inhibition of dysregulated Ras/Raf/ERK signalling may be useful in reversing vascular remodelling in PAH. Raf and ERK1/2 (Ras/Raf/ERK) signalling is constitutively activated after BMPR2 knock-down in human pulmonary EC cells (Awad, Elinoff et al. 2016). The proliferative PASMC and PAEC cell phenotype, infiltration of activated inflammatory cells, vascular remodelling and plexogenic lesions are all considered hallmarks of advanced PAH. Also, activation of p38 MAPK has detrimental effects in PASMCs and PAECs and is linked to cardiac hypertrophy and heart failure. Pharmacological inhibition of p38 MAPK reverses hypoxia induced proliferation in rat pulmonary artery fibroblasts exposed to chronic hypoxia or in the monocrotaline rat model of PAH (Awad, Elinoff et al. 2016). Taken together, these data suggest that the enhanced proliferation of primary PASMC-*BMPR2*$^{+/W9X}$ mutants is mediated via the SMAD-independent TAK1-p38 MAPK pathway. Furthermore, the TGF-β canonical pathway was examined and a small but significant shift in increase of phosphorylated SMAD2/3 protein levels was identified, when the cells were treated with BMP4, strengthening the notion that canonical TGF-β signalling is up-regulated in cases of defective BMP signalling due to a PAH-related *BMPR2* mutation (Morrell 2006). All the above analysis of BMP/TGF-β signalling cascade in primary PASMC-*BMPR2*$^{+/W9X}$ cells fulfils the third aim of this project and provides further insight on the signalling intermediaries that are activated in a SMAD-dependent or SMAD-independent manner in diseased PASMC cells.

Expanding the analysis on BMP and TGF-β signalling cascades in PAH, it has been demonstrated that aged *BMPR2*$^{+/R899X}$ mice are susceptible to PAH and elevated RVSP, along with dysregulation of multiple SMAD-independent pathways like p38 MAPK and p42/44 phosphorylation (West, Harral et al. 2008). In reality, dysfunctional BMP/TGF-β signalling is more widespread than suggested by *BMPR2* mutations alone, in primary and severe PAH. The monocrotaline rat model of PAH exhibited elevated MPAP and RVHI after 28 days of disease induction, where JAB1 and p38 MAPK levels of expression were significantly higher than of those in atorvastatin-treatment and control groups (Gao, Zhu et al. 2010). Heme oxygenase-1 (HO-1), the rate-limiting enzyme in heme catabolism, has been shown to be protective against vascular and lung injury. It has been shown that HO-1 induction is independent of SMAD1/5

signalling, but dependant on activation of p38 MAPK in PASMCs harbouring *BMPR2* KD mutations (Yang, Lee et al. 2007). So, bringing back *BMPR2* mutations in the spotlight, it has been proved that gene transfer of *BMPR2* is enabling BMP4 and BMP7 expression, partially restoring the BMP signal and mediating the growth arrest and differentiation of PASMCs (Yu, Deng et al. 2008). Correlating that with the key finding of this study as of BMP signalling enhancement after BMP4-ligand stimulation in *BMPR2* mutant cells, it is suggested that the abnormal proliferation of PAH cells could be rescued, stepping into a potential reversal of the PAH phenotype during disease progression.

To conclude, while the general notion is that activation of TGF-β signalling pathway generally represses BMP-mediated SMAD1/5 signalling in PASMC cells via SMAD3 pathway (Upton, Davies et al. 2013), it has also been demonstrated in a previous study that TGF-β could also stimulate SMAD1/5 signalling in PASMC and fibroblast cells through ALK1 receptor (Zhang, Du et al. 2017). Reciprocally, impaired BMP signalling may potentiate TGF-β cascade and SMAD2/3 activation, suggesting an opposing balance between the two signalling pathways, a notion which is also enhanced by the fact that BMP stimulation restores the SMAD2/3 signalling in steady-state levels (Han, Hong et al. 2013). However, the biological relevance of this signalling cross-talk in PASMC cells is depicted upon injury and/or initiation of PH disease, in which aberrant growth of PASMCs facilitates cell motility, growth and survival, attributes that activate the anti-proliferating effect of both TGF-β and BMP signalling cascades (Eickelberg, Morty 2007). Both pathways promote apoptosis of PASMCs either in healthy or PAH state (Zhang, Du et al. 2017), whereas when compared with the endothelium, BMP signalling via BMPR-II seems to play an opposite role in PAECs, because BMPR-II promotes PAEC survival and protects them against apoptosis (Eickelberg, Morty 2007)

4.4.5 JAB1 DIFFERENTIALLY REGULATES BMP AND TGF-B SIGNALLING

In order to investigate the potential differential regulation of BMP/TGF-β signalling balance mediated by JAB1 in a SMAD-dependent and SMAD-independent manner in a generic cell line, JAB1 transfection studies revealed a significant

activation of SMAD2/3 pathway, along with significant activation of TAK1 protein in HeLa cells compared with cells transfected with empty vectors controls (Figure 4-7). When the JAB1-transfected cells were subjected in BMP4-ligand stimulation, the activated levels of TAK1 protein were again present, but activated SMAD2/3 signalling was restored to normal as in the control case (Figure 4-7). Unpredictably, the *ID1* mRNA level of expression was up-regulated in all cases, both in HeLa cells and an immortalized PASMC cell line that was employed to represent normal healthy PASMC in the vasculature (Figure 4-8). While *ID1* down-regulation would be the number one expectation in defective BMP signalling, this finding could be explained by the fact that upon inhibition of BMP signalling, the TGF-β signalling cascade is activated via up-regulation of phosphorylated TAK1, which then causes the increase of *ID1* expression. Supportive to that, ID1 is also target of TAK1-mediated signalling, and more specifically, this SMAD-independent cascade is activated upon BMP signalling inhibition and subsequent activation of TGF-β signalling cascade (Augeri, Langenfeld et al. 2016). On the contrary, it has been previously shown that JAB1 can bind ID1 and ID3 proteins, resulting to their ubiquitin-dependent proteolytic degradation mediated by the COP9 signalosome (Bounpheng, Dimas et al. 1999). However, it has also been demonstrated and previously analysed that, JAB1 also down-regulates the I-SMAD7, which primary role is to orchestrate a negative-feedback loop for regulation of the intensity or duration of the TGF-β signal (Kim, Lee et al. 2004). While, I-SMAD6 preferentially inhibits BMP signalling, I-SMAD7 inhibits both BMP and TGF-β signalling cascades, by binding to the activated BMP type-I receptors and complexing with Smurf-1 and 2, inducing the ubiquitin-mediated degradation of the receptors (Miyazono, Maeda et al. 2005). Thus, JAB1-mediated down-regulation of I-SMAD7 results in enhanced activation of SMAD2/3 signalling with subsequent activation of the TGF-β target genes, as the ID transcription factors.

It is not really possible to deduce that this study demonstrates JAB1 as the master-regulator of BMP and TGF-β signalling pathways. However, dysregulation of JAB1 leads to abnormal BMPR-II receptor loss and PAH progression, by disruption of the homeostatic BMP/TFG-β signalling imbalance. This could be justified for the following reasons: a) It has been proven within the context of this

study that JAB1 down-regulates BMPR-II via ubiquitin-mediated proteolytic degradation, b) It antagonizes BMP and TGF-β signalling by inducing SMAD5 and the common SMAD4 degradation via ubiquitin-mediated proteolysis (Haag, Aigner 2006, Wan, Cao et al. 2002), c) It regulates TGF-b signalling and down-stream target ID1, by binding to I-SMAD7 and promoting its degradation via ubiquitin-mediated proteolysis (Kim, Lee et al. 2004), d) Its over-expression promotes impairment of BMP signalling via SMAD-dependant pathways and activation of mitogenic cascades as of p38 MAPK and TAK1 via SMAD-independent signalling (this study), and e) it represses the expression of the BMP/TGF-β down-stream targets ID1 and ID3 by direct binding and promoting their degradation via ubiquitin-mediated proteolysis (Berse, Bounpheng et al. 2004). Thus, BMP/TGF-β signalling pathways are regulated differentially at all main stages of the signal transduction by JAB1 protein, a synergistic rational outcome which combines the findings of this study along with the finding of previous on the field experimentation, also fulfilling the forth aim of this project.

4.4.6 SHRNA KNOCK-DOWN OF JAB1 REVERSES ABNORMAL PROLIFERATION IN PAH

To elucidate the potential anti-proliferative effect of *JAB1* suppression in *BMPR2* mutant primary PASMC cells, RNAi interference technique was employed in order to efficiently knock-down the endogenous levels of *JAB1* mRNA transcript in primary PASMC-*BMPR2*$^{+/W9X}$ cells. As it has been previously demonstrated (Figure 4-4), p.W9X PASMCs exhibit abnormal proliferation rates, indicative to the disease phenotype in cases where *BMPR2* haploinsufficiency is the inherited molecular mechanism for primary PH. Indeed, the PAH phenotype was rapidly developed after 48h in case of the transfected with Scramble shRNA mutants compared to the Scramble shRNA-transfected healthy controls (Figure 4-9). A phenotype that was efficiently rescued at the same time by transfection of healthy and mutant PASMCs with human anti-JAB1 shRNA (Figure 4-9). Thus, it has been confirmed for the first time that *JAB1* is required for human *BMPR2* mutant PASMCs in order to exhibit pro-proliferating responses, and subsequent

depletion of JAB1 protein through specific shRNA knock-down rescues their PAH pathogenic phenotype. This novel finding also fulfils the fifth and last aim of this project.

Previous studies have also addressed the importance of JAB1 depletion regarding the cell proliferation in various experimental systems. Yoshida et al., 2010, targeted the JAMM motif of Jab1 in mouse embryonic fibroblasts (MEF) and JAB1 depletion prevented progression of the cell cycle at multiple points, highlighting also the importance of this motif in the oncogenic activity of the JAB1 protein. JAB1 is also inhibited after interaction with the cytokine macrophage migration inhibitory factor (MIF), along with the JAB1-stimulus enhanced AP-1 and JNK activity (Kleemann, Hausser et al. 2000). Furthermore, X-linked intellectual disability gene CUL4B also targets JAB1 for degradation via proteolytic degradation, potentiating the up-regulation of BMP signalling and suggesting another way to target the oncogenic properties of JAB1 (He, Lu et al. 2013). Of note, micro-mass cultures of limb buds from $JAB1^{flox/flox}$ conditional knock-out mice, that was created as a model for chondrocyte differentiation during early limb development, interestingly exhibited decreased BMP signalling response of down-stream targets ID1 and Ihh (Bashur, Chen et al. 2014). This controversy could be explained by the fact that JAB1 elimination may result in suppression of BMP signalling in certain cells as osteochondral progenitors (OPC), due to enhancement of I-SMAD7 BMP-inhibitory activity, thus the down-stream targets may be repressed as a final effect. Furthermore, it has been proved that JAB1 is over-expressed in hepatocellular carcinoma (HCC tissues) and peroxisome proliferator-activated receptor γ PPARγ ligands troglitazone and rosiglitazone could down-regulate the JAB1 protein expression in HCC cells (Hsu, Huang et al. 2008). In addition, depletion of JAB1 inhibits Ras-mediated tumorigenesis by inducing premature senescence in p53-null cells (Tsujimoto, Yoshida et al. 2012), and also inhibits proliferation in certain pancreatic cell lines (Fukumoto, Tomoda et al. 2006). In regard to cardiovascular disorders, depletion of JAB1 in HEK293T cells expressing the type A and B receptors of the vasoconstricting peptide endothelin-1, resulted in increased cell surface levels of the receptors, as they can also be JAB1 targets for ubiquitin-mediated proteolysis and degradation (Nishimoto, Lu et al. 2010). Therefore, JAB1 may play a key role

in regulation of the physiological control of blood pressure, cardiac function, and also in genesis and development of CVD such as atherosclerosis, cardiac remodelling accompanying chronic heart failure, and pulmonary hypertension (Nishimoto, Lu et al. 2010).

There is no up to date developed RNAi-based therapeutic approach for PAH. It often requires a delivery vehicle to transport the siRNA/shRNA molecules that target complementary mRNA stands for degradation, thus inhibiting gene expression. However, clinical advancements that permit non-invasive topical delivery of siRNA specific for the treatment of asthma and respiratory syncytial virus (RSV) have already been development and currently they are tested in Phase II clinical trials (Burnett, Rossi et al. 2011). For JAB1 shRNA delivery, a systemic or ex vivo delivery is proposed as a first RNAi therapeutical approach, initially by re-infusion of modified cells into an animal model of PAH disease.

4.5 CONCLUSION AND FURTHER WORK

JAB1 appears to be a key regulator of BMP and TGF-β signalling pathways in PAEC and PASMC cells, functioning by differential regulation of all stages of the pathways cascades. It regulates the signalling balance of both main pathways in a SMAD-dependant manner, targeting for proteolysis via ubiquitin-mediated degradation the SMAD5, co-SMAD4 and I-SMAD7. Furthermore, it acts up-stream of BMP pathway, by promoting the proteolytic degradation of BMPR-II and also down-stream of BMP/TGF-β signalling cascades, by suppressing ID1 and ID3 transcription factors through ubiquitination. In addition to that, JAB1 can also promote ID protein expression via up-regulation of SMAD2/3 signalling, if its prior act was to down-regulate the BMP signal via repression of I-SMAD7 or BMPR-II protein expression, counter-balancing the cross-talk of the two main pathways. The role of JAB1 as a regulator of BMP/TGF-β signalling is more complex as it can also regulate the pathways in a SMAD-independent manner, promoting the activation of TAK1 and p38 MAPK mitogenic cascades, thus enhancing the pro-proliferative state of healthy and/or *BMPR2* mutated PASMC cells, whereas it can also down-regulate p38 MAPK protein expression in other

cell types such as cancerous cell lines. However, JAB1 up-regulation itself seems to be *BMPR2* mutation specific in PASMC cells, explaining the enhanced BMPR-II down-regulation of expression in certain PAH cases, which the profound loss of BMPR-II is well beyond of that can be explained by haploinsufficiency mechanism. This study also facilitated to validate the anti-proliferative effect of BMP4-ligand stimulation on hyper-proliferating *BMPR2* mutant PASMC cells, highlighting the suppressive regulatory role of BMP signalling on cell proliferation and differentiation. Finally, successful knock-down of JAB1 in healthy and *BMPR2* mutant PASMC cells resulted in control of their proliferation, a result which is indicative of the essential role of JAB1 protein in positively regulating the cell proliferation. This later finding may well set JAB1 as a rational clinical target for manipulation in the treatment of PAH.

The proposed future directions, based on these finding, include the transfection of BOEC cells with constructs harbouring non-BMP defects (such as Caveolin-1 (CAV-1)/ Potassium Channel Subfamily K Member 3 (KCNK3)) in order to assess JAB1 level and effect upon signalling down-regulation. Finally, these fundamental science studies should be expanded into the two up to date (hypoxia and monocrotaline) murine models of disease. If to continue working in the field, a recommended allowing suitable time for the above-mentioned experimentation, would be a 2-3-year study, for further cell signalling experimentation and *in vivo* studies in animal models.

CHAPTER 5: HAPLOINSUFFICIENCY OF THE NOTCH1 RECEPTOR AS A CAUSE OF ADAMS-OLIVER SYNDROME WITH VARIABLE CARDIAC ANOMALIES

5.1 INTRODUCTION

Adams-Oliver syndrome (AOS) is a rare condition characterized by congenital limb defects and scalp cutis aplasia. In a percentage of cases relatively close to 20%, notable cardiac involvement and HHT along with PH are also apparent. The up to date clinical investigations report that 13.4% of AOS cases have been associated with CHD and a further 10% crude estimate of that cases develop PAH at birth or at later time in their lives. Despite several significant advances in the understanding of the genetic basis of AOS, the underlying molecular defect remains unresolved for the majority of affected subjects (Southgate, Sukalo et al. 2015). This study aimed to identify novel genetic determinants of AOS.

*5.3 Section was contributed in Southgate, Sukalo, Karountzos et al., 2015 paper, that was risen from an international collaboration of studies and the NOTCH1 signalling experimentation of this study.

5.1.1 PRELIMINARY EXPERIMENTATION**

Whole-exome sequencing was performed for 12 unrelated probands, each with a clinical diagnosis of AOS, as per the guidelines by Snape et al., 2009. AOS was segregating as an autosomal dominant trait and the patients were negative for *ARHGAP31* and *RBPJ* mutations. Screening a cohort of 52 unrelated AOS subjects, 8 additional unique *NOTCH1* mutations were detected, including three de novo amino-acid substitutions, all within the ligand-binding domain. Congenital heart anomalies were noted in 47% (8/17) of *NOTCH1*-positive probands and affected family members (Southgate, Sukalo et al. 2015).

**The extensive analysis of the Methods and Materials that were employed for this investigation, is described in (Southgate, Sukalo et al. 2015), including patient cohorts, exome sequencing and mutation detection. Site-directed mutagenesis was conducted by Dr Laura Southgate and the mutagenized constructs were provided to the Thesis Author for transient transfection studies. The total RNA from patient samples was extracted by Dr Laura Southgate, from blood samples

obtained by Dr John Tolmie. The first strand cDNA synthesis was performed by Dr Laura Southgate and samples were provided to the Thesis Author for qPCR analysis. All other techniques were conducted by: Dr Laura Southgate, Dr Maja Sukalo, Dr Claire Collinson and Dr Edward Taylor. The statistical analysis of Figures 5-3 and 5-4 were conducted by Dr Laura Southgate and also verified afresh by the same statistical software (GraphPad Prism 6.02) by the Author for thesis purposes. Furthermore, the extensive analysis of the preliminary Results such as the clinical features of *NOTCH1* positive families and the identification of novel *NOTCH1* variants are also reported in detail in (Southgate, Sukalo et al. 2015). Additionally, the location and conservation of *NOTCH1* mutations (Figure 5-1B) was conducted by Dr Laura Southgate and is reported in (Southgate, Sukalo et al. 2015). Finally, the ball and stick representation of the 3-dimentional structure of human NOTCH1 EGF repeats 11-13 (Figure 5-2A) was produced from Dr Edward Taylor and is also reported in (Southgate, Sukalo et al. 2015).

Contribution of the Author of this Thesis to Chapter 5.

1. All cell culture and transient transfection experiments were conducted by the Thesis Author.
2. The cDNA samples from patients were provided to the Thesis Author for qPCR analysis.
3. The RNA extraction and cDNA synthesis from transfected cells along with all qPCR work (Figures 5-3, 5-4 and 5-5A1-B2) were conducted by the Thesis Author.
4. The statistical analysis of the published Figures 5-3 and 5-4 were verified afresh in GraphPad Prism 6.02 software, by the Thesis Author.

The author of this PhD thesis (Anastasios S. Karountzos) has signed an Authorship Responsibility and Copyright Transfer Agreement (CTA) for the American Heart Association Circulation. Cardiovascular Genetics journal, for the publication of the article: Southgate et al. ‘Haploinsufficiency of the NOTCH1 receptor as a cause of Adams-Oliver syndrome with variable cardiac anomalies’. *Circulation. Cardiovascular Genetics* 2015; 8:572-581; DOI: 0.1161/CIRCGENETICS.115.001086.

The right of the author for reproduction of any published material such as figures or tables for PhD thesis purposes is covered under the CTA act.

5.1.2 *NOTCH1* MISSENSE MUTATIONS ARE LOCATED WITHIN CRITICAL FUNCTIONAL DOMAINS

The MutationTaster2,19 PolyPhen-2,20 and/or SIFT prediction software21 were employed by Dr Laura Southgate to identify the pathogenicity of the ten *NOTCH1* mutations that identified in this study (Table 5-1). Six of them are missense mutations (p.P407R, p.R448Q, p.C449R, p.C456Y, p.C1374R, p.A1740S) with the rest being truncating mutations (frameshifts and nonsense). More specifically, five out of the ten mutations have been predicted as probably damaging (Appendix D – Table D-2). Specifically, four missense mutations (p.P407R, p.R448Q, p.C449R and p.C456Y) occur in or adjacent to the ligand-binding domain, specified by EGF repeats 11-13 (Figure 5-1A, Figure 5-2A), with the remaining mutations to span across the length of the receptor. The majority lie within highly conserved regions of the NOTCH1 protein, and are highly conserved across species (Figure 5-1). In addition, certain cysteine residues are affected by the identified protein mutations p.C449R, p.C456Y and p.C1374R, which possibly disrupt key disulphidic bonds that are critical of the EGF-like domains structure (Figure 5-2). By contrast, the TM domain p.A1740S mutation is not conserved in other vertebrate species apart mammals, and has a less clear impact upon the receptor's structural integrity (Figure 5-1)

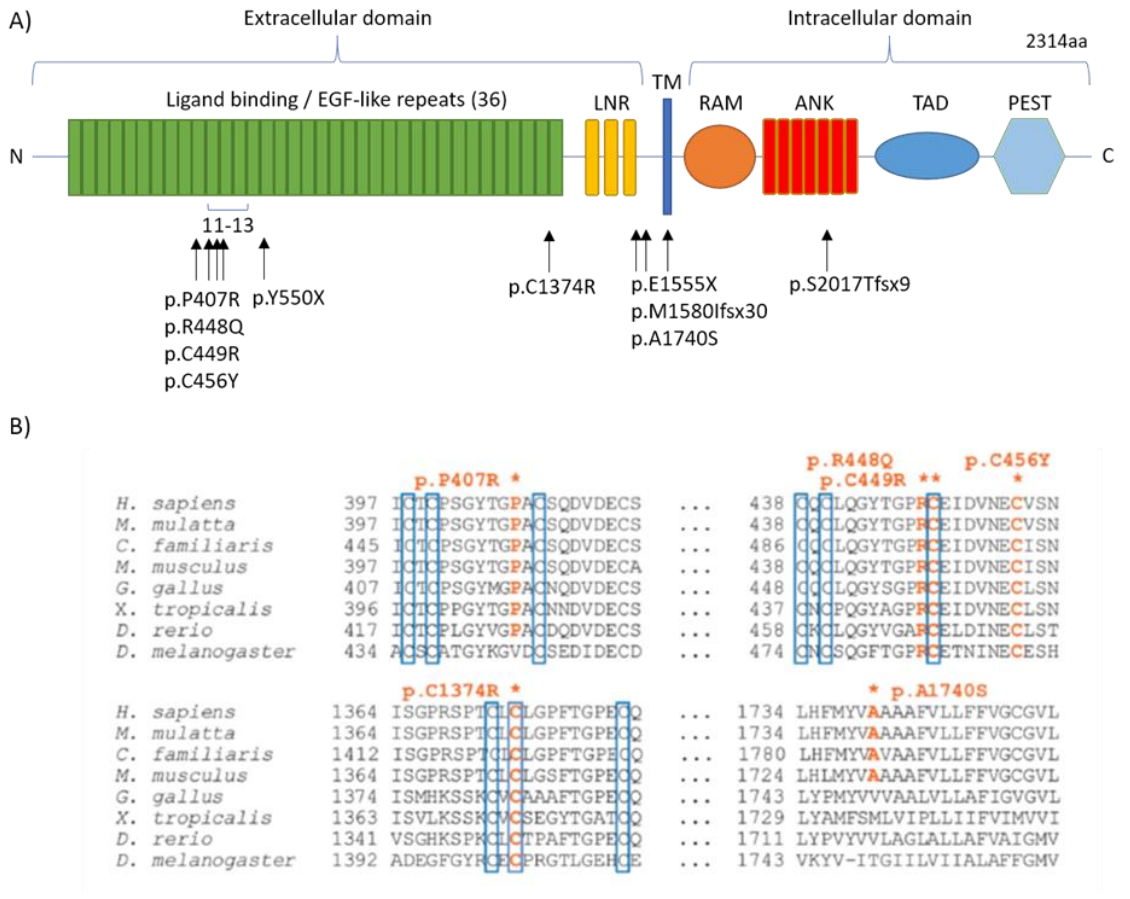

Figure 5-1 Location and conservation of *NOTCH1* mutations
A) Illustration of the NOTCH1 protein highlighting the critical functional domains. The AOS-associated mutations identified within the context of this study are exhibited below the schematic. B) Conservation of the 6 missense mutations across species. Conserved residues are highlighted in orange. The 4th, 5th and 6th conserved cysteines within the EGF domains are boxed. Accession numbers: *H. sapiens*: NP_060087.3; *M. mulatta*: AFH32544.1; *C. lupus familiaris*: XP_005625490.1 (predicted); *M. musculus*: NP_032740.3; *G. gallus*: NP_001025466.1; *X. tropicalis*: NP_001090757.1; *D. rerio*: NP_571377.2; *T. rubripes*: XP_003975158.1 (predicted); *D. melanogaster*: NP_476859.2.

A. 3-D structure of human NOTCH1 EGF repeats 11-13.

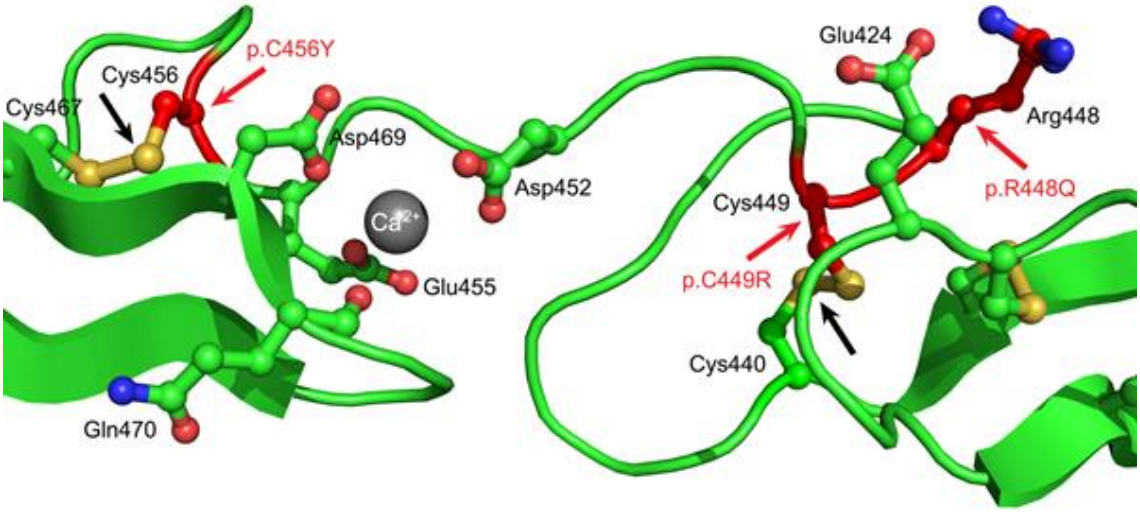

B. EGF11:

```
1234 GACGTGGATGAGTGCTCGCTGGGTGCCAACCCCTGCGAGCATGCGGGCAAGTGCATCAACACGCTG
 412 -D--V--D--E--C--S--L--G--A--N--P--C--E--H--A--G--K--C--I--N--T--L-
                  1                       2                 3
1300 GGCTCCTTCGAGTGCCAGTGTCTGCAGGGCTACACGGGCCCCCGATGCGAGATCGACGTCAACGAG
 434 -G--S--F--E--C--Q--C--L--Q--G--Y--T--G--P--R--C--E--I--D--V--N--E-
                  4     5                       6
```

C. Disruption of di-sulphide bridges

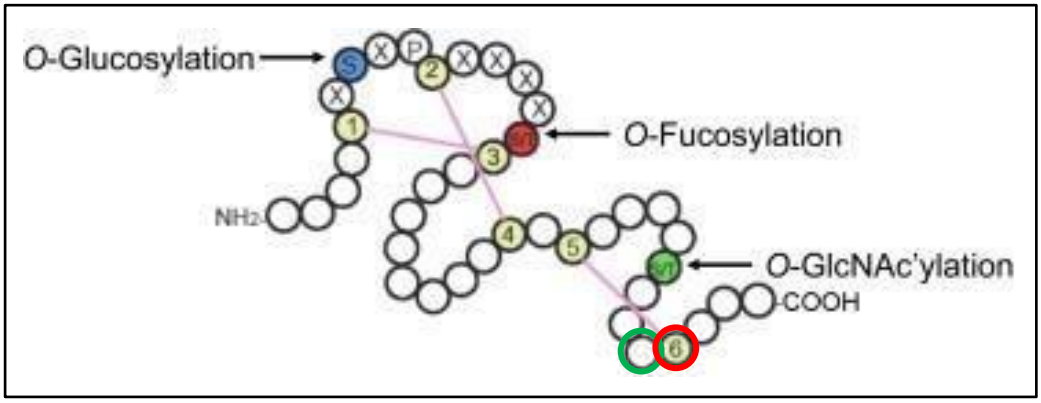

Figure 5-2 NOTCH1 functional effects
A) Ball and stick representation of the 3-dimensional structure of human NOTCH1 EGF repeats 11-13. The positions of the adjacent AOS mutations p.R448Q and p.C449R are highlighted by the solid red arrows. The p.C456Y mutation is similarly marked. The solid black arrows indicate the disulphide bonds which would be abolished by the p.C449R and p.C456Y mutations, respectively. The side chains of the key Ca2+ ion coordinating residues (Asp452, Glu455 and Asp469) and Glu424 are indicated. Water molecules have been removed for clarity. Figure produced from the crystal structure (PDB ID: 2VJ3)22 using the PyMOL Molecular Graphics System. B) EGF11 repeat harbouring the missense mutations c.1343G>A and c.1345T>C, C) Schematic of the EGF11 repeat structure presenting the disruption of the di-sulphide bridge between cysteines 5 and 6 that may be caused by the p.C449R mutation. The NOTCH1 functional effects were studied under supervision of Dr E. Taylor. Schematics are adopted with permission reprints from Dr E. Taylor.

5.1.3 ASSESSMENT OF NOTCH1 SIGNALLING IN AOS PATIENTS

For the purposes of this study, the NOTCH1 canonical signalling and more specifically mRNA transcripts of the receptor along with the key down-stream targets *HEY1* and *HES1*, were investigated in regard to novel *NOTCH1* mutations identified in AOS patient clinical samples. A potential down-regulation of the *NOTCH1* expression levels along with *HEY1/HES1* reduction was expected by impaired signalling due to the missense and frameshift mutations that were investigated *in vivo* and *in vitro*.

Notch crosstalk with BMP signalling was reviewed in an excellent article that focused on regulation of oscillatory gene expression (Beets, Huylebroeck et al. 2013). In endothelial cells, BMP signalling is generally thought to cooperate with Notch signalling to induce quiescence and promote vessel maturation and arterialization. Recent reports have highlighted this cooperative crosstalk between DLL4/NOTCH1 and the BMP9-ALK1-SMAD1/5 pathway. While the role of NOTCH3 has been extensively investigated in cases of PAH and the interactions of Notch signalling with the BMP/TGF-β pathway have been addressed (Zong, Ouyang et al. 2016, Andersson, Sandberg et al. 2011), it was significant to investigate a hypothesised molecular bridge between AOS and PAH. For this purpose, a potential cross-talk of NOTCH1 with BMP signalling was assessed in regards of certain AOS-associated mutations of *NOTCH1* and their direct impact with BMP signalling intermediaries and down-stream target.

5.2 AIMS

- To assess the *in vivo* levels of mutant mRNA transcripts of *NOTCH1*, *HEY1* and *HES1* of three AOS patients harbouring *NOTCH1* mutation (c.1343G>A and c.1649dupA (*2 cases*)), by quantitative RT-PCR of RNA extracted from peripheral blood.
- To assess the *in vitro* levels of *NOTCH1* mRNA receptor in HeLa cell line, after transient transfections with mutated *NOTCH1* constructs harbouring missense AOS-associated *NOTCH1* mutations (c.1220C>G, c.1343G>A, c.4120T>C and c.5128g>T), by quantitative RT-PCR analysis of cultured cells.
- To investigate the impact of c.1343G>A and c.1649dupA *NOTCH1* AOS-associated mutations on BMP signalling in HeLa cell line, by qPCR analysis of the *in vivo* patient data, and by Western blotting analysis after transient transfections of mutated NOTCH1 receptor into HeLa cells.

5.3 RESULTS

5.3.1 *NOTCH1* HAPLOINSUFFICIENCY IS IMPLICATED IN AOS PATHOGENESIS

Quantitative real-time PCR studies were employed for *NOTCH1* mutant mRNA transcript assessment, utilizing RNA extractions from peripheral blood of three individual AOS patients harbouring NOTCH1 c.1343G>A and c.1649dupA mutations (2 cases). The receptor transcript levels were significantly reduced when compared to a healthy individual (Control), exhibiting an approximation of 50% expression reduction in all *in vivo* tested samples (Figure 5-3A). While institutional ethical constraints blocked definite heart assessment of the control subject, it was clarified by individual testimony that there was no family history of developmental abnormalities linking to AOS-CHD.

Following the *in vivo* experimentation, transient transfections of mutagenized *NOTCH1* constructs were conducted to investigate the functional effect of missense mutations, for which patient RNA was not offered. A significant decrease of mutant NOTCH1 expression was also verified from quantitative RT-PCR experimentation of total RNA extracted from HeLa cells, when compared with full-length WT construct (Control). This *in vitro* analysis likewise provided independent confirmation of *NOTCH1* down-regulation for the c.1343G>A mutation, alongside the c.1220C>G, c.4120T>C and c.5218G>T mutations (Figure 5-4).

To further cross-examine the functional effect of *NOTCH1* mutants on down-stream signalling targets, *in vivo* gene expression studies were employed for quantification of *HEY1* and *HES1* transcripts in RNA samples of the mentioned AOS patients. The subjects harbouring the c.1649dupA frameshift mutation revealed a principally marked reduction of *HEY1* transcript levels, when compared to WT control ($p=0.0004$). In addition, *HEY1* expression was also down-regulated, but not at a significant extent for the case of c.1343G>A missense mutation (Figure 5-3B). Following the same pattern of down-regulation, *HES1* transcripts were reduced in the c.1649dupA patients ($p=0.0004$), but no

significant deviation to the WT control was detected in the c.1343G>A sample (Figure 5-3C).

Table 5-1 Summary of identified *NOTCH1* variants

Exon	Coding variant	Protein variant	Variant type	Protein domain
7	c.1220C>G	p.P407R	Missense	EGF 10
8	c.1343G>A	p.R448Q	Missense	EGF 11
8	c.1345T>C	p.C449R	Missense	EGF 11
8	c.1367G>A	p.C456Y	Missense	EGF 11
10	c.1649dupA	p.Y550*	Frameshift	EGF 14
25	c.4120T>C	p.C1374R	Missense	EGF 35
26	c.4663G>T	p.E1555*	Nonsense	LNR 3
26	c.4739dupT	p.M1580lfs*30	Frameshift	-
28	c.5218G>T	p.A1740S	Missense	TM
32	c.6049_6050delTC	p.S2017Tfs*9	Frameshift	ANK 4

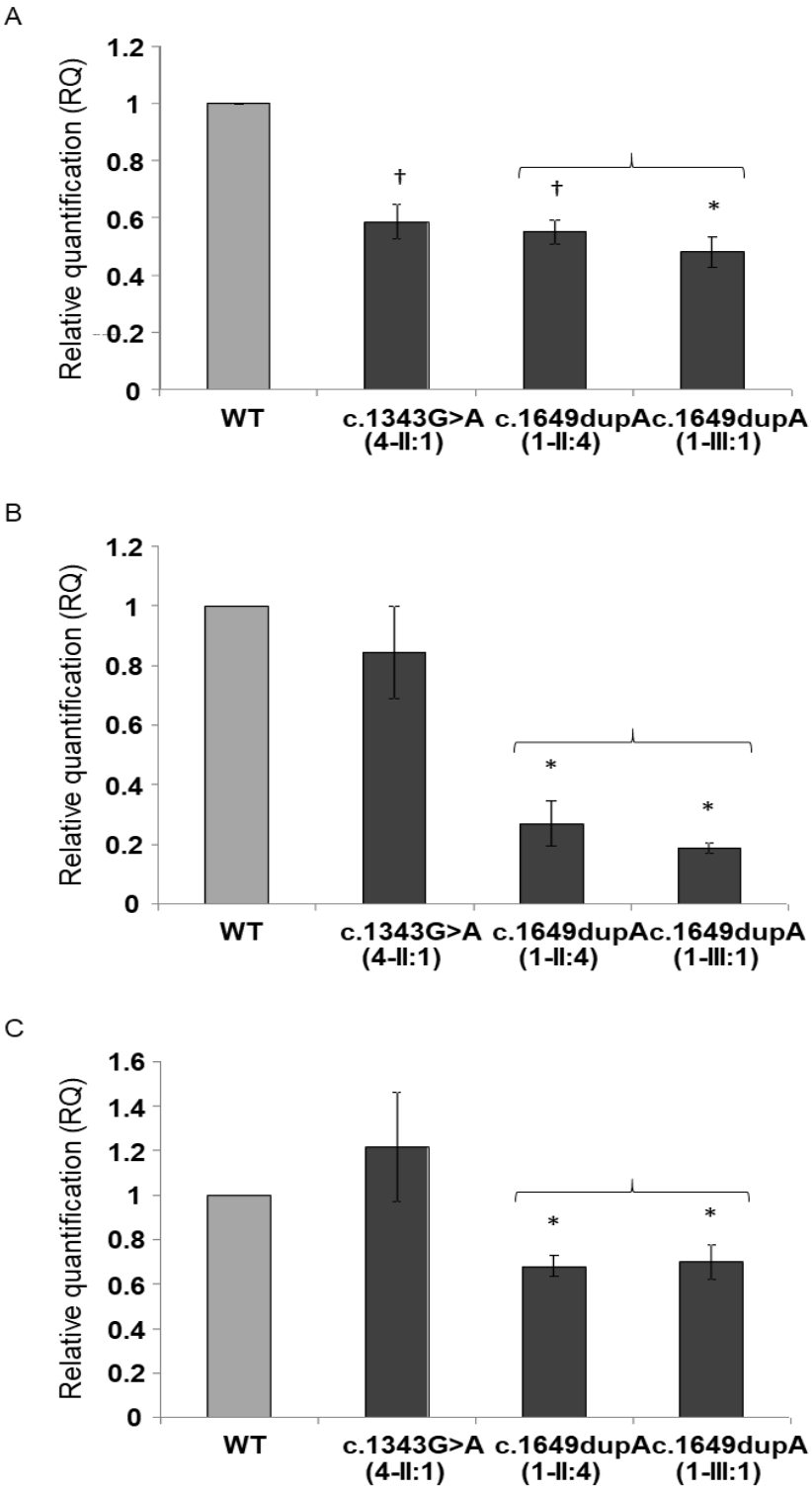

Figure 5-3 Real-time qPCR of *NOTCH1*-positive patient samples
Graphs show levels of gene expression for A) *NOTCH1*, B) *HEY1* and C) *HES1*. Relative quantification (RQ) of mRNA transcripts are calculated relative to the WT baseline and normalised to *GAPDH* and *ACTB* levels. Data are means ±SD of 3 independent experiments;
Key: *P<0.001; †P≤0.01 vs the control group, RM one-way ANOVA,
NOTCH1 mutations: c.1343G>A, c.1649dupA. Subject IDs: 4-II:1, 1-II:4, 1-III:1 (Table D-1, Appendix D)

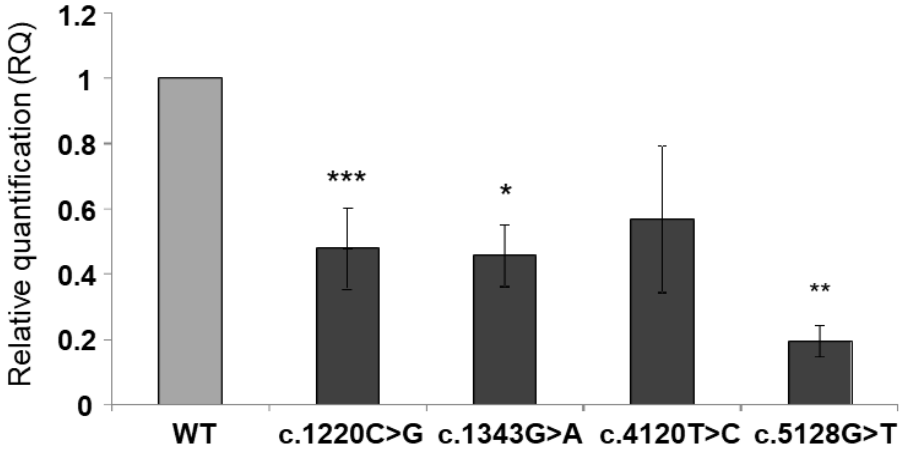

Figure 5-4 Real-time quantitative PCR of cells transiently transfected with mutagenized *NOTCH1* cDNA constructs
All missense mutations show reduced *NOTCH1* expression by comparison to cells transfected with a full-length wild-type construct (WT). Relative quantification (RQ) of gene expression is calculated relative to the WT baseline and normalised to *GAPDH* and *ACTB*. Data are means ±SD of 3 independent experiments;

Key: ***P<0.0001; **P=0.0017; *P=0.0148 vs the control group, RM one-way ANOVA
NOTCH1 mutations: c.1220C>G, c.1343G>A, c.4120T>C, c.5128G>T.

5.3.2 POTENTIAL CROSS-TALK BETWEEN NOTCH1 AND BMP SIGNALLING

For the purposes of identifying a novel cross-talk in molecular level between the defective NOTCH1 signalling cascade in the AOS patients with related cardiac and vascular abnormalities, and the BMP signalling pathway, quantitative RT-PCR was employed to identify potential ID1 dysregulation *in vivo*. The missense *NOTCH1* c.1343G>A mutation and the c.1646dupA frameshift mutation cases were once more examined and very interestingly in both cases ID1 mRNA levels ware up-regulated (Figure 5-5 A1-A2). To further interrogate this novel finding in vitro, transient transfection of WT, c.1343G>A and c.1646dupA NOTCH in HeLa cells was performed to examine the functional impact of the *NOTCH1* missense and frameshift mutation on SMAD1/5 signalling. 48h later the cells were harvested and Western blotting analysis revealed significantly higher phosphorylated levels of SMAD1/5 protein in both WT and mutated NOTCH1 receptor over-expression (Figure 5-5 C1-C2). The effect of WT *NOTCH1* over-expression on *ID1* mRNA levels in HeLa cells was also assessed by qPCR and was also positively correlated with *NOTCH1* up-regulation (Figure 5-5 B1-B2).

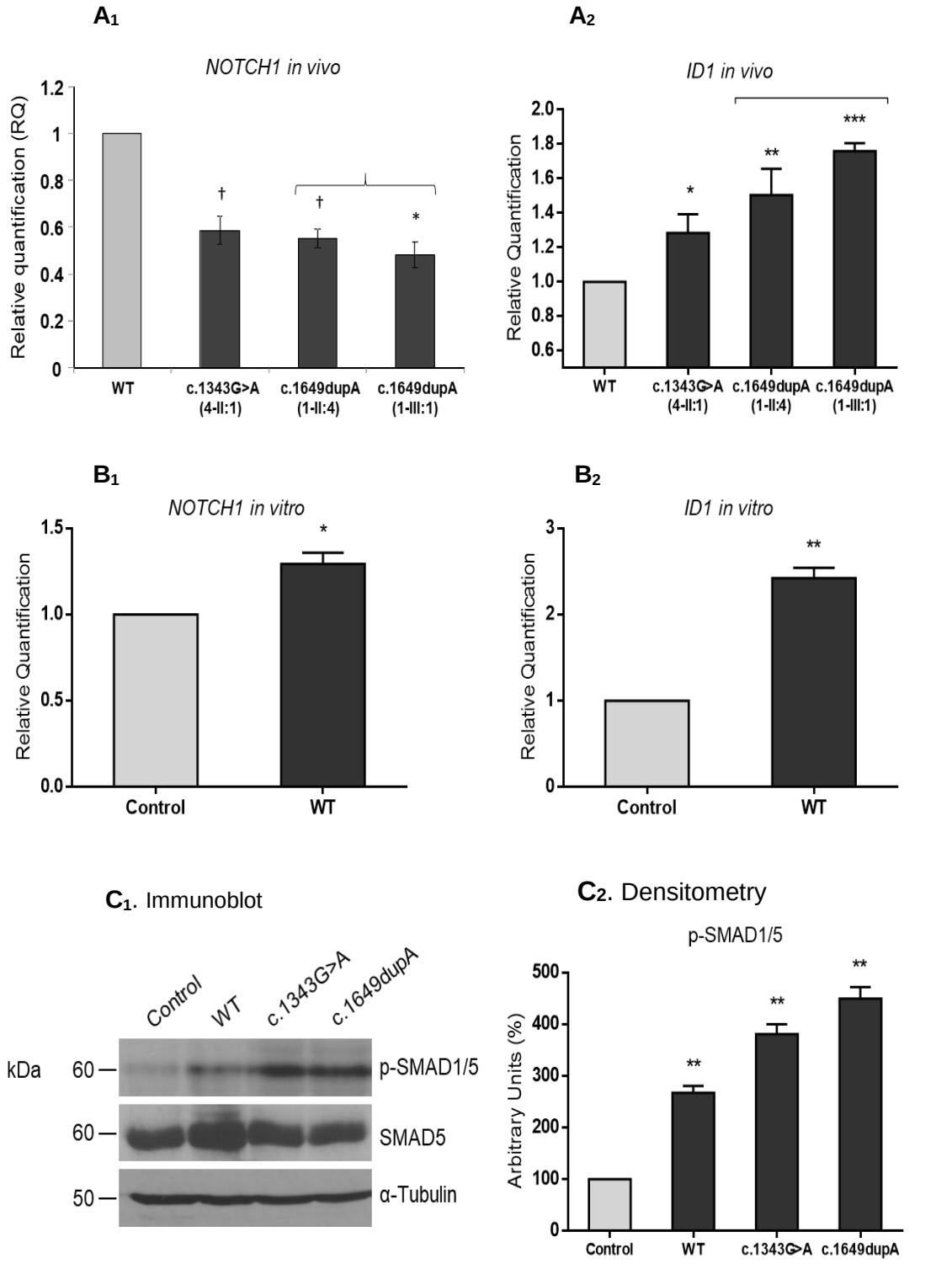

Figure 5-5 *In vivo* and in *vitro ID1* destabilization in the present of *NOTCH1* mutations (A_1 - A2) Real-time PCR of *NOTCH1*-positive patient samples. Graphs show levels of gene expression for *NOTCH1* and *ID1*. Interestingly, *ID1* transcript levels are up-regulated in patient samples. Relative quantification (RQ) of mRNA transcripts are calculated relative to the WT baseline and normalised to *ACTB* levels. (B_1) Real-time quantitative PCR of HeLa cells transiently transfected with WT *NOTCH1* cDNA construct. (B_2) *ID1* mRNA levels significantly up-regulated when WT *NOTCH1* has been ectopically over-expressed. Relative quantification (RQ) of gene expression is calculated relative to

the control baseline (cells transfected with empty vector) and normalised to *ACTB*. (C_1) Immunoblots of endogenous p-SMAD1/5 and SMAD5 of HeLa cells transiently transfected with mutagenized *NOTCH1* and WT cDNA constructs. (C_2) Both mutations plus WT show increased p-SMAD1/5 expression by comparison to cells transfected with empty plasmid (control). Data are means ±SD of 3 independent experiments;

Key: [†,**]P≤0.01; *P<0.05, ***P<0.001 vs the control group, RM one-way ANOVA

5.4 DISCUSSION

5.4.1 HAPLOINSUFFICIENCY OF THE NOTCH1 RECEPTOR AS A CAUSE OF ADAMS-OLIVER SYNDROME WITH VARIABLE CARDIAC ANOMALIES

There is an unusual high degree of locus heterogeneity for this serious morphogenetic disease, termed as AOS. Molecular and genetic studies successfully provided essential knowledge on the identification of multiple causative genes, and further the relevant molecular pathways to the disease pathogenesis. Yet, there is significant unexplained locus heterogeneity with underlying molecular genetic determinants, nevertheless uncharacterized for the majority of cases. It is possible that AOS may represent a cluster of related phenotypes, analogous to RASopathies or cliopathies (Davis, Katsanis 2012, Patel, Taylor et al. 2004). Up to date, there are several proposed mechanisms to explain limb reduction and scalp defects in AOS. For example, vascular obstruction by thromboses during embryonic development is a known cause of TTLD, or endothelial cell dysfunction is a root cause of AOS (Hoyme, Jones et al. 1982, Toriello, Graff et al. 1988, Swartz, Sanatani et al. 1999). Denuted or reduplicated internal elastic laminae in AOS-blood vessels, blood vessel stenosis due to irregular vascular smooth muscle cells coverage, and tortuous ectatic vessels along with a general paucity of small to medium blood vessels are common findings in autopsy of AOS-vasculopathy related cases, suggesting pericyte dysfunction as the basic pathophysiological mechanism in AOS (Patel, Taylor et al. 2004). Both Stittrich et al., 2014, and Southgate et al., 2015, reports added up to this glowing list of wide variety of AOS-related vascular defects, identifying AOS-subjects with pathological conditions cutis marmorata, venous ectasia, thrombophilia, portal hypertension, pulmonary hypertension and right- and left-sided CHD. While relevant academic and clinical bibliography reports the unclear mechanism of how *NOTCH1* mutations and further loss of function cause AOS, it is of critical importance to highlight the dysregulated NOTCH1 signalling due to prevention of translation of effective stabilization of the receptor homotetramers after ligand binding interactions, as Notch signalling strength is the critical element in determining the normal development of the vasculature (Petrovic, Formosa-Jordan et al. 2014).

Southgate et al., 2015, documented 10 novel germline *NOTCH1* mutations identified in 12 AOS clinically diagnosed probands and a 50 unrelated AOS-patient cohort with autosomal dominant and sporadic forms of AOS. Of interest, a significant high proportion of probands (5/11; 45%) diagnosed with a congenital heart abnormality, a percentage considerably higher of reported literature cases (Patel, Taylor et al. 2004, Algaze, Esplin et al. 2013). In addition, 47% (8/17) of all affected variant carries had been diagnosed with a congenital heat anomaly as well (Appendix D – Table D-1). Taken together, *NOTCH1* variants may represent a subtype of AOS, associated with cardiac malformations. Equally importantly, cutis marmorata telangiectatica congenita and several portal vein abnormalities were observed in *NOTCH1*-positive cases, thus *NOTCH1* variants may also represent a distinct subtype of AOS associated with cardiovascular defects. To further support these associations, *NOTCH1* mutations in 5 AOS kindreds with cardiac spectrum defects were reported in a correlated study undertaken by Stittrich et al., 2014.

In the context of this research, the emerged defective NOTCH1 signalling pathway is highlighted in regard to AOS pathogenesis. Existing literature reports numerus times the vital role of Notch family of single-pass transmembrane receptors in multiple cellular processes including cell fate in bilaterally symmetric multicellular eukaryotes, during embryogenesis and development of the cardiovascular system (High, Lu et al. 2008). Mutations of Notch components across the whole signalling cascade, underlie CHDs in humans and mice; for instance, *Jag1* gene and at a lesser extent *NOTCH2* mutations are responsible for the majority of cases in Alagille syndrome (Oda, Elkahloun et al. 1997), or embryonic lethality and cardiovascular defects (High, Lu et al. 2008). Interestingly, distinct *NOTCH2* truncating variants are responsible for Hajdu-Cheney syndrome, an osteolytic developmental disorder with pleiotrofic effects analogous to the NOTCH1 receptor. Furthermore, craniofacial abnormalities, impairment of limb development and positive regulation of angiogenesis and osteogenesis have been reported in vivo for mice lacking Jag2 ligand or conditionally targeting NOTCH1 and NOTCH2 receptors (Francis, Radtke et al. 2005, Pan, Liu et al. 2005). However, more functional studies regarding NOTCH1

receptor have to be undertaken for elucidation of the importance of its signalling cascade, during human foetal development.

In mammalian cells, the canonical NOTCH1 signalling is stimulated by ligand binding (Jag1/2, Delta-like1/3/4) through direct contact of adjacent cells, followed by proteolytic cleavage of NICD, which in turn forms transcriptional complexes with RBPJ and other co-activators (Figure 1-11). Furthermore, RBPJ regulates the expression of certain members of HEY and HES families of transcription factors, which have prominent role in cardiovascular development along with vasculogenesis and vascular remodelling (Fischer, Schumacher et al. 2004). Therefore, stimulation of *HEY1* and *HES1* it is known to be a direct readout of signalling activation.

This study focuses in 10 missense, nonsense or frameshift *NOTCH1* mutations, all identified by Southgate et al., 2015 that four out of ten are predicted protein truncating mutations most likely subject to NMD. Five of the six identified missense mutations are located with EGF-like domains of the receptor (Table 5-1). This particular domain is responsible for the ligand-binding activation of signalling, chelating Ca^{2+} and is characterized by a core-β-pleated sheet, 3 disulphide bonds along with a series of variable loops (Hambleton, Valeyev et al. 2004). p.R448, p.C449R and p.C456Y lie within the EGF11 region, most likely disrupting the tertiary structure and affecting ligand interaction and/or Ca^{2+} binding (Figures 5-1 and 5-2). More specifically, the side chains of Arg448 and Glu424 interact electrostatically as it illustrated at the X-ray structure of this region (Figure 5-2); therefore p.R448Q mutation makes this interaction unstable. In addition, p.C449R and p.C456Y mutations potentially break the disulphide bonds between Cys440 and Cys449, and between Cys456 and Cys469 respectively. An imminent outcome of these breakages is the disruption of the adjacent Ca^{2+} stability coordinated by the side chains Asp469, Glu455 and Asp452 (Figure 5-2). There is no up to date 3-dimentional structure of EGF35 region, but it is highly anticipated that Cys1374 mutation exerts similar effects. Furthermore, EOGT functions as an O-linked N-Acetylglucosamine (GlcNAc) transferase, which catalyses the addition of an O-GlcNAc moiety to the 36 EGF-like repeats of the receptor in both Drosophila and mouse (Sakaidani, Ichiyanagi et al. 2012). Although, AOS-associated EOGT gene functions have not yet been fully

elucidated in humans, it is notable that 4 of the 5 EGF-domain missense identified mutations are located within the $C_5XXGXS/TGXXC_6$ motif located between the fifth and sixth conserved cysteines, which is target of EOGT for O-glycose or O-fucose modification. Moreover, the p.A1740S transmembrane mutation is also investigated in terms of defective signalling, although the functional impact on the receptor is unknown. Taken together, these findings suggest that the structural integrity of NOTCH1 receptor is affected by the majority of the identified missense mutations, thus its vital signalling activity is highly compromised.

In the context of this research, gene expression studies have been performed to demonstrate that *NOTCH1* expression is down-regulated in AOS-subjects harbouring *NOTCH1* mutations *in vivo*. The control subject was a single healthy female aged 26 years old. Additional controls have been employed as part of the experimental design of the real-time PCR studies (Figure 5-3). Further *in vitro* transient transfection studies have been designed and undertaken to support and corroborate the *in vivo* data**.** Indeed, the generated data (Figure 5-4) support the prediction of partial *NOTCH1* transcript loss by NMD or potential perturbation of mRNA stability in case of the missense mutations, when compared to control cells that had been transfected with WT *NOTCH1*. To further support the notion of NOTCH1 dysregulated signalling, the NOTCH1 down-stream targets *HEY1* and *HES1* at a lesser extent, were down-regulated *in vivo* for the tested *NOTCH1* mutations. Of interest, perturbation of both *HEY1* and *HES1* expression vary between the mutations tested, indicating allele-specific effects on downstream signalling (Southgate, Sukalo et al. 2015). Despite the limited available number of patient samples, *HEY1* down-regulation suggests a common mechanism in AOS molecular pathology. Moreover, these data are highly compatible with the previous hypothesis that *RBPJ* mutations, a known causal factor in AOS pathogenesis, contribute to dysregulated Notch signalling. Taken together, these data solidify the project hypothesis; that loss-of-function haploinsufficiency of *NOTCH1* is an important factor in AOS pathogenesis. They also provide a genotype-phenotype correlation between *NOTCH1* mutation and AOS-subjects with cardiac anomalies. Therefore, the first two aims of this project have been fulfilled both *in vivo* and *in vitro* case studies of *NOTCH1* key missense and frameshift mutations, with subsequent receptor and down-stream targets down-

regulation, a verified result which supports the notion of dysregulated NOTCH1 signalling in AOS with variable cardiac abnormalities.

5.4.2 SIGNALLING CROSS-TALK BETWEEN NOTCH1 AND BMP PATHWAYS

This study also provides novel evidence of synergism between NOTCH1 and BMP signalling in a proportion of AOS-associated cases. The loss in regulation of NOTCH1 and NOTCH3 signalling, has been recently associated with the pathogenesis of several lung diseases, such as chronic obstructive pulmonary disease, asthma, pulmonary fibrosis, PAH, lung cancer and lung lesions in some congenital diseases (Zong, Ouyang et al. 2016). In the case of PAH and NOTCH3 signalling in particular, the pathway is activated in primary human coronary artery and vascular smooth muscle cells, with several biological implications including reduction of cell proliferation rates and resistance to PAH development under hypoxic situations (Campos, Wang et al. 2002, Li, Zhang et al. 2009). Further molecular studies in the field, empowered the notion that spontaneous PAH in mouse models may arise via the dysregulation of Notch signalling (Yu, Mao et al. 2013). While a direct convergence between Notch and BMP/TGF-β signalling is already evident in relevant bibliography, highlighting the NICD interactions with SMAD3 for TGF-β and SMAD1 for BMP signalling, there is no up to date study to bridge at a molecular lever AOS NOTCH1 signalling with potential alterations in BMP signalling. Thus, novel experimentation was designed to elucidate the potential synergism of BMP signalling in case of defective AOS-NOTCH1 signalling, both *in vivo* and *in vitro*. Indeed, *ID1* transcription levels were significantly up-regulated in AOS-patients harbouring p.R448Q and p.Y550* *NOTCH1* mutations. Of note, phosphorylated SMAD1/5 levels were also significantly up-regulated in transient transfections studies of the above mutations in a generic cell line, a finding which correlates with the hypothesis of BMP signalling activation upon dysregulated NOTCH1 signalling and fulfils the last aim of the project. Taken together, these data agree with the general notion of BMP signalling cooperation, and synergistic and subsequent antagonism of BMP-SMAD and Notch-mediated signalling pathways that have been demonstrated in

EC and VSMC cultures (Beets, Huylebroeck et al. 2013, Rostama, Peterson et al. 2014).

5.5 CONCLUSION AND FURTHER WORK

This report solidifies *NOTCH1* mutations as the primary cause of AOS, in a proportion of cases in the cohort study (17%), while establishes *NOTCH1* as an important genetic factor in AOS with associated cardiovascular complications. This finding warrants further epidemiological investigation in a future AOS-cohort study, that will be examined for cardiovascular complications. The functional studies have indicated links to previously associated genes of this condition, which together accentuate the central importance of NOTCH1 signalling in a series of key developmental systems in human embryogenesis. Further X-ray crystallography studies of the identified *NOTCH1* missense mutations of the EGF-like domain will also elucidate the extend of the structural perturbation of the receptor and subsequent impairment of the signalling cascade. Finally, the cross talk of BMP and NOTCH1 signalling is highlighted as a synergistic effect in AOS pathology, underlined by forms of non-canonical signalling and potentiating the suppressive BMP cell signalling effect in AOS-cases of dysfunctional NOTCH1 signalling and further cardiovascular defects. A future goal of research could be established in regards the potential BMP signalling up-regulation in AOS-subjects that suffer from certain vasculopathies and/or PAH. If to continue working in the field, a recommended allowing suitable time-frame for the above-mentioned experimentation, would be a 2-3 years' study, as X-ray crystallographic studies along with tissue-based work would require a substantial amount of time for the evolution of this crucial research on AOS and PAH linkage, in terms of aberrant signalling and cardiovascular malformations.

CHAPTER 6: DISCUSSION

In order to summarise the findings regarding the differential regulation of the BMP and TGF-β signalling pathways mediated by JAB1 and its control of several target genes in healthy and/or disease state, a schematic was produced (Figure 6-1).

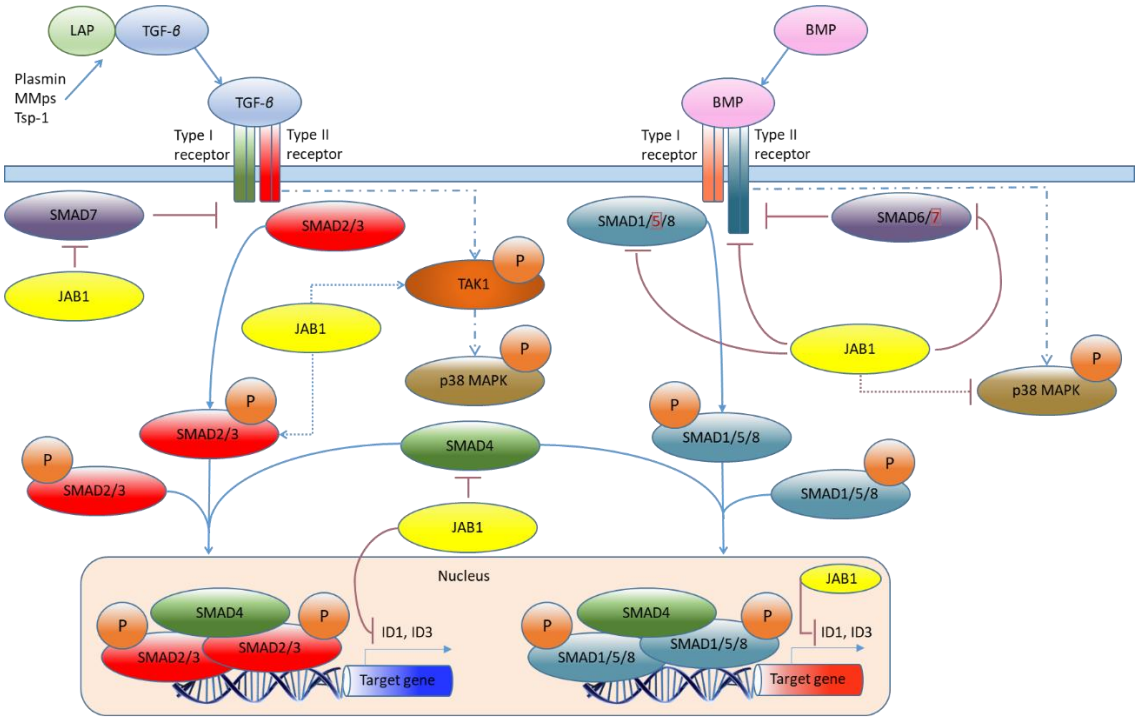

Figure 6-1 JAB1 differentially regulates BMP and TGF-β signalling pathways
Upon BMP or TGF-β ligand stimulation, the type-II receptors activate and phosphorylate through their kinase domain, type I receptors. In turn, type-I receptors phosphorylate R-SMADs 1/5/8 (for BMP signal) or R-SMADS2/3 (for TGF-β signal) and through association with the common-SMAD4 they form trimers which translocate to the nucleus and form complexes with other transcription co-factors, regulating SMAD-dependant gene expression. The receptor complexes could also activate SMAD-independent signalling such as TAK1 and p38MAPK pathways. Inhibitory SMADs 6 (for BMP signalling) and 7 (for TFG-β signalling) act as negative regulators of BMP/TGF-β signalling, targeting the activated receptor complexes for proteasomal degradation. As it has been shown within the context of this study, pulmonary arterial endothelial and smooth muscle cells undergo differential regulation of the signal transduction by JAB1 protein, in all main steps of the BMP/TGF-β signalling cascades, by targeting for proteasomal degradation BMP type II receptor, co-SMAD4, SMAD5, I-SMAD7, and the transcription factors ID1 and ID3. Furthermore, JAB1 over-expression can up-regulate SMAD2/3 signalling and activate the mitogenic cascades of TAK1 and p38 MAPK, via SMAD-independent signalling. In certain cell types as carcinomas, JAB1 over-expression could lead to down-regulation of p38 MAPK, as it has been demonstrated in this study's early findings.

The main aim of this study was to examine the respective roles of JAB1 and NOTCH1 in the development of cardiovascular disorders. Previous studies have shown both proteins to be involved in BMP signalling pathways; JAB1 has been identified as a BMPR-II interacting protein, whilst NOTCH1 intracellular domain interacts with SMADs and enhances the canonical NOTCH1 signalling (Andersson et al. 2011). We therefore seek to better understand the processes by which these pathways are regulated and their function in cardiac disease pathogenesis, both with and without a PAH phenotype.

A principal study goal was to verify the interaction of JAB1 and BMPR-II in vivo and in vitro for which evidence has been presented in HeLa and HEK293T generic cell lines. Moreover, over-expression of monomeric JAB1 has been shown to modulate the down-regulation of BMPR-II. Further BMP4-ligand stimulation of the BMP pathway did not alter the mechanistic effect of JAB1 on down-stream BMPR-II outcomes, in particular the effect on SMAD1/5 activation, thus it was considered definitive. An additional feature that was identified was the up-regulation of JAB1 protein expression in PASMC cells harbouring two distinctive HPAH *BMPR2* mutations. However, this finding did not come into synergy with a third HPAH *BMPR2* mutation that has been extensively studied, indicating that JAB1 dysregulation is *BMPR2* mutation specific in PAH cells. Through the study of JAB1 and BMPR-II protein interaction, a novel finding has been identified, whereby JAB1 down-regulation of BMPR-II is mediated via the proteasomal pathway in the normal and/or disease circulation. Thus, the currently unsolved elevated receptor loss in PAH progression could be explained through this identified protein-protein interaction with JAB1. Taken together, these data provide insights into the role of this interaction, that when disrupted, may lead to a disease phenotype. Further functional studies may elucidate the minimal JAB1 interacting regions, by domain, with the BMPR-II receptor and the definition of the real-time interaction of BMPR-II with JAB1 by fluorescence resonance energy transfer (FRET) analysis.

In recent studies, JAB1 has been characterized as an oncogene (Hsu et al. 2008, Yoshida, et al. 2010, Shackleford and Claret 2010), and here the tumorigenic potential of JAB1 is indicated by demonstrating increased proliferation of JAB1-transfected cells by comparison to control. However, present studies have not

examined this finding in the context of monoclonal growth of tested cells. These data are important in the context of PAH because they may play a significant role for explanation of the uncontrolled proliferation of PAECs and PASCMs in disease state. The up-regulation of JAB1 remains to be extensively investigated in multiple human PAH lines with a range of in *vivo* mutations and primary murine cells to determine whether genotype may influence JAB1 level. It would also be of interest to examine stable clones expressing a BMPR-II KD mutation, such as p.D485G, a highly penetrant missense mutation.

In case of BMPR2 mutant PASMC cells, it has also been demonstrated that selective BMP4 treatment inhibited their abnormal proliferation, a finding that verifies the reported use of TGF-β1 and BMPs as BMP2, 4 and 7 anti-proliferative effects on vascular smooth muscle cells (Morrell, Yang et al. 2001), and complements the first use of BMP7 ligand to target and enhance endothelial BMPR-II signalling and reverse established PAH in animal model of disease (Long, Ormiston et al. 2015). Further experimentation on PASMC cells indicated that *BMPR2* haploinsufficiency potentiates TGF-B signalling in PAH, mainly via mitogenic SMAD-independent signalling pathways such p38MAPK and TAK1, underlining the importance of restoration of the BMP signal and its suppressive role on cell proliferation. Taken together, this study underscores a role for BMP4 as a vascular stability and quiescence factor and provide a translational framework for delivery of the BMP ligand as a treatment strategy for PAH.

This study mainly characterizes JAB1 as a key regulator of BMP and TGF-β signalling pathways, because as it has been shown it differentially regulates their signalling balance, by mainly repressing or enhancing at a lesser extent the relevant up-stream, intermediaries and down-stream transcription factors. The manner in which JAB1 mediates regulation of the BMP/TGF-β signal indicates that is happening via SMAD-dependent or SMAD-independent pathways, as it was verified in a generic cell line. More specifically, it has been evidenced that JAB1 over-expression down-regulates BMPR-II protein expression, along with SMAD5, co-SMAD4 and I-SMAD7, whereas JAB1 dysregulation could shift the BMP and TGF-β balance towards the later, potentiating *ID1* expression via either repressing the I-SMAD7 or activating SMAD non-canonical signalling by TAK1 up-regulation. In addition, p38 MAPK activation by JAB1 over-expression was

considered to be cell type specific, because an opposite effect on p38 MAPK regulation was observed in HeLa cells that JAB1 was ectopically over-expressed. Most importantly and through RNAi interference studies, the endogenous knock-down of JAB1 from healthy and mutant PASMCs, managed to suppress cell proliferation and reverse abnormal proliferation in mutants, rescuing the PAH disease phenotype. Thus, JAB1 oncogenic activity may potentiate a clinical target for manipulation in the treatment of PAH.

Novel patient data analysis has demonstrated that *NOTCH1* gene expression is down-regulated in AOS subjects harbouring *NOTCH1* mutation *in vivo*, supporting the initial prediction of transcript loss by molecular mechanisms as NMD or perturbation of mRNA stability (Cartegni et al. 2002). Transient transfection studies of mutant constructs further supported *in vitro* the patient data, solidifying the hypothesis that haploinsufficiency of the NOTCH1 receptor is a cause of AOS. Moreover, reduction of *HEY1* and, to a lesser extent, *HES1* transcript levels confirms the prediction that these identified mutations potentially lead to dysregulated Notch signalling, as previously reported with mutations of the *RBPJ* gene in AOS (Hassed et al. 2012). Furthermore, reduction of *HEY1*, which is mainly associated with cardiovascular development (Fischer, Schumacher et al. 2004), is a fact which may explain the increased incidence of the reported cardiovascular findings in these patients. In the context of NOTCH1 defective signalling, future X-Ray crystallographic studies should be employed to assess the effects of the identified missense mutations of NOTCH1 in the extracellular domain, specifically in EGF repeats 11-13 encoding the ligand-binding domain. Finally and within the context of this study, novel compelling evidence of synergism between NOTCH1 and BMP signalling has been identified in a proportion of AOS-associated cases. While BMP and Notch signalling cross-talk is well described in available bibliography, this was the first time that a BMP/NOTCH1 molecular bridge has been investigated, linking defective AOS-associated NOTCH1 signalling with up-regulated BMP signalling both *in vivo* and *in vitro* cases. This later finding may be indicative of potentiation of the suppressive BMP regulatory effect in AOS-cases of dysfunctional NOTCH1 signalling and further cardiovascular defects. In summary, these data support the hypothesis that AOS may be a disorder of vasculogenic origin, and further provide

novel evidence of a genotype-phenotype correlation between *NOTCH1* mutations and AOS-related congenital heart defects.

6.1 CONCLUSION

During PAH progression, JAB1 protein is up-regulated under certain *BMPR2* mutations, a dysregulation which results in down-regulation of the BMPR-II receptor via ubiquitin-mediated proteolysis and further impairment of BMP signalling. JAB1 over-expression potentiates cells into a proliferative and anti-apoptotic response, promoting a differentiated phenotype. In addition, the BMP/TGF-β signalling balance is greatly affected by JAB1 dysregulation, both in SMAD-dependant and SMAD-independent manners. Thus, JAB1 can be characterized as a regulator of the BMP and TGF-β signalling pathways. Finally, haploinsufficiency of the NOTCH1 receptor has also been identified as the primary cause of AOS, and an important genetic factor in AOS with associated cardiovascular complications.

CHAPTER 7: APPENDIX A

Buffer recipes and SDS-PAGE conditions

Extraction Buffer for co-IPs

20mM HEPES pH 7.5
100mM NaCl
10% Glycerol
1% Triton X-100
20 mM sodium fluoride (NaF),
1 mM sodium orthovanadate (Na3VO4),
1 mM phenylmethylsulphonyl fluoride (PMSF),
10x Protein Inhibitors Cocktail
dH_2O

General Extraction Buffer for WBs

1M Tris base pH 7.4
5M NaCl
1M $MgCl_2$
10% SDS
1% Triton X-100
20 mM sodium fluoride (NaF),
1 mM sodium orthovanadate (Na3VO4),
1 mM phenylmethylsulphonyl fluoride (PMSF),
10x Protein Inhibitors Cocktail
dH_2O

SDS-PAGE Running Buffer

25mM Tris
192mM Glycine
0.1% SDS
dH_2O

Transfer Buffer (for Western blotting)

25mM Tris
192mM Glycine
20% Methanol
dH_2O

SDS Sample-Loading Buffer

50mM Tris-HCl pH 6.8
2% SDS
10% Glycerol
1% β-mercaptoethanol
12.5 mM EDTA
0.02% bromophenol blue

CHAPTER 8: APPENDIX B

Growth curves of project key cell lines

In order to study the growth and the doubling time of the studied cell lines, HeLa and HEK293T cells were maintained in culture for 6 days, and PASMC (WT) were maintained for 7 days, without media change (Figure A-1). The Population Doubling Time (PDT) from the linear part of each curve was defined using the formula: $T_d = (t_2 - t_1) \times \frac{\log_e 2}{\log_e\left(\frac{N_2}{N_1}\right)}$, where N being cell numbers at the two times. The PDTs of HeLa, HEK293T and PASMC cells were 27.23h, 17.89h and 35.00h respectively.

The hTERT-immortalized PASMC-*Bmpr2*$^{+/R899X}$ cell line was discarded from experimentation, because of abnormal proliferation (Figure A-2). Whilst not investigated, the human Telomerase Reverse transcriptase (hTERT) treatment of primary cells for immortalization may cause altering of their phenotypic characteristics and proliferation rates.

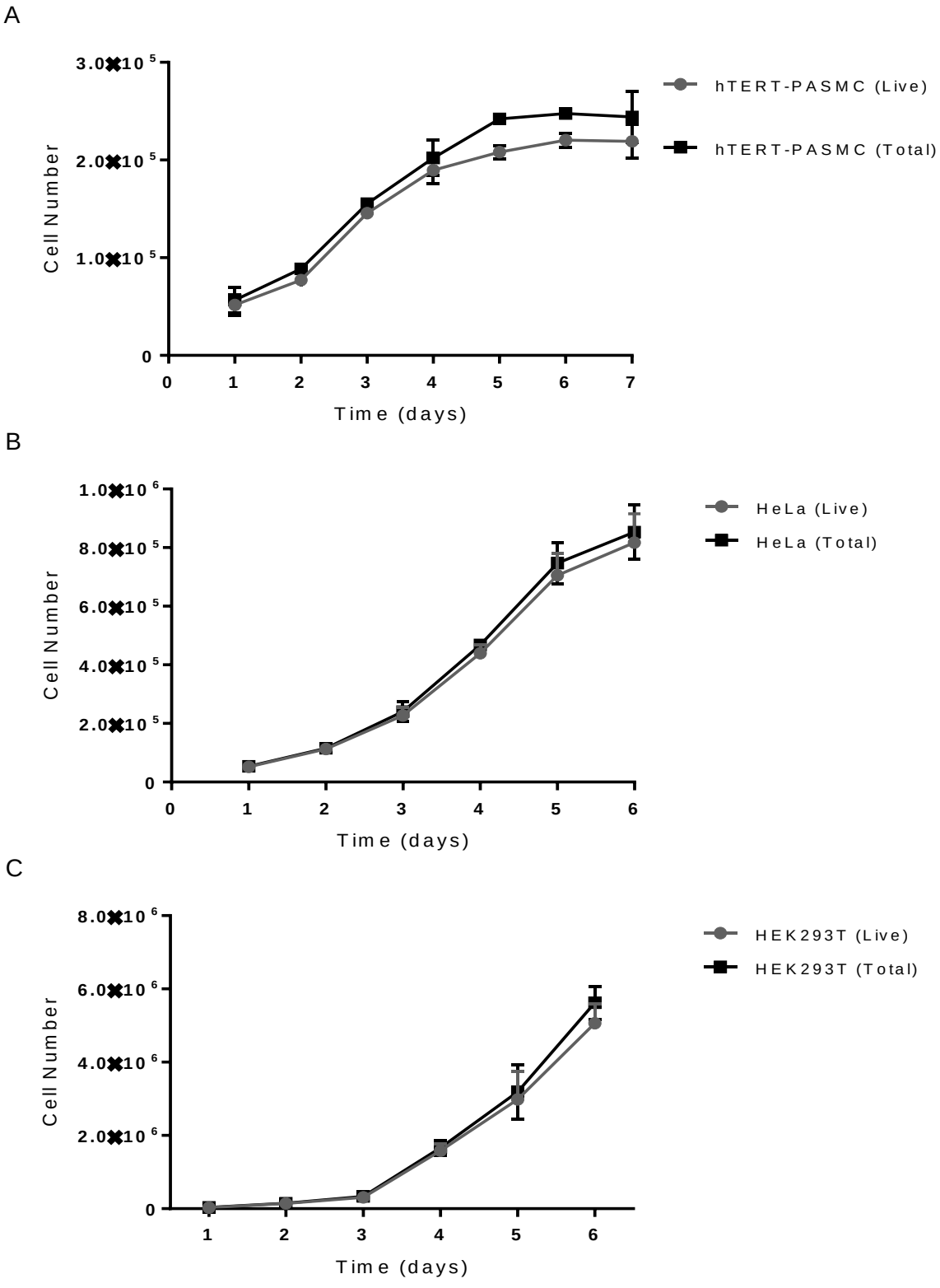

Figure A-1 Growth curves of human PASMC (WT), HeLa and HEK293T cell lines
The PDT for A) PASMC cells was 37.00h, for B) HeLa cells was 27.23h and for C) HEK293T cells was 17.89h. The results of 3 independent experiments in technical triplicates (mean ±SD) are shown.

A

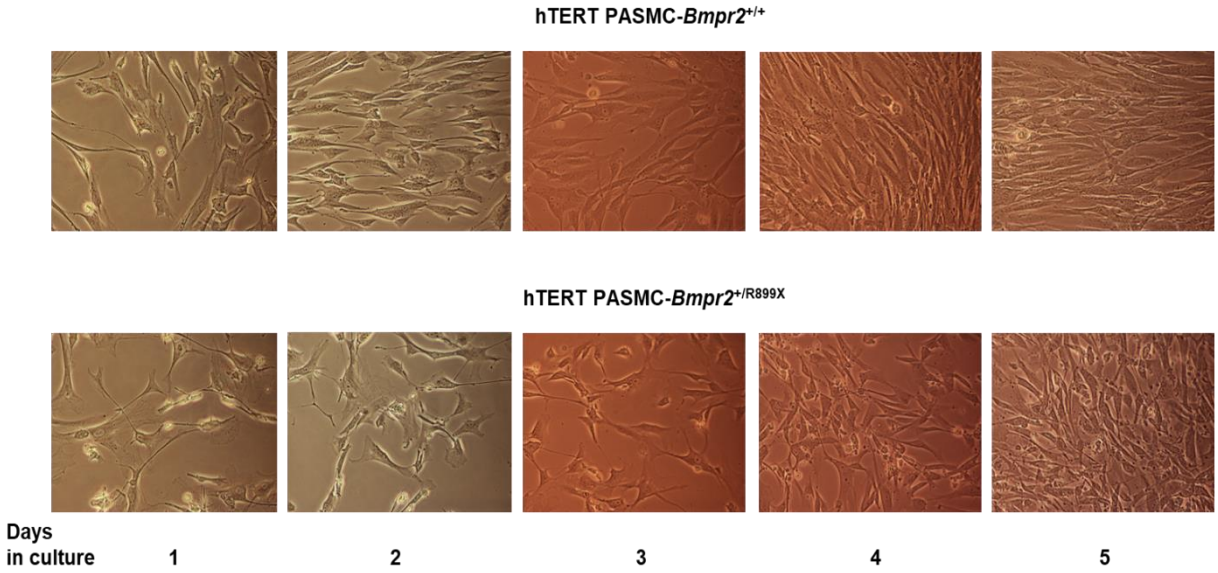

B

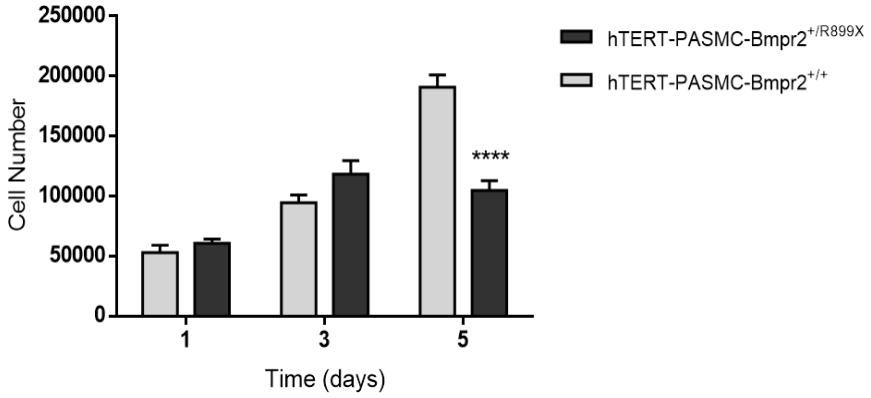

Figure A-2 Abnormal proliferation of hTERT PASMC-*BMPR2*$^{+/R899X}$ cell line
A) 10x Optical Magnification of hTERT PASMC-*BMPR2*$^{+/R899X}$ and WT cells in 5 days culture experiments. B) A significant difference in proliferation between p.R899X cells and control at day 5 was identified. Mutant cells were behaving in an abnormal and unexpected way, slowing down their proliferation compared to healthy cells, for all experimentation that took place in our laboratories. The cells were found to be inappropriate for further proliferation and transfection studies, within the context of the project. P values were calculated by Sidak's multiple comparison test in a 2 way Analysis of Variance (ANOVA).
Key: ****p<0.0001

CHAPTER 9: APPENDIX C

Transient Transfections

Chemical methods (Figures 1-3)

Non-liposomal reagents: Fugene HD (Promega) and Turbofectin 8.0

Liposomal Reagents: Lipofectamine 2000 and Lipofectamine 3000

Detection time: 48h post transfection

Generic cell lines: HeLa and HEK293T

Regent (μL): pDNA (μg) ratio of 3:1 after optimization in each above case (Lipofectamine 2000 and Fugene HD have similar results with 2.5:1 as well)

Cell viabilities and transfection efficiencies in HeLa cell line, 48h post-transfection. The viabilities were verified using Trypan Blue stain, after repeated experimentation in 6 well plates / 10cm dishes.

Reagent	Viability (48h)	Efficiency of Transfection (48h)
Fugene HD	95%	44%
Turbofectin 8.0	90%	50%
Lipofectamine 2000	60%	50 %
Lipofectamine 3000	80%	45%

Comments:

1) 24h post transfection time is limited in efficient gene expression (verified by WB)
2) JAB1 – BMPR-II interaction, due BMPR-II down-regulation after ectopic Jab1 expression, visible at 48h
3) Experiments with HEK293T cells gave better Western blotting results in regard to ectopic expression of Jab1; yet after 48h and due to high proliferation rate of the cells the episome copies are being reduced.
4) Extremely low reproducibility of positive results – loss of valuable lab. Time
5) No transfection of hTERT Pulmonary Arterial Smooth Muscle Cells (verified by WB)
6) High laboratory costs due time (t/c media and flasks, reagents, antibodies for WB)

Electroporation / Microporation (Neon System – Life Technologies) (Figure 4)

Detection time: 24h post transfection

Generic cell lines: HeLa and hTERT-PASMC

Cell viabilities: Highly comparable to Control cells in optimised experiments (remains to be verified by TB staining)

Comments:

1) The transfection efficiency in hTERT PASMCs reaches up to 66% with 1200V, 20msec, 2 pulses, but with less viability (when compared to control cells).
2) Cost effective (app. £4 per transfection)
3) Highly reproducible results (the mini-optimization experiment in HeLa cells was repeated twice, using 10ul and 100ul tips)
4) The cells can be transfected with pDNA, si/miRNA and protein (no need for specific reagents per experiment)
5) Universal electroporation buffer for all cells types.
6) Reduced experimental time by 1 day (no need for pre-transfection cell plating and overnight incubation)
7) Triple transfections will be performed and further be assessed with WB technique.
8) Easy handling of the equipment even for beginners / storage of optimal settings per cell type.

Transfection efficiencies

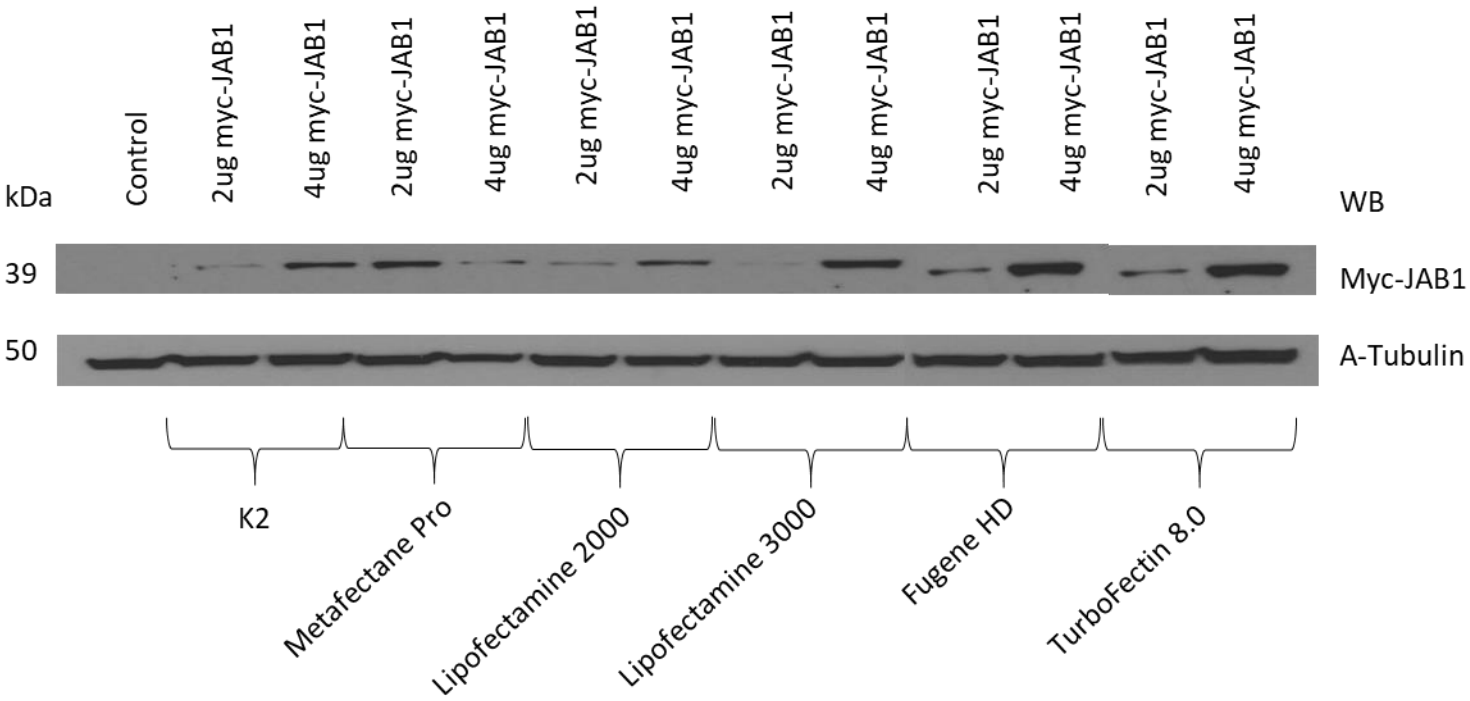

Figure C-1 Identification of Transfection Efficiencies of various liposomal and non-liposomal transfection reagents using myc-tagged JAB1 pDNA in HeLa cell line. Immunoblots of myc-tagged JAB1 and A-Tubulin (endogenous control) in HeLa cells transfected with 2 or 4µg of myc-JAB1 pDNA, utilizing various commercial liposomal and non-liposomal formulations of transfection reagents (liposomal: K2, Metafectane Pro, Lipofectamine 2000 and Lipofectamine 3000; non-liposomal: Fugene HD and Turbofectin 8.0). $3x10^5$ cells per well were plated in 6 well plates the day before transfection in order to accomplish an 80% confluence on the following day. The cells were transfected according to manufacturer's instruction at a 3:1 ratio of reagent(µl) to DNA(µg) and the transfection media was changed after 6 hours of incubation time. The cells were lysed for protein collection after 48h of total incubation time. Lipofectamine 3000, Fugene HD and TurboFectin 8.0 gave optimal results in transfection efficiencies and Fugene HD transfected samples retained high levels of viability after 48h incubation time (viability was assessed microscopically).

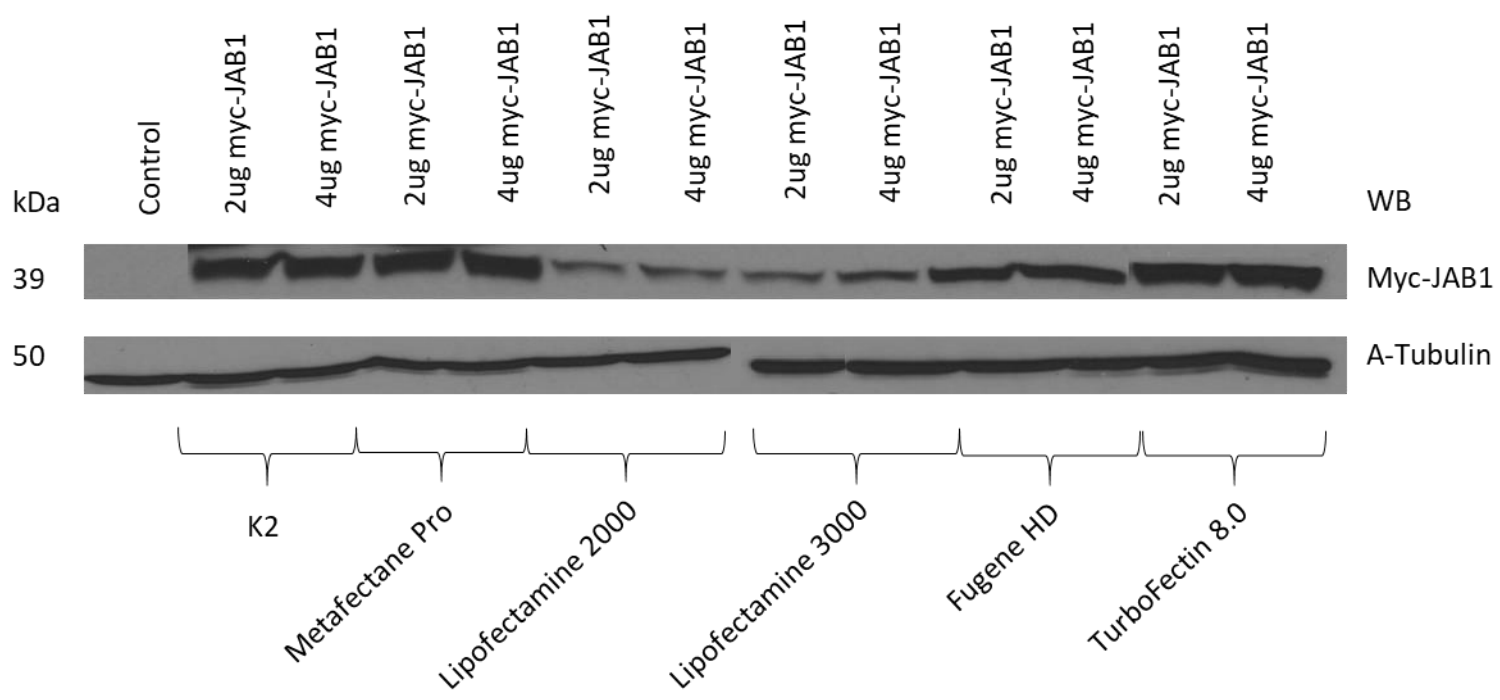

Figure C-2 Identification of Transfection Efficiencies of various liposomal and non-liposomal transfection reagents using myc-tagged JAB1 pDNA in HEK293T cell line. Immunoblots of myc-tagged JAB1 and A-Tubulin (endogenous control) in HEK293T cells transfected with 2 or 4μg of myc-JAB1 pDNA, utilizing various commercial liposomal and non-liposomal formulations of transfection reagents (liposomal: K2, Metafectane Pro, Lipofectamine 2000 and Lipofectamine 3000; non-liposomal: Fugene HD and Turbofectin 8.0). $5x10^5$ cells per well were plated in 6 well plates the day before transfection in order to accomplish an 80% confluence on the following day. The cells were transfected according to manufacturer's instruction at a 3:1 ratio of reagent(μl) to DNA(μg) and the transfection media was changed after 6 hours of incubation time. The cells were lysed for protein collection after 48h of total incubation time. Interestingly, only a small fold increase in ectopic JAB1 expression is observed between the 2 and the 4μg of pDNA transfected samples, utilizing Lipofectamine 3000. The above reagents did not affect significantly the viability of the cells after 48h incubation time (viability was assessed microscopically.

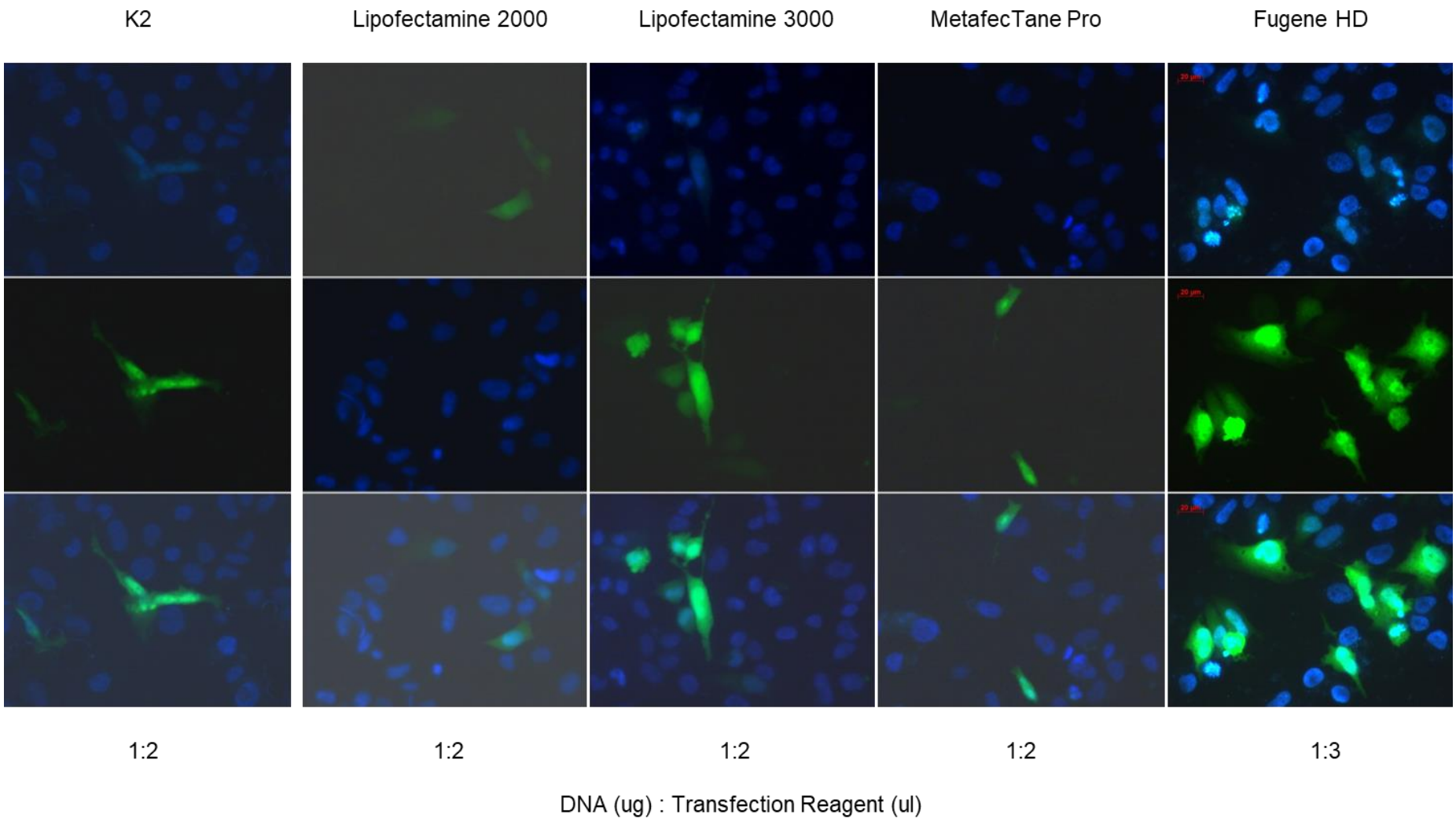

Figure C-3 Optimisation of commercial liposome and non-liposomal transfection reagents. A transfection titration experiment with K1,

Lipofectamine 2000, Lipofectamine 3000, Metafectane PRO and Fugene HD in various Transfection Reagent volumes to plasmid DNA ratios (5:1. 4:1, 3:1, 2:1 and 1:1) and fluorescent analysis of HeLa cells transfected with eGFP protein and incubated for 48h in 37oC - 5% CO2, revealed the best ratios for each reagent as indicated above. Fugene HD gave undoubtedly the best transfection efficiency amongst them with the lowest toxicity effect on the cells with reagent to DNA ratio of 3:1

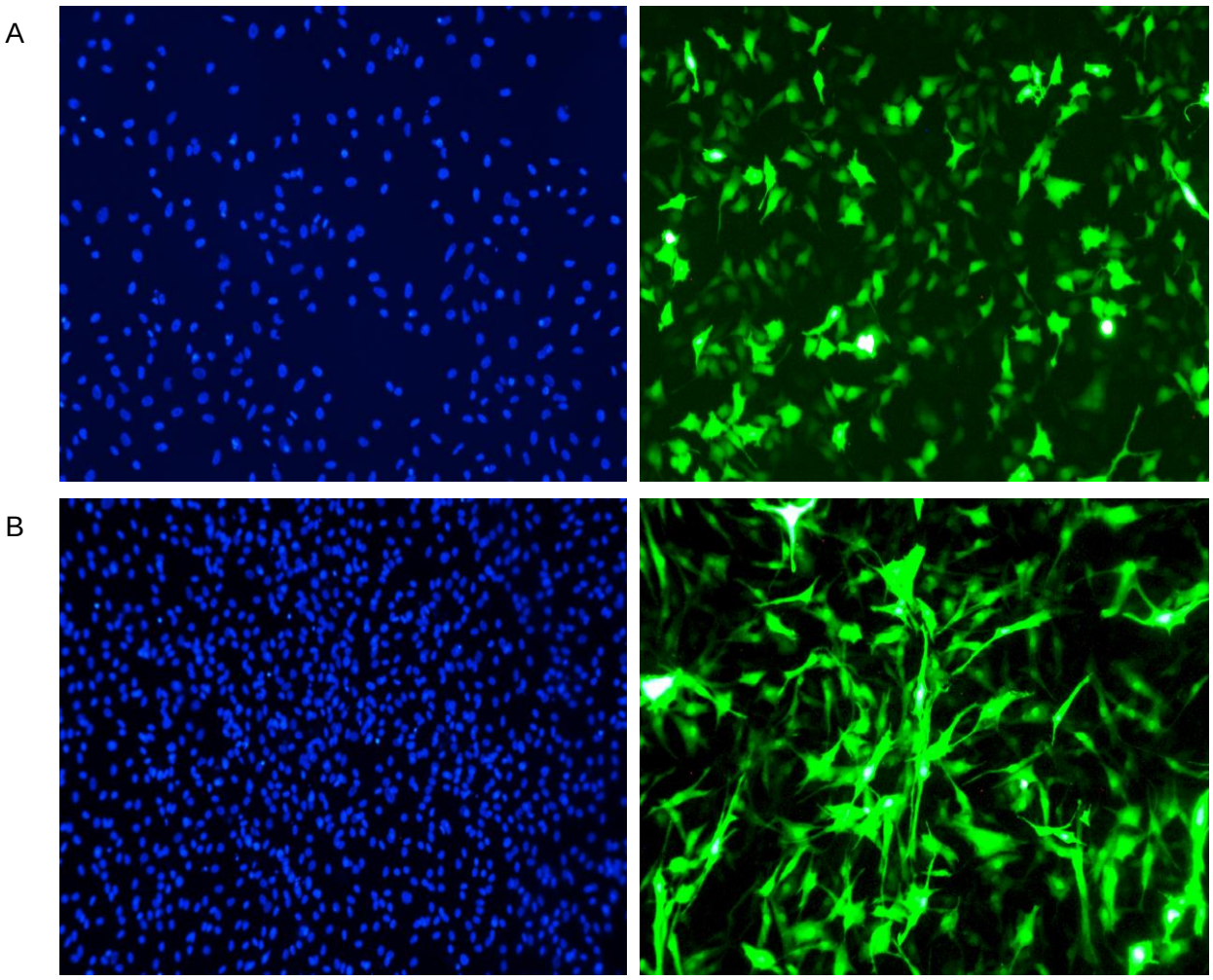

Figure C-4 Optimised electroporation parameters for HeLa and hTERT-PASMC cell lines A) 75% transfection efficiency in Hela cells after a mini optimization experiment – 24h post-transfection time – minimal amount of pDNA encoding GFP, verifying the application note of life technologies (1005V, 35msec, 2 pulses, 100ul tip), 10x magnification, B) 40% transfection efficiency in hTERT-PASMCs after a full optimization experiment – 24 well plate - 24h post-transfection time – minimal amount of pDNA encoding GFP, novel data for hTERT PASMC transfection using the Neon System. (1100V, 20msec, 1 pulse, 10ul tip), 10x magnification. The electroporator device was Neon® Transfection System (ThermoFisher SCIENTIFIC).

CHAPTER 10: APPENDIX D

Supplementary data on AOS affected subjects and identified NOTCH1 variants

In this section, the clinical characteristics of AOS affected subjects harbouring NOTCH1 mutations, are summarized in Table 1 along with pedigree structures and sequence chromatograms of identified *NOTCH1* mutations, that are illustrated in Figure 1.

Moreover, the predicted pathogenicity of the identified NOTCH1 variants is identified in Table 2 (MutationTaster2,19 PolyPhen-2,20 and/or SIFT prediction software21).

*All the Figures and Tables of this section can be also found online in Southgate, Sukalo et al. 2015 paper.

Table D-1 Clinical characteristics of AOS subjects harbouring *NOTCH1* mutations

Subject ID	Country of origin	Current Age	Sex	Scalp ACC	TTLD	Cardiac or Vascular Features [Age at Diagnosis]	Echocardiographic Assessment [Age at Assessment]	Other features [Age at Diagnosis]
1-II:1*	UK	29 y	Male	++	+	ND	Not assessed	Undefined heart murmur
1-II:2		28 y	Male	++	+	ND	Not assessed	Undefined heart murmur
1-II:4		35 y	Female	–	++	[34 y]: AR; AS; CMTC on abdomen and legs	[34 y]: mild AS and AR (PV: 2.04 m/s, PG: 16.65 mm Hg), mildly increased velocities through pulmonary valve (2.06 m/s) and descending aorta (2 m/s)	–
1-III:1		17 y	Male	+	++	ND	Not assessed	–
1-III:2		10 y	Female	–	–	[9 yr]: AR	[9 yr]: mild AR (PV: 2.21 m/s, PG: 19.54 mm Hg), mildly increased velocities through pulmonary valve (1.91 m/s) and descending aorta (2.3 m/s)	–
2-II:1*	Italy	27 y	Male	+	–	[15 d]: BAV; CoA; PMV; [5 mo]: subclavian flap coarctectomy	[15 d]: nonstenotic PMV with mild regurgitation	Reference: Dallapiccola et al15 1992 (patient 2)
3-II:3	Germany	35 y	Male	–	+	None	[34 y]: normal	–

3-III:1*		8 y	Male	++	+	None	[7 yr]: normal	–
4-I:2	Italy	47 y	Female	–	–	AR; AS	[47 y]: thick fibrotic semilunar valves; moderate AR (PG: 34 mm Hg, MG: 20 mm Hg); mild to moderate LVH	Long palpebral fissures
4-II:1*		25 y	Female	+	++	[15 d]: AS; CoA; PMV; VSD	[15 d]: subaortic membranous VSD; severe AS (PG: 80 mm Hg, MG: 60 mm Hg); PMV with valvular insufficiency	Long palpebral fissures
5-II:1*	UK	10 y	Male	++	–	[1 d]: PA-VSD; [6 d]: right MBTS; [2 yr]: Rastelli correction	[1 d]: PA, VSD Fallot type; [10 y]: some narrowing of shunt, free pulmonary regurgitation	[5 y]: portal vein thrombosis; portal hypertension; T-cell lymphopenia; complex learning disability; autism
6-II:1*	Russia	Deceased	Female	++	+	[In utero]: truncus arteriosus communis type I; [1 d]: VSD	[1 d]: membrane VSD, right-sided aortic bow descending on left-hand side	–
7-II:1*	Italy	8 y	Male	+	+	None	[7 y]: normal	Bilateral cryptorchidism; bilateral abdominal wall hernia; hypertelorism; downslanting palpebral fissures
8-II:1*	Italy	15 y	Male	+	+	[1 d]: CMTC	[15 y]: normal	Epilepsy; dyslexia

9-II:1*	Germany	33 y	Female	+	++	ND	Not assessed	–
10-II:1*	France	16 y	Female	++	++	[3.5 y]: ASD; surgically closed at 4 y; arteriography: EHPVT, hepatopetal and hepatofugal collateral veins	[3.5 y]: ASD, suspected portopulmonary hypertension (mPAP: 30 mm Hg); [7 yr]: mPAP: 45 mm Hg, PVR: 8.1 Wood U/m2, PWP: <15 mm Hg; [12 yr]: mPAP: 27 mm Hg with Sildenafil treatment	[3.5 y]: HSM and portal hypertension with GI bleeding; OPV. Reference: Girard et al,16 2005 (patient 1); Franchi-Abella et al,17 2014
11-II:1*	Greece	19 y	Male	++	++	[6.5 y]: arteriography: EPVO, large hepatofugal coronary vein, tiny hepatopetal cavernoma	[6.5 y]: normal; [14 y]: normal	[6.5 y]: HSM and portal hypertension; OPV. Reference: Girard et al,16 2005 (patient 2); Franchi-Abella et al,17 2014

Subject identifiers refer to the pedigree structures in Figure 1. The proband for each family is marked with an asterisk. – indicates absent; +, present (for ACC: +, small defect [<5 cm]; ++, large defect [>5 cm] with underlying osseous skull defect; for TTLD: +, feet or hands only; ++, both feet and hands affected); ACC, aplasia cutis congenita; AR, aortic regurgitation; AS, aortic valve stenosis; ASD, atrial septal defect; BAV, bicuspid aortic valve; CMTC, cutis marmorata telangiectatica congenita; CoA, coarctation of the aorta; EPVO, extrahepatic portal vein obstruction; EHPVT, extrahepatic portal vein thrombosis; GI, gastrointestinal; HSM, hepatosplenomegaly; LVH, left ventricular hypertrophy; MBTS, modified Blalock–Taussig shunt; MG: median gradient; mPAP, mean pulmonary arterial pressure (measured by right heart catheterization); Nd, not determined; OPV, obliterative portal venopathy; PA, pulmonary atresia; PG, peak gradient; PMV, parachute mitral valve; PV, peak velocity; PVR, pulmonary vascular resistance; PWP, pulmonary wedge pressure; TTLD, terminal transverse limb defects; and VSD, ventral septal defect.

Table D-2 Predicted pathogenicity of identified *NOTCH1* variants

Variant	MutationTaster2	PolyPhen-2	SIFT
p.P407R	Disease causing (prob: 0.999976877874958)	Probably damaging (0.968)	Tolerated (0.326)
p.R448Q	Disease causing (prob: 0.999999768941672)	Probably damaging (0.984)	Damaging (0.009)
p.C449R	Disease causing (prob: 0.999999999999999)	Probably damaging (1.000)	Damaging (0.001)
p.Y550*	Disease causing (prob: 1)	n/a	n/a
p.C1374R	Disease causing (prob: 0.999999999999986)	Probably damaging (0.999)	Damaging (0)
p.E1555*	Disease causing (prob: 1)	n/a	n/a
p.M1580Ifs*30	Disease causing (prob: 1)	n/a	n/a
p.A1740S	Polymorphism (prob: 0.980152316967981)	Benign (0.134)	Damaging (0.027)
p.S2017Tfs*9	Disease causing (prob: 1)	n/a	n/a

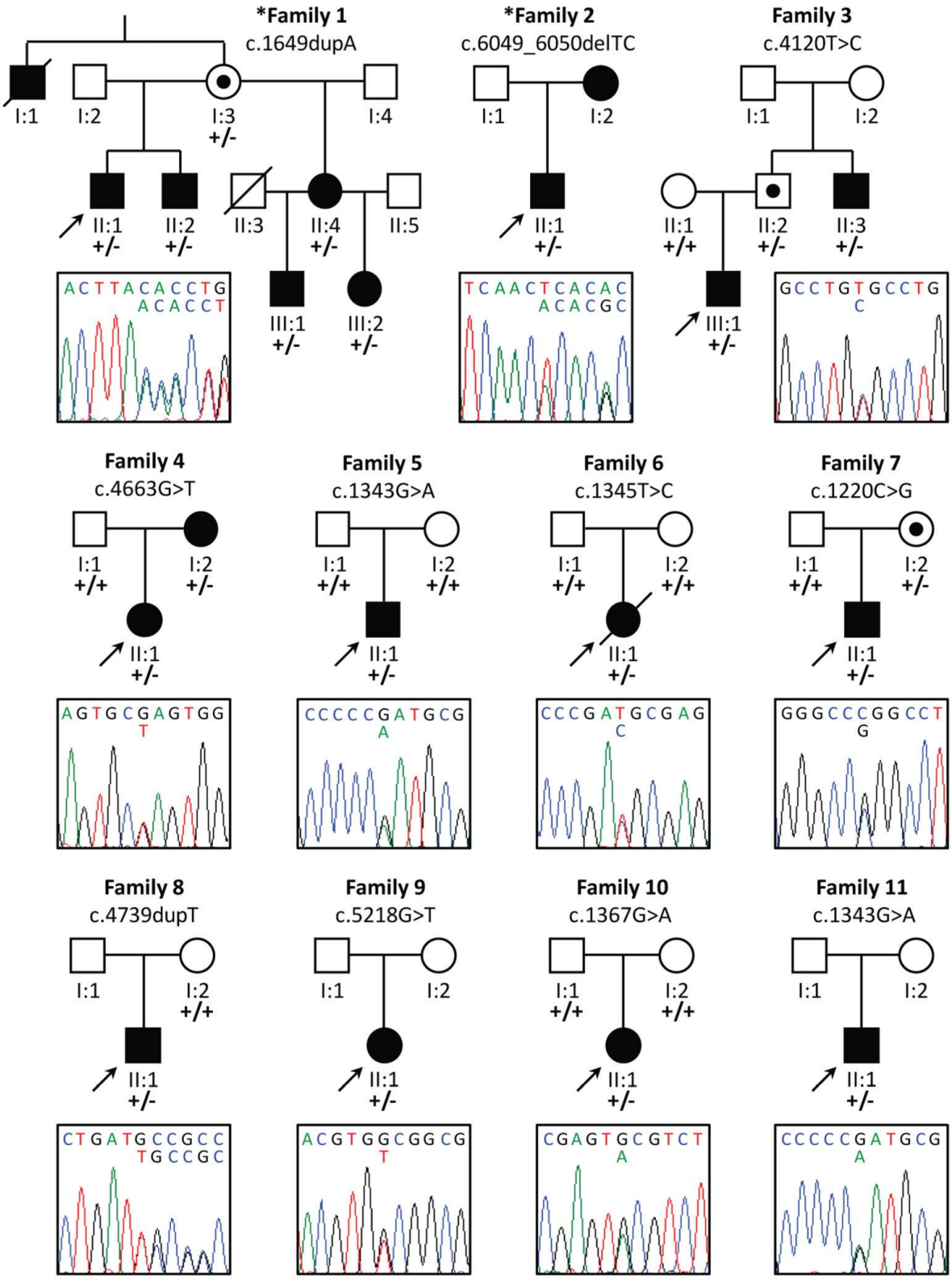

Figure D-1 Pedigree structures and sequence chromatograms of identified *NOTCH1* mutations

Asterisks denote the families included in the exome sequencing discovery cohort. Probands are marked by the black arrows and asymptomatic carriers are indicated with black dots. For *de novo* mutations, paternity was confirmed by microsatellite analysis (data not shown). Key: +, wild-type allele; −, mutant allele

CHAPTER 11: APPENDIX E

Miscellaneous data

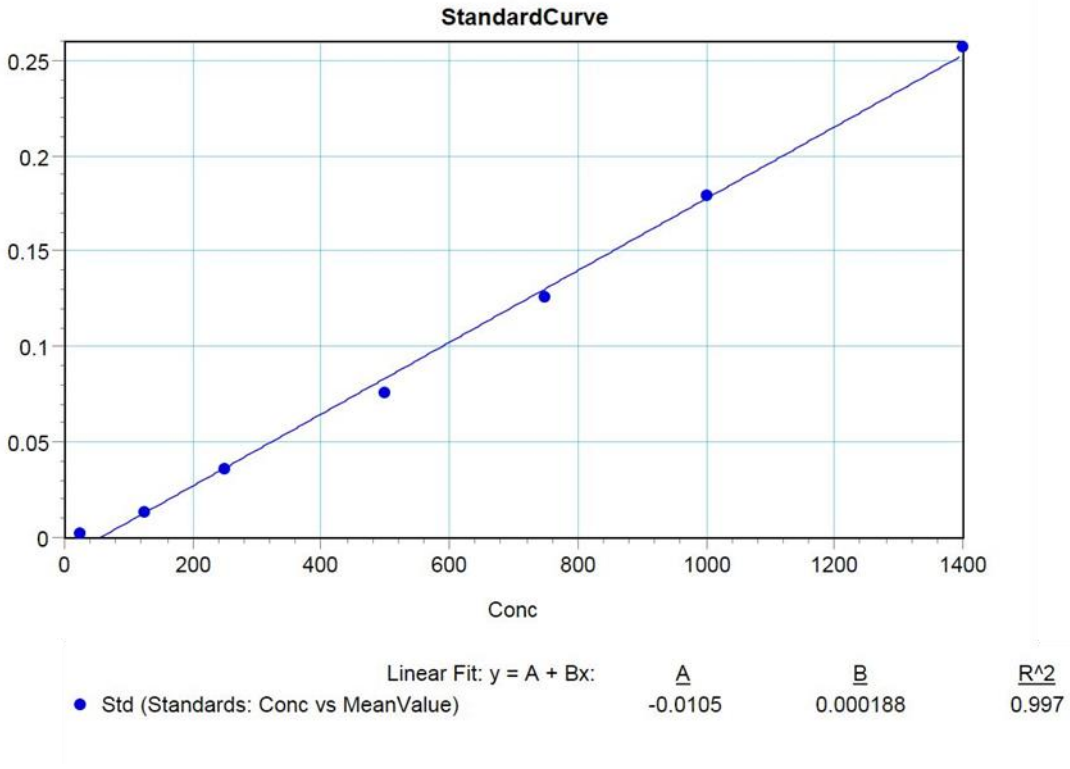

Figure E-1 Example of Lowry Assay standard curve with DC Protein micro-Assay Kit (BIO-RAD) for protein quantitation of cell culture extracts

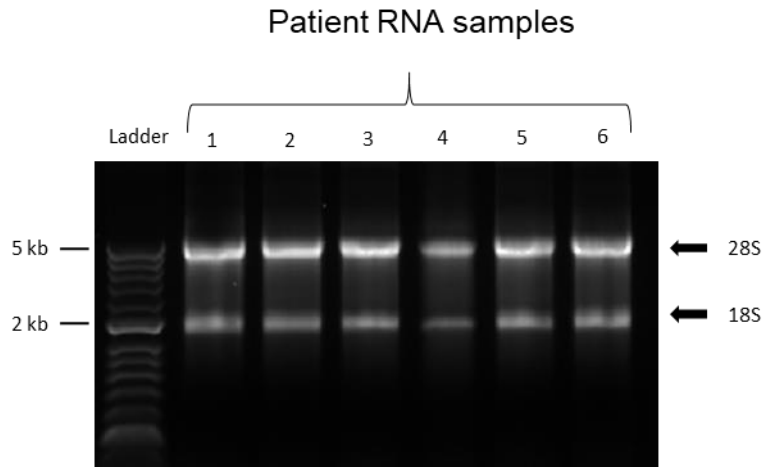

Figure E-2 Example of the quality of RNA isolation samples using RNeasy Plus Mini Kit (QIAGEN)
The 18S and 28S ribosomal RNA bands are clearly visible in the intact RNA samples, that were used for cDNA synthesis and qPCR following relative quantification of expression of transfected Notch1 mutations in HeLa cells (see Figure 5-4).

A. Immunoblot

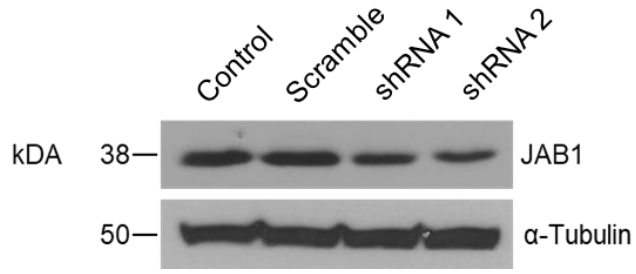

B. Densitometry

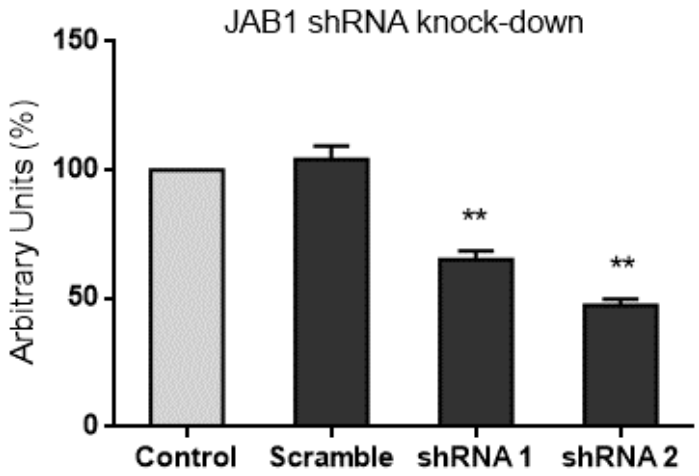

Figure E-3 JAB1 down-regulation of expression after shRNA specific knock-down
A) Indicative preliminary immunoblotting revealing effective JAB1 down-regulation of protein expression, after transient transfections with 5ug/transfection per 1million HeLa cells, of Scramble (control) or shRNAs against Jab1 mRNA. α-Tubulin was used as endogenous control. B) Densitometric analysis in arbitrary units (%) from the immunoblots for JAB1 shRNA knock-downs. Data are means ±SD of 3 independent experiments; **P < 0.01 vs the control group, RM one-way ANOVA.

Table E-1 List of JAB1 interacting proteins

JAB1 interacting proteins				
Protein	Description	Effect of JAB1 interaction	Overall signalling effect	References
Proteins degraded by JAB1				
p27	Cyclin-dependent kinase inhibitor and tumor suppressor	Nuclear export and degradation	Increased cellular proliferation	Tomoda, Kubota et al. 2002
LHR	Lutropin/choriogonadotropin receptor	Degradation	Reproductive disorders	Li, Liu et al. 2000
p53	Transcription factor and tumor suppressor	Nuclear export and degradation	Inhibit p53 tumor suppressor function	Oh, Lee et al. 2006 Berg, Zhou et al. 2007 Zhang, Chen et al. 2008
SMAD4	Co-Smad, positive regulator of TGFß signaling	Ubiquitination and degradation	Inhibit TGFß signaling	Wan, Cao et al. 2002
SMAD7	Inhibitory Smad, negative regulator of TGFß signaling	Nuclear export and degradation	Increase TGFß signaling	Kim, Park et al. 2004
ERα	Estrogen receptor α	Degradation	Increase hormone induced transcription	Callige, Kieffer et al. 2005
West nile virus Capsid	Activates caspase-3 and caspase-9 in the apoptosis pathway	Nuclear translocation and degradation	Protective against West Nile Virus	Tanaka, Kanai et al. 2006
Cyclin E	Cell cycle control, G1 to S phase	Degradation	Cell cycle	Doronkin, Djagaeva et al. 2002
Rad9-Rad1-Hus complex	Involved in DNA damage sensing and DNA repair	Degradation	Impair DNA checkpoint and repair response to DNA damage	Huang, Yuan et al. 2007
RUNX-3	Runt-related transcription factors	Nuclear export and degradations	Inhibition of a tumour suppressor	Kim, Choi et al. 2009
MIF	Cytokine with tautomerase and oxidoreductases activities	Inhibition of MIF secretion	Inhibits MIF-mediated AKT signaling	Lue, Thiele et al. 2007
DNA topoisomerase (topo) II alpha	Enzyme that is essential for cell proliferation that segregates chromosome pairs during chromosome condensation	Degradation in a MPN dependent manner under glucose starvation	Decreased cell proliferation under stress conditions such as glucose starvation	Yun, Tomida et al. 2004

Endothelin type A and B receptors	G protein-coupled receptors whose overexpression is correlated with chronic heart failure and in infiltrating cells of atherosclerotic lesions	Ubiquitination and degradation	Decreased Endothelin-1 induced intracellular signalling through ERK1/2	Nishimoto, Lu et al. 2010
Proteins affected by JAB1				
c-Jun	Member of the AP-1 transcription factor family	Transcriptional co-activator and specificity factor	Increased transcriptional activity and cellular proliferation	Claret, Hibi et al. 1996
Myc	Oncogenic transcription factor	Promotes transcription of MYC target genes and induces MYC ubiquitination and turnover	Activates a wound signature and induced cell proliferation and invasion in breast cancer cells	Adler, Lin et al. 2006
HIF-1α	Hypoxia inducible factor α	Competes with p53 for binding, stabilizes protein HIF-1α levels	Increased expression of VEGF and angiogenesis	Bae, Ahn et al. 2002 Bemis, Chan et al. 2004
HAND2	Transcription factor important for development of the heart, limbs, and neural crest-derived lineages	Enhances HAND2 DNA binding	Tissue-specific transcription	Dai, Bonin et al. 2004
53BP1	P53 binding protein, cellular response to stress conditions	Hyperphosphorylation under stress conditions	Activation of mitotic checkpoint mechanism	Kwak, Kim et al. 2005
SMAD5	Receptor associated Smad protein, positive regulator of TGFß signaling	Inhibits bone morphogenetic signaling	Affect matrix turnover	Haag, Aigner et al. 2006
Brn-2	POU transcription factor, development of neocortex and neural cell lineage	Increases Brn-2 transcriptional activity	Neuronal development and neurodegenerative diseases	Huang, Iwamoto et al. 2005
Bcl-3	Member of Iκ-B family, proto-oncogene, can activate or inhibit NF-κB transcription	Bridges binding between Jab1/CSN5 and NF-κB	Link NF-κB and AP-1 gene activation	Dechend, Hirano et al. 1999
E2F-1	Transcription factor important for cell cycle progression, DNA damage repair, apoptosis	Cofactor for E2F-1 dependent apoptosis, but not cell cycle entry	Enhances E2F-1 mediated apoptosis	Hallstrom, Nevins et al. 2006
PR, SRC-1	Progesterone receptor, steroid receptor coactivator	Stabilized PR-SRC-1 complexes	Increased transcriptional activity	Chauchereau, Georgiakaki et al. 2000
SMYD3	A histone methyltransferase	Suppressed transcription of the	Negative regulation of p16 and	Mori, Yoneda-

		tumour suppressor p16	possible increased in hematopoietic progenitors	Kato et al. 2008
Cullin	Subunit of SCF ubiquitin ligases	Cleavage of NEDD8 from Cul1	Required for optimal SCF ubiquitin ligase activity	Cope, Suh et al. 2002
PAR-2	G protein-coupled receptor for trypsin and tryptase	Increased PAR-2 transcription	Increased AP-1 activation	Luo, Wang et al. 2006
MDM2	Mediates p53 degradation	Reduces MDM2 self-ubiquitination	Negative regulation of p53	Zhang, Chen et al. 2008
TRAF-2	TNFR-associated factor 2, mediator of TNFα prosurvival response	Ubiquitination of TRAF-2	Necessary for TNF-α prosurvival signalling and MMP production	Wang, Li et al. 2006
Rad51	DNA repair protein involved in homologous recombination	Increases expression through negative regulation of p53	Increased ability of cell to repair DNA	Tian, Peng et al. 2010
FcαRI/CD89	Receptor for IgA expressed on myeloid cells and involved in phagocytosis, Ab-dependent cellular cytotoxicity, antigen presentation, and cytokine release	Binds directly to the intracellular domain and is involved in regulating stabilization of surface expression	Decreased expression of FcαR1 and possible defective antigen recognition response	Bakema, Hiemstra et al. 2010
5-HT(6)R	Serotonin receptor involved in the control of mood and emotion as well as involved in neurological disorders	Reduced Jab1/CSN5 expression decreases expression and activity	Reduced signaling through 5-HT(6)R, increased c-Jun activity and enhanced cell survival under hypoxia	Yun, Baik et al. 2010

Abbreviations: 5-HT(6)R, serotonin 6 receptor; AP-1, activator protein ; Bcl-3, B-cell lymphoma 3-encoded protein; ERα, estrogen receptor α; FcαRI, FCalphaRI; HAND2, heart- and neural crest derivatives-expressed protein 2; HIF-1α, hypoxia inducible factor α; LHR, lutropin/choriogonadotropin receptor; MIF, macrophage migration inhibitory factor; MDM2, murine double minute; NEDD8, neural precursor cell-expressed developmentally down-regulated; NF-kB, nuclear factor kappa-light-chain-enhancer of activated B cells; 53BP-1, p53 binding protein 1; PAR-2, abnormal embryonic PARtitioning of cytoplasm 2; PR, Progesterone receptor; SCF, Skp1-Cullin-F-box; SRC-1, steroid receptor coactivator 1; TRAF-2, TNF receptor-associated factor 2; VEGF, vascular endothelial growth factor

CHAPTER 12: REFERENCES

AARONSON, P.I., ROBERTSON, T.P., KNOCK, G.A., BECKER, S., LEWIS, T.H., SNETKOV, V. and WARD, J.P., 2006. Hypoxic pulmonary vasoconstriction: mechanisms and controversies. *The Journal of physiology,* **570**(Pt 1), pp. 53-58.

ADLER, A.S., LIN, M., HORLINGS, H., NUYTEN, D.S., VAN DE VIJVER, M.J. and CHANG, H.Y., 2006. Genetic regulators of large-scale transcriptional signatures in cancer. Nature genetics, 38(4), pp. 421-430.

AMEYAR, M., WISNIEWSKA, M. and WEITZMAN, J.B., 2003. A role for AP-1 in apoptosis: the case for and against. *Biochimie,* **85**(8), pp. 747-752.

ANDERSEN, P., UOSAKI, H., SHENJE, L.T. and KWON, C., 2012. Non-canonical Notch signaling: emerging role and mechanism. *Trends in cell biology,* **22**(5), pp. 257-265.

ANDERSSON, E.R., SANDBERG, R. and LENDAHL, U., 2011. Notch signaling: simplicity in design, versatility in function. *Development (Cambridge, England),* **138**(17), pp. 3593-3612.

ANDRAWES, M.B., XU, X., LIU, H., FICARRO, S.B., MARTO, J.A., ASTER, J.C. and BLACKLOW, S.C., 2013. Intrinsic selectivity of Notch 1 for Delta-like 4 over Delta-like 1. *The Journal of biological chemistry,* **288**(35), pp. 25477-25489.

ATKINSON, C., STEWART, S., UPTON, P.D., MACHADO, R., THOMSON, J.R., TREMBATH, R.C. and MORRELL, N.W., 2002. Primary Pulmonary Hypertension Is Associated With Reduced Pulmonary Vascular Expression of Type II Bone Morphogenetic Protein Receptor. *Circulation,* **105**(14), pp. 1672-1678.

AUGERI, D.J., LANGENFELD, E., CASTLE, M., GILLERAN, J.A. and LANGENFELD, J., 2016. Inhibition of BMP and of TGFbeta receptors downregulates expression of XIAP and TAK1 leading to lung cancer cell death. *Molecular cancer,* **15**, pp. 27-016-0511-9.

AWAD, K.S., ELINOFF, J.M., WANG, S., GAIRHE, S., FERREYRA, G.A., CAI, R., SUN, J., SOLOMON, M.A. and DANNER, R.L., 2016. Raf/ERK drives the proliferative and invasive phenotype of BMPR2-silenced pulmonary artery endothelial cells. *American journal of physiology.Lung cellular and molecular physiology,* **310**(2), pp. L187-201.

AWAD, K.S., WEST, J.D., DE JESUS PEREZ, V. and MACLEAN, M., 2016. Novel signaling pathways in pulmonary arterial hypertension (2015 Grover Conference Series). *Pulmonary circulation,* **6**(3), pp. 285-294.

BAE, M.K., AHN, M.Y., JEONG, J.W., BAE, M.H., LEE, Y.M., BAE, S.K., PARK, J.W., KIM, K.R. and KIM, K.W., 2002. Jab1 interacts directly with HIF-1alpha and regulates its stability. *The Journal of biological chemistry,* **277**(1), pp. 9-12.

BAGAROVA, J., VONNER, A.J., ARMSTRONG, K.A., BORGERMANN, J., LAI, C.S., DENG, D.Y., BEPPU, H., ALFANO, I., FILIPPAKOPOULOS, P., MORRELL, N.W., BULLOCK, A.N., KNAUS, P., MISHINA, Y. and YU, P.B., 2013. Constitutively active ALK2 receptor mutants require type II receptor cooperation. *Molecular and cellular biology,* **33**(12), pp. 2413-2424.

BAI, G., SHENG, N., XIE, Z., BIAN, W., YOKOTA, Y., BENEZRA, R., KAGEYAMA, R., GUILLEMOT, F. and JING, N., 2007. Id sustains Hes1 expression to inhibit precocious neurogenesis by releasing negative autoregulation of Hes1. *Developmental cell,* **13**(2), pp. 283-297.

BAKEMA, J.E., HIEMSTRA, I.H., BAKKER, J., DE HAIJ, S., KOK, Y., ADEMA, G., VAN EGMOND, M., COFFER, P.J., VAN DE WINKEL, J.G. and LEUSEN, J.H., 2010. c-Jun activating binding protein 1 binds to the IgA receptor and modulates protein levels of FcalphaRI and FcRgamma-chain. *European journal of immunology,* **40**(7), pp. 2035-2040.

BAKER, K.E. and PARKER, R., 2004. Nonsense-mediated mRNA decay: terminating erroneous gene expression. *Current opinion in cell biology,* **16**(3), pp. 293-299.

BARON, M., 2003. An overview of the Notch signalling pathway. *Seminars in cell & developmental biology,* **14**(2), pp. 113-119.

BASHUR, L.A., CHEN, D., CHEN, Z., LIANG, B., PARDI, R., MURAKAMI, S. and ZHOU, G., 2014. Loss of jab1 in osteochondral progenitor cells severely impairs embryonic limb development in mice. *Journal of cellular physiology,* **229**(11), pp. 1607-1617.

BEETS, K., HUYLEBROECK, D., MOYA, I.M., UMANS, L. and ZWIJSEN, A., 2013. Robustness in angiogenesis: notch and BMP shaping waves. *Trends in genetics : TIG,* **29**(3), pp. 140-149.

BEMIS, L., CHAN, D.A., FINKIELSTEIN, C.V., QI, L., SUTPHIN, P.D., CHEN, X., STENMARK, K., GIACCIA, A.J. and ZUNDEL, W., 2004. Distinct aerobic and hypoxic mechanisms of HIF-alpha regulation by CSN5. *Genes & development,* **18**(7), pp. 739-744.

BERG, J.P., ZHOU, Q., BREUHAHN, K., SCHIRMACHER, P., PATIL, M.A., CHEN, X., SCHAFER, N., HOLLER, T.T., FISCHER, H.P., BUTTNER, R. and GUTGEMANN, I., 2007. Inverse expression of Jun activation domain binding protein 1 and cell cycle inhibitor p27Kip1: influence on proliferation in hepatocellular carcinoma. *Human pathology,* **38**(11), pp. 1621-1627.

BERSE, M., BOUNPHENG, M., HUANG, X., CHRISTY, B., POLLMANN, C. and DUBIEL, W., 2004. Ubiquitin-dependent degradation of Id1 and Id3 is mediated by the COP9 signalosome. *Journal of Molecular Biology,* **343**(2), pp. 361-370.

BOUNPHENG, M.A., DIMAS, J.J., DODDS, S.G. and CHRISTY, B.A., 1999. Degradation of Id proteins by the ubiquitin-proteasome pathway. *FASEB journal : official publication of the Federation of American Societies for Experimental Biology,* **13**(15), pp. 2257-2264.

BURNETT, J.C., ROSSI, J.J. and TIEMANN, K., 2011. Current progress of siRNA/shRNA therapeutics in clinical trials. *Biotechnology journal,* **6**(9), pp. 1130-1146.

BURTON, V.J., CIUCLAN, L.I., HOLMES, A.M., RODMAN, D.M., WALKER, C. and BUDD, D.C., 2011. Bone morphogenetic protein receptor II regulates pulmonary artery endothelial cell barrier function. *Blood,* **117**(1), pp. 333-341.

CALLIGE, M., KIEFFER, I. and RICHARD-FOY, H., 2005. CSN5/Jab1 is involved in ligand-dependent degradation of estrogen receptor {alpha} by the proteasome. *Molecular and cellular biology,* **25**(11), pp. 4349-4358.

CAMPOS, A.H., WANG, W., POLLMAN, M.J. and GIBBONS, G.H., 2002. Determinants of Notch-3 receptor expression and signaling in vascular smooth muscle cells: implications in cell-cycle regulation. *Circulation research,* **91**(11), pp. 999-1006.

CHAMOVITZ, D.A. and SEGAL, D., 2001. JAB1/CSN5 and the COP9 signalosome. A complex situation. *EMBO reports,* **2**(2), pp. 96-101.

CHAUCHEREAU, A., GEORGIAKAKI, M., PERRIN-WOLFF, M., MILGROM, E. and LOOSFELT, H., 2000. JAB1 interacts with both the progesterone receptor and SRC-1. *The Journal of biological chemistry,* **275**(12), pp. 8540-8548.

CHAN, M.C., NGUYEN, P.H., DAVIS, B.N., OHOKA, N., HAYASHI, H., DU, K., LAGNA, G. and HATA, A., 2007. A novel regulatory mechanism of the bone morphogenetic protein (BMP) signaling pathway involving the carboxyl-terminal tail domain of BMP type II receptor. *Molecular and cellular biology,* **27**(16), pp. 5776-5789.

CHAN, M.C., NGUYEN, P.H., DAVIS, B.N., OHOKA, N., HAYASHI, H., DU, K., LAGNA, G. and HATA, A., 2007. A novel regulatory mechanism of the bone morphogenetic protein (BMP) signaling pathway involving the carboxyl-terminal tail domain of BMP type II receptor. *Molecular and cellular biology,* **27**(16), pp. 5776-5789.

CHAO, C.C., 2015. Mechanisms of p53 degradation. *Clinica chimica acta; international journal of clinical chemistry,* **438**, pp. 139-147.

CHEN, D., BASHUR, L.A., LIANG, B., PANATTONI, M., TAMAI, K., PARDI, R. and ZHOU, G., 2013. The transcriptional co-regulator Jab1 is crucial for chondrocyte differentiation in vivo. *Journal of cell science,* **126**(Pt 1), pp. 234-243.

CHILLAKURI, C.R., SHEPPARD, D., LEA, S.M. and HANDFORD, P.A., 2012. Notch receptor-ligand binding and activation: insights from molecular studies. *Seminars in cell & developmental biology,* **23**(4), pp. 421-428.

CHUN, Y., LEE, M., PARK, B. and LEE, S., 2013. CSN5/JAB1 interacts with the centromeric components CENP-T and CENP-W and regulates their proteasome-mediated degradation. *The Journal of biological chemistry,* **288**(38), pp. 27208-27219.

CLARET, F.X., HIBI, M., DHUT, S., TODA, T. and KARIN, M., 1996. A new group of conserved coactivators that increase the specificity of AP-1 transcription factors. *Nature,* **383**(6599), pp. 453-457.

COHEN, I., SILBERSTEIN, E., PEREZ, Y., LANDAU, D., ELBEDOUR, K., LANGER, Y., KADIR, R., VOLODARSKY, M., SIVAN, S., NARKIS, G. and BIRK, O.S., 2014. Autosomal recessive Adams-Oliver syndrome caused by homozygous mutation in EOGT, encoding an EGF domain-specific O-GlcNAc transferase. *European journal of human genetics : EJHG,* **22**(3), pp. 374-378.

COPE, G.A., SUH, G.S., ARAVIND, L., SCHWARZ, S.E., ZIPURSKY, S.L., KOONIN, E.V. and DESHAIES, R.J., 2002. Role of predicted metalloprotease motif of Jab1/Csn5 in cleavage of Nedd8 from Cul1. *Science (New York, N.Y.),* **298**(5593), pp. 608-611.

CROSSWHITE, P. and SUN, Z., 2014. Molecular mechanisms of pulmonary arterial remodeling. *Molecular medicine (Cambridge, Mass.),* **20**, pp. 191-201.

CUSHING, L., JIANG, Z., KUANG, P. and LU, J., 2015. The roles of microRNAs and protein components of the microRNA pathway in lung development and diseases. *American journal of respiratory cell and molecular biology,* **52**(4), pp. 397-408.

DAI, Y.S., HAO, J., BONIN, C., MORIKAWA, Y. and CSERJESI, P., 2004. JAB1 enhances HAND2 transcriptional activity by regulating HAND2 DNA binding. *Journal of neuroscience research,* **76**(5), pp. 613-622.

DAVIES, R.J., HOLMES, A.M., DEIGHTON, J., LONG, L., YANG, X., BARKER, L., WALKER, C., BUDD, D.C., UPTON, P.D. and MORRELL, N.W., 2012. BMP type II receptor deficiency confers resistance to growth inhibition by TGF-beta in pulmonary artery smooth muscle cells: role of proinflammatory cytokines. *American journal of physiology.Lung cellular and molecular physiology,* **302**(6), pp. L604-15.

DAVIS, E.E. and KATSANIS, N., 2012. The ciliopathies: a transitional model into systems biology of human genetic disease. *Current opinion in genetics & development,* **22**(3), pp. 290-303.

DECHEND, R., HIRANO, F., LEHMANN, K., HEISSMEYER, V., ANSIEAU, S., WULCZYN, F.G., SCHEIDEREIT, C. and LEUTZ, A., 1999. The Bcl-3 oncoprotein acts as a bridging factor between NF-kappaB/Rel and nuclear co-regulators. *Oncogene,* **18**(22), pp. 3316-3323.

DEMAGNY, H., ARAKI, T. and DE ROBERTIS, E.M., 2014. The tumor suppressor Smad4/DPC4 is regulated by phosphorylations that integrate FGF, Wnt, and TGF-beta signaling. *Cell reports,* **9**(2), pp. 688-700.

DEN BESTEN, W., VERMA, R., KLEIGER, G., OANIA, R.S. and DESHAIES, R.J., 2012. NEDD8 links cullin-RING ubiquitin ligase function to the p97 pathway. *Nature structural & molecular biology,* **19**(5), pp. 511-6, S1.

DENG, Z., MORSE, J.H., SLAGER, S.L., CUERVO, N., MOORE, K.J., VENETOS, G., KALACHIKOV, S., CAYANIS, E., FISCHER, S.G., BARST, R.J., HODGE, S.E. and KNOWLES, J.A., 2000. Familial primary pulmonary hypertension (gene PPH1) is caused by mutations in the bone morphogenetic protein receptor-II gene. *American Journal of Human Genetics,* **67**(3), pp. 737-744.

DIGILIO, M.C., MARINO, B. and DALLAPICCOLA, B., 2008. Autosomal dominant inheritance of aplasia cutis congenita and congenital heart defect: a possible link to the Adams-Oliver syndrome. *American journal of medical genetics.Part A,* **146A**(21), pp. 2842-2844.

DORONKIN, S., DJAGAEVA, I. and BECKENDORF, S.K., 2002. CSN5/Jab1 mutations affect axis formation in the Drosophila oocyte by activating a meiotic checkpoint. *Development (Cambridge, England),* **129**(21), pp. 5053-5064.

DRAKE, K.M., DUNMORE, B.J., MCNELLY, L.N., MORRELL, N.W. and ALDRED, M.A., 2013. Correction of nonsense BMPR2 and SMAD9 mutations by ataluren in pulmonary arterial hypertension. *American journal of respiratory cell and molecular biology,* **49**(3), pp. 403-409.

DRAKE, K.M., ZYGMUNT, D., MAVRAKIS, L., HARBOR, P., WANG, L., COMHAIR, S.A., ERZURUM, S.C. and ALDRED, M.A., 2011. Altered MicroRNA processing in heritable pulmonary arterial hypertension: an important role for Smad-8. *American journal of respiratory and critical care medicine,* **184**(12), pp. 1400-1408.

DUNMORE, B.J., DRAKE, K.M., UPTON, P.D., TOSHNER, M.R., ALDRED, M.A. and MORRELL, N.W., 2013. The lysosomal inhibitor, chloroquine, increases cell surface BMPR-II levels and restores BMP9 signalling in endothelial cells harbouring BMPR-II mutations. *Human molecular genetics,* **22**(18), pp. 3667-3679.

DURRINGTON, H.J., UPTON, P.D., HOER, S., BONAME, J., DUNMORE, B.J., YANG, J., CRILLEY, T.K., BUTLER, L.M., BLACKBOURN, D.J., NASH, G.B., LEHNER, P.J. and MORRELL, N.W., 2010. Identification of a lysosomal pathway

regulating degradation of the bone morphogenetic protein receptor type II. *The Journal of biological chemistry,* **285**(48), pp. 37641-37649.

DYER, L.A., PI, X. and PATTERSON, C., 2014. The role of BMPs in endothelial cell function and dysfunction. *Trends in endocrinology and metabolism: TEM,* **25**(9), pp. 472-480.

ECHALIER, A., PAN, Y., BIROL, M., TAVERNIER, N., PINTARD, L., HOH, F., EBEL, C., GALOPHE, N., CLARET, F.X. and DUMAS, C., 2013. Insights into the regulation of the human COP9 signalosome catalytic subunit, CSN5/Jab1. *Proceedings of the National Academy of Sciences,* **110**(4), pp. 1273-1278.

EGNATCHIK, R.A., BRITTAIN, E.L., SHAH, A.T., FARES, W.H., FORD, H.J., MONAHAN, K., KANG, C.J., KOCUREK, E.G., ZHU, S., LUONG, T., NGUYEN, T.T., HYSINGER, E., AUSTIN, E.D., SKALA, M.C., YOUNG, J.D., ROBERTS, L.J.,2ND, HEMNES, A.R., WEST, J. and FESSEL, J.P., 2017. Dysfunctional BMPR2 signaling drives an abnormal endothelial requirement for glutamine in pulmonary arterial hypertension. *Pulmonary circulation,* **7**(1), pp. 186-199.

EICKELBERG, O. and MORTY, R.E., 2007. Transforming growth factor beta/bone morphogenic protein signaling in pulmonary arterial hypertension: remodeling revisited. *Trends in cardiovascular medicine,* **17**(8), pp. 263-269.

ESTEVA, F.J., SAHIN, A.A., RASSIDAKIS, G.Z., YUAN, L.X., SMITH, T.L., YANG, Y., GILCREASE, M.Z., CRISTOFANILLI, M., NAHTA, R., PUSZTAI, L. and CLARET, F.X., 2003. Jun activation domain binding protein 1 expression is associated with low p27(Kip1)levels in node-negative breast cancer. *Clinical cancer research : an official journal of the American Association for Cancer Research,* **9**(15), pp. 5652-5659.

EVANS, J.D., GIRERD, B., MONTANI, D., WANG, X.J., GALIE, N., AUSTIN, E.D., ELLIOTT, G., ASANO, K., GRUNIG, E., YAN, Y., JING, Z.C., MANES, A., PALAZZINI, M., WHEELER, L.A., NAKAYAMA, I., SATOH, T., EICHSTAEDT, C., HINDERHOFER, K., WOLF, M., ROSENZWEIG, E.B., CHUNG, W.K., SOUBRIER, F., SIMONNEAU, G., SITBON, O., GRAF, S., KAPTOGE, S., DI ANGELANTONIO, E., HUMBERT, M. and MORRELL, N.W., 2016. BMPR2 mutations and survival in pulmonary arterial hypertension: an individual participant data meta-analysis. *The Lancet.Respiratory medicine,* **4**(2), pp. 129-137.

FENTEANY, G. and SCHREIBER, S.L., 1998. Lactacystin, proteasome function, and cell fate. *The Journal of biological chemistry,* **273**(15), pp. 8545-8548.

FISCHER, A., SCHUMACHER, N., MAIER, M., SENDTNER, M. and GESSLER, M., 2004. The Notch target genes Hey1 and Hey2 are required for embryonic vascular development. *Genes & development,* **18**(8), pp. 901-911.

FOLETTA, V.C., LIM, M.A., SOOSAIRAJAH, J., KELLY, A.P., STANLEY, E.G., SHANNON, M., HE, W., DAS, S., MASSAGUE, J. and BERNARD, O., 2003. Direct signaling by the BMP type II receptor via the cytoskeletal regulator LIMK1. *The Journal of cell biology,* **162**(6), pp. 1089-1098.

FOX, S.I., 2016. Blood, Heart, and Circulation. *Human Physiology.* 14 edn. McGraw-Hill, pp. 388-418.

FRANCIS, J.C., RADTKE, F. and LOGAN, M.P., 2005. Notch1 signals through Jagged2 to regulate apoptosis in the apical ectodermal ridge of the developing limb bud. *Developmental dynamics : an official publication of the American Association of Anatomists,* **234**(4), pp. 1006-1015.

FU, Y., CHANG, A., CHANG, L., NIESSEN, K., EAPEN, S., SETIADI, A. and KARSAN, A., 2009. Differential regulation of transforming growth factor beta signaling pathways by Notch in human endothelial cells. *The Journal of biological chemistry,* **284**(29), pp. 19452-19462.

FUKUMOTO, A., TOMODA, K., YONEDA-KATO, N., NAKAJIMA, Y. and KATO, J.Y., 2006. Depletion of Jab1 inhibits proliferation of pancreatic cancer cell lines. *FEBS letters,* **580**(25), pp. 5836-5844.

GAINE, S., 2000. Pulmonary hypertension. *Jama,* **284**(24), pp. 3160-3168.

GAO, Y.F., ZHU, X.D., SHI, D.M., JING, Z.C., LI, L., MA, D., FAN, Z.X., LI, J., WANG, Y.W. and WU, B.X., 2010. The effects of atorvastatin on pulmonary arterial hypertension and expression of p38, p27, and Jab1 in rats. *International journal of molecular medicine,* **26**(4), pp. 541-547.

GBD 2013 MORTALITY AND CAUSES OF DEATH COLLABORATORS, 2015. Global, regional, and national age-sex specific all-cause and cause-specific mortality for 240 causes of death, 1990-2013: a systematic analysis for the Global Burden of Disease Study 2013. *Lancet (London, England),* **385**(9963), pp. 117-171.

GBD 2015 MORTALITY AND CAUSES OF DEATH COLLABORATORS, 2016. Global, regional, and national life expectancy, all-cause mortality, and cause-specific mortality for 249 causes of death, 1980-2015: a systematic analysis for the Global Burden of Disease Study 2015. *Lancet (London, England),* **388**(10053), pp. 1459-1544.

GE, B., GRAM, H., DI PADOVA, F., HUANG, B., NEW, L., ULEVITCH, R.J., LUO, Y. and HAN, J., 2002. MAPKK-independent activation of p38alpha mediated by TAB1-dependent autophosphorylation of p38alpha. *Science (New York, N.Y.),* **295**(5558), pp. 1291-1294.

GEORGE, M.G., SCHIEB, L.J., AYALA, C., TALWALKAR, A. and LEVANT, S., 2014. Pulmonary hypertension surveillance: United States, 2001 to 2010. *Chest,* **146**(2), pp. 476-495.

GHATAORHE, P., RHODES, C.J., HARBAUM, L., ATTARD, M., WHARTON, J. and WILKINS, M.R., 2017. Pulmonary arterial hypertension - progress in understanding the disease and prioritizing strategies for drug development. *Journal of internal medicine,* .

GIANFELICI, V., 2012. Activation of the NOTCH1 pathway in chronic lymphocytic leukemia. *Haematologica,* **97**(3), pp. 328-330.

GLICKMAN, M.H. and CIECHANOVER, A., 2002. The ubiquitin-proteasome proteolytic pathway: destruction for the sake of construction. *Physiological Reviews,* **82**(2), pp. 373-428.

GO, A.S., MOZAFFARIAN, D., ROGER, V.L., BENJAMIN, E.J., BERRY, J.D., BORDEN, W.B., BRAVATA, D.M., DAI, S., FORD, E.S., FOX, C.S., FRANCO, S., FULLERTON, H.J., GILLESPIE, C., HAILPERN, S.M., HEIT, J.A., HOWARD, V.J., HUFFMAN, M.D., KISSELA, B.M., KITTNER, S.J., LACKLAND, D.T., LICHTMAN, J.H., LISABETH, L.D., MAGID, D., MARCUS, G.M., MARELLI, A., MATCHAR, D.B., MCGUIRE, D.K., MOHLER, E.R., MOY, C.S., MUSSOLINO, M.E., NICHOL, G., PAYNTER, N.P., SCHREINER, P.J., SORLIE, P.D., STEIN, J., TURAN, T.N., VIRANI, S.S., WONG, N.D., WOO, D., TURNER, M.B. and AMERICAN HEART ASSOCIATION STATISTICS COMMITTEE AND STROKE STATISTICS SUBCOMMITTEE, 2013. Heart disease and stroke statistics--2013 update: a report from the American Heart Association. *Circulation,* **127**(1), pp. e6-e245.

GOLLOB, J.A., WILHELM, S., CARTER, C. and KELLEY, S.L., 2006. Role of Raf kinase in cancer: therapeutic potential of targeting the Raf/MEK/ERK signal transduction pathway. *Seminars in oncology,* **33**(4), pp. 392-406.

GOUMANS, M.J., VALDIMARSDOTTIR, G., ITOH, S., LEBRIN, F., LARSSON, J., MUMMERY, C., KARLSSON, S. and TEN DIJKE, P., 2003. Activin receptor-like kinase (ALK)1 is an antagonistic mediator of lateral TGFbeta/ALK5 signaling. *Molecular cell,* **12**(4), pp. 817-828.

GREENBAUM, D., COLANGELO, C., WILLIAMS, K. and GERSTEIN, M., 2003. Comparing protein abundance and mRNA expression levels on a genomic scale. *Genome biology,* **4**(9), pp. 117.

HAAG, J. and AIGNER, T., 2006. Jun activation domain-binding protein 1 binds Smad5 and inhibits bone morphogenetic protein signaling. *Arthritis and Rheumatism,* **54**(12), pp. 3878-3884.

HALLSTROM, T.C. and NEVINS, J.R., 2006. Jab1 is a specificity factor for E2F1-induced apoptosis. *Genes & development,* **20**(5), pp. 613-623.

HAMBLETON, S., VALEYEV, N.V., MURANYI, A., KNOTT, V., WERNER, J.M., MCMICHAEL, A.J., HANDFORD, P.A. and DOWNING, A.K., 2004. Structural and functional properties of the human notch-1 ligand binding region. *Structure (London, England : 1993),* **12**(12), pp. 2173-2183.

HAN, C., HONG, K.H., KIM, Y.H., KIM, M.J., SONG, C., KIM, M.J., KIM, S.J., RAIZADA, M.K. and OH, S.P., 2013. SMAD1 deficiency in either endothelial or smooth muscle cells can predispose mice to pulmonary hypertension. *Hypertension (Dallas, Tex.: 1979),* **61**(5), pp. 1044-1052.

HARPER, R.L., REYNOLDS, A.M., BONDER, C.S. and REYNOLDS, P.N., 2016. BMPR2 gene therapy for PAH acts via Smad and non-Smad signalling. *Respirology (Carlton, Vic.),* **21**(4), pp. 727-733.

HARRISON, R.E., FLANAGAN, J.A., SANKELO, M., ABDALLA, S.A., ROWELL, J., MACHADO, R.D., ELLIOTT, C.G., ROBBINS, I.M., OLSCHEWSKI, H., MCLAUGHLIN, V., GRUENIG, E., KERMEEN, F., HALME, M., RAISANEN-SOKOLOWSKI, A., LAITINEN, T., MORRELL, N.W. and TREMBATH, R.C., 2003. Molecular and functional analysis identifies ALK-1 as the predominant cause of pulmonary hypertension related to hereditary haemorrhagic telangiectasia. *Journal of medical genetics,* **40**(12), pp. 865-871.

HARTUNG, A., BITTON-WORMS, K., RECHTMAN, M.M., WENZEL, V., BOERGERMANN, J.H., HASSEL, S., HENIS, Y.I. and KNAUS, P., 2006. Different routes of bone morphogenic protein (BMP) receptor endocytosis influence BMP signaling. *Molecular and cellular biology,* **26**(20), pp. 7791-7805.

HARVEY, R.P. and ROSENTHAL, N.(.)., 1998. *Heart Development.* San Diego: Academic Press.

HASSED, S.J., WILEY, G.B., WANG, S., LEE, J.Y., LI, S., XU, W., ZHAO, Z.J., MULVIHILL, J.J., ROBERTSON, J., WARNER, J. and GAFFNEY, P.M., 2012. RBPJ mutations identified in two families affected by Adams-Oliver syndrome. *American Journal of Human Genetics,* **91**(2), pp. 391-395.

HASSEL, S., EICHNER, A., YAKYMOVYCH, M., HELLMAN, U., KNAUS, P. and SOUCHELNYTSKYI, S., 2004. Proteins associated with type II bone morphogenetic protein receptor (BMPR-II) and identified by two-dimensional gel electrophoresis and mass spectrometry. *Proteomics,* **4**(5), pp. 1346-1358.

HASSKARL, J., MERN, D.S. and MUNGER, K., 2008. Interference of the dominant negative helix-loop-helix protein ID1 with the proteasomal subunit S5A causes centrosomal abnormalities. *Oncogene,* **27**(12), pp. 1657-1664.

HAYFLICK, L., 1973. Subculturing human diploid fibroblast cultures. In: P.F.J. KRUSE and M.K.J. PATTERSON, eds, *Tissue culture methods and applications.* Academic Press edn. New York: pp. 220–223.

HE, F., LU, D., JIANG, B., WANG, Y., LIU, Q., LIU, Q., SHAO, C., LI, X. and GONG, Y., 2013. X-linked intellectual disability gene CUL4B targets Jab1/CSN5 for degradation and regulates bone morphogenetic protein signaling. *Biochimica et biophysica acta,* **1832**(5), pp. 595-605.

HIGH, F.A., LU, M.M., PEAR, W.S., LOOMES, K.M., KAESTNER, K.H. and EPSTEIN, J.A., 2008. Endothelial expression of the Notch ligand Jagged1 is required for vascular smooth muscle development. *Proceedings of the National Academy of Sciences of the United States of America,* **105**(6), pp. 1955-1959.

HOYME, H.E., JONES, K.L., VAN ALLEN, M.I., SAUNDERS, B.S. and BENIRSCHKE, K., 1982. Vascular pathogenesis of transverse limb reduction defects. *The Journal of pediatrics,* **101**(5), pp. 839-843.

HSU, M.C., HUANG, C.C., CHANG, H.C., HU, T.H. and HUNG, W.C., 2008. Overexpression of Jab1 in hepatocellular carcinoma and its inhibition by peroxisome proliferator-activated receptor{gamma} ligands in vitro and in vivo. *Clinical cancer research : an official journal of the American Association for Cancer Research,* **14**(13), pp. 4045-4052.

HUANG, J., YUAN, H., LU, C., LIU, X., CAO, X. and WAN, M., 2007. Jab1 mediates protein degradation of the Rad9-Rad1-Hus1 checkpoint complex. *Journal of Molecular Biology,* **371**(2), pp. 514-527.

HUANG, Y.T., IWAMOTO, K., KUROSAKI, T., NASU, M. and UEDA, S., 2005. The neuronal POU transcription factor Brn-2 interacts with Jab1, a gene involved in the onset of neurodegenerative diseases. *Neuroscience letters,* **382**(1-2), pp. 175-178.

INTERNATIONAL PPH CONSORTIUM, LANE, K.B., MACHADO, R.D., PAUCIULO, M.W., THOMSON, J.R., PHILLIPS, J.A.,3RD, LOYD, J.E., NICHOLS, W.C. and TREMBATH, R.C., 2000. Heterozygous germline mutations in BMPR2, encoding a TGF-beta receptor, cause familial primary pulmonary hypertension. *Nature genetics,* **26**(1), pp. 81-84.

ITOH, F., ITOH, S., GOUMANS, M.J., VALDIMARSDOTTIR, G., ISO, T., DOTTO, G.P., HAMAMORI, Y., KEDES, L., KATO, M. and TEN DIJKE PT, P., 2004. Synergy and antagonism between Notch and BMP receptor signaling pathways in endothelial cells. *The EMBO journal,* **23**(3), pp. 541-551.

IZZI, L. and ATTISANO, L., 2004. Regulation of the TGFbeta signalling pathway by ubiquitin-mediated degradation. *Oncogene,* **23**(11), pp. 2071-2078.

IZZI, L. and ATTISANO, L., 2004. Regulation of the TGFbeta signalling pathway by ubiquitin-mediated degradation. *Oncogene,* **23**(11), pp. 2071-2078.

JONES, R., CAPEN, D.E. and REID, L., 2014. *Chapter 5 - Pulmonary Vascular Development.* Boston: Academic Press.

JONIGK, D., GOLPON, H., BOCKMEYER, C.L., MAEGEL, L., HOEPER, M.M., GOTTLIEB, J., NICKEL, N., HUSSEIN, K., MAUS, U., LEHMANN, U., JANCIAUSKIENE, S., WELTE, T., HAVERICH, A., RISCHE, J., KREIPE, H. and LAENGER, F., 2011. Plexiform lesions in pulmonary arterial hypertension composition, architecture, and microenvironment. *The American journal of pathology,* **179**(1), pp. 167-179.

JUMPERTZ, S., HENNES, T., ASARE, Y., VERVOORTS, J., BERNHAGEN, J. and SCHUTZ, A.K., 2014. The beta-catenin E3 ubiquitin ligase SIAH-1 is regulated by CSN5/JAB1 in CRC cells. *Cellular signalling,* **26**(9), pp. 2051-2059.

KATO, J.Y. and YONEDA-KATO, N., 2009. Mammalian COP9 signalosome. *Genes to cells : devoted to molecular & cellular mechanisms,* **14**(11), pp. 1209-1225.

KERSTJENS-FREDERIKSE, W.S., VAN DE LAAR, I.M., VOS, Y.J., VERHAGEN, J.M., BERGER, R.M., LICHTENBELT, K.D., KLEIN WASSINK-RUITER, J.S., VAN DER ZWAAG, P.A., DU MARCHIE SARVAAS, G.J., BERGMAN, K.A., BILARDO, C.M., ROOS-HESSELINK, J.W., JANSSEN, J.H., FROHN-MULDER, I.M., VAN SPAENDONCK-ZWARTS, K.Y., VAN MELLE, J.P., HOFSTRA, R.M. and WESSELS, M.W., 2016. Cardiovascular malformations caused by NOTCH1 mutations do not keep left: data on 428 probands with left-sided CHD and their families. *Genetics in medicine : official journal of the American College of Medical Genetics,* **18**(9), pp. 914-923.

KIM, B.C., LEE, H.J., PARK, S.H., LEE, S.R., KARPOVA, T.S., MCNALLY, J.G., FELICI, A., LEE, D.K. and KIM, S.J., 2004. Jab1/CSN5, a component of the COP9 signalosome, regulates transforming growth factor beta signaling by binding to Smad7 and promoting its degradation. *Molecular and cellular biology,* **24**(6), pp. 2251-2262.

KIM, J.H., CHOI, J.K., CINGHU, S., JANG, J.W., LEE, Y.S., LI, Y.H., GOH, Y.M., CHI, X.Z., LEE, K.S., WEE, H. and BAE, S.C., 2009. Jab1/CSN5 induces the cytoplasmic localization and degradation of RUNX3. *Journal of cellular biochemistry,* **107**(3), pp. 557-565.

KINOSHITA, S.M., KRUTZIK, P.O. and NOLAN, G.P., 2012. COP9 signalosome component JAB1/CSN5 is necessary for T cell signaling through LFA-1 and HIV-1 replication. *PloS one,* **7**(7), pp. e41725.

KLEEMANN, R., HAUSSER, A., GEIGER, G., MISCHKE, R., BURGER-KENTISCHER, A., FLIEGER, O., JOHANNES, F.J., ROGER, T., CALANDRA, T., KAPURNIOTU, A., GRELL, M., FINKELMEIER, D., BRUNNER, H. and BERNHAGEN, J., 2000. Intracellular action of the cytokine MIF to modulate AP-1 activity and the cell cycle through Jab1. *Nature,* **408**(6809), pp. 211-216.

KOMANDER, D., 2009. The emerging complexity of protein ubiquitination. *Biochemical Society transactions,* **37**(Pt 5), pp. 937-953.

KOUVARAKI, M.A., KORAPATI, A.L., RASSIDAKIS, G.Z., TIAN, L., ZHANG, Q., CHIAO, P., HO, L., EVANS, D.B. and CLARET, F.X., 2006. Potential role of Jun activation domain-binding protein 1 as a negative regulator of p27kip1 in pancreatic adenocarcinoma. *Cancer research,* **66**(17), pp. 8581-8589.

KWAK, H.J., KIM, S.H., YOO, H.G., PARK, S.H. and LEE, C.H., 2005. Jun activation domain-binding protein 1 is required for mitotic checkpoint activation via its involvement in hyperphosphorylation of 53BP1. *Journal of cancer research and clinical oncology,* **131**(12), pp. 789-796.

LANE, K.B., BLACKWELL, T.R., RUNO, J., WHEELER, L., PHILLIPS, J.A.,3RD and LOYD, J.E., 2005. Aberrant signal transduction in pulmonary hypertension. *Chest,* **128**(6 Suppl), pp. 564S-565S.

LARSEN, M., HOG, A., LUND, E.L. and KRISTJANSEN, P.E., 2005. Interactions between HIF-1 and Jab1: balancing apoptosis and adaptation. Outline of a working hypothesis. *Advances in Experimental Medicine and Biology,* **566**, pp. 203-211.

LAU, E.M.T., GIANNOULATOU, E., CELERMAJER, D.S. and HUMBERT, M., 2017. Epidemiology and treatment of pulmonary arterial hypertension. *Nature reviews.Cardiology,* .

LI, S., LIU, X. and ASCOLI, M., 2000. p38JAB1 binds to the intracellular precursor of the lutropin/choriogonadotropin receptor and promotes its degradation. *The Journal of biological chemistry,* **275**(18), pp. 13386-13393.

LI, Q., QIU, Y., MAO, M., LV, J., ZHANG, L., LI, S., LI, X. and ZHENG, X., 2014. Antioxidant mechanism of Rutin on hypoxia-induced pulmonary arterial cell proliferation. *Molecules (Basel, Switzerland),* **19**(11), pp. 19036-19049.

LI, X., ZHANG, X., LEATHERS, R., MAKINO, A., HUANG, C., PARSA, P., MACIAS, J., YUAN, J.X., JAMIESON, S.W. and THISTLETHWAITE, P.A., 2009. Notch3 signaling promotes the development of pulmonary arterial hypertension. *Nature medicine,* **15**(11), pp. 1289-1297.

LO, A.K., DAWSON, C.W., LO, K.W., YU, Y. and YOUNG, L.S., 2010. Upregulation of Id1 by Epstein-Barr virus-encoded LMP1 confers resistance to TGFbeta-mediated growth inhibition. *Molecular cancer,* **9**, pp. 155-4598-9-155.

LONG, L., ORMISTON, M.L., YANG, X., SOUTHWOOD, M., GRAF, S., MACHADO, R.D., MUELLER, M., KINZEL, B., YUNG, L.M., WILKINSON, J.M., MOORE, S.D., DRAKE, K.M., ALDRED, M.A., YU, P.B., UPTON, P.D. and MORRELL, N.W., 2015. Selective enhancement of endothelial BMPR-II with BMP9 reverses pulmonary arterial hypertension. *Nature medicine,* **21**(7), pp. 777-785.

LOPEZ-ROVIRA, T., CHALAUX, E., MASSAGUE, J., ROSA, J.L. and VENTURA, F., 2002. Direct binding of Smad1 and Smad4 to two distinct motifs mediates bone morphogenetic protein-specific transcriptional activation of Id1 gene. *The Journal of biological chemistry,* **277**(5), pp. 3176-3185.

LUCA, V.C., JUDE, K.M., PIERCE, N.W., NACHURY, M.V., FISCHER, S. and GARCIA, K.C., 2015. Structural biology. Structural basis for Notch1 engagement of Delta-like 4. *Science (New York, N.Y.),* **347**(6224), pp. 847-853.

LUE, H., THIELE, M., FRANZ, J., DAHL, E., SPECKGENS, S., LENG, L., FINGERLE-ROWSON, G., BUCALA, R., LUSCHER, B. and BERNHAGEN, J., 2007. Macrophage migration inhibitory factor (MIF) promotes cell survival by activation of the Akt pathway and role for CSN5/JAB1 in the control of autocrine MIF activity. *Oncogene,* **26**(35), pp. 5046-5059.

LUO, W., WANG, Y., HANCK, T., STRICKER, R. and REISER, G., 2006. Jab1, a novel protease-activated receptor-2 (PAR-2)-interacting protein, is involved in PAR-2-induced activation of activator protein-1. *The Journal of biological chemistry,* **281**(12), pp. 7927-7936.

MACHADO, R.D., 2012. The molecular genetics and cellular mechanisms underlying pulmonary arterial hypertension. *Scientifica,* **2012**, pp. 106576.

MACHADO, R.D., EICKELBERG, O., ELLIOTT, C.G., GERACI, M.W., HANAOKA, M., LOYD, J.E., NEWMAN, J.H., PHILLIPS, J.A.,3RD, SOUBRIER, F., TREMBATH, R.C. and CHUNG, W.K., 2009. Genetics and genomics of pulmonary arterial hypertension. *Journal of the American College of Cardiology,* **54**(1 Suppl), pp. S32-42.

MACHADO, R.D., PAUCIULO, M.W., THOMSON, J.R., LANE, K.B., MORGAN, N.V., WHEELER, L., PHILLIPS, J.A.,3RD, NEWMAN, J., WILLIAMS, D., GALIE, N., MANES, A., MCNEIL, K., YACOUB, M., MIKHAIL, G., ROGERS, P., CORRIS, P., HUMBERT, M., DONNAI, D., MARTENSSON, G., TRANEBJAERG, L., LOYD, J.E., TREMBATH, R.C. and NICHOLS, W.C., 2001. BMPR2 haploinsufficiency as the inherited molecular mechanism for primary pulmonary hypertension. *American Journal of Human Genetics,* **68**(1), pp. 92-102.

MACHADO, R.D., RUDARAKANCHANA, N., ATKINSON, C., FLANAGAN, J.A., HARRISON, R., MORRELL, N.W. and TREMBATH, R.C., 2003. Functional interaction between BMPR-II and Tctex-1, a light chain of Dynein, is isoform-specific and disrupted by mutations underlying primary pulmonary hypertension. *Human molecular genetics,* **12**(24), pp. 3277-3286.

MACHADO, R.D., SOUTHGATE, L., EICHSTAEDT, C.A., ALDRED, M.A., AUSTIN, E.D., BEST, D.H., CHUNG, W.K., BENJAMIN, N., ELLIOTT, C.G., EYRIES, M., FISCHER, C., GRAF, S., HINDERHOFER, K., HUMBERT, M., KEILES, S.B., LOYD, J.E., MORRELL, N.W., NEWMAN, J.H., SOUBRIER, F.,

TREMBATH, R.C., VIALES, R.R. and GRUNIG, E., 2015. Pulmonary Arterial Hypertension: A Current Perspective on Established and Emerging Molecular Genetic Defects. *Human mutation,* **36**(12), pp. 1113-1127.

MACHADO, R.D., ALDRED, M.A., JAMES, V., HARRISON, R.E., PATEL, B., SCHWALBE, E.C., GRUENIG, E., JANSSEN, B., KOEHLER, R., SEEGER, W., EICKELBERG, O., OLSCHEWSKI, H., GREGORY ELLIOTT, C., GLISSMEYER, E., CARLQUIST, J., KIM, M., TORBICKI, A., FIJALKOWSKA, A., SZEWCZYK, G., PARMA, J., ABRAMOWICZ, M.J., GALIE, N., MORISAKI, H., KYOTANI, S., NAKANISHI, N., MORISAKI, T., HUMBERT, M., SIMONNEAU, G., SITBON, O.,

MAHMUD, E., MADANI, M.M., KIM, N.H., POCH, D., ANG, L., BEHNAMFAR, O., PATEL, M.P. and AUGER, W.R., 2018. Chronic Thromboembolic Pulmonary Hypertension: Evolving Therapeutic Approaches for Operable and Inoperable Disease. *Journal of the American College of Cardiology,* **71**(21), pp. 2468-2486.

MAJKA, S., HAGEN, M., BLACKWELL, T., HARRAL, J., JOHNSON, J.A., GENDRON, R., PARADIS, H., CRONA, D., LOYD, J.E., NOZIK-GRAYCK, E., STENMARK, K.R. and WEST, J., 2011. Physiologic and molecular consequences of endothelial Bmpr2 mutation. *Respiratory research,* **12**, pp. 84-9921-12-84.

MARTINEZ-FRIAS, M.L., ARROYO CARRERA, I., MUNOZ-DELGADO, N.J., NIETO CONDE, C., RODRIGUEZ-PINILLA, E., URIOSTE AZCORRA, M., OMENACA TERES, F. and GARCIA ALIX, A., 1996. The Adams-Oliver syndrome in Spain: the epidemiological aspects. *Anales Espanoles de Pediatria,* **45**(1), pp. 57-61.

MASSAGUE, J., 2012. TGFbeta signalling in context. *Nature reviews.Molecular cell biology,* **13**(10), pp. 616-630.

MASSAGUE, J., SEOANE, J. and WOTTON, D., 2005. Smad transcription factors. *Genes & development,* **19**(23), pp. 2783-2810.

MATON, A., 1993. *Human biology and health.* First Edition edn. Englewood Cliffs, N.J.: Prentice Hall.

MCGILL, H.C.,JR, MCMAHAN, C.A. and GIDDING, S.S., 2008. Preventing heart disease in the 21st century: implications of the Pathobiological Determinants of Atherosclerosis in Youth (PDAY) study. *Circulation,* **117**(9), pp. 1216-1227.

MCLAUGHLIN, V.V. and MCGOON, M.D., 2006. Pulmonary arterial hypertension. *Circulation,* **114**(13), pp. 1417-1431.

MEESTER, J.A., SOUTHGATE, L., STITTRICH, A.B., VENSELAAR, H., BEEKMANS, S.J., DEN HOLLANDER, N., BIJLSMA, E.K., HELDERMAN-VAN DEN ENDEN, A., VERHEIJ, J.B., GLUSMAN, G., ROACH, J.C., LEHMAN, A., PATEL, M.S., DE VRIES, B.B., RUIVENKAMP, C., ITIN, P., PRESCOTT, K., CLARKE, S., TREMBATH, R., ZENKER, M., SUKALO, M., VAN LAER, L., LOEYS,

B. and WUYTS, W., 2015. Heterozygous Loss-of-Function Mutations in DLL4 Cause Adams-Oliver Syndrome. *American Journal of Human Genetics,* **97**(3), pp. 475-482.

MENDIS, S., PUSKA, P. and NORRVING, B., 2011. *Global Atlas on cardiovascular disease prevention and control.* Geneva: World Health Organization 2011.

MIYAZONO, K., MAEDA, S. and IMAMURA, T., 2005. BMP receptor signaling: transcriptional targets, regulation of signals, and signaling cross-talk. *Cytokine & growth factor reviews,* **16**(3), pp. 251-263.

MONTANI, D., GUNTHER, S., DORFMULLER, P., PERROS, F., GIRERD, B., GARCIA, G., JAIS, X., SAVALE, L., ARTAUD-MACARI, E., PRICE, L.C., HUMBERT, M., SIMONNEAU, G. and SITBON, O., 2013. Pulmonary arterial hypertension. *Orphanet journal of rare diseases,* **8**, pp. 97-1172-8-97.

MORAN, A.E., FOROUZANFAR, M.H., ROTH, G.A., MENSAH, G.A., EZZATI, M., MURRAY, C.J. and NAGHAVI, M., 2014. Temporal trends in ischemic heart disease mortality in 21 world regions, 1980 to 2010: the Global Burden of Disease 2010 study. *Circulation,* **129**(14), pp. 1483-1492.

MORI, M., YONEDA-KATO, N., YOSHIDA, A. and KATO, J.Y., 2008. Stable form of JAB1 enhances proliferation and maintenance of hematopoietic progenitors. *The Journal of biological chemistry,* **283**(43), pp. 29011-29021.

MORRELL, N.W., 2006. Pulmonary hypertension due to BMPR2 mutation: a new paradigm for tissue remodeling? *Proceedings of the American Thoracic Society,* **3**(8), pp. 680-686.

MORRELL, N.W., YANG, X., UPTON, P.D., JOURDAN, K.B., MORGAN, N., SHEARES, K.K. and TREMBATH, R.C., 2001. Altered growth responses of pulmonary artery smooth muscle cells from patients with primary pulmonary hypertension to transforming growth factor-beta(1) and bone morphogenetic proteins. *Circulation,* **104**(7), pp. 790-795.

MURAKAMI, K., MATHEW, R., HUANG, J., FARAHANI, R., PENG, H., OLSON, S.C. and ETLINGER, J.D., 2010. Smurf1 ubiquitin ligase causes downregulation of BMP receptors and is induced in monocrotaline and hypoxia models of pulmonary arterial hypertension. *Experimental biology and medicine (Maywood, N.J.),* **235**(7), pp. 805-813.

NASIM, M.T., GHOURI, A., PATEL, B., JAMES, V., RUDARAKANCHANA, N., MORRELL, N.W. and TREMBATH, R.C., 2008. Stoichiometric imbalance in the receptor complex contributes to dysfunctional BMPR-II mediated signalling in pulmonary arterial hypertension. *Human molecular genetics,* **17**(11), pp. 1683-1694.

NASIM, M.T., OGO, T., AHMED, M., RANDALL, R., CHOWDHURY, H.M., SNAPE, K.M., BRADSHAW, T.Y., SOUTHGATE, L., LEE, G.J., JACKSON, I., LORD, G.M., GIBBS, J.S., WILKINS, M.R., OHTA-OGO, K., NAKAMURA, K., GIRERD, B., COULET, F., SOUBRIER, F., HUMBERT, M., MORRELL, N.W., TREMBATH, R.C. and MACHADO, R.D., 2011. Molecular genetic characterization of SMAD signaling molecules in pulmonary arterial hypertension. *Human mutation,* **32**(12), pp. 1385-1389.

NASIM, M.T., OGO, T., CHOWDHURY, H.M., ZHAO, L., CHEN, C.N., RHODES, C. and TREMBATH, R.C., 2012. BMPR-II deficiency elicits pro-proliferative and anti-apoptotic responses through the activation of TGFbeta-TAK1-MAPK pathways in PAH. *Human molecular genetics,* **21**(11), pp. 2548-2558.

NISHIHARA, A., WATABE, T., IMAMURA, T. and MIYAZONO, K., 2002. Functional heterogeneity of bone morphogenetic protein receptor-II mutants found in patients with primary pulmonary hypertension. *Molecular biology of the cell,* **13**(9), pp. 3055-3063.

NISHIMOTO, A., LU, L., HAYASHI, M., NISHIYA, T., HORINOUCHI, T. and MIWA, S., 2010. Jab1 regulates levels of endothelin type A and B receptors by promoting ubiquitination and degradation. *Biochemical and biophysical research communications,* **391**(4), pp. 1616-1622.

ODA, T., ELKAHLOUN, A.G., PIKE, B.L., OKAJIMA, K., KRANTZ, I.D., GENIN, A., PICCOLI, D.A., MELTZER, P.S., SPINNER, N.B., COLLINS, F.S. and CHANDRASEKHARAPPA, S.C., 1997. Mutations in the human Jagged1 gene are responsible for Alagille syndrome. *Nature genetics,* **16**(3), pp. 235-242.

OH, W., LEE, E.W., SUNG, Y.H., YANG, M.R., GHIM, J., LEE, H.W. and SONG, J., 2006. Jab1 induces the cytoplasmic localization and degradation of p53 in coordination with Hdm2. *The Journal of biological chemistry,* **281**(25), pp. 17457-17465.

PAN, L., WANG, S., LU, T., WENG, C., SONG, X., PARK, J.K., SUN, J., YANG, Z.H., YU, J., TANG, H., MCKEARIN, D.M., CHAMOVITZ, D.A., NI, J. and XIE, T., 2014. Protein competition switches the function of COP9 from self-renewal to differentiation. *Nature,* **514**(7521), pp. 233-236.

PAN, Y., LIU, Z., SHEN, J. and KOPAN, R., 2005. Notch1 and 2 cooperate in limb ectoderm to receive an early Jagged2 signal regulating interdigital apoptosis. *Developmental biology,* **286**(2), pp. 472-482.

PATAN, S., 2004. Vasculogenesis and angiogenesis. *Cancer treatment and research,* **117**, pp. 3-32.

PATEL, M.S., TAYLOR, G.P., BHARYA, S., AL-SANNA'A, N., ADATIA, I., CHITAYAT, D., SUZANNE LEWIS, M.E. and HUMAN, D.G., 2004. Abnormal

pericyte recruitment as a cause for pulmonary hypertension in Adams-Oliver syndrome. *American journal of medical genetics.Part A,* **129A**(3), pp. 294-299.

PENG, T. and MORRISEY, E.E., 2013. Development of the pulmonary vasculature: Current understanding and concepts for the future. *Pulmonary Circulation,* **3**(1), pp. 176-178.

PERIZ, J., GILL, A.C., KNOTT, V., HANDFORD, P.A. and TOMLEY, F.M., 2005. Calcium binding activity of the epidermal growth factor-like domains of the apicomplexan microneme protein EtMIC4. *Molecular and biochemical parasitology,* **143**(2), pp. 192-199.

PETROVIC, J., FORMOSA-JORDAN, P., LUNA-ESCALANTE, J.C., ABELLO, G., IBANES, M., NEVES, J. and GIRALDEZ, F., 2014. Ligand-dependent Notch signaling strength orchestrates lateral induction and lateral inhibition in the developing inner ear. *Development (Cambridge, England),* **141**(11), pp. 2313-2324.

PIAZZA, A.J., BLACKSTON, D. and SOLA, A., 2004. A case of Adams-Oliver syndrome with associated brain and pulmonary involvement: further evidence of vascular pathology? *American journal of medical genetics.Part A,* **130A**(2), pp. 172-175.

PIETRA, G.G., EDWARDS, W.D., KAY, J.M., RICH, S., KERNIS, J., SCHLOO, B., AYRES, S.M., BERGOFSKY, E.H., BRUNDAGE, B.H. and DETRE, K.M., 1989. Histopathology of primary pulmonary hypertension. A qualitative and quantitative study of pulmonary blood vessels from 58 patients in the National Heart, Lung, and Blood Institute, Primary Pulmonary Hypertension Registry. *Circulation,* **80**(5), pp. 1198-1206.

PUGH, M.E. and HEMNES, A.R., 2010. Pulmonary hypertension in women. *Expert review of cardiovascular therapy,* **8**(11), pp. 1549-1558.

RABINOVITCH, M., 2012. Molecular pathogenesis of pulmonary arterial hypertension. *The Journal of clinical investigation,* **122**(12), pp. 4306-4313.

RAJKUMAR, R., KONISHI, K., RICHARDS, T.J., ISHIZAWAR, D.C., WIECHERT, A.C., KAMINSKI, N. and AHMAD, F., 2010. Genomewide RNA expression profiling in lung identifies distinct signatures in idiopathic pulmonary arterial hypertension and secondary pulmonary hypertension. *American journal of physiology.Heart and circulatory physiology,* **298**(4), pp. H1235-48.

RAND, M.D., LINDBLOM, A., CARLSON, J., VILLOUTREIX, B.O. and STENFLO, J., 1997. Calcium binding to tandem repeats of EGF-like modules. Expression and characterization of the EGF-like modules of human Notch-1 implicated in receptor-ligand interactions. *Protein science : a publication of the Protein Society,* **6**(10), pp. 2059-2071.

ROSTAMA, B., PETERSON, S.M., VARY, C.P. and LIAW, L., 2014. Notch signal integration in the vasculature during remodeling. *Vascular pharmacology,* **63**(2), pp. 97-104.

RUDARAKANCHANA, N., FLANAGAN, J.A., CHEN, H., UPTON, P.D., MACHADO, R., PATEL, D., TREMBATH, R.C. and MORRELL, N.W., 2002. Functional analysis of bone morphogenetic protein type II receptor mutations underlying primary pulmonary hypertension. *Human molecular genetics,* **11**(13), pp. 1517-1525.

RUNO, J.R. and LOYD, J.E., 2003. Primary pulmonary hypertension. *Lancet (London, England),* **361**(9368), pp. 1533-1544.

RUSANESCU, G., WEISSLEDER, R. and AIKAWA, E., 2008. Notch signaling in cardiovascular disease and calcification. *Current cardiology reviews,* **4**(3), pp. 148-156.

RYAN, J., DASGUPTA, A., HUSTON, J., CHEN, K.H. and ARCHER, S.L., 2015. Mitochondrial dynamics in pulmonary arterial hypertension. *Journal of Molecular Medicine (Berlin, Germany),* **93**(3), pp. 229-242.

SABBA, C., PASCULLI, G., LENATO, G.M., SUPPRESSA, P., LASTELLA, P., MEMEO, M., DICUONZO, F. and GUANT, G., 2007. Hereditary hemorrhagic telangiectasia: clinical features in ENG and ALK1 mutation carriers. *Journal of thrombosis and haemostasis : JTH,* **5**(6), pp. 1149-1157.

SAKAIDANI, Y., ICHIYANAGI, N., SAITO, C., NOMURA, T., ITO, M., NISHIO, Y., NADANO, D., MATSUDA, T., FURUKAWA, K. and OKAJIMA, T., 2012. O-linked-N-acetylglucosamine modification of mammalian Notch receptors by an atypical O-GlcNAc transferase Eogt1. *Biochemical and biophysical research communications,* **419**(1), pp. 14-19.

SANGADALA, S., YOSHIOKA, K., ENYO, Y., LIU, Y., TITUS, L. and BODEN, S.D., 2014. Characterization of a unique motif in LIM mineralization protein-1 that interacts with jun activation-domain-binding protein 1. *Molecular and cellular biochemistry,* **385**(1-2), pp. 145-157.

SHACKLEFORD, T.J. and CLARET, F.X., 2010. JAB1/CSN5: a new player in cell cycle control and cancer. *Cell division,* **5**, pp. 26-1028-5-26.

SHAHEEN, R., AGLAN, M., KEPPLER-NOREUIL, K., FAQEIH, E., ANSARI, S., HORTON, K., ASHOUR, A., ZAKI, M.S., AL-ZAHRANI, F., CUETO-GONZALEZ, A.M., ABDEL-SALAM, G., TEMTAMY, S. and ALKURAYA, F.S., 2013. Mutations in EOGT confirm the genetic heterogeneity of autosomal-recessive Adams-Oliver syndrome. *American Journal of Human Genetics,* **92**(4), pp. 598-604.

SHAHEEN, R., FAQEIH, E., SUNKER, A., MORSY, H., AL-SHEDDI, T., SHAMSELDIN, H.E., ADLY, N., HASHEM, M. and ALKURAYA, F.S., 2011.

Recessive mutations in DOCK6, encoding the guanidine nucleotide exchange factor DOCK6, lead to abnormal actin cytoskeleton organization and Adams-Oliver syndrome. *American Journal of Human Genetics,* **89**(2), pp. 328-333.

SHIM, J.H., GREENBLATT, M.B., XIE, M., SCHNEIDER, M.D., ZOU, W., ZHAI, B., GYGI, S. and GLIMCHER, L.H., 2009. TAK1 is an essential regulator of BMP signalling in cartilage. *The EMBO journal,* **28**(14), pp. 2028-2041.

SHINTANI, M., YAGI, H., NAKAYAMA, T., SAJI, T. and MATSUOKA, R., 2009. A new nonsense mutation of SMAD8 associated with pulmonary arterial hypertension. *Journal of medical genetics,* **46**(5), pp. 331-337.

SIMONNEAU, G., GATZOULIS, M.A., ADATIA, I., CELERMAJER, D., DENTON, C., GHOFRANI, A., GOMEZ SANCHEZ, M.A., KRISHNA KUMAR, R., LANDZBERG, M., MACHADO, R.F., OLSCHEWSKI, H., ROBBINS, I.M. and SOUZA, R., 2013. Updated clinical classification of pulmonary hypertension. *Journal of the American College of Cardiology,* **62**(25 Suppl), pp. D34-41.

SNAPE, K.M., RUDDY, D., ZENKER, M., WUYTS, W., WHITEFORD, M., JOHNSON, D., LAM, W. and TREMBATH, R.C., 2009. The spectra of clinical phenotypes in aplasia cutis congenita and terminal transverse limb defects. *American journal of medical genetics.Part A,* **149A**(8), pp. 1860-1881.

SOBOLEWSKI, A., RUDARAKANCHANA, N., UPTON, P.D., YANG, J., CRILLEY, T.K., TREMBATH, R.C. and MORRELL, N.W., 2008. Failure of bone morphogenetic protein receptor trafficking in pulmonary arterial hypertension: potential for rescue. *Human molecular genetics,* **17**(20), pp. 3180-3190.

SOMMER, N., HECKER, M., TELLO, K., RICHTER, M., LIEBETRAU, C., WEIGAND, M.A., SEEGER, W., GHOFRANI, A. and GALL, H., 2016. Pulmonary hypertension : What is new in therapy? *Der Anaesthesist,* **65**(8), pp. 635-652.

SOUBRIER, F., COULET, F., MORRELL, N.W. and TREMBATH, R.C., 2006. Mutations of the TGF-? type II receptor BMPR2 in pulmonary arterial hypertension. *Human mutation,* **27**(2), pp. 121-132.

SOUBRIER, F., CHUNG, W.K., MACHADO, R., GRUNIG, E., ALDRED, M., GERACI, M., LOYD, J.E., ELLIOTT, C.G., TREMBATH, R.C., NEWMAN, J.H. and HUMBERT, M., 2013. Genetics and genomics of pulmonary arterial hypertension. *Journal of the American College of Cardiology,* **62**(25 Suppl), pp. D13-21.

SOUTHGATE, L., MACHADO, R.D., SNAPE, K.M., PRIMEAU, M., DAFOU, D., RUDDY, D.M., BRANNEY, P.A., FISHER, M., LEE, G.J., SIMPSON, M.A., HE, Y., BRADSHAW, T.Y., BLAUMEISER, B., WINSHIP, W.S., REARDON, W., MAHER, E.R., FITZPATRICK, D.R., WUYTS, W., ZENKER, M., LAMARCHE-VANE, N. and TREMBATH, R.C., 2011. Gain-of-function mutations of ARHGAP31, a Cdc42/Rac1

GTPase regulator, cause syndromic cutis aplasia and limb anomalies. *American Journal of Human Genetics,* **88**(5), pp. 574-585.

SOUTHGATE, L., SUKALO, M., KAROUNTZOS, A.S.V., TAYLOR, E.J., COLLINSON, C.S., RUDDY, D., SNAPE, K.M., DALLAPICCOLA, B., TOLMIE, J.L., JOSS, S., BRANCATI, F., DIGILIO, M.C., GRAUL-NEUMANN, L.M., SALVIATI, L., COERDT, W., JACQUEMIN, E., WUYTS, W., ZENKER, M., MACHADO, R.D. and TREMBATH, R.C., 2015. Haploinsufficiency of the NOTCH1 Receptor as a Cause of Adams-Oliver Syndrome With Variable Cardiac Anomalies. *Circulation.Cardiovascular genetics,* **8**(4), pp. 572-581.

STITTRICH, A.B., LEHMAN, A., BODIAN, D.L., ASHWORTH, J., ZONG, Z., LI, H., LAM, P., KHROMYKH, A., IYER, R.K., VOCKLEY, J.G., BAVEJA, R., SILVA, E.S., DIXON, J., LEON, E.L., SOLOMON, B.D., GLUSMAN, G., NIEDERHUBER, J.E., ROACH, J.C. and PATEL, M.S., 2014. Mutations in NOTCH1 cause Adams-Oliver syndrome. *American Journal of Human Genetics,* **95**(3), pp. 275-284.

SWARTZ, E.N., SANATANI, S., SANDOR, G.G. and SCHREIBER, R.A., 1999. Vascular abnormalities in Adams-Oliver syndrome: cause or effect? *American Journal of Medical Genetics,* **82**(1), pp. 49-52.

TANAKA, Y., KANAI, F., ICHIMURA, T., TATEISHI, K., ASAOKA, Y., GULENG, B., JAZAG, A., OHTA, M., IMAMURA, J., IKENOUE, T., IJICHI, H., KAWABE, T., ISOBE, T. and OMATA, M., 2006. The hepatitis B virus X protein enhances AP-1 activation through interaction with Jab1. *Oncogene,* **25**(4), pp. 633-642.

TANG, Y., URS, S., BOUCHER, J., BERNAICHE, T., VENKATESH, D., SPICER, D.B., VARY, C.P. and LIAW, L., 2010. Notch and transforming growth factor-beta (TGFbeta) signaling pathways cooperatively regulate vascular smooth muscle cell differentiation. *The Journal of biological chemistry,* **285**(23), pp. 17556-17563.

TIAN, L., PENG, G., PARANT, J.M., LEVENTAKI, V., DRAKOS, E., ZHANG, Q., PARKER-THORNBURG, J., SHACKLEFORD, T.J., DAI, H., LIN, S.Y., LOZANO, G., RASSIDAKIS, G.Z. and CLARET, F.X., 2010. Essential roles of Jab1 in cell survival, spontaneous DNA damage and DNA repair. *Oncogene,* **29**(46), pp. 6125-6137.

TOMODA, K., KATO, J.Y., TATSUMI, E., TAKAHASHI, T., MATSUO, Y. and YONEDA-KATO, N., 2005. The Jab1/COP9 signalosome subcomplex is a downstream mediator of Bcr-Abl kinase activity and facilitates cell-cycle progression. *Blood,* **105**(2), pp. 775-783.

TOMODA, K., KUBOTA, Y., ARATA, Y., MORI, S., MAEDA, M., TANAKA, T., YOSHIDA, M., YONEDA-KATO, N. and KATO, J.Y., 2002. The cytoplasmic shuttling and subsequent degradation of p27Kip1 mediated by Jab1/CSN5 and the COP9 signalosome complex. *The Journal of biological chemistry,* **277**(3), pp. 2302-2310.

TORIELLO, H.V., GRAFF, R.G., FLORENTINE, M.F., LACINA, S. and MOORE, W.D., 1988. Scalp and limb defects with cutis marmorata telangiectatica congenita: Adams-Oliver syndrome? *American Journal of Medical Genetics,* **29**(2), pp. 269-276.

TOWBIN, J.A., CASEY, B. and BELMONT, J., 1999. The molecular basis of vascular disorders. *American Journal of Human Genetics,* **64**(3), pp. 678-684.

TRAN, H.J., ALLEN, M.D., LOWE, J. and BYCROFT, M., 2003. Structure of the Jab1/MPN domain and its implications for proteasome function. *Biochemistry,* **42**(39), pp. 11460-11465.

TSUJIMOTO, I., YOSHIDA, A., YONEDA-KATO, N. and KATO, J.Y., 2012. Depletion of CSN5 inhibits Ras-mediated tumorigenesis by inducing premature senescence in p53-null cells. *FEBS letters,* **586**(24), pp. 4326-4331.

TSUKAMOTO, S. and YOKOSAWA, H., 2009. Targeting the proteasome pathway. *Expert opinion on therapeutic targets,* **13**(5), pp. 605-621.

TUDER, R.M., STACHER, E., ROBINSON, J., KUMAR, R. and GRAHAM, B.B., 2013. Pathology of pulmonary hypertension. *Clinics in chest medicine,* **34**(4), pp. 639-650.

UPTON, P.D., DAVIES, R.J., TAJSIC, T. and MORRELL, N.W., 2013. Transforming growth factor-beta(1) represses bone morphogenetic protein-mediated Smad signaling in pulmonary artery smooth muscle cells via Smad3. *American journal of respiratory cell and molecular biology,* **49**(6), pp. 1135-1145.

VALDIMARSDOTTIR, G., GOUMANS, M.J., ROSENDAHL, A., BRUGMAN, M., ITOH, S., LEBRIN, F., SIDERAS, P. and TEN DIJKE, P., 2002. Stimulation of Id1 expression by bone morphogenetic protein is sufficient and necessary for bone morphogenetic protein-induced activation of endothelial cells. *Circulation,* **106**(17), pp. 2263-2270.

VAN ALBADA, M.E. and BERGER, R.M., 2008. Pulmonary arterial hypertension in congenital cardiac disease--the need for refinement of the Evian-Venice classification. *Cardiology in the young,* **18**(1), pp. 10-17.

VLODAVSKY, I., JOHNSON, L.K. and GOSPODAROWICZ, D., 1979. Appearance in confluent vascular endothelial cell monolayers of a specific cell surface protein (CSP-60) not detected in actively growing endothelial cells or in cell types growing in multiple layers. *Proceedings of the National Academy of Sciences of the United States of America,* **76**(5), pp. 2306-2310.

WAITE, K.A. and ENG, C., 2003. From developmental disorder to heritable cancer: it's all in the BMP/TGF-beta family. *Nature reviews.Genetics,* **4**(10), pp. 763-773.

WAN MAKHTAR, W.R., BROWNE, G., KAROUNTZOS, A., STEVENS, C., ALGHAMDI, Y., BOTTRILL, A.R., MISTRY, S., SMITH, E., BUSHEL, M., PRINGLE, J.H., SAYAN, A.E. and TULCHINSKY, E., 2017. Short stretches of rare codons regulate translation of the transcription factor ZEB2 in cancer cells. *Oncogene,* .

WAN, M., CAO, X., WU, Y., BAI, S., WU, L., SHI, X., WANG, N. and CAO, X., 2002. Jab1 antagonizes TGF-beta signaling by inducing Smad4 degradation. *EMBO reports,* **3**(2), pp. 171-176.

WANG, J., LI, C., LIU, Y., MEI, W., YU, S., LIU, C., ZHANG, L., CAO, X., KIMBERLY, R.P., GRIZZLE, W. and ZHANG, H.G., 2006. JAB1 determines the response of rheumatoid arthritis synovial fibroblasts to tumor necrosis factor-alpha. *The American journal of pathology,* **169**(3), pp. 889-902.

WANG, L., ZHENG, J. and PEI, D., 2016. The emerging roles of Jab1/CSN5 in cancer. *Medical Oncology,* **33**(8), pp. 90.

WARD, J.P. and AARONSON, P.I., 1999. Mechanisms of hypoxic pulmonary vasoconstriction: can anyone be right? *Respiration physiology,* **115**(3), pp. 261-271.

WEI, N., SERINO, G. and DENG, X.W., 2008. The COP9 signalosome: more than a protease. *Trends in biochemical sciences,* **33**(12), pp. 592-600.

WELCHMAN, R.L., GORDON, C. and MAYER, R.J., 2005. Ubiquitin and ubiquitin-like proteins as multifunctional signals. *Nature reviews.Molecular cell biology,* **6**(8), pp. 599-609.

WELSH, D.J., HARNETT, M., MACLEAN, M. and PEACOCK, A.J., 2004. Proliferation and signaling in fibroblasts: role of 5-hydroxytryptamine2A receptor and transporter. *American journal of respiratory and critical care medicine,* **170**(3), pp. 252-259.

WEST, J., HARRAL, J., LANE, K., DENG, Y., ICKES, B., CRONA, D., ALBU, S., STEWART, D. and FAGAN, K., 2008. Mice expressing BMPR2R899X transgene in smooth muscle develop pulmonary vascular lesions. *American journal of physiology.Lung cellular and molecular physiology,* **295**(5), pp. L744-55.

WHITEMAN, P., DOWNING, A.K., SMALLRIDGE, R., WINSHIP, P.R. and HANDFORD, P.A., 1998. A Gly --> Ser change causes defective folding in vitro of calcium-binding epidermal growth factor-like domains from factor IX and fibrillin-1. *The Journal of biological chemistry,* **273**(14), pp. 7807-7813.

WICKER, C.A. and IZUMI, T., 2016. Analysis of RNA expression of normal and cancer tissues reveals high correlation of COP9 gene expression with respiratory chain complex components. *BMC Genomics,* **17**, pp. 983.

WIDEMAN, R.F.,JR and HAMAL, K.R., 2011. Idiopathic pulmonary arterial hypertension: an avian model for plexogenic arteriopathy and serotonergic vasoconstriction. *Journal of pharmacological and toxicological methods,* **63**(3), pp. 283-295.

WONG, W.P., KNOWLES, J.A. and MORSE, J.H., 2005. Comparative analysis of BMPR2 gene and its mutations in idiopathic pulmonary arterial hypertension. *Chest,* **128**(6 Suppl), pp. 615S.

WOTTON, D., LO, R.S., LEE, S. and MASSAGUE, J., 1999. A Smad transcriptional corepressor. *Cell,* **97**(1), pp. 29-39.

WRANA, J.L. and ATTISANO, L., 2000. The Smad pathway. *Cytokine & growth factor reviews,* **11**(1-2), pp. 5-13.

WRIGHT, A.F., EWART, M.A., MAIR, K., NILSEN, M., DEMPSIE, Y., LOUGHLIN, L. and MACLEAN, M.R., 2015. Oestrogen receptor alpha in pulmonary hypertension. *Cardiovascular research,* **106**(2), pp. 206-216.

WU, T.W., AZHIBEKOV, T. and SERI, I., 2016. Transitional Hemodynamics in Preterm Neonates: Clinical Relevance. *Pediatrics and neonatology,* **57**(1), pp. 7-18.

XU, P., LIU, J. and DERYNCK, R., 2012. Post-translational regulation of TGF-beta receptor and Smad signaling. *FEBS letters,* **586**(14), pp. 1871-1884.

YANG, J., LI, X., AL-LAMKI, R.S., SOUTHWOOD, M., ZHAO, J., LEVER, A.M., GRIMMINGER, F., SCHERMULY, R.T. and MORRELL, N.W., 2010. Smad-dependent and smad-independent induction of id1 by prostacyclin analogues inhibits proliferation of pulmonary artery smooth muscle cells in vitro and in vivo. *Circulation research,* **107**(2), pp. 252-262.

YANG, J., LI, X., LI, Y., SOUTHWOOD, M., YE, L., LONG, L., AL-LAMKI, R.S. and MORRELL, N.W., 2013. Id proteins are critical downstream effectors of BMP signaling in human pulmonary arterial smooth muscle cells. *American journal of physiology.Lung cellular and molecular physiology,* **305**(4), pp. L312-21.

YANG, J., LI, X. and MORRELL, N.W., 2014. Id proteins in the vasculature: from molecular biology to cardiopulmonary medicine. *Cardiovascular research,* **104**(3), pp. 388-398.

YANG, X., LEE, P.J., LONG, L., TREMBATH, R.C. and MORRELL, N.W., 2007. BMP4 induces HO-1 via a Smad-independent, p38MAPK-dependent pathway in pulmonary artery myocytes. *American journal of respiratory cell and molecular biology,* **37**(5), pp. 598-605.

YANG, X., LONG, L., SOUTHWOOD, M., RUDARAKANCHANA, N., UPTON, P.D., JEFFERY, T.K., ATKINSON, C., CHEN, H., TREMBATH, R.C. and MORRELL,

N.W., 2005. Dysfunctional Smad signaling contributes to abnormal smooth muscle cell proliferation in familial pulmonary arterial hypertension. *Circulation research,* **96**(10), pp. 1053-1063.

YANG, X., LONG, L., REYNOLDS, ,PAUL N. and MORRELL, N.W., 2011. Expression of mutant BMPR-II in pulmonary endothelial cells promotes apoptosis and a release of factors that stimulate proliferation of pulmonary arterial smooth muscle cells. *Pulmonary Circulation,* **1**(1), pp. 103-110.

YOSHIDA, A., YONEDA-KATO, N., PANATTONI, M., PARDI, R. and KATO, J.Y., 2010. CSN5/Jab1 controls multiple events in the mammalian cell cycle. *FEBS letters,* **584**(22), pp. 4545-4552.

YOUNG-HOON PARK^{1, #}, MI, S.J., #</SUP>, KI-TAE HA², HAK, S.Y., BOK, A.S. and *</SUP>, 2017. Structural characterization of As-MIF and hJAB1 during the inhibition of cell-cycle regulation. *BMB Reports,* **50**(5), pp. 269-274.

YU, P.B., DENG, D.Y., BEPPU, H., HONG, C.C., LAI, C., HOYNG, S.A., KAWAI, N. and BLOCH, K.D., 2008. Bone morphogenetic protein (BMP) type II receptor is required for BMP-mediated growth arrest and differentiation in pulmonary artery smooth muscle cells. *The Journal of biological chemistry,* **283**(7), pp. 3877-3888.

YU, Y.R., MAO, L., PIANTADOSI, C.A. and GUNN, M.D., 2013. CCR2 deficiency, dysregulation of Notch signaling, and spontaneous pulmonary arterial hypertension. *American journal of respiratory cell and molecular biology,* **48**(5), pp. 647-654.

YUN, H.M., BAIK, J.H., KANG, I., JIN, C. and RHIM, H., 2010. Physical interaction of Jab1 with human serotonin 6 G-protein-coupled receptor and their possible roles in cell survival. *The Journal of biological chemistry,* **285**(13), pp. 10016-10029.

YUN, J., TOMIDA, A., ANDOH, T. and TSURUO, T., 2004. Interaction between glucose-regulated destruction domain of DNA topoisomerase IIalpha and MPN domain of Jab1/CSN5. *The Journal of biological chemistry,* **279**(30), pp. 31296-31303.

ZANOTTI, S. and CANALIS, E., 2016. Notch Signaling and the Skeleton. *Endocrine reviews,* **37**(3), pp. 223-253.

ZAPATA, H.H., SLETTEN, L.J. and PIERPONT, M.E., 1995. Congenital cardiac malformations in Adams-Oliver syndrome. *Clinical genetics,* **47**(2), pp. 80-84.

ZHANG, X.C., CHEN, J., SU, C.H., YANG, H.Y. and LEE, M.H., 2008. Roles for CSN5 in control of p53/MDM2 activities. *Journal of cellular biochemistry,* **103**(4), pp. 1219-1230.

ZHANG, H., DU, L., ZHONG, Y., FLANDERS, K.C. and ROBERTS, J.D.,JR, 2017. Transforming growth factor-beta stimulates Smad1/5 signaling in pulmonary artery smooth muscle cells and fibroblasts of the newborn mouse through ALK1. *American journal of physiology.Lung cellular and molecular physiology,* **313**(3), pp. L615-L627.

ZHANG, H., DU, L., ZHONG, Y., FLANDERS, K.C. and ROBERTS, J.D.,JR, 2017. Transforming growth factor-beta stimulates Smad1/5 signaling in pulmonary artery smooth muscle cells and fibroblasts of the newborn mouse through ALK1. *American journal of physiology.Lung cellular and molecular physiology,* **313**(3), pp. L615-L627.

ZHOU, G., CHEN, T. and RAJ, J.U., 2015. MicroRNAs in pulmonary arterial hypertension. *American journal of respiratory cell and molecular biology,* **52**(2), pp. 139-151.

ZHOU, X.L. and LIU, J.C., 2014. Role of Notch signaling in the mammalian heart. *Brazilian journal of medical and biological research = Revista brasileira de pesquisas medicas e biologicas,* **47**(1), pp. 1-10.

ZONG, D., OUYANG, R., LI, J., CHEN, Y. and CHEN, P., 2016. Notch signaling in lung diseases: focus on Notch1 and Notch3. *Therapeutic advances in respiratory disease,* **10**(5), pp. 468-484.